CRCLEME
Cooperative Research Centre for
Landscape Evolution & Mineral Exploration

CSIRO
AUSTRALIA
EXPLORATION
AND MINING

AMIRA
Australian Mineral Industries Research Association Limited ACN 004 448 266

OPEN FILE
REPORT
SERIES

ATLAS OF WEATHERED ROCKS

I.D.M. Robertson and C.R.M. Butt

CRC LEME OPEN FILE REPORT 1

August 1997

(CSIRO Division of Exploration Geoscience Report 390, 1st revision)

CRC LEME is an unincorporated joint venture between The Australian National University, University of Canberra, Australian Geological Survey Organisation and CSIRO Exploration and Mining, established and supported under the Australian Government's Cooperative Research Centres Program.

CRC

AMIRA
9th Floor, 128 Exhibition Street
Melbourne, 3000, Australia
Telephone: (03) 9679 9955 Fax: (03) 9679 9900
Australian Mineral Industries Research Association Limited ACN 004 448 266

CRCLEME
Cooperative Research Centre for
Landscape Evolution & Mineral Exploration

CSIRO
AUSTRALIA
EXPLORATION
AND MINING

ATLAS OF WEATHERED ROCKS

I.D.M. Robertson and C.R.M. Butt

CRC LEME OPEN FILE REPORT 1

August 1997

(CSIRO Division of Exploration Geoscience Report 390, 1st revision)

CRC LEME is an unincorporated joint venture between The Australian National University, University of Canberra, Australian Geological Survey Organisation and CSIRO Exploration and Mining
Headquarters: CRC LEME c/o CSIRO Exploration and Mining, Private Bag, PO Wembley, Western Australia, 6014

RESEARCH ARISING FROM CSIRO/AMIRA REGOLITH GEOCHEMISTRY PROJECTS 1987-1993

In 1987, CSIRO commenced a series of multi-client research projects in regolith geology and geochemistry which were sponsored by companies in the Australian mining industry, through the Australian Mineral Industries Research Association Limited (AMIRA). The initial research program, "Exploration for concealed gold deposits, Yilgarn Block, Western Australia" (1987-1993) had the aim of developing improved geological, geochemical and geophysical methods for mineral exploration that would facilitate the location of blind, buried or deeply weathered gold deposits. The program included the following projects:

P240: Laterite geochemistry for detecting concealed mineral deposits (1987-1991). Leader: Dr R.E. Smith.
Its scope was development of methods for sampling and interpretation of multi-element laterite geochemistry data and application of multi-element techniques to gold and polymetallic mineral exploration in weathered terrain. The project emphasised viewing laterite geochemical dispersion patterns in their regolith-landform context at local and district scales. It was supported by 30 companies.

P241: Gold and associated elements in the regolith - dispersion processes and implications for exploration (1987-1991). Leader: Dr C.R.M. Butt.
The project investigated the distribution of ore and indicator elements in the regolith. It included studies of the mineralogical and geochemical characteristics of weathered ore deposits and wall rocks, and the chemical controls on element dispersion and concentration during regolith evolution. This was to increase the effectiveness of geochemical exploration in weathered terrain through improved understanding of weathering processes. It was supported by 26 companies.

These projects represented "an opportunity for the mineral industry to participate in a multi-disciplinary program of geoscience research aimed at developing new geological, geochemical and geophysical methods for exploration in deeply weathered Archaean terrains". This initiative recognised the unique opportunities, created by exploration and open-cut mining, to conduct detailed studies of the weathered zone, with particular emphasis on the near-surface expression of gold mineralisation. The skills of existing and specially recruited research staff from the Floreat Park and North Ryde laboratories (of the then Divisions of Minerals and Geochemistry, and Mineral Physics and Mineralogy, subsequently Exploration Geoscience and later Exploration and Mining) were integrated to form a task force with expertise in geology, mineralogy, geochemistry and geophysics. Several staff participated in more than one project. Following completion of the original projects, two continuation projects were developed.

P240A: Geochemical exploration in complex lateritic environments of the Yilgarn Craton, Western Australia (1991-1993). Leaders: Drs R.E. Smith and R.R. Anand.
The approach of viewing geochemical dispersion within a well-controlled and well-understood regolith-landform and bedrock framework at detailed and district scales continued. In this extension, focus was particularly on areas of transported cover and on more complex lateritic environments typified by the Kalgoorlie regional study. This was supported by 17 companies.

P241A: Gold and associated elements in the regolith - dispersion processes and implications for exploration. Leader: Dr. C.R.M. Butt.
The significance of gold mobilisation under present-day conditions, particularly the important relationship with pedogenic carbonate, was investigated further. In addition, attention was focussed on the recognition of primary lithologies from their weathered equivalents. This project was supported by 14 companies.

Although the confidentiality periods of the research reports have expired, the last in December 1994, they have not been made public until now. Publishing the reports through the CRC LEME Report Series is seen as an appropriate means of doing this. By making available the results of the research and the authors' interpretations, it is hoped that the reports will provide source data for future research and be useful for teaching. CRC LEME acknowledges the Australian Mineral Industries Research Association and CSIRO Division of Exploration and Mining for authorisation to publish these reports. It is intended that publication of the reports will be a substantial additional factor in transferring technology to aid the Australian Mineral Industry.

This report (CRC LEME Open File Report 1) is a First revision (second printing) of CSIRO, Division of Exploration Geoscience Restricted Report 390R, first issued in 1993, which formed part of the CSIRO/AMIRA Project P241A.

Copies of this publication can be obtained from:
The Publication Officer, c/- CRC LEME, CSIRO Exploration and Mining, PMB, Wembley, WA 6014, Australia. Information on other publications in this series may be obtained from the above or from http://leme.anu.edu.au/
Cataloguing-in-Publication:
Robertson, I.D.M.
Atlas of weathered rocks
ISBN 0 958 68572 X
1. Regolith 2. Chemical weathering 3. Weathering 4. Petrology 5. Cementation (Petrology) 6. Rock--Analysis 7. Yilgarn--Western Australia 8. Geochemistry.
I. Butt, C.R.M. II. Title
CRC LEME Open File Report 1.
ISSN 1329-4768

PREFACE

The CSIRO - AMIRA Project "Exploration for Concealed Gold Deposits, Yilgarn Block, Western Australia" has, as its overall aim, the development of improved geological, geochemical and geophysical methods for mineral exploration that will facilitate the location of blind, concealed or deeply weathered gold deposits.

One of the chief problems encountered by the exploration geologist, when working in intensely weathered terrain, is in determining the bedrock type from its weathered counterpart. This is particularly difficult for the junior geologist, who inevitably has the task of field and pit mapping and the logging of drill chips, as weathered rock interpretive skills are only gathered with experience.

A specific objective of Project P241A was an Atlas of Weathered Rocks. This Atlas has been assembled, where possible, from exposures of single rock types to illustrate the changes that take place as rocks weather. Inevitably it is incomplete, not only in the number of rock types that could be covered but, due to the degree of truncation of the laterite profile, the depths to which material could be obtained and the climatic variations under which rocks weather. It begins with a summary of regolith terminology and the principles and mineralogy of weathering. The Atlas itself illustrates fabric and mineralogical changes which occur with weathering, focusing on what can be gained by relating microscopic evidence to what can be gained from intelligent use of the hand-lens. It also records the changes in major and trace element contents which occur up the weathered profile; being able to recognize the position in the profile from weathering fabrics will lead to a better understanding and prediction of geochemical dispersion.

It was not intended to produce a complete catalogue of the weathering of all lithologies - an almost impossible task. The principal aim has been to demonstrate the amount of lithological information that can be obtained from careful observation and chemical analysis of weathered materials. The data has been presented in loose-leaf format and are the basis of continuing work, so that results of similar studies of other lithologies can be added subsequently.

C.R.M. Butt
Project Leader, P241A (Dispersion Processes)
May, 1993

TABLE OF CONTENTS

1 INTRODUCTION

1.1 Regolith terminology and classification

The regolith comprises the entire altered, unconsolidated or secondarily re-cemented cover that overlies more coherent bedrock, which has been formed by the weathering, erosion, transport and/or deposition of older material. The regolith, thus, includes fractured and weathered basement rocks, saprolites, soils, organic accumulations, glacial deposits, colluvium, alluvium, evaporitic sediments and aeolian deposits. The regolith in deeply weathered terrains is particularly complex and may exhibit great variations in mineralogical and chemical composition, fabric and origin even within a single profile or toposequence.

Well-defined systems of terminology and classification are essential to provide an accurate description of regolith materials and units and to permit valid comparisons between sites. The regolith is polygenetic, hence descriptive attributes must recognize characteristics due to different events. The classification must be able to discriminate these characteristics accordingly and to emphasize those events considered to be the most important. In the Yilgarn Block and, indeed, in much of Australia, the regolith consists of a deep, partly residual, lateritic weathering profile, formed under warm, humid climates. It was later modified by physical and chemical alterations induced by tectonic and climatic changes (generally, uplift and a change to an arid climate). Accordingly, the terminology and classification are based on the fundamental characteristics of this profile, with modifications due to later events or features attributable to parent lithology added as descriptors. For example, the present-day formation of calcrete may, because of erosion, be superimposed on different horizons of the pre-existing profile. Classification of the product, therefore, may be either according to the later event (i.e., presence of calcrete) or to the earlier event (i.e., the horizon in which the calcrete has precipitated). The former recognizes a single "calcrete unit" and the latter subdivides the calcrete between the various horizons. The latter is the preferred classification but, in some circumstances, identification of the calcrete unit may be paramount, in which case the alternative classification could be adopted. Providing the descriptions of the material are adequate, classification according to either scheme should be possible.

The scheme described here is derived, in part, from Anand and Butt, 1988. The terms conform, as far as possible, with established national and international usage. As in all natural systems, many changes are gradational, consequently the limits to some defined units are arbitrary (e.g., saprock). Similarly, the placement of some units can be equivocal and may depend upon the purpose of the classification, as discussed above for calcrete. Sedimentary units deposited on bedrock or pre-existing regolith are usually considered as part of the regolith. However, with respect to post-depositional weathering, the unaltered sediment could be regarded as the bedrock and the altered sediment as regolith. Such distinctions are rarely significant in exploration, although they arise in the Yilgarn Block, where Permian glacial deposits and Tertiary sediments occur, e.g., in palaeodrainages.

1.1.1 Classification of the lateritic regolith

The classification and terminology are summarized in Figure 1. The classification is broadly hierarchical, with sub-divisions of each unit defined in terms of a given set of attributes. Increasing sub-division requires a greater level of detail for correct classification. However, the detail and precision that can be achieved are limited by the sampling procedures and the nature and sophistication of the observations. Thus, samples obtained by rotary or percussion drilling cannot be described using the same set of attributes as those obtained by core drilling or from outcrop and hence cannot be classified with the same precision. For example, the "clay zone", as observed by rotary drill cuttings, may include more than one horizon of the lateritic profile (e.g.,

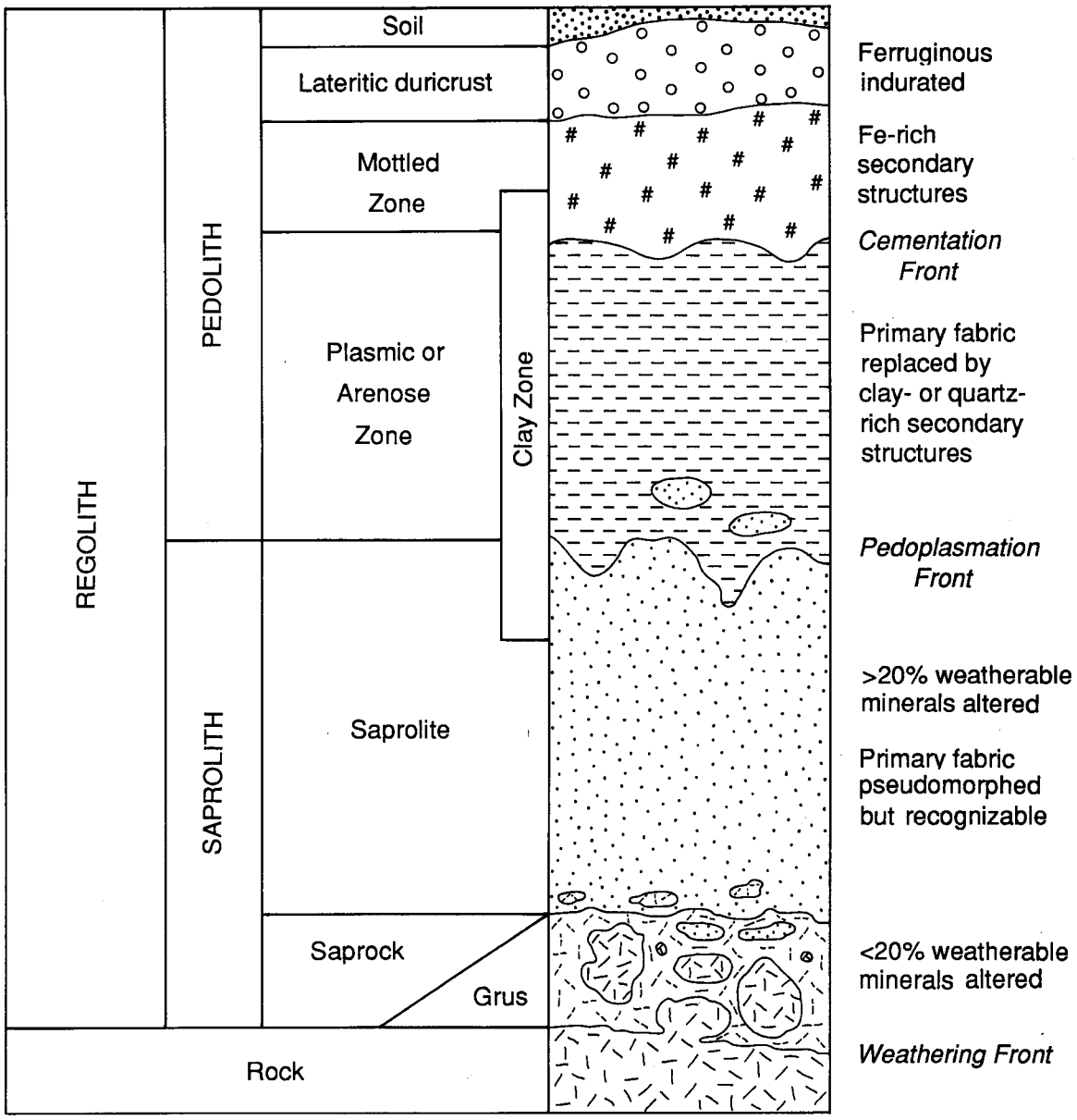

Figure 1. Regolith Terminology

saprolite and mottled zone) and show none of the distinctive fabric elements, which may have been present, as they were destroyed by the act of drilling.

1.1.2 ***Principal units.*** The profile consists of two major components, the saprolith and the pedolith. These are distinguished by their fabrics, which, in turn, reflect their genesis. The base of the saprolith is in contact with fresh rock. This contact defines the base of the regolith (Figure 2B).

Saprolith: The saprolith is the (generally lower) part of the regolith that has retained the fine fabric originally expressed by the arrangement of the primary minerals (e.g., crystals, grains) of the parent material. The definition may include weathered rocks in which only larger structures including bedding, schistosity, veining or lithological contacts are preserved. The presence of these fabrics implies that weathering has been essentially isovolumetric and pseudomorphic.

Pedolith: The pedolith is the upper part of the regolith in which the fabric of the parent material has been destroyed by one or more pedological processes, including non-isovolumetric weathering or soil formation and/or the development of new fabrics. Some horizons are characterized by concentration of particular elements (e.g., Fe and Al oxides in lateritic profiles) and the presence of distinctive secondary structures such as pisoliths. The boundary between saprolith and pedolith is termed the "pedoplasmation front". Further subdivision is into the commonly recognized horizons of the lateritic weathering profile.

Saprolith: Only two major saprolith horizons, saprock and saprolite, are recognized at present, with a minor subdivision, grus. Although the saprolite commonly comprises at least two thirds of a complete laterite profile, there is, as yet, no satisfactory procedure for its subdivision. The principal criterion for any such subdivision should be a weathering index but there is little agreement as to how such an index can be defined. These horizons may be developed on any rock type, although a distinctive variant, grus, resulting from considerable physical disintegration, may be present over granitoids.

Saprock: Saprock is a compact, slightly weathered rock of low porosity with less than 20% of the *weatherable* minerals altered[1] . Weathering effects are present along mineral boundaries and intra-mineral fissures, along cleavages, shears, joints and fractures or affecting only a few individual mineral grains or mineral species.

Grus: Grus is the fragmental disintegration product of largely unweathered granitic rock. It is commonly applied to surface products, but is also present as a porous horizon ranging in thickness from a few cm to 10 m or more at the base of the saprolite. Grus differs from saprock in that it is friable rather than compact.

Saprolite: Saprolite is weathered bedrock in which fine fabrics, originally expressed by the arrangement of the primary minerals (e.g., crystal, grains), are retained. Compared to saprock, more than 20% of the weatherable minerals have been altered. The definition may be extended to include weathered rocks in which only larger structures (e.g., Figures 2A and 3A) such

---

[1] Although saprock begins with the first signs of weathering, joints, shears and quartz veins may be penetrated by significant staining by Fe oxides, even though the surrounding rocks may be quite fresh. Thus scale is a factor. These stains may even penetrate the fresh rock cleavage but, since this Fe oxide staining is essentially imported, the surrounding rock could still be regarded as fresh. The first signs of weathering are generally oxidation of rock sulphides or breakdown of feldspars to clays.

The upper boundary of the saprock may be difficult to locate on the hand specimen scale as it is difficult to determine the proportion of weatherable minerals in the fresh rock without a detailed petrographic study. However this boundary is gradational; saprock and saprolite are notoriously inhomogenous here.

SAPROCK AND SAPROLITE

Figure 2A. Tholeiitic lava saprolite showing relatively undeformed pillow structures. Telegraph Pit, Laverton, WA.

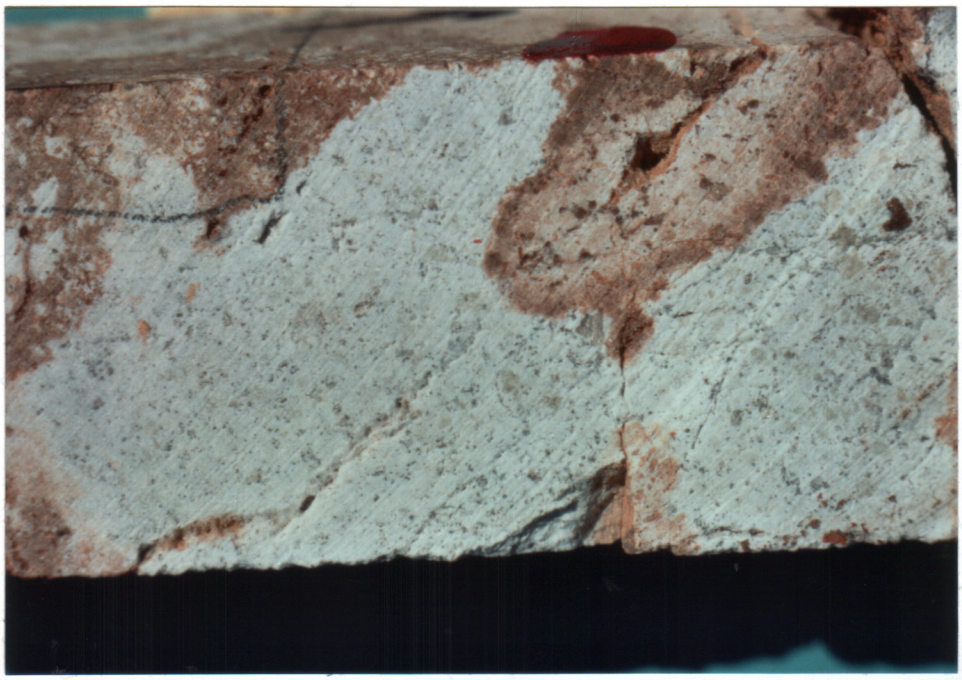

Figure 2B. Junction between fresh rock and saprock in drillcore. Brown staining due to release of Fe from oxidation of pyrite, spreading from fractures, due to increased water access. Wau, Papua New Guinea.

as bedding, schistosity, veining, pillows or lithological contacts are preserved. Saprolite may become more massive upwards, as the proportion of clay increases and cementation by secondary silica, carbonates, aluminosilicates and, especially, Fe oxides is not uncommon.

The term "pallid zone" should not be used synonymously for saprolites; saprolites exhibit a wide variety of colours. Although saprolites are commonly white over felsic rocks, over some felsic and most mafic and ultramafic rocks they are not; conversely, not all pale or white horizons are saprolite. Recognition of saprolite in percussion and RAB drill cuttings may be difficult, particularly at shallow depths, where the weathering has been intense and the material is soft and clay rich, so that fabrics are easily destroyed by drilling. The "clay zone", seen in such cuttings, may include saprolite, plasmic clay and even some mottled zone.

Pedolith: Subdivision of the pedolith is based on fabric, particularly secondary structures, and/or on the concentration of particular elements. The principal horizons are a mottled zone, a ferruginous zone (laterite or lateritic residuum), soil and lag. Generally, fabric loss and accumulation of Fe and Al oxides appear to coincide fairly closely, defining the mottled zone. Where Fe and Al accumulation occurs without fabric loss, the material remains saprolite. Where fabric loss occurs without oxide accumulation, there is a transitional zone of consolidation and settling, the plasmic or arenose horizons[2], which occur just above the pedoplasmation front at the base of the pedolith, between the saprolite and the mottled zone. Major structural features, such as quartz veins and lithological contacts, may still be preserved, generally with some distortion or change in orientation (dip), indicating non-isovolumetric weathering.

Plasmic horizon: Massive clays or silty clays, commonly having a mesoscopically homogeneous plasmic fabric, are developed over rocks poor in quartz. The loss of lithic fabric is caused by solution and authigenesis of minerals and various mechanical processes, such as shrinking and swelling of clays, and settling of resistant primary and secondary minerals through instability induced by leaching.

Arenose horizon: This is a sandy horizon with a grain-supported (or nearly so) fabric. The loss of lithic fabric appears to be caused by solution of weatherable primary and secondary minerals (dominantly kaolinite) and settling of resistant minerals, dominantly quartz.

Mottled zone: This is characterized by localized spots, blotches and streaks of Fe oxides that, with further mobilization and concentration, become reorganized into secondary structures, such as pisoliths and nodules, and that surround tubular voids (Figure 3B). Nodule growth progressively destroys pre-existing fabrics, although pseudomorphic lithic, plasmic or arenose fabrics and micro-fabrics may be preserved in the nodule core.

The definition of the mottled zone inherently includes fabric changes in the matrix and the development of secondary structures by the oxides themselves; colour variegation alone is not diagnostic. The mottled zone is part of the lateritic profile, probably formed at or above the water-table. As such, it is distinct from mottling associated with later weathering episodes, e.g., at lower water-tables or in soils formed on partly stripped profiles.

Pisoliths, nodules and voids (both open and infilled) of various shapes that develop in the mottled zone become upwardly more numerous. In the ferruginous zone (or laterite), the pisoliths and nodules are either cemented, to form an ironstone or duricrust, or become dominant over any intervening matrix.

---

[2] Plasmic horizons tend to form on mafic, ultramafic and argillaceuos rocks. Arenose horizons are common on granitic or arkosic rocks. They are equivalent in the stratigraphy of the regolith.

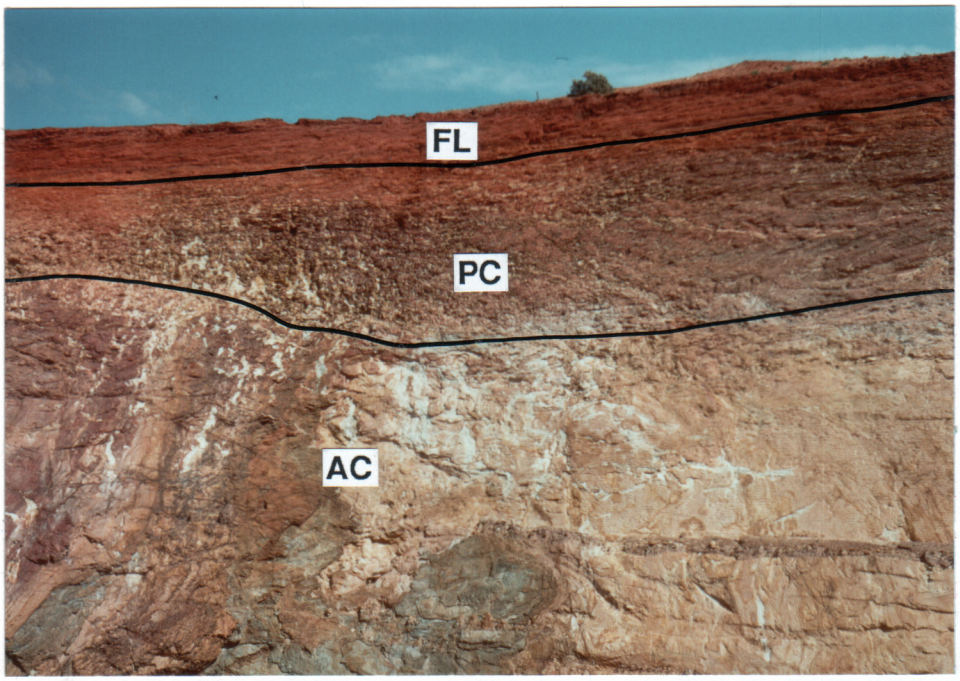

Figure 3A. Steep-dipping saprolite of Archaean schists (AC), overlain by Permian clays (PC) in which a mottled zone occurs, in turn overlain by hardpanized, brown, very ferruginous fluvial sands and grits (FL) produced from erosion of the upper regolith. Telegraph Pit, Laverton, WA.

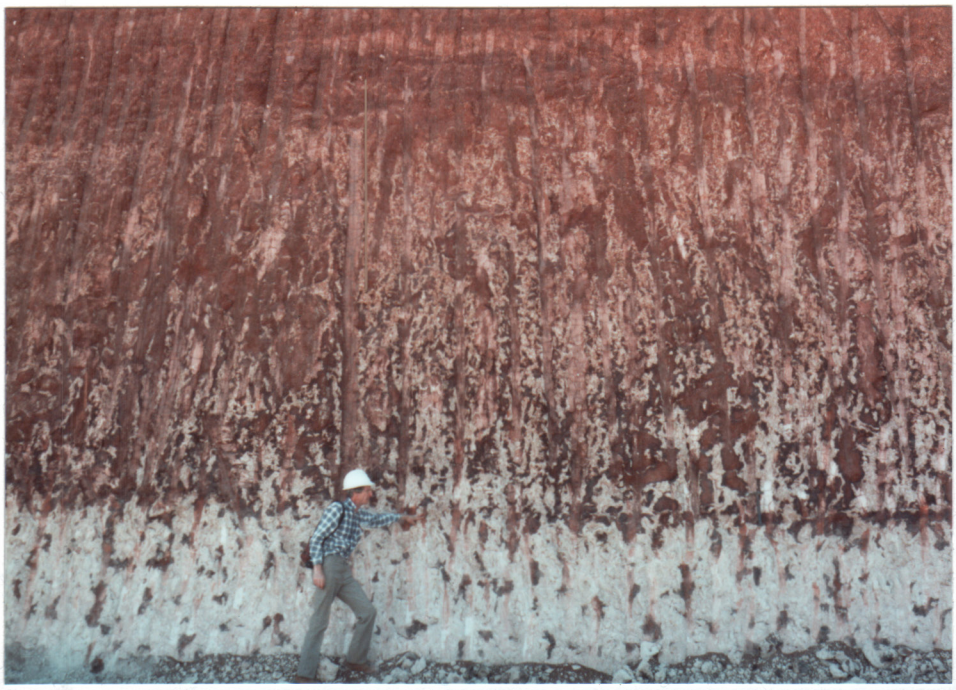

Figure 3B. The base of the mottled zone in transported overburden, showing the cementation front and unusually coarse mottles, resembling root casts. Kanowna, WA.

LATERITE AND MOTTLED ZONE

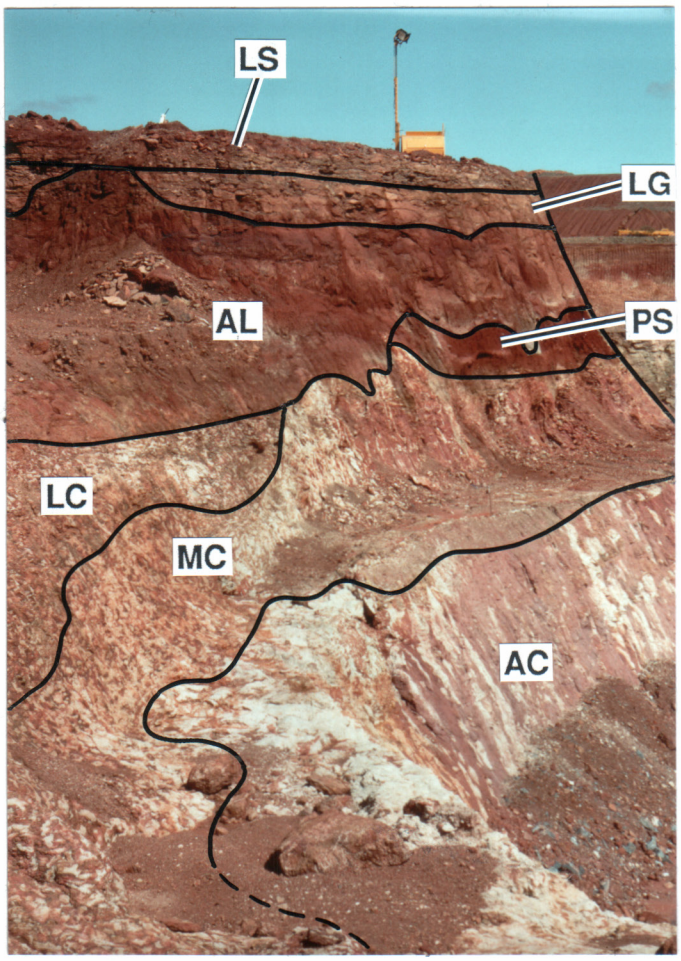

Figure 4. Complexities of the regolith are illustrated by the Genesis Pit at Lawlers. The saprolite and part of the mottled zone are developed in Archaean rocks (AC) but the upper mottled zone (MC) and lateritic horizon (LC) are developed in Permian clays. These, in turn, are overlain unconformably by various colluvial/alluvial horizons (AL), including upper layers of lateritic gravel (LG) and silt (LS), silicified to hardpan. A small, rare wedge of palaeosol (PS) occurs between mottled Permian clays and the colluvium/alluvium.

Ferruginous Zone, "Laterite": A highly weathered material, depleted in alkalis and alkaline earth elements, that is composed principally of secondary oxides and oxyhydroxides of iron (goethite, hematite, maghemite) and hydroxides of aluminium (e.g., gibbsite). These oxides may incorporate other minerals including clays and other secondary minerals (e.g., kaolinite, halloysite, anatase), resistant primary minerals (e.g., quartz, zircon, rutile) and weatherable primary minerals (e.g., ilmenite, muscovite). The laterite horizon is hard or subject to hardening upon exposure. (Definition after Sivarajasingham *et al.*, 1962).

Laterite may be either indurated or unconsolidated. *Lateritic duricrust* or *cuirasse* is indurated laterite, composed of various structural forms of secondary segregations such as mottles, nodules, pisoliths and ooliths, cemented by a matrix of clay and aluminium and/or iron oxides. *Lateritic gravels* consist of unconsolidated ferruginous segregations and fragments. A classification of these materials has been developed by Anand *et al.*, (1989).

Lateritization is dominantly a chemical process. Erosion of the lateritized regolith by sheetwash can occur later (e.g., Figures 3A and 4), with sedimentation on plains and in valleys. These sediments, which may already be weathered, may then be reweathered (e.g., Figure 3B). For geochemical exploration purposes, recognition of the sedimentary origin is critical and may require comparisons of immobile element and resistant mineral compositions of overburden and known residuum. Investigation of the degree of homogeneity of the fragments or clasts and of the characteristics of surface lag can assist with identification.

The processes that formed the above components of the regolith on the Yilgarn Block are thought to be associated with a humid climate when intense chemical weathering dominated. Modification of these materials occurred with changes in climate and increased erosion.

1.2 Post-lateritic modification of the regolith

1.2.1 Partial truncation. Erosion has occurred due to instability resulting from climatic change or drainage rejuvenation following uplift. Removal of the upper horizons of the profile has exposed lower horizons (e.g., Figure 3A), including unweathered rock. The exposed lower horizon may outcrop, become the parent material of newly formed soils or be overlain by transported overburden. The erosion products occur as extensive transported overburden including alluvium, lag, colluvium, sheet-wash, lake sediments, evaporitic sediments and aeolian material on fresh or weathered bedrock. These sediments may be unconsolidated, friable or partially or wholly consolidated, cemented by iron oxide, silica, carbonates, gypsum or clays.

1.2.2 Cementation by introduced components. Cementation is one of the most recognizable modifications to a lateritic profile occurring in response to the change from a humid to an arid climate. The most common cements are iron oxides (ferricrete), silica (silcrete, hardpan), Ca and Mg carbonates (calcrete), aluminosilicates and gypsum.

Ferricrete: Ferricrete is an indurated material formed by the *in situ* cementation of pre-existing regolith by Fe oxides. The fabric, mineralogy and composition of ferricretes may reflect those of the parent (regolith) material and hence, if residual, the underlying lithology. Some authors restrict the term to the ferruginous horizon of lateritic regoliths (and therefore synonymous with cuirasse, lateritic duricrust) but the more general definition is preferred. Cementation can occur during or after lateritic weathering.

Silcrete: These strongly silicified, indurated regolith components, commonly have a conchoidal fracture with a vitreous lustre. Silcretes appear to represent the complete or near-complete silicification of a precursor regolith horizon by the infilling of available voids with silica. They may be broadly subdivided into pedogenic or groundwater types. Most are dense and massive,

Figure 5A. Blocky outcrop of silicified dunite saprolite at Mt. Hope.

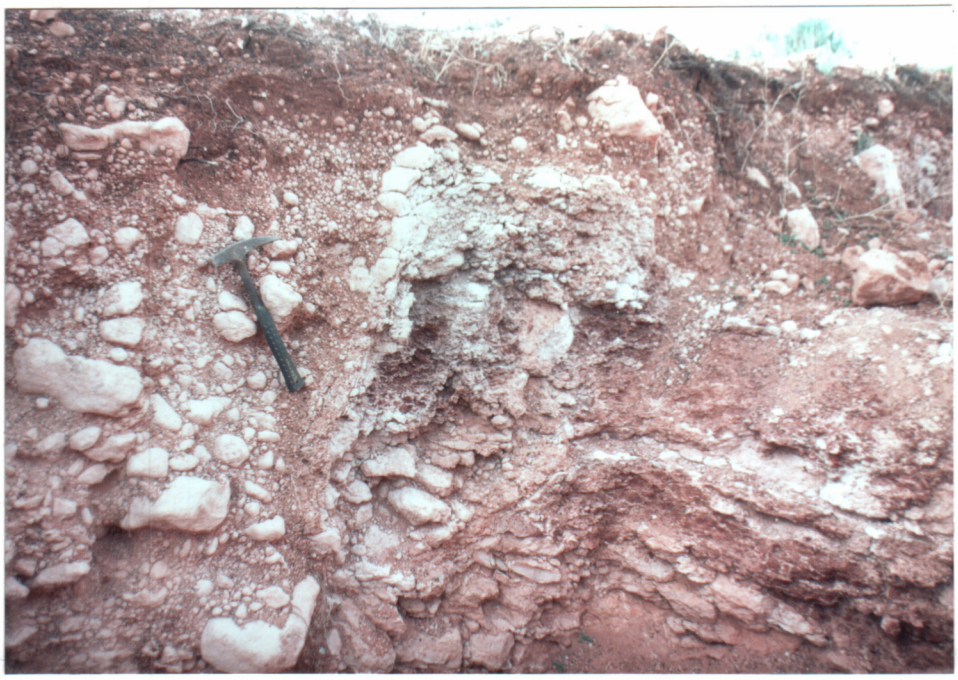

Figure 5B. Cobbles of calcrete on left and carbonate-infused lateritic gravels, with a marked platey structure, on right, all set in a highly calcareous friable earth at Peach Tree, Mulline, WA.

HARDPAN AND LAG

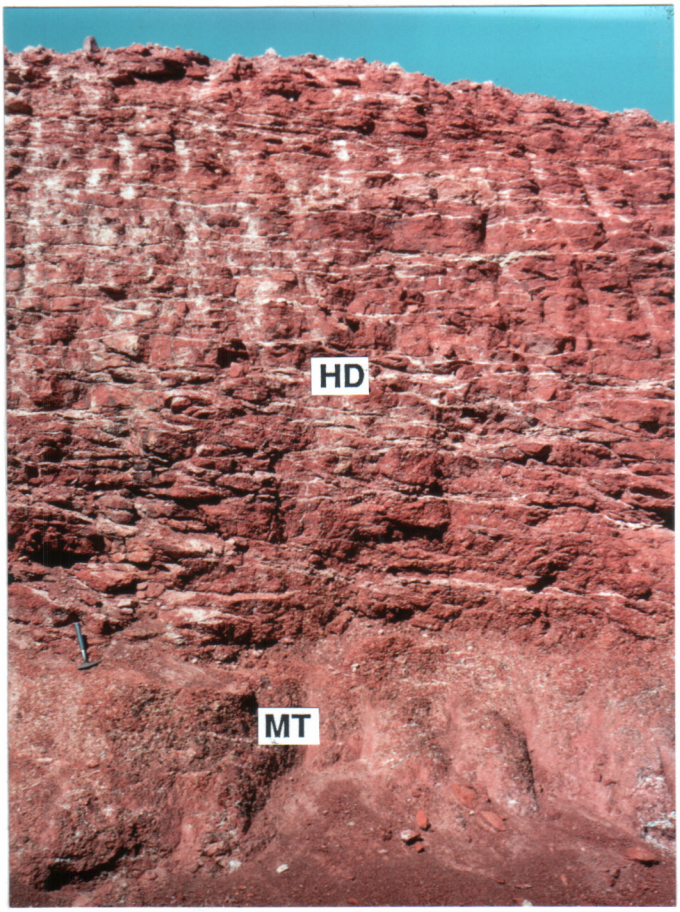

Figure 6. Hardpan (HD) developed in pisolitic, lateritic residuum at Bottle Creek, north-west of Menzies WA.. The hardpan has well-developed horizontal partings, along which occurs flakey and powdery, fine silica and coatings of Mn oxides. The unsilicified mottled zone (MT) appears towards the base. Photo HMC.

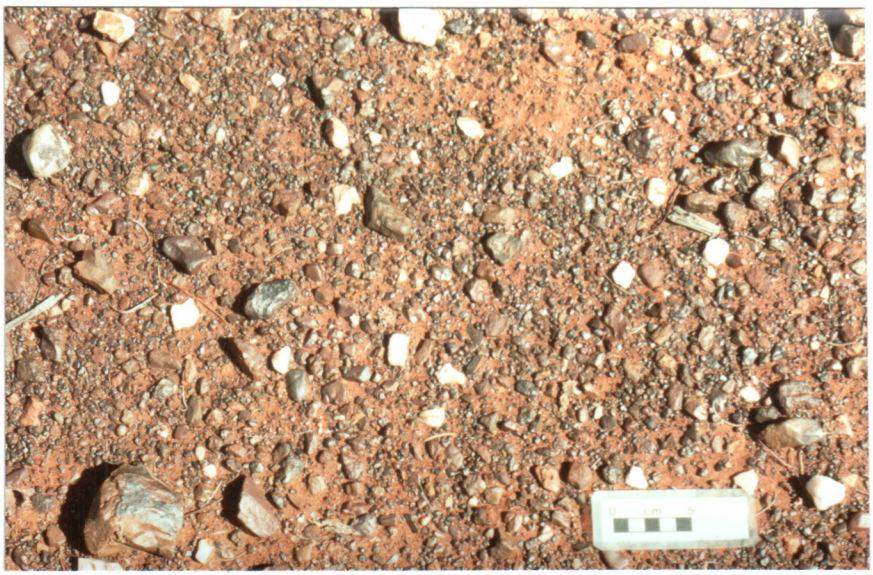

Figure 7. A lag or desert armour of angular to subrounded fragments of ferruginized saprolite and chips of vein quartz, produced by deflation of soil by wind and water. Beasley Creek, Laverton, WA

but some may be cellular, with boxwork fabrics. The fabric, mineralogy and composition of silcretes may reflect those of the parent (regolith) material and hence, if residual, the underlying lithology. Thus, silcretes over granites and sandstones are silicified arenose zone, have a floating or terrazzo quartz fabric and tend to be enriched in Ti and Zr; silcretes with lithic fabrics (e.g., on dunites) are silicified saprolites (Figure 5A) with initial constituents diluted or replaced by silica.

Hardpan: Hardpan is a near-surface indurated horizon. Red-brown hardpans, such as the Wiluna Hardpan (Figure 6), consist of a variety of transported or residual host materials, including colluvium, pisolitic horizons and brecciated saprolite, set in a porous, red-brown, earthy matrix, cemented by silica (generally hyalite). The material has a coarsely laminated appearance and commonly has Mn oxides on partings. Wiluna Hardpan is generally 0.5-10.0 m thick, and is generally found north of latitude 30°S (the Menzies Line). It is commonly overlain by a red-brown, gravelly, clay soil.

Calcrete: This is an indurated to powdery material, formed by the *in situ* cementation or replacement, or both, of pre-existing regolith by secondary carbonates. Calcretes vary widely in carbonate content and properties, from friable, fine grained soils to coarse nodular horizons to limestone rock. There are two principal genetic types, (1) pedogenic or vadose calcretes (e.g., Figure 5B) and (2) groundwater or phreatic calcretes. Most consist of calcite and/or dolomite; magnesite occurs over some ultramafic rocks. Groundwater calcretes may have minor aragonite and Mg clays such as sepiolite. Pedogenic calcretes are most abundant south of 30°S (Menzies Line); groundwater calcretes occur to the north.

1.2.3 Formation of soil and lag. Few soils which originally overlay the developing lateritic profiles (ferralsols) are preserved, although it is possible that they have contributed to some of the extensive sand plains over granites. Most soils are developed from, rather than with, the material they overlie, whether these are the ferruginous zones of complete profiles or the exposed horizons (e.g., mottled zone, saprolite, fresh rock) of truncated profiles, and have characteristics inherited from these parent materials. Those soils to the south of the Menzies Line, in an environment dominated by winter rainfall and eucalypt woodland, may contain nodular and powdery soil carbonates. Those to the north of the Menzies Line, in an environment of dominantly summer rainfall and having acacia woodland, have little soil carbonate. Many of the soils of the Yilgarn, particularly those towards the arid interior, contain a significant wind-blown component of fine, silty quartz, with rounded grains.

Erosion of the upper layers of soil by wind and water removes the fine materials and leaves a desert armour or lag (Figure 7). Lag may also develop by upward displacement of coarser fragments by eluviation, bioturbation and root plucking. The composition of the lag is related to the regolith substrate. Lag of saprolite or ferruginous saprolite occurs over erosional areas, a lag of pisoliths and nodules occurs over areas of preserved laterite. Allochthonous lag of mixed origin, comprising lithic fragments, quartz and lateritic pisoliths is generally abundant on colluvial-alluvial outwash plains. Lags developed on mafic and ultramafic rocks tend to be very ferruginous. Careful petrographic examination reveals a variety of primary and secondary fabrics (Robertson, 1989; Robertson, 1990; Robertson and Tenhaeff, 1992) preserved in, and pseudomorphed by, Fe oxides and oxyhydroxides, illustrating the incompleteness of the various weathering processes.

2 THE WEATHERING PROCESS

2.1 Initiation of weathering

Rainwater contains highly reactive hydrogen ions and this is a powerful weathering agent, as shown below. Surface water has access to the rock along faults, joints and cleavage. This occurs on a scale of metres to tens of metres, and high fluid flow rates are possible. Penetration of solid rock is more difficult. Initial access is along the margins of quartz veins and along intergranular boundaries, on the scale of a few mm, and fluid flow rates are slow. Access to the minerals occurs along mineral cleavages, twin boundaries and lattice dislocations on the scale of a few microns to nanometres, with minute rates of fluid movement, probably governed largely by diffusion. Thus, *initial* penetration of a fresh mineral is a slow process and its rate depends on factors such as mineral cleavage and strain. Weathering solutions etch tube-like channels that spread outward into a grain, improving fluid access and so accelerating the rate of weathering. Dissolved ions diffuse away from the weathering front, where they are in high concentration, to large voids and fractures, where they are in low concentration and come in contact with flowing solutions.

2.2 Weathering reactions

Weathering of igneous and metamorphic rocks consists of the conversion of a suite of high temperature *primary* minerals to a suite of new, low temperature *secondary* minerals stable in the weathering environment. This proceeds largely by oxidation, and hydrolysis. The various components of the rocks are removed sequentially. The losses are shown by a decrease in the volume of the product minerals (reflected by Δv in Table 1), and a decrease in bulk density that progressively increases the porosity of the rocks. This, in turn, allows improved fluid access and accelerates weathering, particularly in the saprolite. Some of this porosity is lost in the plasmic zone, where clay deposition and structural collapse take place, though vesicular structures and root channels locally increase porosity. Although weathering releases many elements into solution, new minerals are formed and these capture mobile elements by incorporating them into their crystal structures or by surface adsorbtion. Where cementation (by Ca, Si, Fe or Al) occurs, fluid movement decreases but weathering is then relatively complete.

Pyrite. Sulphide oxidation generally occurs at the weathering front and occurs in two steps, particularly if available oxygen is limited. First pyrite oxidizes and releases soluble Fe^{2+}, SO_4^{2-} and H^+ (Table 1, Equation 1). The acid conditions so produced may be locally buffered by decomposition of any carbonates present in the gangue and wall rocks, and by silicate weathering reactions which require a low pH to proceed. The second stage may be remote from the first, where oxygen is more plentiful, and involves the combined oxidation and hydrolysis of the Fe^{2+} to precipitate iron oxyhydroxides and release more protons (Table 1, Equations 2 and 3). Sulphide oxidation is another prime source of hydrogen ions for weathering reactions, thus, where oxidizing sulphides are present, weathering generally proceeds to far greater depths than would normally occur. Oxidation of sulphides releases a very large suite of chalcophile elements.

Feldspar. Transmission electron microscopy by several workers (Eggleton and Buseck, 1980; Anand *et al.*, 1985) has shown that feldspar may weather either (a) directly to kaolinite, halloysite or gibbsite or (b), via a two step reaction in which plagioclase feldspar converts to smectite (Table 1, Equation 4, Figure 8B) and then the smectite alters to kaolinite (Table 1, Equation 5). Both are hydrolysis reactions, requiring a source of hydrogen ions (acid conditions) and release alkalis and alkaline earth elements. Potassium feldspar weathering proceeds similarly, though via illite (which may be expressed as a smectite with interlayered K) and occurs higher in the profile (Robertson, 1990). Development of smectite is commonly not seen in laterite profiles and may either not occur or be a transitory phase, occurring only on the sub-micron scale. The widespread occurrence of smectite in some regoliths is probably due to weathering under arid conditions, in which leaching of alkalis and alkaline earth elements was less severe.

TABLE 1 - MINERAL REACTION EQUATIONS

Pyrite

1) $2FeS_2 + 7O_2 + 2H_2O \rightarrow 2Fe^{2+} + 4SO_4^{2-} + 4H^+$
pyrite

2) $2Fe^{2+} + 0.5O_2 + H_2O \Longleftrightarrow 2Fe^{3+} + 2OH^-$

3) $2Fe^{3+} + 6H_2O \rightarrow 2Fe(OH)_3 + 6H^+$
goethite

Feldspar

4) $4Ca_{0.5}Na_{1.5}(Si_{5.5}Al_{2.5})O_{16} + 8H^+ + 16H_2O \rightarrow$
plagioclase

$4Ca_{0.25}Al_2[Si_{3.5}Al_{0.5}]O_{10}(OH)_2 + 6Na^+ + Ca^{2+} + 8H_4SiO_4$
smectite

Δv *100:87*

5) $4Ca_{0.25}Al_2[Si_{3.5}Al_{0.5}]O_{10}(OH)_2 + 2H^+ + 13H_2O \rightarrow$
smectite

$5Al_2Si_2O_5(OH)_4 + 4H_4SiO_4 + Ca(OH)_2$
kaolinite

Δv *100:79.*

Alkali Feldspar

6) $2[Na,K]Al\,Si_3O_8 + 9H_2O + 2H^+ \rightarrow Al_2Si_2O_5(OH)_4 + 2[Na,K]^+ + 4H_4SiO_4$
alkali feldspar — kaolinite

Δv *100:49*

Calcic Plagioclase

7) $2CaAl_2Si_2O_8 + 2H_2O + 4H^+ \rightarrow 2Al_2Si_2O_5(OH)_4 + 2Ca^2$
anorthite — kaolinite

Δv *100:98*

TABLE 1 - MINERAL REACTION EQUATIONS (CONTD)

Chlorite

8) $(Mg_3\ Fe^{2+}_2\ Al)(Si_3\ Al)O_{10}(OH)_8 + 0.5O_2 + 4.6H^+ + 0.5H_4SiO_4 \rightarrow$
chlorite

$Mg_{0.4}(Al_{1.5}\ Mg_{0.3}\ Fe^{3+}_{0.2})(Si_{3.5}\ Al_{0.5})O_{10}(OH)_2 + 2.3Mg^{2+} + 1.8Fe(OH)_3 + 3.6H_2O$
smectite

$\Delta v \sim 100{:}87$

Muscovite

9) $2KAl_3Si_3O_{10}(OH)_2 + 8H^+ + 2H_2O \rightarrow 2Al_2Si_2O_5(OH)_4 + 2K^+ + 2Al^{3+} + 2H_4SiO_4$
muscovite — kaolinite

$\Delta v\ 100{:}70$

10) $2Al^{3+} + 2H_4SiO_4 \rightarrow Al_2Si_2O_5(OH)_4 + 2H_2O$
kaolinite

Kaolinite

11) $Al_2Si_2O_5(OH)_4 + 2H_2O \rightarrow Al_2Si_2O_5(OH)_4.(2H_2O)$
kaolinite — halloysite

$\Delta v\ 100{:}116$

12) $Al_2Si_2O_5(OH)_4 + 5H_2O \rightarrow 2Al(OH)_3 + 2H_2SiO_4$
kaolinite — gibbsite

$\Delta v\ 100{:}49$

13) $Al_2Si_2O_5(OH)_4 + 2H_2O \leftrightarrow 2Al^{3+} + 2H_4SiO_4$
kaolinite

Tremolite

14) $Ca_2Mg_5Si_8O_{22}(OH)_2 + 14H^+ + 8H_2O \rightarrow 2Ca^{2+} + 5Mg^{2+} + 8H_4SiO_4$
tremolite

$\Delta v\ 100{:}0$

Talc

15) $Mg_6Si_8O_{20}(OH)_4 + 8Al^{3+} + 12H^+ \rightarrow 4Al_2Si_2O_5(OH)_4 + 6Mg^{2+}$
talc — kaolinite

$\Delta v\ 100{:}101$

If the reaction for alkali feldspar (Table 1, Equation 6) is compared with that of calcic plagioclase (Table 1, Equation 7), it is clear that more kaolinite is produced from the calcic plagioclase, resulting in a very compact kaolinite; the alkali feldspar loses more silica and results in a porous product (compare Δv values for Equations 6 and 7). Where plagioclase and K-feldspar occur intimately intergrown in a perthite, the plagioclase weathers first (Figure 8A). The rigid structure provided by the relatively unaltered K-feldspar prevents collapse and provides plenty of fluid access. The kaolinite produced from the plagioclase hydrates to halloysite (see below). Elements released by feldspar weathering include minor Ba, Rb, Sr, REE and, rarely, trace Pb, Ag and B.

Chlorite. Weathering of chlorite to smectite requires oxidizing, acid conditions and yields Fe oxides which cause turbidity in the chlorite (Table 1 Equation 8). The smectite then hydrolyses to kaolinite, requiring more hydrogen ions to do so and releases Fe and alkaline earth elements. Weathering chlorite releases minor Cr, Li, Mn, Ni and Ti. At Mt. Percy (Butt, 1991), chlorite is the principal host of chromium.

Micas. Some muscovite survives (Anand and Gilkes, 1987) but other muscovite loses its K, converting to illite or hydromuscovite, and then loses a Si tetrahedral layer (Robertson and Eggleton, 1991) and changes to kaolinite (Table 1, Equation 9). This is an hydrolysis reaction requiring hydrogen ions. Both Si and Al from the tetrahedral layer dissolve, later to combine and deposit elsewhere as more kaolinite (Table 1, Equation 10). This soluble Al could alternatively participate in the kaolinization of talc (Table 1, Equation 15). In some micas, discrete layers, that are visible optically, alter to kaolinite (Robertson, 1990), leaving layers of highly birefringent muscovite alternating with layers of low birefringent kaolinite. Sericitic micas, however, alter to a material of moderate (yellow to white) birefringence that is muscovite and kaolinite intimately mixed on a sub-micron scale (Figure 8C). Weathering of muscovite releases minor Cr, F, Li, Rb, V and Ti, and, from some micas, traces of B, Cu, Nb, Pb, Sn, W and Zn. Weathering of biotite and phlogopite proceeds more readily than muscovite; biotite releases a similar element suite to muscovite, together with much Fe. Generally, the more complex the silicate, especially sheet and chain silicates, the richer and more varied their contained suite of trace elements.

Kaolinite. Halloysite is a common secondary mineral in Si-rich groundwater environments such as those in the Yilgarn Block. Kaolinite may hydrate to halloysite (Table 1, Equation 11). Sheets of kaolinite alter inhomogeneously to halloysite and so buckle and curl into spiral structures (Figure 8D), much like a rolled newspaper (Robertson and Eggleton, 1991). This type of halloysite is generally Fe-poor, but smaller halloysite tubes contain more Fe (~2%) and very Fe-rich halloysite tends to a spherical morphology. Near the coastal margin of the Yilgarn Block, where rainfall is more plentiful and drainage more effective, the groundwater is poor in Si so that kaolinite dissolves and gibbsite is precipitated (Table 1, Equation 12) with silica removed by the groundwater. Some kaolinite in upper parts of the profile, above the pedoplasmation front, may dissolve and precipitate elsewhere, causing extensive fabric changes (Table 1, Equation 13).

Tremolite and talc. Both these magnesian minerals contain little Al. Although both require significant quantities of hydrogen ions to weather, their weathering behaviour is markedly different. Tremolite dissolves near the base of the profile, leaving hollow voids, and releases alkaline earth elements and Si to solution (Table 1, Equation 14). In contrast, talc remains stable to near the top of the profile and then weathers to kaolinite (Table 1, Equation 15), but for this it requires an external source of Al ions, possibly supplied by weathering of muscovite and kaolinite. Talc and tremolite have fairly simple compositions and release Mg, Ca, Fe, Si and traces of Ti.

Hornblende. Hornblende and other amphiboles alter to smectite deep in the profile and thence to kaolinite higher up. Alteration begins along the amphibole cleavage and is generally nearly complete before chlorite is attacked (Llorca, 1989). Weathering of amphiboles, particularly hornblende, may release small amounts of Cr, Cu, F, K, Li, Mn, Ni, Sn, Ti, V and Zn.

FIGURE 8

Partial weathering of perthitic feldspar

A. Partly weathered vein perthite showing a mesh of halloysite rods (HO) pseudomorphing the plagioclase of the perthite, surrounded by a relatively unaltered lacework of etched microcline (MC). Granitic saprolite from Trial Hill, Queensland. Specimen MJ6. Scanning electron micrograph.

Partial weathering of plagioclase

B. Rounded, cellular encrustations of smectite (SM), showing a typical 'cornflake' fabric, coating plagioclase. This illustrates smectite as an intermediate product in the weathering of plagioclase to kaolinite. Granite saprock from Trial Hill, Queensland. Specimen MJ10 Scanning electron micrograph.

Intimate mixture of sericite and kaolinite on sub-micron scale

C. An intimate mixture of mica (MS), showing mottled diffraction contrast and 10 Å diffraction fringes, with kaolinite (KA). This intimate mixture, which cannot be resolved optically, results in a material with a birefringence intermediate between that of muscovite and kaolinite (yellow to white). Granite saprolite from Trial Hill, Queensland. Specimen MJ6 Transmission electron micrograph.

Halloysite spirals forming from flakes of kaolinite

D. Strips of kaolinite (KA) continuous with polygonal and oval rolls of halloysite (HO). Parts of the halloysite spirals contain straight sections reinforced by relict kaolinite with a mottled diffraction contrast (MX). This illustrates the hydrolysis of kaolinite sheets to halloysite rolls, like the rolling of a newspaper. Preserved patches of kaolinite reinforce the linear parts of the rolls. As the kaolinite is progressively hydrolysed, the rolls become oval or round in section. Kaolinized plagioclase of granite saprolite, Trial Hill, Queensland. Transmission electron micrograph.

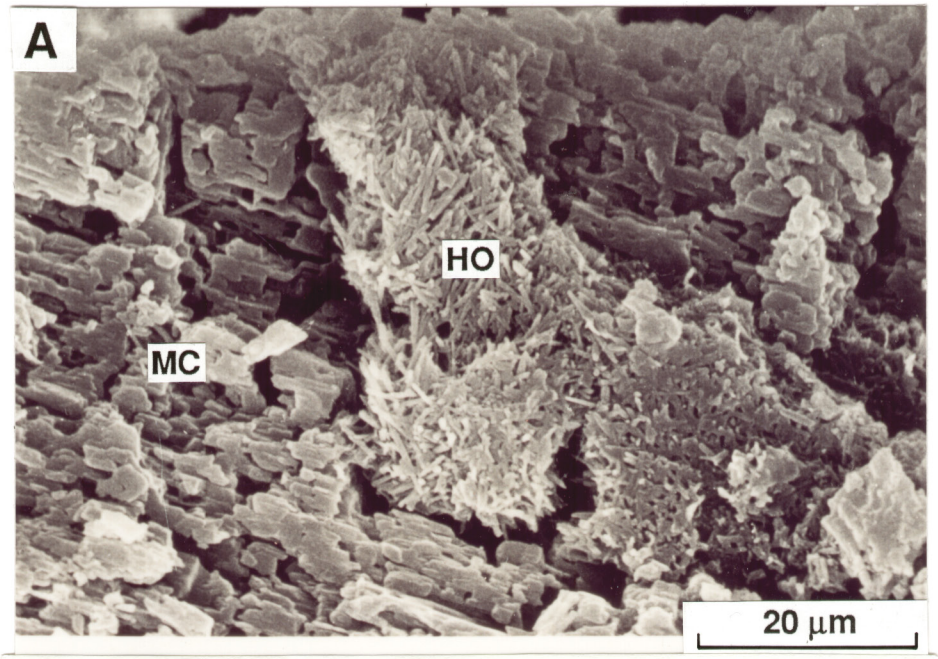
A
HO
MC
20 μm

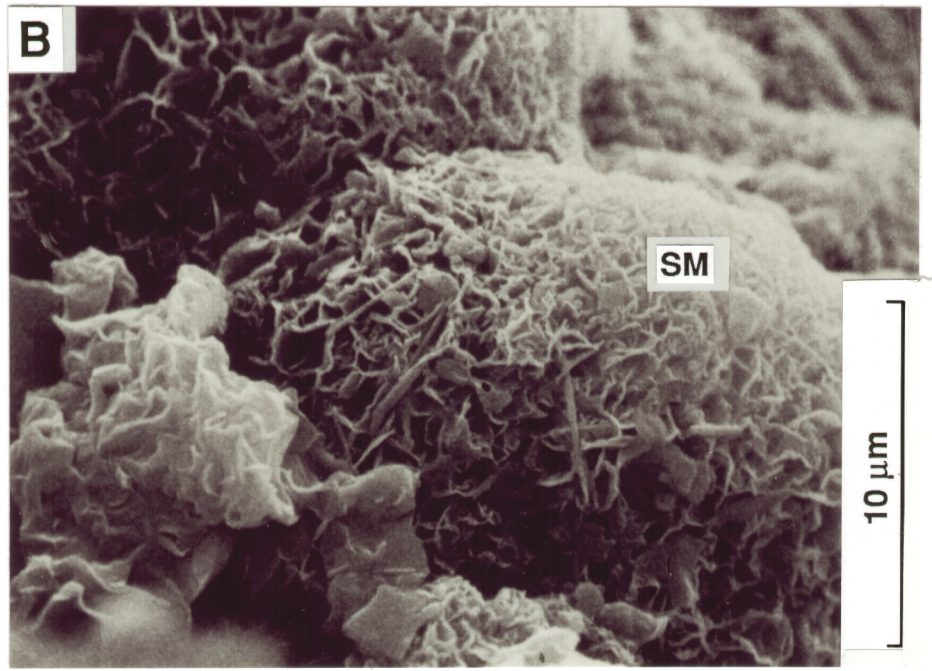
B
SM
10 μm

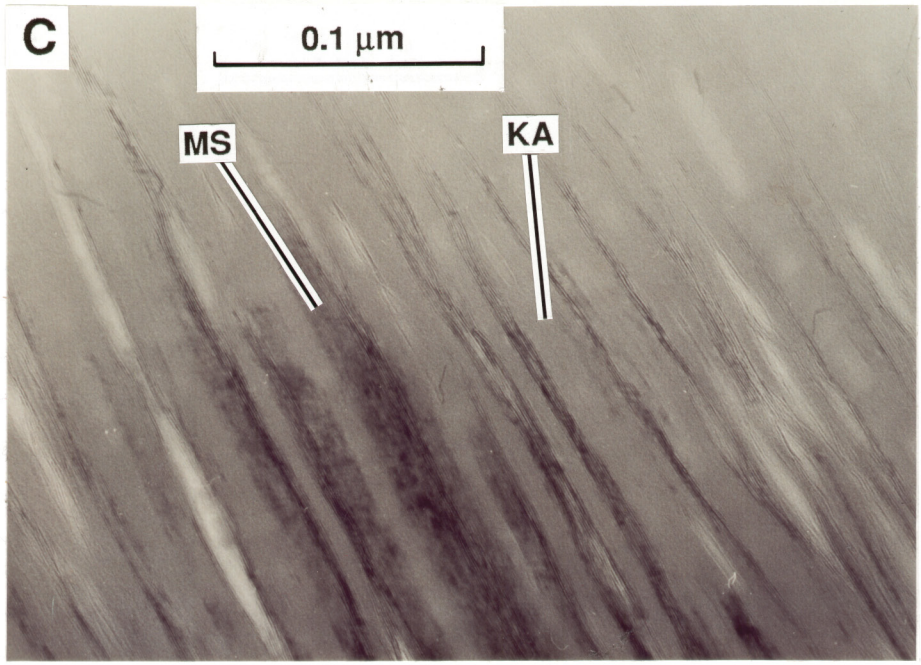
C
0.1 μm
MS
KA

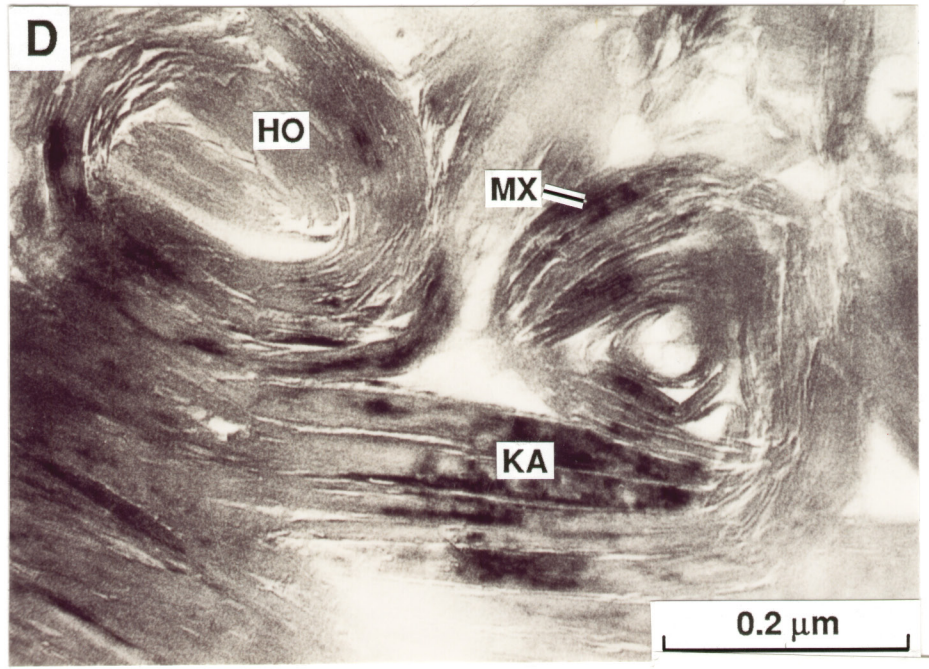
D
HO
MX
KA
0.2 μm

Carbonates. Primary carbonates (siderite, ankerite, dolomite and calcite) all weather at the base of the profile. If this occurs with sulphide oxidation, the breakdown of excess carbonates buffers the reaction, keeping the pH neutral. Calcium, Mg, Fe and traces of Mn, Sr and Ba are released on weathering of these carbonates. Iron and Ba tend to be retained as oxides and barite respectively, but most Mn and Sr are leached from the profile.

2.3 Secondary minerals

Although a few minerals remain unaffected or relatively so (such as quartz, chromite, rutile and zircon), weathering generally produces a range of completely new minerals. The most abundant are the clays (kaolinite, its hydrated equivalent, halloysite, and smectites) together with Fe oxides and oxyhydroxides (goethite, hematite and maghemite), several Mn oxides (commonly pyrolusite, cryptomelane and lithiophorite), cryptocrystalline or amorphous silica, and carbonates. A number of secondary carbonates and hydroxy-carbonates may be formed from Ca, Mg, Fe, Mn, Sr, Ba, Bi, Cu, Ce, La, Pb, U and Zn. Some secondary minerals can absorb, or incorporate into their lattices, significant quantities of trace elements released by weathering. Most important of these are the Fe oxides, which may concentrate Ag, As, Bi, Cr, Cu, Mn, Ni, Sb, Se, Ti and Zn; the Mn oxides adsorb Ag, Ba, Co, Cu, Ni, Pb, Sb, Li, W and Zn. The high sorption capacity is due to the very high surface areas; for example, goethite generally has a very small crystal size (~0.03 μm) and hence a very high surface area (~100 m^2/g). Smectites have a high ion exchange capacity and, apart from Si and Al, are able to incorporate significant amounts of Fe, Mg, Zn, Mn and Ni variously in octahedral and tetrahedral sites. The exchange cations are Ca, Na, K, Cs, Sr and Mg; the exchange capacity varies with the type of smectite and the physical conditions. Ions of a greater valency (e.g., Ca) are more readily retained. Kaolinite has only about 2% of the capacity of smectite to hold other ions.

2.4 Mineral stability

Mineral stability in the weathered profile is illustrated by using the Rand Pit (at Reedy; Robertson *et al.,* 1990) as an example, supported by evidence from other deposits.

Chlorite is an important component of many mafic and ultramafic rocks. It may be particularly abundant in the lower two thirds of the profile, where it can be closely associated with the cleavage. Further up the profile, but still within the saprolite, *smectite* progressively replaces chlorite. This is particularly marked where sulphides have oxidized, causing an acid environment that enhances the breakdown of chlorite, so promoting weathering. Higher in the saprolitic profile *kaolinite*, in turn, replaces smectite. Alternately chlorite may weather directly to kaolinite, without intermediate smectite, though smectite probably occurs as a transitory phase. Chlorite may host chromium and the resultant kaolinite is green.

Feldspar is an important primary mineral in mafic rocks (plagioclase) and in felsic porphyries, where it occurs as albite, microcline and microcline perthite. Plagioclase degrades readily to kaolinite deep in the saprolite but, although microcline survives higher in the profile, it also ultimately weathers to kaolinite.

Talc is a very resistant mineral and may survive to the upper saprolite or mottled zone, so that it is a useful indicator of ultramafic rocks. It weathers in part to kaolinite but, as it contains little Al, a source of soluble Al is needed before this reaction can occur. *Tremolite*, another indicator of ultramafic rocks, weathers readily and is completely dissolved near the base of the weathering profile.

Muscovite and fuchsite generally persists throughout weathering profiles (e.g., Mt. Percy and Beasley Creek). Flakes of muscovite, partly altered to hydromuscovite, may occur even in the

ferruginous components of the duricrust and overlying lag, where they are set in, and apparently protected by goethite. Muscovite may partially weather to kaolinite in or just below the lateritic cuirasse. Apart from being rock-forming minerals, micas (muscovite, paragonite or fuchsite) are important components of phyllic alteration haloes around mineralization and their survival has exploration implications.

Primary *carbonates* occur near the base of the profile where they may either form part of an alteration halo or be due to widespread greenstone carbonation. Because they weather and dissolve so readily, carbonates are absent from all but the top of the profile, where they reappear as secondary carbonates (calcrete and pedogenic soil carbonates). Likewise sulphur-bearing minerals such as *sulphides* are consumed at the base of the profile but sulphates (barite, gypsum and alunite) appear within the regolith. Deposition of secondary carbonates and sulphates, except for some barite, is not linked to a particular part of the lateritic profile and deposition appears to be a late event. Alunite has a greater depth range than gypsum, which tends to occur in the soil or shallow saprolite.

Kaolinite and *goethite* are the ultimate products of a number of primary minerals (sulphides, pyroxene, amphibole, feldspar, chlorite, talc and muscovite). They are stable throughout the weathered profile, though kaolinite may dissolve and reprecipitate in the plasmic zone, producing much of the observed fabric changes characteristic of this zone; Fe oxides cements are important in the mottled zone and duricrust. *Quartz* is also stable from fresh rock through the weathered profile, though quartz grains become progressively corroded and siliceous cements are important near the top of the profile in some rocks.

Some minerals, such as *chromite* and *zircon* are particularly stable and survive virtually unaltered to the top of the profile. However, etched zircons occur in silcretes in the arenose zone over granite; chromite weathers very slightly in the lateritic duricrust. *Rutile* is stable but other Ti-rich minerals such as *sphene, ilmenite* and *titanomagnetite* weather to *anatase*, which, in itself, is stable. Thus, Cr, Zr and Ti are among the most geochemically stable elements (see below) but their behaviour is very dependent on the minerals that contain them.

2.5 Trends in major element weathering

The alkalis and alkaline earth elements are removed during the earliest stages of weathering (saprock to saprolite), leaving major Si, Al, Fe and a trace of Ti. Thus, subsequent major element weathering trends are effectively displayed using the Si-Al-Fe ternary diagram (Figure 9). There are two major evolutionary trends, with minor variations depending on the rock type and the style of weathering.

Fresh rock to saprolite and plasmic clay: The first trend is away from the Si apex, approximately maintaining the Fe:Al ratio of the original rock, as all felsic or mafic minerals are weathered to kaolinite and/or smectite, releasing felsic and mafic mineral-associated silica to the groundwater. In quartz-deficient rocks of the poorly drained lower regolith of the central Yilgarn Block, this trend has a natural limit at a SiO_2/Al_2O_3 ratio of 54:46, equivalent to kaolinite; in quartz-bearing rocks the trend is shorter as crystalline quartz remains behind. Where the rainfall is greater, the regolith better-drained and the groundwaters deficient in Si, there is no such limitation as gibbsite can form instead of kaolinite; the Si content of mafic and felsic minerals is progressively lost, only crystalline quartz remaining (bauxitization).

Saprolite and plasmic clay to mottled zone and duricrust/silcrete: In rocks with a substantial mafic component, the second trend is towards the Fe Apex, either approximately maintaining the Si:Al ratio or parallel to the Si-Fe axis. This reflects Fe-oxide cementation with or without some loss of Si by dissolution of quartz. The resulting duricrusts have a fundamentally different major

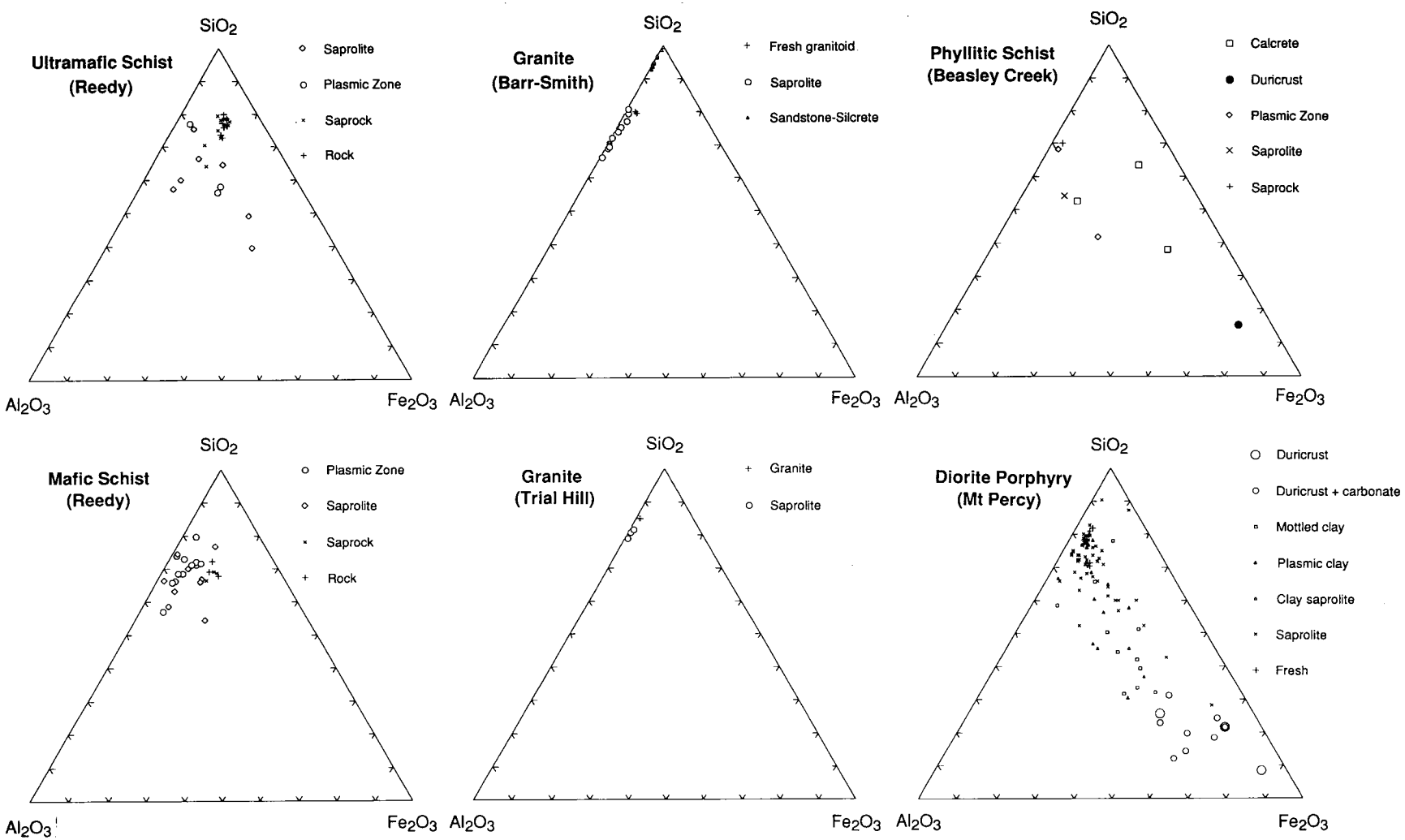

Figure 9. Ternary Si-Al-Fe diagrams comparing major element changes in granites, porphyries, phyllites, ultramafic and mafic rocks due to weathering.

element composition from their progenitors. Rocks with little mafic component (e.g., granite), the trend is back towards the Si apex, reflecting dissolution and loss of kaolinite, resulting in an arenose horizon or silcrete.

2.6 Weathering fabrics

Fabric changes in a weathering profile are only one of the consequences of the reactions between weathering minerals. Although some secondary minerals replace their precursors, pseudomorphing and, thus, preserving the fabric, others dissolve and reprecipitate elsewhere, causing the greatest fabric changes. Pseudomorphic replacements tend to dominate the lower part of the profile where original rock fabrics tend to be well-preserved, defining the saprock and saprolite. Pseudomorphic replacements of feldspar by kaolinite or gibbsite, and pyroxene or amphiboles by goethite, leave the original rock fabric perfectly preserved or even accentuated. Fabrics are best preserved where the sizes of the elements of the original fabric are significantly greater than the crystal sizes of the replacing minerals.

Above the pedoplasmation front, where pedogenic processes are dominant, mineral dissolution and distant precipitation are important and fabric changes become more marked. Such changes involve dissolution of clays, the formation of clay blasts, clay accordion structures and quartz segregation fabrics, the development of vesicular structures and channelways and the appearance of root casts, which become infilled with clays or fragments from higher levels in the regolith. Pedoplasmation tends to be incomplete and pockets of the original fabric may be found preserved very close to the surface. The importance of these processes increases into the mottled zone and lateritic residuum where segregation, concentration and cementation by Fe oxide minerals occur. The Fe oxides, chiefly goethite with some hematite and maghemite, replace and so preserve the plasmic and any surviving saprolitic or primary structures.

2.7 Optimal mapping conditions

Mapping a pit face dominated by weathered rocks is not easy. Initial mapping is started at the surface, where the rocks are most weathered (lateritic residuum or mottled zone), and recognition of the original rock types is particularly difficult. Single rock types are quite variable, even in the relatively fresh state, and this variability is increased by weathering. However, the conversion of most weatherable minerals to kaolinite in the plasmic zone makes very different rock types remarkably alike.

A freshly cut or dust covered pit face, seen in the stark noon light of summer will yield the least geological information. Strong sunlight, falling on the pit face at an acute angle, throws shadows which accentuate irregularities in the surface of the pit face. These are governed more by the means of excavation than by geology. Washing and etching by rainwater of the face of a pit greatly increases the observable structural, fabric and field relation detail. Although mapping of pits cannot be delayed, minor preparation of the pit face, by hosing down, and mapping the pit face while in shadow or when the day is overcast, will increase the yield of geological information.

3 GEOCHEMICAL DATABASE

3.1 Analysis

The objectives of compiling a geochemical database of weathered rocks are to illustrate variations in major, minor and trace element composition as weathering proceeds and to aid rock type discrimination, generally excluding elements associated with mineralisation. While it would assist to provide information on typical background elemental abundances; achieving this is difficult for pathfinder and target elements (e.g., Au, As, Sb, Cu, Pb, Zn, Cd, W) because much of the material collected for this study was from open cut mines. It is inevitable that some parts of their distributions will be anomalous.

The chemical compositions are tabulated with each profile study. A standard analytical package, shown below, has been used to provide as much consistency as possible.

A. Neutron activation analysis (INAA), 30 g aliquots except for some where 10 g used (Becquerel Laboratories Pty. Ltd.): As, Au, Ce, Co, Cr, La, Mo, Sb, W.

B. X-Ray fluorescence (XRF) on pressed powders, using a Philips PW1220C by the methods of Norrish and Chappell (1977) and Hart (1989), with Fe determined for matrix correction (CSIRO): Ba, Ce, Cu, Ga, Ge, Mn, Nb, Ni, Pb, Rb, Sr, V, Y, Zn, Zr.

C. X-Ray fluorescence (XRF) of fused discs (0.7 g sample and 6.4 g Li borate) using a Philips PW1480 instrument by the method of Norrish and Hutton (1969) (CSIRO): Si, Al, Fe, Mg, Ca, Na, K, Ti, P.

D. Inductively coupled plasma emission spectrometry (ICP-ES) on a Hilger E-1000 following fusion of 0.25 g samples with Li metaborate and solution in dilute HNO_3 (CSIRO): Si, Al, Fe, Mg, Ca, Ti, Be.

E. Inductively-coupled plasma mass spectrometry (ICP-MS), following digestion with hot HCl, HF and $HClO_4$ and solution in HCl (Analabs): Ag, Cd, In, Sn, Bi.

3.2 Selection of database for discriminant analysis

A wide range of igneous lithologies has been included (Table 2) from all regolith horizons (unweathered through to duricrust where available). To these were added some less typical rocks (fuchsite-altered ultramafic rocks from Mt. Percy; quartz-rich mafic and ultramafic schists from Reedy; xenolith-contaminated porphyries from Mt. Percy). Metasediments were not included as most immature clastics of the Archaean tend to reflect their provenance materials and any subsequent diagenetic alteration. The sizes of each segment of the data base and the sources are given in Table 2.

TABLE 2 GEOCHEMICAL DATA BASE

Rock Type	Location	Number of Samples	Source
Fuchsite Ultramafic	Mt. Percy	302	Report 156R
Ultramafic rocks	Mt. Percy	155	Report 156R
Pyroxenite	Ora Banda	11	Unpublished
Ultramafic Schist	Reedy	31	Report 102R
Amphibolite	Lights of Israel	123	Report 393R
Mafic Schist	Reedy	27	Report 102R
Porphyry	Reedy	7	Report 102R
Porphyry	Mt. Percy	111	Report 156R
Granite	Barr-Smith Range	30	This volume

Most of the data are from samples collected within or close to mineralization. Hence, it was necessary to ignore target and pathfinder elements in the database as they are likely to be atypical, may vary with proximity to mineralisation and may be independent of rock type. On this basis Ag, Au, As, Sb, Bi, Pb, Zn, Cd, W, Se, Ge, Mo and W were eliminated for rock type discrimination. Some elements were excluded as their concentrations were too close to detection (Be, Nb, Sn) and others were eliminated due to incomplete data (B, Br, Cs, Eu, Hf, In, Ir, Li, Lu, Sc, Sm, Ta, Te, Th, Tl, U, Yb) and yet others as their concentrations are too widely varied by weathering processes (Ca, Mg, Sr, Na, K). Many of these were excluded due to combinations of these reasons. Sixteen elements were chosen (Si, Fe, Al, Ti, Ba, Ce, Co, Cr, Ga, La, Mn, Ni, Rb, V, Y and Zr) to be assessed with multivariate discriminant analysis.

4 ROCK TYPE DISCRIMINATION

There are several means of discriminating rock types in the weathered profile, including colour, fabric, mineralogy and geochemistry. Geochemical changes that take place in a rock are complex, but geochemistry probably shows the most promise of all, particularly if a suite of elements is considered and processed as a multivariate data set. Ore-related elements should be excluded since these tend to confuse the rock type discrimination. It is best to interpret a combination of fabric, geochemistry, colour and mineralogy which, with experience, gives the best possible discrimination.

4.1 Colour

Colour variations are impressive in weathered rocks but are rarely diagnostic of either lithology or weathering horizon. They are also very dependent on the ambient light conditions at the time, on experience and colour perception. The colours white (kaolinite, talc), red, yellow (Fe oxides), green (smectite, Cr, Ni or Fe^{2+}), and confusing mixtures of these, result in inaccuracy and personal bias. Classification of colours using the Munsell system can be used to standardize terminology, but it cannot be used satisfactorily by those with defective colour vision. Spectrometry in the visible to short-wave infrared is perhaps more precise and can distinguish some minerals. Colour is generally leached, together with the transition elements that produce it, in the so-called 'pallid zone'.

4.2 Fabric

Fabric is very useful in fresh rock, saprock and much of the saprolite for identifying lithologies but its value is greatly diminished where the weathered rock has been largely pulverized by drilling. Above the pedoplasmation front, fabrics are altered by pedogenic processes. However, relict fabrics survive in places, because the processes are incomplete, or the fabrics have been protected from pedogenic action by extensive ferruginization. Interpretation of weathered rock fabrics takes time and requires experience.

4.3 Mineralogy

Where weathering has been intense, kaolinite and Fe oxides are commonly the end products of weathering of mafic and felsic rocks. Relict talc and muscovite help to identify ultramafic rocks, argillaceous metasediments or alteration zones but, where they are fine grained, separating them from kaolinite can be extremely difficult. X-ray diffraction or infra-red spectrometry are the only certain means.

Micas occur as part of the halo around mineralization, where they persist throughout most of the saprolite and mottled zone, being significantly weathered only in the duricrust. Remnants of micas have been found preserved in ferruginous nodules in the saprolite and at the surface in lag but this preservation is generally accompanied by partial loss of contained alkalis. Although muscovite occurs within both barren and mineralized weathered shales, the sodic mica, paragonite, seems much less abundant in mineralized shale profiles. Paragonite is probably a negative indicator of mineralization.

Carbonates are also associated with alteration zones around mineralization and may be significant deep in the profile but these carbonates are readily destroyed near oxidizing sulphides. Pedogenic carbonates and calcretes occur near the surface and are related not to mineralization but to Ca-rich, and, some Mg-rich rocks, and specific parts of the landscape. However, the occurrence of carbonate near the surface has an additional exploration significance as a sampling medium for Au.

Concentrations of S over ore have been noted in some soils and in the saprolite overlying sulphidic orebodies, where it occurs as gypsum and minor barite and as alunite in the mid to upper saprolite. Alunite-jarosite minerals are formed in some gossans. Sulphur is a labile component and most has been introduced into the landscape as aeolian gypsum; there are, in some locations, close spatial relationships to underlying weathered sulphides that require further field and isotopic investigation.

Microprobe analysis of the Cr contents of rutile, mica, chlorite and, where present, spinel may be used to indicate original ultramafic, mafic or felsic bedrocks. Proximity to mineralization may be indicated by a decrease in Fe content in tourmaline and mica, and a decreased Na content in the mica.

4.4 Geochemistry

During the course of the geochemical investigation, a number of elements emerged as rock-type identifiers. These may be used singly, in pairs, in threes and in n-dimensional space by multivariate (e.g., discriminant) analysis. As the number of elements used increases so too, to a limiting degree, does the reliability of discrimination.

4.4.1 Univariate and bivariate analysis

Elements such as Cr are enriched in ultramafic rocks, but Mg, Co and Ni are less effective because they are leached (or even enriched) in the upper parts of the profile. Some ultramafic rocks have high concentrations of Cr, V and Sc. Felsic rocks are rich in Al, Ga and Zr, but metasedimentary rocks vary considerably in their compositions due to their differing provenances. Thus, single elements show considerable overlap, may have only local application and their use may be severely limited to particular parts of the weathered profile.

Bivariate plots (element pairs) are slightly more successful. The most useful is Ti-Zr (or Ti-Hf) which is discussed in detail below. Some argillaceous metasedimentary rocks may be distinguished from mafic-ultramafic and felsic metavolcanic rocks by their Al-Ga relationships, though this separation is not distinct near the top of the profile. Some success was obtained with Rb-Nb, Rb-Sc and Rb-Li plots to separate the mafic-ultramafic suite from the metasedimentary and felsic suites. Partial discrimination was achieved between unweathered ultramafic variants (talcose, chloritic, biotitic and fuchsitic) using plots of Ba, Zr and K.

Ti, Zr and Cr: Titanium, Zr and Cr are considered to be among the most stable in the weathered environment (Hallberg, 1984) but their effectiveness as discriminators of lithology depends on the stability of their host minerals. Zirconium is largely held in zircon, which is generally quite stable. The presence of leached, skeletal zircons and, conversely, reports of the presence of overgrowths on zircon, indicate that even Zr can become mobile under certain circumstances. Titanium is held in rutile, ilmenite and sphene and, when the latter two are weathered, their weathering products are stable Ti oxides (anatase) and rutile. However, silicates, notably amphiboles and chlorite, also contain significant quantities of Ti and these are highly weatherable. If Cr is held in chromite it is relatively stable, but if it occurs in silicates such as pyroxene, chlorite or amphibole, it is readily released by weathering.

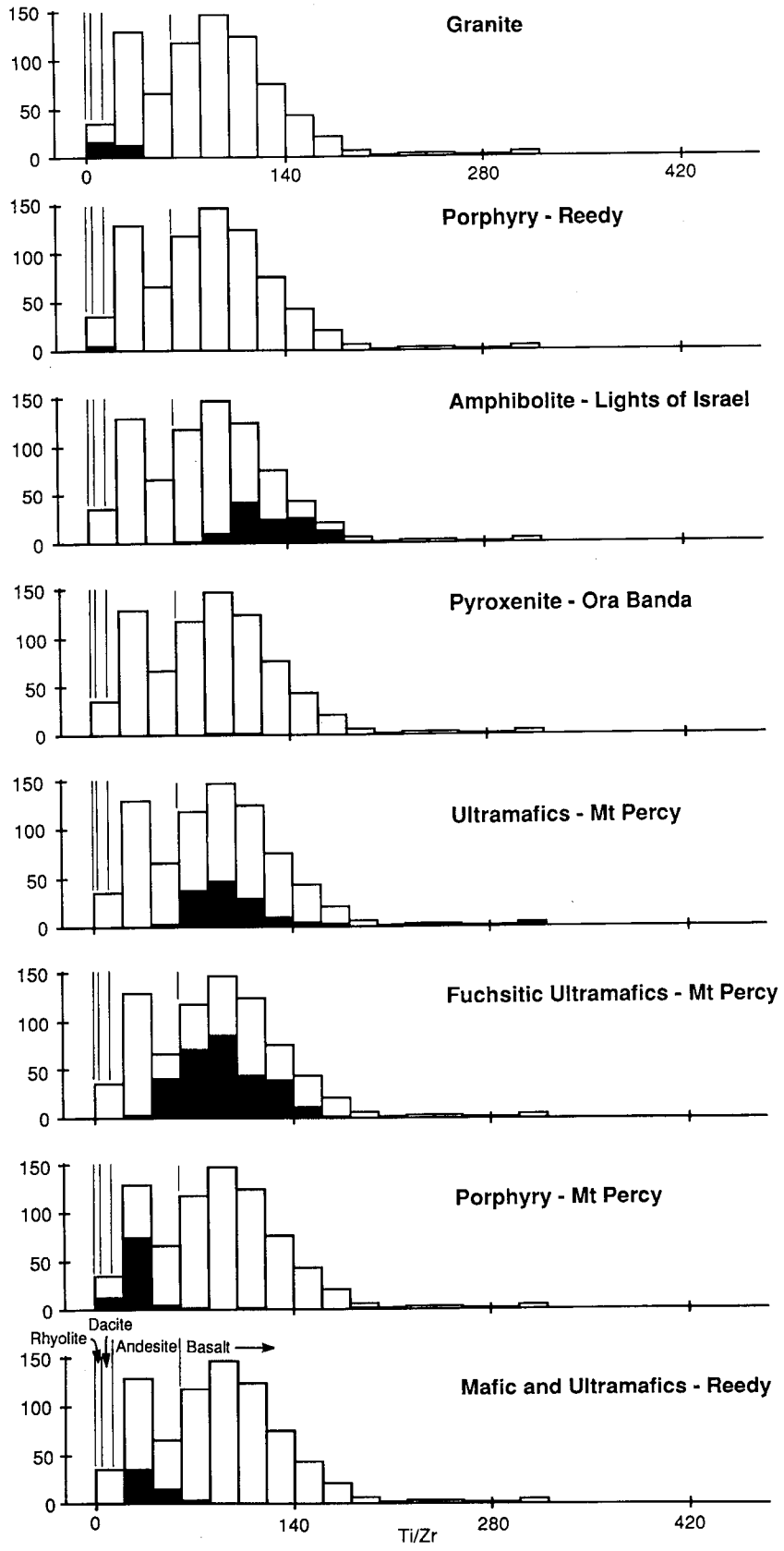

Figure 10. Histograms of Ti/Zr ratios for rock groups of database. Whole data set - open. Specific lithology - solid.

Hallberg (1984) showed that the major groups of igneous rocks could be distinguished, even in the weathered state, by the Ti/Zr ratio. Basalt has a Ti/Zr ratio of greater than 60, andesite ranges from 60-12, dacite from 12-4 and rhyolite is generally less than 4. Inevitably, the fields show some overlap. The ultramafic rocks have a similar Ti/Zr ratio to basaltic rocks, but are richer in Cr. This method of distinction also works well for moderate weathering in the saprolite and the clay zone. However, if the saprolites and plasmic zone are considered separately from the surficial materials (mottled zone and duricrust), some of the latter near-surface material has an abnormally low Ti/Zr ratio. Thus, this method has limited application in the mottled zone and in the duricrust where Ti is only partly stable. Most ultramafic and mafic rocks are indistinguishable on their Ti/Zr ratios, but the higher Cr contents of ultramafic rocks are commonly diagnostic. In some duricrusts on ultramafic rocks at Mt. Percy, Cr-rich chlorite and kaolinite has been replaced by Fe oxides and some of the Cr has been leached. This duricrust is also contaminated by Zr, Ti and other elements from adjacent porphyries so that it has a quite anomalous composition (Butt, 1991).

The major rock groups of the database may be distinguished using the Ti/Zr ratio and Cr. As expected, the granite and the porphyry from Reedy have low Ti/Zr ratios, typical of felsic rocks; the amphibolites from Lights of Israel and the pyroxenites from Ora Banda have high Ti/Zr ratios typical of mafic-ultramafic rocks (Figure 10). The majority of the ultramafic material from Mt Percy are also classified as mafic-ultramafic but the fuchsitic rocks have a much wider range than their unaltered counterparts and spread into the upper part of the 'andesite' range, which is clearly an incorrect classification. Similarly, the xenolith-rich porphyries from Mt. Percy are not classified as felsic rocks and the mafic-ultramafic, Cr- and tremolite-rich schists from Reedy fall in the 'andesite' range. The mafic-ultramafic schists from Reedy, classified by the method of Jensen (1976) as komatiites to basaltic komatiites, are unusually Zr-rich and form a radial trend on the Ti-Zr diagram (Figure 11). The amphibolites from Lights of Israel show the normal radial basaltic trend.

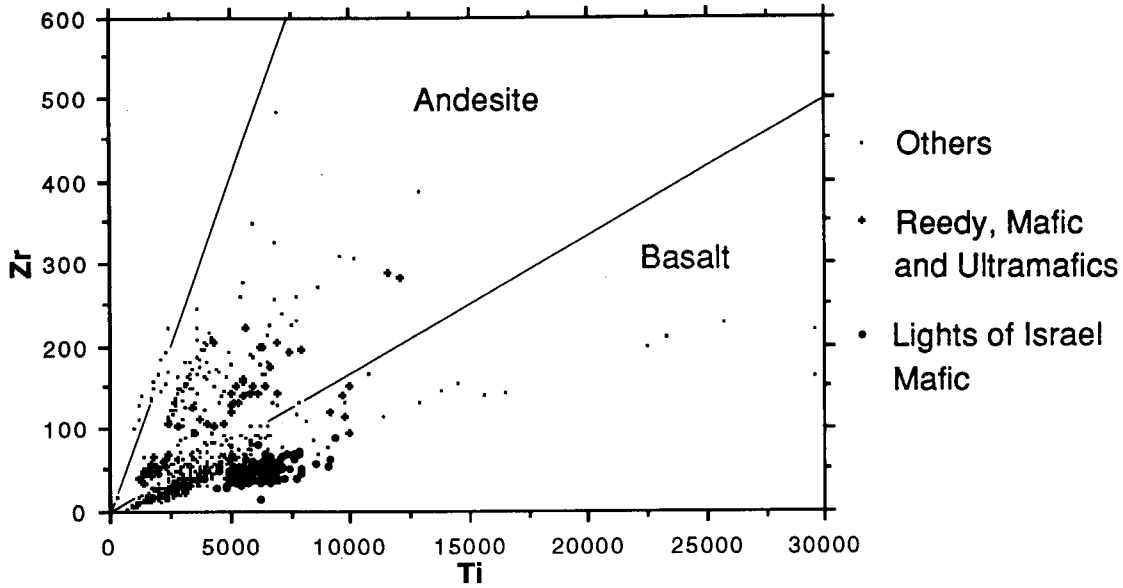

Figure 11. Ti-Zr 'Hallberg' plot of database comparing basaltic trend of amphibolites from Lights of Israel and 'andesitic' trend of rocks from Reedy.

Plots of Ti/Zr-Cr have been used to investigate the porphyry from Mt. Percy. Two trends are shown; a major trend towards increasing Cr at a relatively low Ti/Zr ratio and a minor spread of Ti/Zr ratios at a low Cr content (Figure 13). There are similar trends on the Ti/Zr-Cr plot of the ultramafic schists that contain these porphyries (Figure 13), suggesting two types of material, a

Ti-rich, Cr-poor and a Ti-poor, Cr-rich type within this population. This clearly illustrates the contamination of the porphyries by the ultramafic schists, confirmed petrographically by numerous xenoliths.

Simple univariate and bivariate analyses are clearly insufficient to classify these complex rocks and their weathered equivalents reliably. Therefore, it was necessary to use a greater range of elements and assess them simultaneously.

4.4.2 Multi-element discriminant analysis

This technique attempts to maximize the differences between pre-determined groups. It is essential to supply well-controlled data to define these groups geochemically as training sets. It is limited by a number of assumptions that may be met only in part by geochemical data. It is assumed that the data have a normal distribution, but this is seldom true, so that log or power transformations may have to be applied. The data should have no extreme values, which, again, is seldom the case. The data should not sum to a constant value, consequently major elements should be excluded and only minor and trace elements used. The number of samples in each training set should exceed the number of elements by a factor of at least three and preferably by ten. Although this is a complex technique, it is a powerful discrimination tool but the results must be be used and interpreted with care.

The elements that provide the best rock type discrimination are, virtually by definition, not pathfinder or target elements, because these are far more dependent on mineralisation than on lithology. Thus, the important discriminating elements will be those that are less commonly determined by exploration geochemists and geologists; mainly lithophile elements present in low abundance.

Multivariate analysis of the database was accomplished in steps, largely using Sun-resident software written by CSIRO Division of Mathematics and Statistics (Campbell, 1980; 1982; 1986).

Data normalization: Data from each element of each rock group were investigated separately, using both an interactive, graphical Q-Q plot program and an iterative computational technique (Box and Cox, 1964). A series of power transforms were applied until the data distributions were as near normal as possible. A separate, 'averaged' value for λ was selected to transform each variable of the pooled groups during all subsequent phases of data analysis (see Grunsky, 1991). Data censorship by the detection limits was considered in the calculations.

Statistics and canonical variate analysis: Robust estimations of means, standard deviations and correlations were followed by robust canonical variate analysis. The results of this canonical variate analysis of nine reference groups are eight canonical variates, of which the first five (CV1-5) contain most of the useful information. The extreme end members, granite and pyroxenite are very well separated on the CV1-CV2 plot (Figure 12), as are the mafic amphibolites from Lights of Israel, which form a close group. As expected, the granitic porphyries from Reedy fall within the edge of the granite field. The orthogonal trend of some granite members reflect a high variance due to extreme weathering (arenose zone). The ultramafic rocks from Mt. Percy are extensively overplotted by their fuchsite-altered variants. All the well-contrasted types are quite distinct. The more difficult lithologies are not so distinct; the xenolith-contaminated porphyries from Mt. Percy form a trend between felsic rocks and the ultramafic rocks, with which they are contaminated. The quartz- and Zr-rich mafic schists from Reedy fall between the felsic rocks and the mafic amphibolites from Lights of Israel. Their ultramafic equivalents form a trend between them and the ultramafic rocks of Mt. Percy. Thus, if these difficult rocks are removed, the distinction would be good; the positions of these difficult rocks on the CV1-CV2 plot closely reflect their affinities.

Figure 12. CV1 - CV2 plot of all rock types in discriminant analysis. Although there is good separation of the more extreme rock groups, there is considerable convergence of the ultramafics from Mt. Percy and their fuchsite-altered counterparts. This is largely resolved by CV3.

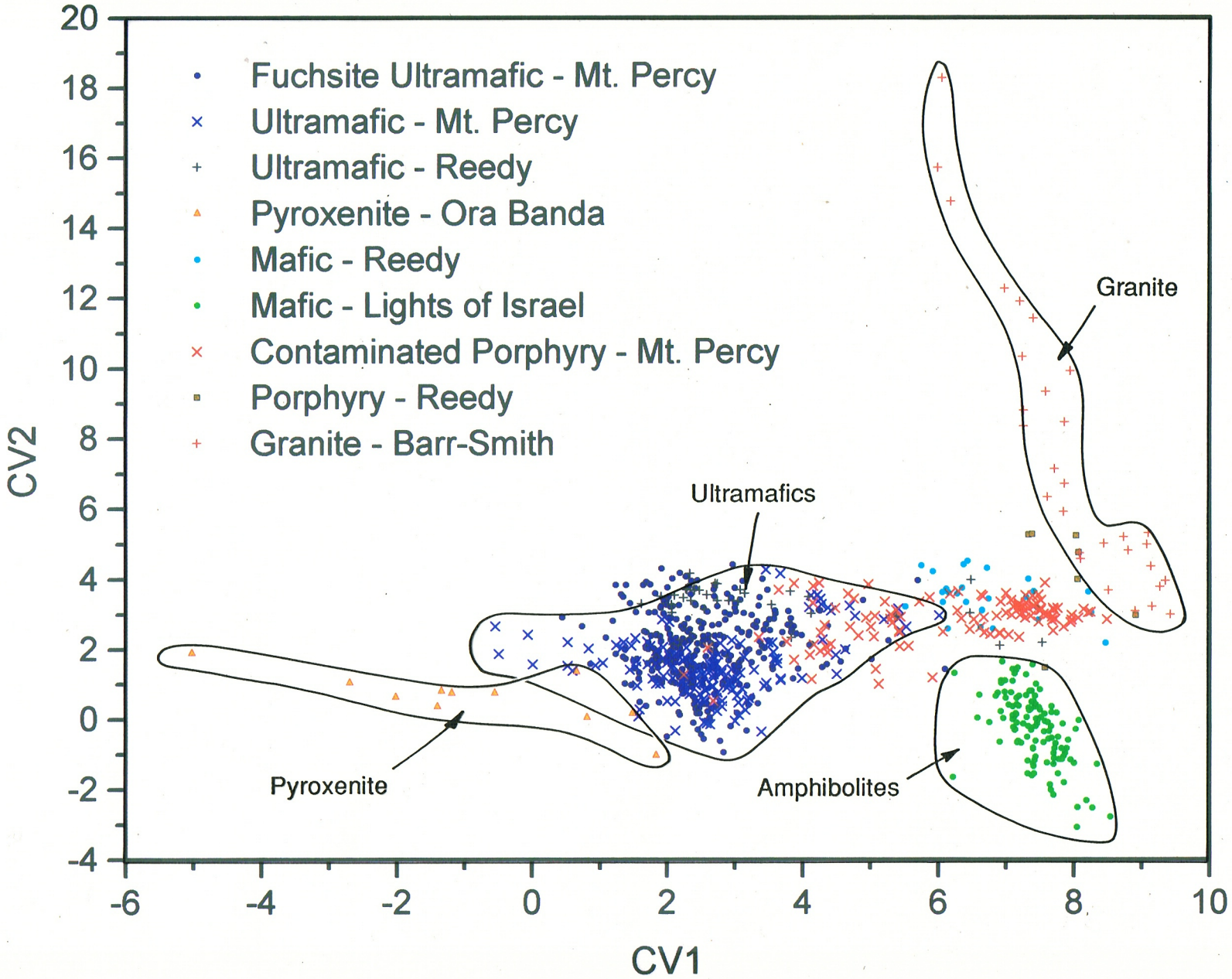

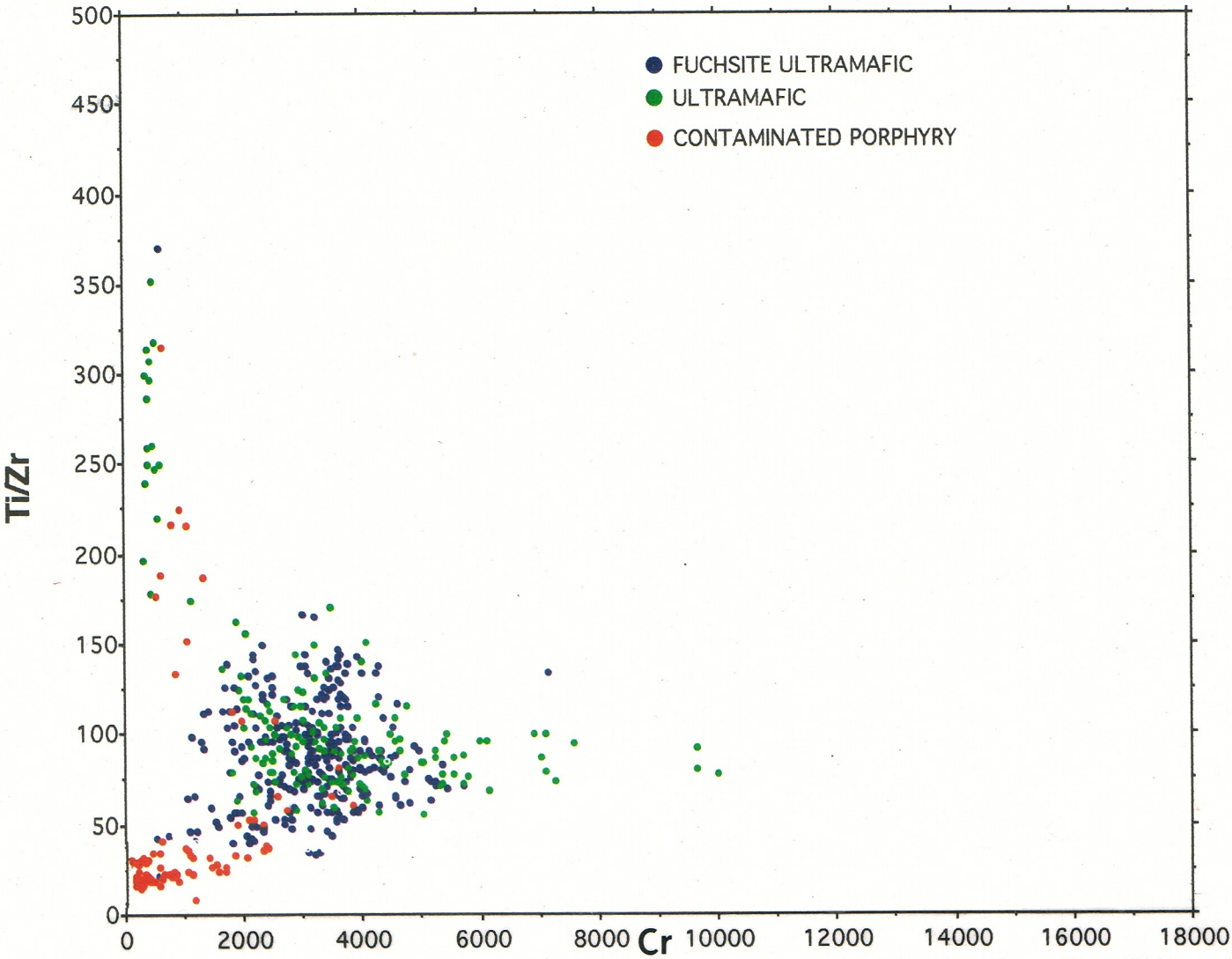

Figure 13. Ti/Zr - Cr plot of contaminated porphyry and their contaminating ultramafic schists.

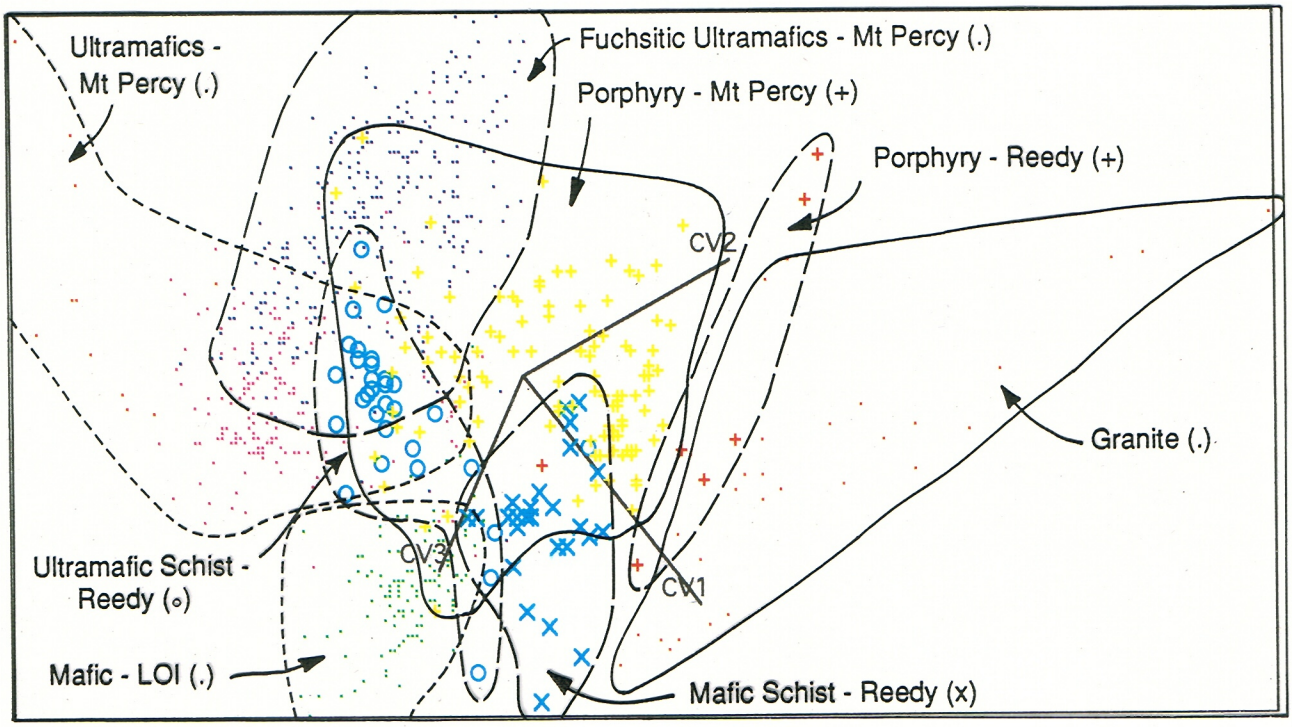

Figure 14. CV1 - CV2 - CV3 plot rotated to achieve maximum separation of all groups.

Although they extensively overplot on the CV1-CV2 diagram, the fuchsitic and the chloritic ultramafic rocks from Mt. Percy are largely separated by CV3. Similarly, overplotting of the Mt. Percy contaminated porphyries on the mafic schists from Reedy on the CV1-CV2 diagram can be separated by CV3. A three dimensional plot of CV1-CV2-CV3 may be rotated to maximize this separation (Figure 14). Thus, though most of the separation is achieved with the first two canonical variates, the others should not be ignored. The rotated three dimensional plot of Figure 14 is about as far as any graphical representation may be taken. Statistical analysis is not limited by three dimensions; each case (geological sample) may be assessed on the basis of its probability of belonging to one or more groups in terms of its group membership and typicality.

Group membership and typicality: Group membership and typicality probabilities for individual samples were calculated and assessed using the 95% confidence level for the typicality. Assessment of the results (Appendix 1;) showed (Table 3) that most rock types could be distinguished with 71-95% accuracy, the exceptions being the pyroxenite (36%; a small data set) and the granite (23%; ideally the granites should have been broken into two contrasting data sets, saprolite and arenose zone). There were, inevitably, a number of cases that could not be classified; even though their membership probabilities indicated a particular group (almost always the correct *a priori* group), their typicalities were below the set confidence limit. The proportion of unclassified cases was high for the pyroxenite and granite because of their high variances; in each *there were no misclassified cases.* This is a far more statistically rigorous procedure than plotting the first two canonical variates but, as probabilities are used, data normalization is essential; it is also more effective as it makes use of the full dimensionality of the analysis. Having completed this type of analysis with a known training set, a group of unknowns may be appended and these identified in a similar manner.

TABLE 3 ACCURACY OF CLASSIFICATION OF DATABASE

A priori	*A posteriori*									
	FUUMaf MtPercy	UMafic MtPercy	UMafic Reedy	Pxenite O Banda	Mafic Reedy	Mafic L.O.I.	Porph MtPercy	Porph Reedy	Granite Barr-Sm	Un-class'd
Fuchsite UMafic	76.74	12.29	0.33	0.00	0.00	0.00	2.65	0.00	0.00	8.31
UMafic MtPercy	0.65	76.77	0.65	0.00	0.65	0.00	0.00	0.00	0.00	13.55
UMafic Reedy	3.23	3.23	77.42	0.00	12.90	0.00	3.23	0.00	0.00	0.00
Pxenite O Banda	0.00	0.00	0.00	36.36	0.00	0.00	0.00	0.00	0.00	63.64
Mafic Reedy	0.00	0.00	7.41	0.00	81.48	0.00	3.70	0.00	0.00	7.41
Mafic L.O.I.	0.00	0.00	0.00	0.00	0.00	95.12	0.00	0.00	0.00	4.88
Porph MtPercy	5.41	5.41	0.90	0.00	0.90	0.00	71.17	0.00	0.00	16.22
Porph Reedy	0.00	0.00	0.00	0.00	0.00	14.29	0.00	71.43	0.00	14.29
Granite Barr-Sm	0.00	0.00	0.00	0.00	0.00	0.00	0.00	0.00	23.33	76.67

Classifying Elements: Those elements which contribute most to the classification are shown in Figure 15. These are, in very nearly equal proportions, Ni>Cr>Co>Rb>Zr>Ti, with a slightly lesser contribution from Ba>Y>Al>Mn etc. The element suite, defined by this technique, has chosen elements that have already been shown to be useful for classification on a univariate and bivariate basis which, when combined, are even more effective. This has not been an easy classification, requiring numerous elements - at least six - to accomplish an imperfect result. These classifying elements are those pertinent to the classification of the whole data set; their order would be modified if subsets of the data (e.g., Mt Percy chloritic and fuchsitic ultramafic rocks) were considered alone and the classification may well be more efficient.

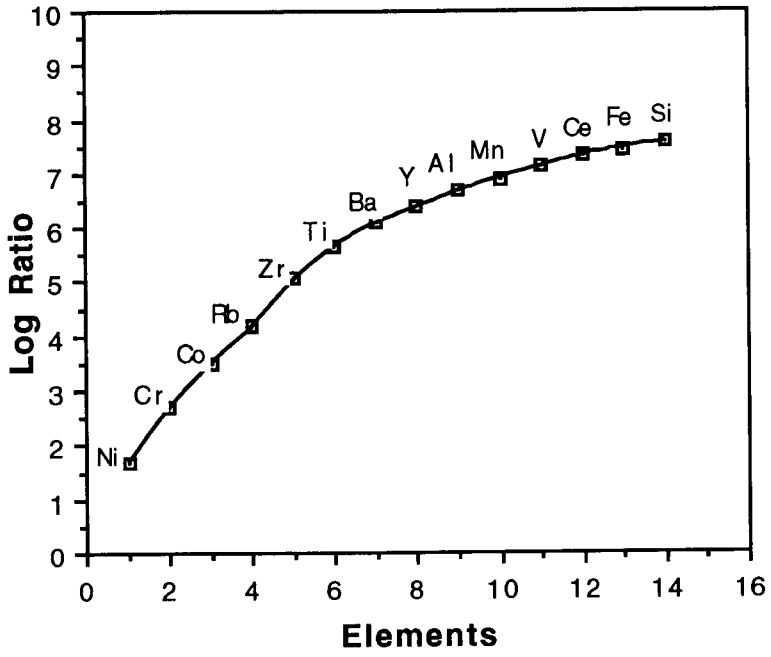

Figure 15. Element contributions to discriminant analysis.

5 ATLAS OF WEATHERED ROCK FABRICS

The objectives of a petrographic study of weathered rocks is to trace the mineralogical and fabric changes that occur in each rock type with progressive weathering up the profile and to relate this to what the field geologist can see using a hand-lens or binocular stereo-microscope. Fabrics seen with the petrographic microscope are shown together with and beside equivalent close-up photographs of the sawn surfaces of the blocks used for making thin sections. Some have been lightly varnished to simulate a 'wet' or 'damp' surface. This is to enhance the meaning of the petrography to the field geologist. Each rock type has been described in detail and, in some cases several occurrences of a rock type. With this are included tabulated bulk XRD data (if available) and bulk major, minor and trace element geochemistry as well as details of specific gravity (if available).

The whole is presented in loose-leaf format, so that additional information may be added as it comes available. The various horizons of the regolith are described from the least weathered to the most weathered, so that the changes due to weathering can be best understood. The photographs of some of the larger figures have been arranged with the most weathered at the top, as they would appear in a profile. In some, two plates were necessary to show the variety of fabrics; the least weathered are on the first plate. All figure and page numbers in the Atlas are preceded by the rock type identifier (e.g., G1 = Granite No 1) so that this section can be expanded conveniently.

Metamorphic Grade	:	Greenschist Facies (Qtz-Ab-Ep-Alm subfacies)
Structural Attributes	:	Schistose
Gross Features	:	At least two mineralized horizons
Profile Truncation	:	Truncation at base of duricrust
Depth to Fresh Rock	:	Unknown
Location	:	Beasley Ck, Laverton, Western Australia
Reference	:	Robertson, and Gall, 1988; Robertson, 1989; Robertson, 1991

Geomorphology and regolith

Although the geomorphology of the Beasley Creek Mine Site is similar to that of regoliths elsewhere in the north-east Goldfields, in which hardpan is abundant, its landscape gives a first, though erroneous impression of simplicity. It is situated on a small rise 3.5 m high, surrounded by wash plains, which form a low tabular divide between broad drainages to the north and south. The rise is asymmetric, with a very gentle western slope, marked by calcrete and small, sparse, saprolite outcrops, a crest with scattered ironstone outcrops and subcrop of phyllitic saprolite and a steeper eastern slope, protected by lateritic duricrust. This steeper slope appears to be maintained by more active erosion at the foot of the rise. The crest of the rise is protected by calcrete and surficial ironstone.

The whole area is mantled by red, friable sandy-clay soil and strewn with multi-component lag. The soils on the low-lying areas are deeper (0.3 - 0.45 m) than on the rise (0.1 - 0.2 m), are relatively acidic (pH 5.0 - 5.5) and are underlain by Wiluna hardpan, but become alkaline and thin on the rise where they are underlain by saprolite and calcrete. Ironstone lag and a duricrust-related khaki lag show only slight dispersion from their sources. A coarse, black, ferruginous lag has a wider distribution but seems associated with the subcrop of the carbonaceous phyllite ore host. A finer, brown, ferruginous lag has a wider distribution and its finest fractions seem to have been separated by down-slope colluvial sedimentation. Quartz lag is dispersed around small quartz veins unrelated to ore.

That the regolith at Beasley Creek has been partly stripped is indicated by the absence of a lateritic duricrust over all but the eastern flank of the rise. Saprolitic Permian sediments overlap only the eastern margin of the mine site. The ferruginous lateritic duricrust closely follows the upper surface of the phyllitic host rock. Ironstones overlie both the host rock and meta-dolerites.

Regolith profile

The petrographic study was made difficult by intense mineralization-related alteration, weathering and ferruginization. Drillhole (BCD1) passes across the stratigraphy from the hangingwall of the phyllite, at the top of the profile, where it is effectively in duricrust, to the footwall at a depth of 41.9 m, in saprolite; a small repeat (0.6 m) occurs at 60 m (Figure Ar1-1). Thus the material is not all directly comparable.

The phyllites are quite variable in composition as they constitute much of the ore zone and have been extensively altered by mineralisation, weathering and associated Fe-oxide deposition. The phyllite is pale yellowish green to yellowish brown, fibrous, slightly mottled and friable, with a weak foliation that has been largely re-cemented by clay minerals and Fe-oxides. Where quartz is seen, it is shard-like or occurs as lenses marking a silicified cleavage. Apart from quartz, the rock consists of kaolinite, sericite and an intimately mixed kaolinite-sericite phase. These phyllosilicates are stained and penetrated to a varying extent by fine-grained goethite. Garnet

pseudomorphs occur in the phyllosilicate groundmass, veined with goethite. All of the garnet has been subsequently dissolved away, leaving an open pseudomorphic boxwork of goethite veinlets (with the form of a garnet). Where Fe-oxide deposition is more prevalent, the phyllites are dark brown, dense and their foliation is extensively cemented by iron oxides. Although they still contain kaolinite, sericite and the common kaolinite-sericite mixture in parts, where goethite is concentrated, only relict books of sericite are preserved in some of the goethite patches.

Iron-rich rocks are dominant near the top of the drillhole (Figure Ar1-1), where they constitute a duricrust. Where goethite is abundant, it forms spongy masses and the foliation of the rock is progressively destroyed. Sericite relics are common in the massive goethite. Some of these goethite-rich rocks are vesicular and colloform structures have developed in the goethite, close to the surface, which show rims of fibrous goethite and an outer layer of Al-poor goethite or hematite with dehydration fractures.

Calcite cementation has occurred in some near-surface samples (7 and 1 m depth), where they have formed Fe-oxide- and carbonate-rich breccias in which cellular goethite and phyllosilicate rock fragments are set in a carbonate matrix. Later leaching has removed much of this carbonate cement, leaving a carbonate coating on the breccia fragments. The carbonate has, in places, formed ellipsoidal granules. Examination of these by SEM shows worm-like carbonate excrescences attached to their surfaces. The quartz is generally angular though some grains show re-entrant boundaries, indicating corrosion.

Saprock

The small intercalation of phyllite, which lies in the footwall at a depth of 60.5 m, consists of pale yellow to white, fibrous micas and quartz. Etching and pale yellow Fe oxide staining is evident along the cleavage planes. It consists of two lensoid phases. (i) Shard-like quartz , which is quite porous, containing abundant voids, is cut by small veinlets of chlorite and, in places, is stained by powdery goethite. (ii) A very fine grained, matted, intimate mixture of kaolinite and sericite (Figure AR1-2A, B), which results in a mixed mineral with a yellowish birefringence and has been stained, to a varying extent, by secondary iron oxides, mainly goethite. The quartz and clay-mica layers are generally quite distinct but in places are mixed, indicating a possibly graded argillaceous-psammitic sediment. XRD examination indicates additional traces of amphibole and talc. The rock has a Ti/Zr ratio and Cr, V, Ce, Y and Rb geochemistry typical of basaltic rocks, so it was probably an inter-flow argillaceous sediment, derived from local basaltic detritus.

Saprolite

At a depth of 42 m, the weathered phyllite is a stained, lightly mottled, pale, yellowish-brown, friable rock with very few small [1-2 mm] nodules of Fe-oxides and a weak foliation. Widely dispersed sericite gives it a slight sheen. The mottling is caused by patches of white kaolinite and pale yellow sericite (Figure Ar1-2C).

The rock consists of a mat of sericite, intimately mixed kaolinite-sericite, showing white birefringence, very fine-grained, low birefringent kaolinite and some quartz. This mat is, in places, broken into patches (Figure Ar1-2D) which are separated by powdery goethite and secondary kaolinite. XRD examination also shows a trace of talc. The kaolinite-sericite mat is set with brown, intensively veined, goethite pseudomorphs (Figure Ar1-2C) after garnet [1-3 mm]; very narrow goethite veins follow the fractures of the garnet but the garnet itself has been completely dissolved. There are a few quartz inclusions within the garnet.

Plasmic zone

At 34 m, the phyllite is weakly foliated and friable. Patches and blasts of structureless, white, very fine-grained, pedogenic kaolinite form a mottled fabric in a matrix of yellowish-brown, goethite-stained sericite and mixed kaolinite-sericite (Figure Ar1-2E, F). Very small, tabular specks of

fresh, black tourmaline are scattered in the foliation. Larger flakes of sericite [0.4 mm] as well as isolated quartz grains and lensoid quartz aggregates [1 mm] occur within the kaolinite-sericite areas, marking a siliceous foliation. XRD examination shows a trace of talc.

At 30 m, infusion of Fe-oxides is more marked, producing a compact, dark-brown rock consisting of an intimate mixture of Fe-oxides and phyllosilicates (kaolinite and sericite). There is a weak foliation which has been largely cemented by Fe-oxides. In detail, the rock consists of fine-grained flakes of kaolinite, set with flakes of mixed kaolinite-sericite. This phyllic groundmass is set with garnet pseudomorphs (Figure Ar1-2G; 0.5 mm). Fractures in the garnet have been filled with goethite and the garnet between the fractures has been leached out (Figure Ar1-2H). Blasts of white, pedogenic kaolinite have partly restructured the saprolite and patches of the groundmass have been stained and invaded by goethite. In many instances, where this is intense, goethite has pseudomorphed the phyllosilicates; where less intense, it has divided the kaolinitic groundmass into small domains and has intensively stained the edges of these domains. The rock also contains large areas rich in Mn-oxide, possibly cryptomelane or manganite.

Mottled zone, duricrust and calcrete

Higher in the profile, at 11 m depth, the rock is highly ferruginous. Pale yellow-brown masses of kaolinite and sericite are interspersed with patches of yellowish cellular or spongy goethite and quartz (Figure Ar1-2I). Ferruginization has destroyed most of the foliation. In places, the goethite is massive with inclusions of remnant sericite (vermicular books and stacks; Figure Ar1-2J), possibly clastic quartz and kaolinite; vesicles walls are lined with fibrous, colloform goethite. Although little clastic materials remain, the rock seems to have consisted of banded phyllitic and psammitic layers.

Although minor carbonate occurs in the rocks deeper in the profile, carbonates become important at 9 m depth and above. Here the rock consists of bands of goethite- and hematite-stained, yellow to pinkish brown phyllitic sericite, kaolinite and minor quartz with a preserved goethite-stained foliation (Figure Ar1-2L). It is cut both parallel to the foliation and to a lesser extent across the foliation by numerous veinlets filled with crystalline calcite (Figure Ar1-2K, L) and by patches of cellular, yellow goethite.

Carbonate is more abundant at 7 m depth, where the regolith is a polymictic breccia (Figure Ar1-2M, N). Disoriented lithofragments of dark-brown, cellular goethite, pale, yellowish-brown phyllite (sericite and kaolinite) and small fragments of quartz, stained with powdery goethite, are set in a porous carbonate matrix. Some of the carbonate matrix is nodular. Some goethite clasts enclose mica relics (Figure Ar1-2N) and quartz shards and the goethite shows partial dehydration to hematite. There are some hematite pseudomorphs after magnetite (martite). The surrounding, slightly stained carbonate is fine-grained and contains numerous irregular vesicles but the walls of the voids and the interiors of a few carbonate veins are lined with a clear, slightly coarser-grained carbonate.

At a depth of 1 m, the breccia is even more carbonate-rich. It consist of round to angular fragments of black to brown, partly cellular and partly massive goethite and khaki brown, iron-stained phyllosilicate, with no remnant foliation, set in and supported by nodular carbonate. The clasts [3-10 mm] are very heterogeneous. They vary from fragments consisting of fine-grained goethite with minor quartz, to fragments of shard-like quartz and lithorelics, set in a goethite-carbonate matrix, to spongy goethite with included carbonate fragments. Parts of the matrix contain oval structures of carbonate and clay. Some are almost oolitic (Figure Ar1-2O,) and have formed as concretions around quartz grains, patches of goethite or carbonate. The matrix in which they are set is a slightly coarser-grained carbonate which has been partly leached away. The goethite in the clasts contains sericite remnants.

Lag

The lag (Figure Ar1-2Q) overlying the phyllite host shows well-preserved schistose phyllitic fabrics, clearly visible under the binocular microscope (Figure Ar1-2R). Islands of preserved original, saprolitic fabric, now largely replaced by goethite (Figures Ar1-2T), are set in bright, massive, to spongy goethite (Figure Ar1-2U). The secondary goethite is fibrous to colloform where it lines vesicles. Saprolitic fabrics (fine-textured layer silicate pseudomorphs, probably after kaolinite and interstratified kaolinite and mica), preserved in the lag, contain sericite relics (10-100 μm), some of which have been split along their cleavages by the enclosing goethite (Figure Ar1-2S). The sericite is poorly crystalline but still contains some K. These sericite relics may be compared to similar relics and to unferruginized saprolitic, phyllitic mica and kaolinite fabrics throughout the profile and illustrate the resistance of mica to extreme weathering.

Mineral stability

Micas are particularly stable and survive from the fresh rock to the lag, provided they have been enclosed in goethite in the mottled zone. If not, micas progressively break down, at least in part, to kaolinite within the upper saprolite and plasmic zone. Quartz survives the saprolite but is readily corroded and replaced by carbonates and Fe oxides in the duricrust. Identification of pre-existing garnet within the saprolite is very dependent on garnet pseudomorphs being correctly identified. No remnant garnet was found. Garnets are generally hardy minerals and readily survive into soils and stream sediments so this weathering process is problematical. Kerogen survives into the saprolite but oxidises close to the surface.

References

Robertson, I.D.M. and Gall, S.F. 1988. A mineralogical, geochemical and petrographic study of the rocks of drillhole BCD1 from the Beasley Creek Gold Mine - Laverton, WA. CSIRO Division of Exploration Geoscience Restricted Report MG67R.

Robertson, I.D.M. 1989. Geochemistry, petrography and mineralogy of ferruginous lag overlying the Beasley Creek Gold Mine - Laverton, WA. CSIRO Division of Exploration Geoscience Restricted Report 27R.

Robertson, I.D.M. 1991. Multi-element dispersion in the saprolite at the Beasley creek Gold Mine, Laverton, Western Australia. CSIRO Division of Exploration Geoscience Restricted Report 152R. 122 pp.

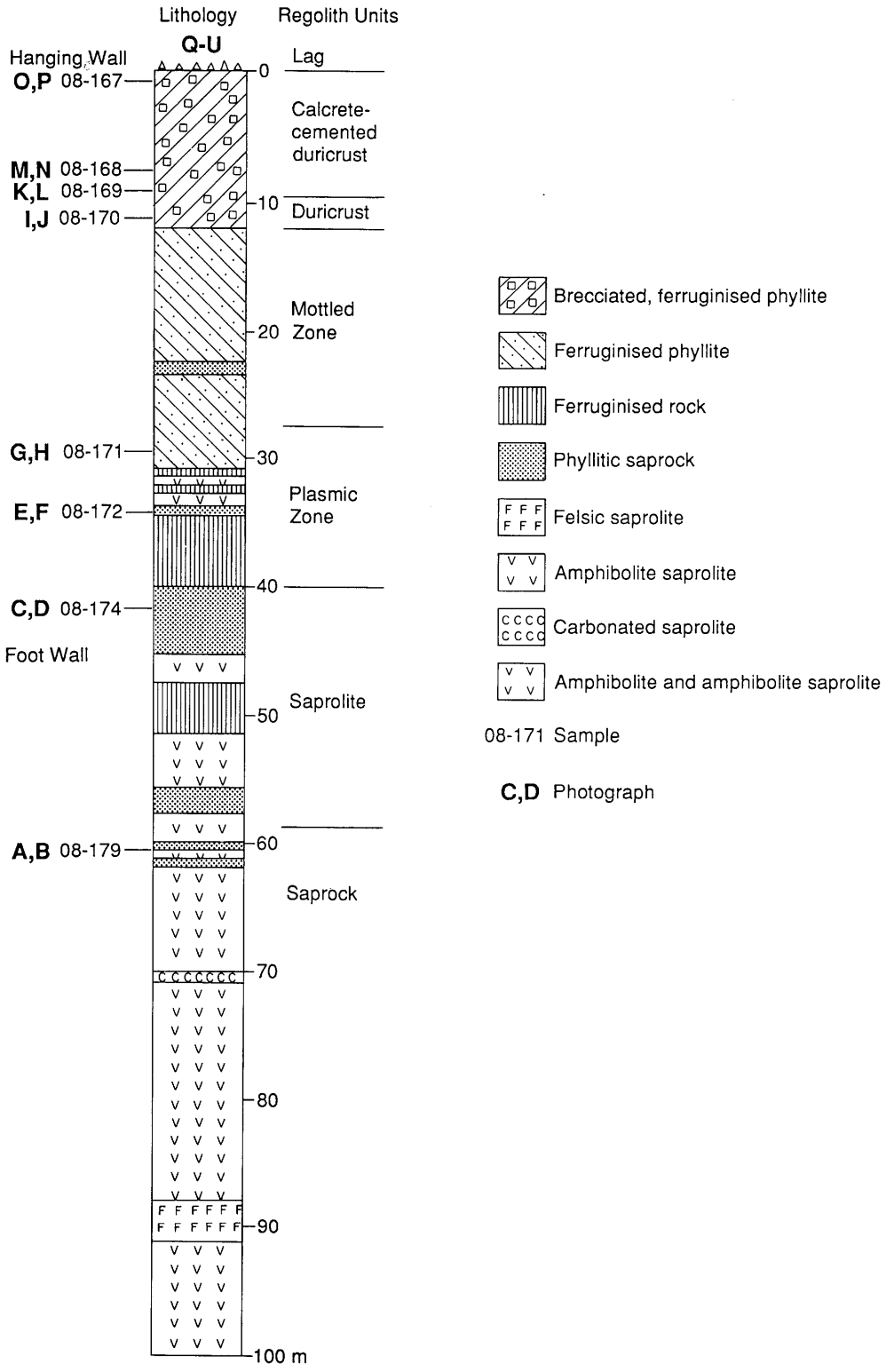

Figure Ar1- 1. Drillhole BCD1 passes from hangingwall to footwall of the mineralized phyllite and intersects the regolith from duricrust to saprock.

FIGURE Ar1-2

Plasmic Zone

G. Numerous white kaolinite blasts (KS) which have partly restructured a schistose saprolitic fabric of kaolinite and mica (MK), set with garnet pseudomorphs (GP). Specimen 08-171. Depth 29.6 m. Close-up photograph of 'wet' surface.

H. Weathered phyllite showing garnet pseudomorphs (GP) set in a fine-grained kaolinite and sericite fabric (MK). The fractures in the garnet are filled with goethite (GO) and the garnet has subsequently been dissolved. Specimen 08-171. Depth 29.6 m. Photomicrograph in normally reflected light.

E. Patches and blasts of very fine-grained, white, secondary kaolinite (KS) developed in a schistose saprolitic fabric of kaolinitic clays (KA) and lenses of kerogen (KG). Specimen 08-172. Depth 34.2 m Close-up photograph of 'wet' surface.

F. Petrographic detail of a secondary kaolinite blast, showing its very fine-grained nature and low birefringence. This kaolinite blast indicates the onset of saprolite restructuring by pedogenic processes. Specimen 08-172. Depth 34.2 m. Photomicrograph with crossed polarizers.

Saprolite

C. Grey patches of kaolinite and mixed kaolinite and mica (Mk) are separated by a mesh of clays stained lightly by goethite (GO). A small goethite pseudomorph after garnet (GP) gives an indication of the metamorphic grade reached by these rocks. The fabric is still weakly schistose. Specimen 08-174. Depth 41.9 m. Close-up photograph of "wet" surface.

D. Petrographic detail of C. Patches of very fine-grained goethite-stained kaolinite (KA) set with coarser flakes of a mixed kaolinite and mica phase (MK) are surrounded by cracks filled with and stained by goethite (GO). Specimen 08-174. Depth 41.9 m. Photomicrograph with crossed polarizers.

Saprock

A. Patches of grey kaolinite (KA) and lenses rich in mixed mica and kaolinite (MK) with flecks of kerogen (KG) make up the schistose fabric of this interflow sediment. The fabric has been slightly stained by goethite (GO). Specimen 08-179. Depth 60.5 m. Close-up photograph of "dry" surface.

B. Part of an argillaceous layer, consisting of a fine-grained mat of low birefringent kaolinite (KA) and coarser flakes of intimately mixed kaolinite-sericite with a yellowish to white birefringence (MK). Specimen 08-179. Depth 60.5 m. Photomicrograph with crossed polarizers.

FIGURE Ar1-2

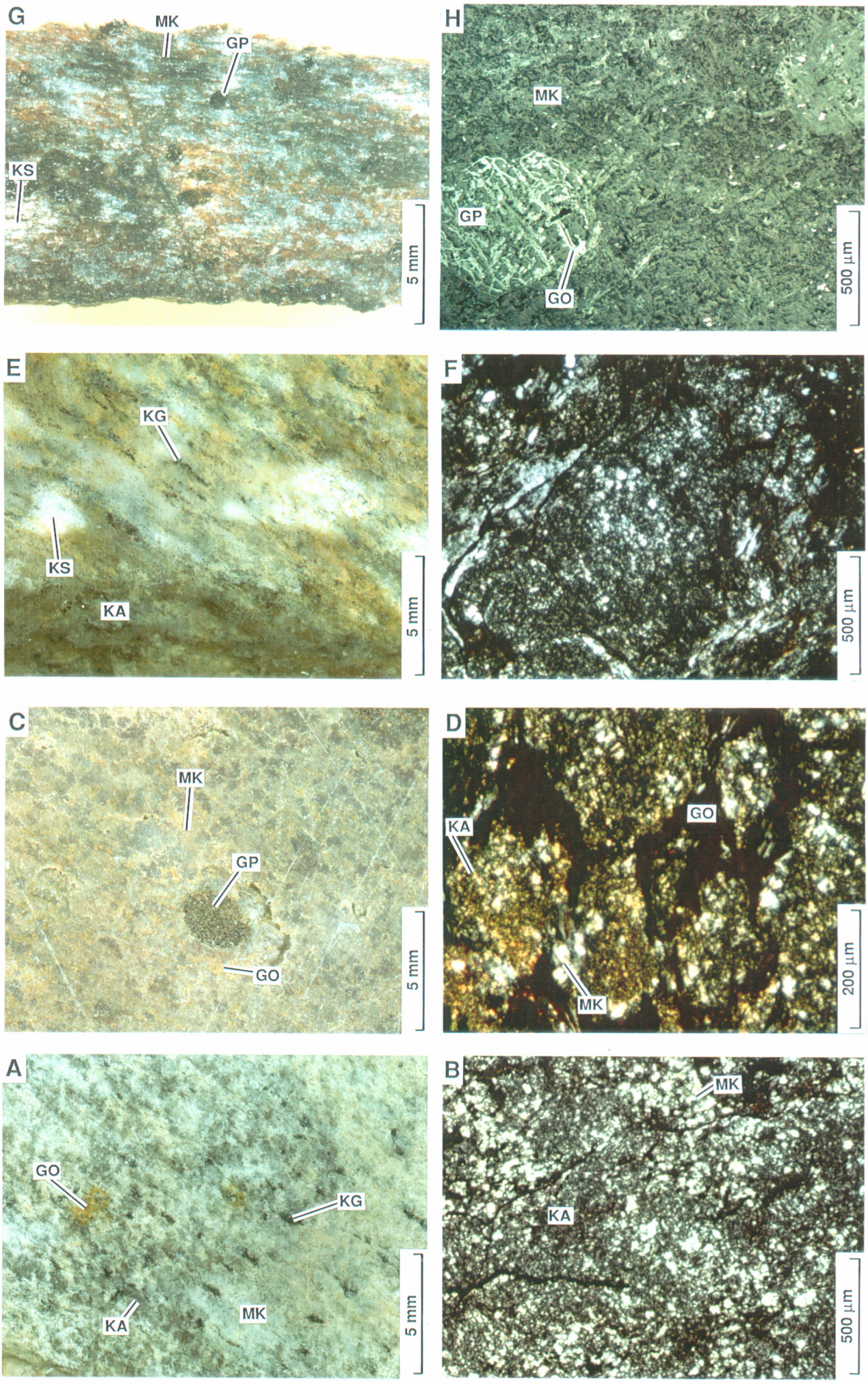
G
MK
GP
KS
5 mm
H
MK
GP
GO
500 µm
E
KG
KS
KA
5 mm
F
500 µm
C
MK
GP
GO
5 mm
D
KA
GO
MK
200 µm
A
GO
KG
KA
MK
5 mm
B
MK
KA
500 µm

FIGURE Ar1-2 (Contd)

Calcrete- brecciated and carbonate cemented duricrust

O A wide variety of disordered, highly ferruginous (PF) and non-ferruginous (PP) angular phyllitic saprolite fragments coated with thin carbonate cutans (CS), set in a breccia with smaller, similar fragments and cemented by porous calcite (CC). Specimen 08-167. Depth 1.0 m. Close-up photograph of 'wet' surface.

P. Petrographic detail of O. Ferruginous phyllitic fragments (PF) and pieces of quartz (QZ) coated in an early phase of carbonate and clay (CS). This has been cemented by clear, coarse-grained calcite (CC) . Specimen 08-167. Depth 1.0 m. Photomicrograph with crossed polarizers.

M. Disoriented fragments of brown, ferruginous, schistose phyllite (PP), set in a calcrete breccia (CC) pitted with small vesicles (VS). Specimen 08-168. Depth 7.4 m. Close-up photograph of 'wet' surface.

N. Petrographic detail of M. A goethite pisolith (GO) set with mica remnants (MU), enclosed in goethite-stained phyllitic material (PH) and cemented into a calcrete breccia (CS). Specimen 08-168. Depth 7.4 m. Photomicrograph with crossed polarizers.

K. A very ferruginous, though slightly schistose phyllite (PP) has been partly dissolved and its stylolitic cavities have been filled and cemented with crystalline calcite (CC). Specimen 08-169. Depth 9.0 m. Close-up photograph of "wet" surface.

L. Petrographic detail of K. The schistose mat of brown, goethite-stained kaolinite (KA) and blue, birefringent sericite (MU) are cut by crystalline calcite (CC). Specimen 08-169. Depth 9.0 m. Photomicrograph with crossed polarizers.

Duricrust

I. Yellow, stained patches of mixed clay and sericite (MK), enclosed in secondary goethite (GO). The goethite contains numerous remnant flakes of mica (see J). Cementation and replacement by goethite is very incomplete. Specimen 08-170. Depth 11.0 m. Close-up photograph of "wet" surface.

J. Petrographic detail of I. Sheets of dark-grey sericite (MU) lie enclosed in light-grey goethite (GO) which has split some of the mica sheets. The mica still contains K but has been partly hydrated. Small vesicles (VS) pock-mark the goethite. Specimen 08-170. Depth 11.0 m. Photomicrograph in normally reflected light.

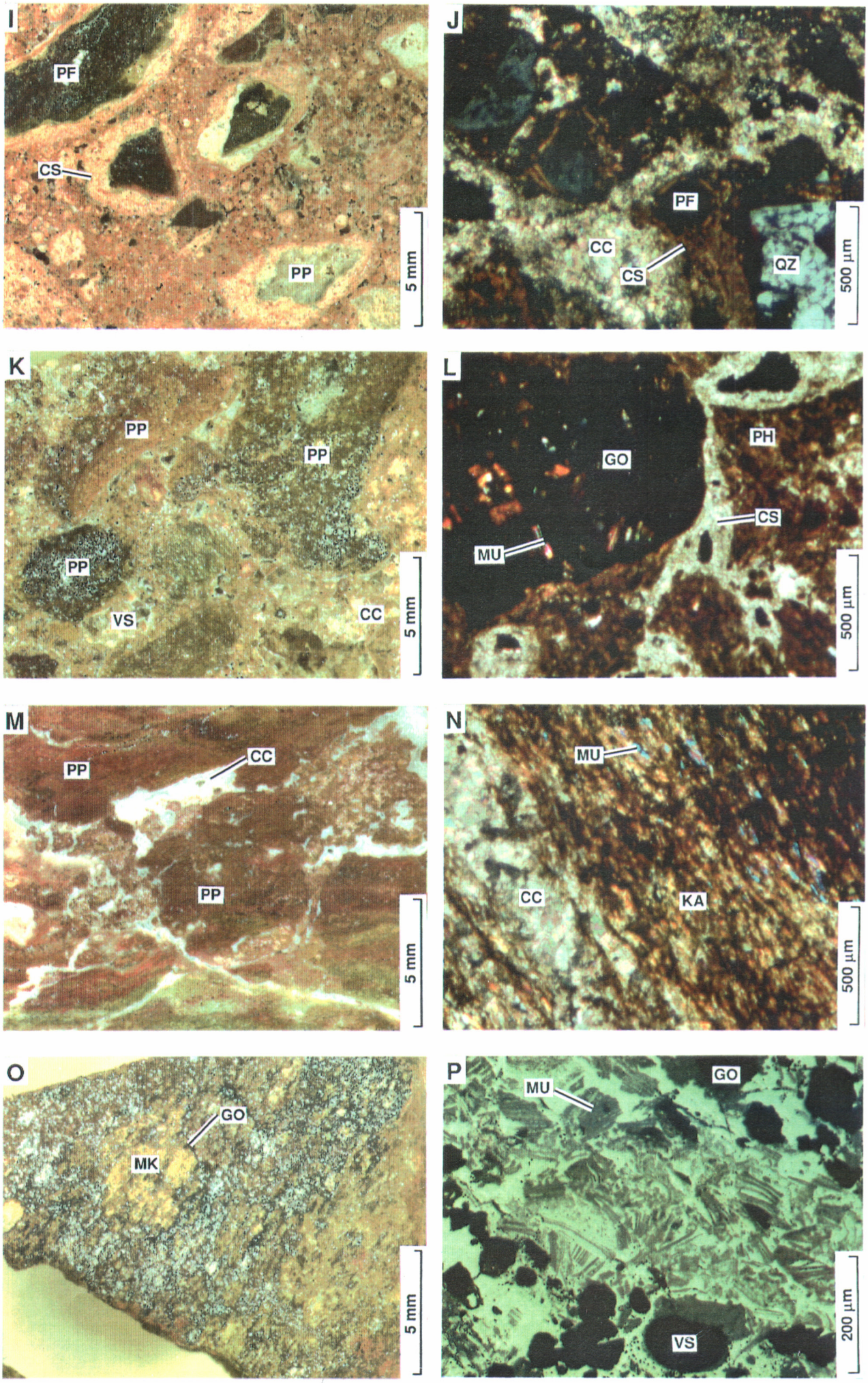
I
PF
CS
PP
5 mm
J
PF
CC
CS
QZ
500 µm
K
PP
PP
PP
VS
CC
5 mm
L
PH
GO
CS
MU
500 µm
M
PP
CC
PP
5 mm
N
MU
CC
KA
500 µm
O
GO
MK
5 mm
P
MU
GO
VS
200 µm

ARI-7

FIGURE Ar1-2 (Contd)

Lag at Beasley Creek

Q. A soil surface strewn with black goethite-rich lag, with minor quartz lag, overlying the ore body at Beasley Creek. Some of the larger fragments are cellular and gossanous.

Preserved phyllite fabrics

R. A deep red-brown, ferruginized lithorelic of ore zone phyllite, showing a preserved, folded schistosity with a high proportion of glistening mica relics. Specimen 08-108D. Close-up photograph of 'wet' surface.

S. Mica relics (MK) set in spongy goethite (GO). The goethite has wedged the mica cleavage sheets apart. Specimen 08-108B. Photomicrograph in normally reflected light.

Partial obliteration of primary fabrics by secondary goethite

T. A very fine-grained, ferruginized lithorelic of ore zone phyllite. Although some schistosity is preserved, much of the original fabric has been replaced by dark brown, secondary goethite. Specimen 08-108B. Close-up photograph of 'wet' surface.

U. Islands of layer silicate pseudomorphs and a few mica remnants (MK) set in dull goethite (GO), invaded by and set in bright hematitic goethite (GH). A few lozenge-shaped hematite crystals (HM) are scattered in the fabric. Specimen 08-104A. Photomicrograph in normally reflected light.

FIGURE Ar1-2 (Contd)

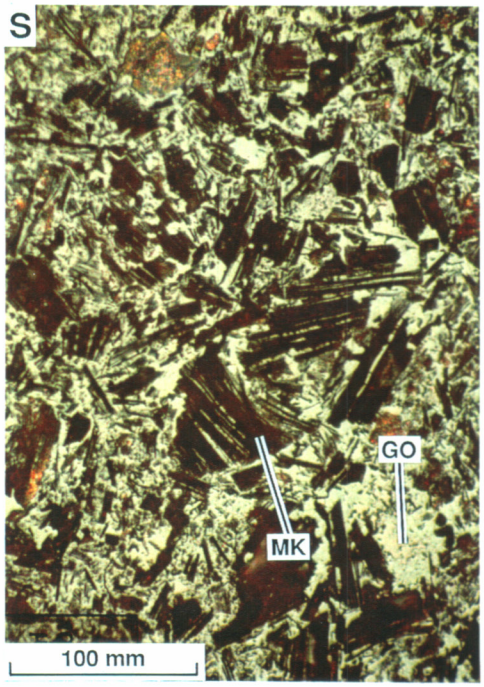

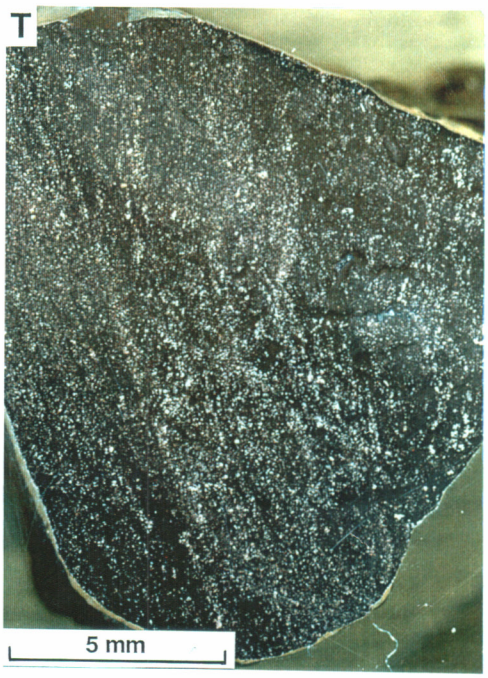

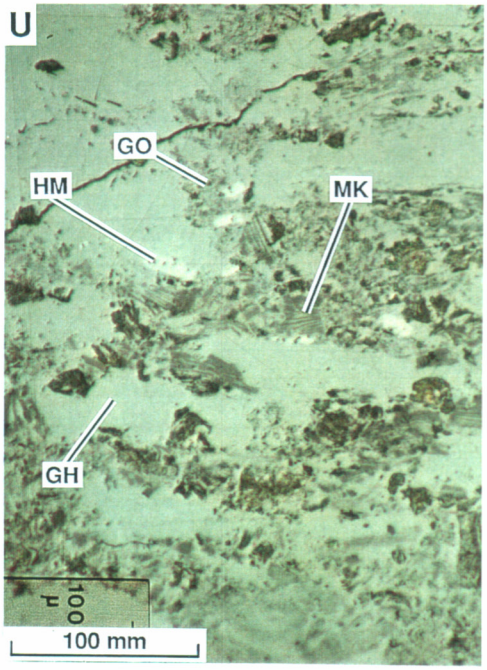

PHYLLITE Ar1
GEOCHEMISTRY

LIB NO	DEPTH	SiO2	Al2O3	Fe2O3	MgO	CaO	TiO2	P2O5	Ag	As	Ba	Be	Bi	Cd	Ce	Co	Cr	Cu	Ga	Ge	In	La	Mn	Mo	Nb
08 - 167	1.00	39.70	6.61	16.16	0.71	14.80	0.33	0.04	1	17	1340	0.0	0	3	8	7	91	61	9	0	0	9	849	3	2
08 - 168	7.40	25.70	10.70	30.60	2.90	8.62	0.43	0.03	0	37	129	0.0	0	3	0	30	187	261	5	0	0	7	886	2	0
08 - 169	9.00	33.20	20.40	9.29	2.35	12.60	1.40	0.01	1	15	485	0.0	3	0	11	2	184	64	28	2	0	1	267	4	9
08 - 170	11.00	9.49	5.56	46.89	0.92	11.80	0.22	0.36	0	126	456	4.4	0	1	2	7	87	252	0	0	0	8	1516	0	0
08 - 171	29.60	31.00	24.00	19.30	0.46	0.20	2.16	0.02	0	94	9918	0.0	0	0	410	383	150	393	32	0	3	128	96629	23	4
08 - 172	34.20	57.90	24.60	2.14	0.20	0.07	2.33	0.00	0	27	23	0.0	0	0	44	0	401	20	30	1	0	7	170	4	10
08 - 174	41.90	44.10	28.20	9.01	0.25	0.09	2.54	0.01	3	226	63	0.0	0	1	15	4	288	352	35	1	0	7	181	3	8
08 - 179	60.50	60.90	23.90	2.43	0.26	0.09	2.42	0.01	0	46	63	0.0	1	1	17	3	60	136	32	1	1	1	146	3	6

LIB NO	Ni	Pb	Rb	Sb	Se	Sn	Sr	V	W	Y	Zn	Zr	Qtz	Goet	Kao	Musc	Chlor	Smec	Talc	Trem	Feld	Calc
08 - 167	34	31	24	3	0	0	191	193	1	9	119	63	16	113	35	23	0	0	5	0	0	58
08 - 168	36	26	37	6	0	0	211	630	57	13	170	37	33	177	220	82	0	0	0	0	0	13
08 - 169	11	5	209	1	0	0	120	789	20	16	23	260	16	62	150	250	0	18	0	0	0	42
08 - 170	73	24	14	8	0	0	88	1403	35	41	327	17	0	200	88	22	0	0	5	0	0	18
08 - 171	218	0	75	3	0	6	226	877	21	53	145	78	0	28	300	270	0	0	0	0	0	0
08 - 172	46	4	5	1	0	0	8	256	11	33	54	438	158	212	400	7	0	0	5	0	0	0
08 - 174	34	5	64	1	1	1	15	679	5	14	61	144	55	177	350	78	0	0	8	0	0	0
08 - 179	13	10	16	3	2	3	13	592	4	19	79	133	182	150	400	16	0	0	5	5	0	0

PHYLLITE Ar1 - BEASLEY CREEK ORE ZONE
GEOCHEMISTRY

Lib No	Depth	SiO2	Al2O3	Fe2O3	MgO	CaO	Na2O	TiO2	S	Ag	As	Au	Ba	Bi	Cd	Ce	Co	Cr	Cu
08-702	10	33.9	13.1	15.01	4.74	11.9	0.12	1.02	0.02	0.6	17	856	289	<0.1	0.36	66	95	103	142
08-703	11	30.5	14.9	20.87	2.71	6.22	0.18	1.41	0.016	0.56	16	247	1371	0.16	0.7	89	254	126	225
08-668	12	47.35	4.46	31.17	0.63	1.78	0.06	0.23	0.025	0.41	266	160	47	0.16	0.29	10	31	78	159
08-669	13	49.7	5.55	21.3	1.34	7.09	0.07	0.26	0.03	0.32	248	286	214	0.16	<0.1	11	18	80	129
08-704	13	22.7	12.9	23.45	3.36	9.89	0.15	1.29	0.021	0.3	53	647	988	0.13	0.32	80	215	196	274
08-670	14	46.2	9.84	10.72	3.5	13.97	0.16	0.78	0.033	0.3	320	300	179	0.12	<0.1	34	3	139	134
08-705	15	25.1	15.9	31.74	1.26	7.16	0.16	1.3	0.013	0.33	89	302	705	0.12	0.23	75	187	181	292
08-706	16	31.6	10.7	22.73	1.4	11	0.15	0.92	0.02	0.49	104	409	916	0.27	0.42	139	273	75	271
08-671	16	36.13	13.01	17.16	1.8	14.2	0.13	0.98	0.026	0.47	277	435	167	0.11	0.13	9	8	166	185
08-707	18	20.6	13.6	26.02	1.46	11.4	0.13	0.94	0.017	0.53	66	1343	2199	0.16	1.44	239	380	91	365
08-672	19	25.33	17.45	25.45	1.05	10.66	0.1	1.54	0.013	1.19	132	582	896	0.15	0.86	144	311	223	344
08-708	21	36.9	7.3	19.16	0.83	12.7	0.09	0.18	0.021	0.13	44	1345	1041	<0.1	0.58	179	795	110	745
08-673	22	18.98	10.39	36.74	0.63	9.7	0.1	0.99	0.019	1.24	180	1505	1187	<0.1	2.09	117	382	148	333
08-709	23	38.8	16.8	29.74	0.38	0.67	0.11	1.48	0.005	0.6	28	169	385	0.11	0.21	13	71	110	310
08-674	24	31.32	25.78	22.88	0.36	1.15	0.14	2.06	0.004	1.26	34	880	464	0.19	0.68	57	227	202	167
08-675	27	26.62	16.91	37.32	0.32	0.43	0.1	1.54	0.015	1.28	41	444	804	0.6	0.97	56	119	156	139
08-741	28	83.1	3.64	9.15	0.35	2.36	0.12	0.26	0.013	1.11	77	494	103	1.3	0.13	31	24	117	265
08-742	29	73.9	3.91	12.01	0.38	0.4	0.15	0.33	0.023	1.19	75	1154	127	1.58	0.19	19	22	227	198
08-676	29	14.46	8.79	52.47	0.4	0.93	0.08	0.73	0.015	1.53	116	1013	1392	0.3	1.47	100	160	147	206
08-743	31	55.52	14.42	19.73	0.54	0.14	0.16	1.1	0.014	1.4	303	676	721	0.31	0.66	120	146	319	373
08-677	32	32.32	21.47	27.02	0.34	0.13	0.13	1.81	0.005	2.18	87	1845	639	0.21	1.47	50	51	182	152
08-744	34	49.77	17.71	23.45	0.34	0.16	0.12	0.84	0.015	0.66	456	20488	322	0.17	<0.1	36	40	195	273
08-678	35	27.65	19.78	30.31	0.43	0.13	0.1	1.63	0.001	0.91	108	3156	930	0.35	0.88	52	51	186	219
08-745	36	37.28	20.2	25.02	0.45	0.17	0.18	1.85	0.002	1.06	131	7384	982	0.25	1.3	71	223	208	323
08-679	37	25.03	15.98	36.31	0.22	0.14	0.08	0.72	0.004	0.71	113	1148	1160	0.23	1.52	77	89	85	339
08-746	39	34.05	17.39	31.6	0.43	0.24	0.15	1.65	0.005	1.11	156	746	1587	0.16	1.41	102	167	150	293
08-680	40	39.23	13.83	28.45	0.23	0.19	0.1	0.73	0.004	1.06	78	1666	2356	0.31	1.93	156	746	70	932
08-681	41	48.78	24.27	12.3	0.15	0.08	0.08	1.8	0	0.4	44	475	223	0.43	0.32	15	44	38	166
08-747	42	38.85	15.53	30.74	0.37	0.2	0.12	1.27	0.003	0.49	154	7067	592	0.26	1.24	39	65	185	248
08-682	42	44.76	15.91	23.16	0.21	0.16	0.11	1.25	0.004	0.63	65	925	1382	0.35	0.99	91	344	51	496
08-748	44	39.47	12.13	30.6	0.47	0.32	0.14	1.16	0.012	0.74	212	3223	539	0.25	1.48	42	68	163	243
08-749	47	33.2	8.54	30.74	0.53	0.29	0.17	1.01	0.005	0.89	222	1873	778	0.44	2.02	25	65	130	450
08-636	48	81.28	6.42	8.72	0.17	0.06	0.08	0.36	0	0.77	132	1105	134	1.61	0.31	22	57	182	85
08-637	49	62.79	11.14	19.02	0.24	0.07	0.08	0.74	0	1.22	154	1210	328	1.94	0.43	45	234	198	365
08-750	49	30.3	11.1	36.89	0.56	0.42	0.14	1.07	0.009	0.74	235	5154	791	0.32	1.63	25	69	151	466
08-638	50	73.49	6.4	15.73	0.19	0.09	0.08	0.45	0.007	0.5	131	699	166	0.85	0.29	28	104	123	174
08-751	52	34.1	9.72	31.88	0.4	0.26	0.13	1.07	0.005	0.68	138	2139	784	0.33	1.38	25	60	153	338
08-639	52	58.58	10.4	23.73	0.19	0.08	0.07	0.8	0.008	1.24	1270	1782	130	0.39	0.37	65	44	125	253
08-752	55	25.5	6.61	41.89	0.36	0.32	0.1	0.8	0.007	0.6	128	5301	1561	0.27	2.06	21	93	114	444
08-640	55	42.53	12.1	33.88	0.23	0.13	0.08	0.95	0.002	1.02	746	1591	398	0.25	0.75	65	307	185	296
08-753	57	66.3	5.42	15.44	0.22	0.19	0.1	0.41	0.011	0.29	67	3312	1108	0.15	0.95	31	72	98	226
08-641	59	46.7	14.22	25.88	0.19	0.09	0.12	1.25	0.009	1.77	394	1531	359	0.26	0.62	34	192	214	289
08-754	60	77.7	4.69	11.87	0.2	0.2	0.1	0.19	0.005	0.24	54	3226	623	<0.1	0.73	34	101	100	306
08-755	62	73.4	2.68	12.01	0.16	0.18	0.09	0.13	0.007	0.22	62	5231	333	<0.1	0.62	22	45	77	158
08-642	62	43.82	12.49	29.88	0.22	0.14	0.1	1.11	0.002	1.12	695	4871	499	0.18	0.85	81	260	160	293
08-756	65	72.47	1.56	23.3	0.18	0.16	0.07	0.08	0.007	0.37	70	15226	207	<0.1	0.63	14	65	124	259
08-643	66	38.32	11.38	34.03	0.22	0.29	0.07	1.08	0.003	1.16	271	2360	270	0.21	0.7	41	255	251	276
08-757	67	63.82	1.22	28.59	0.18	0.15	0.08	0.08	0.008	0.6	89	46072	185	0.13	0.82	8	25	119	188
08-644	69	21.91	5.84	56.33	0.17	0.18	0.06	0.62	0.004	1.07	198	9379	167	<0.1	0.91	18	126	140	187
08-645	73	14.33	3.89	59.76	0.11	0.12	0.03	0.51	0.001	0.83	142	4154	136	<0.1	0.91	3	67	112	159
08-646	76	22.01	3.91	57.47	0.17	0.2	0.02	0.51	0.002	0.48	272	2770	176	0.13	1.04	13	81	166	166
08-647	80	23.44	3.39	56.19	0.17	0.21	0.03	0.41	0.002	1.09	367	3337	184	0.15	1.17	4	58	150	103
08-648	83	44.44	9.76	25.31	2.07	0.62	0	0.92	0.002	1	126	6765	594	<0.1	0.58	17	76	72	188
08-649	86	36.58	9.73	29.17	3.19	0.35	0.21	1	0.008	0.42	120	953	354	<0.1	0.49	12	64	85	127

PHYLLITE Ar1 - BEASLEY CREEK ORE ZONE
GEOCHEMISTRY

Lib No	Ga	Ge	In	La	Mn	Mo	Nb	Ni	Pb	Rb	Sb	Sn	Sr	V	W	Y	Zn	Zr
08-702	15	1	0.13	6.4	11551	3.8	1	33	3	33	0.35	0.57	166	303	2.8	5	35	57
08-703	18	0	0.17	14.4	46473	4.2	5	48	2	47	0.18	0.5	162	450	2.5	10	56	81
08-668	1	3	0.09	11.5	617	3.2	1	48	48	15	4.14	<0.5	27	207	6.1	16	273	20
08-669	3	3	0.08	14.9	462	3.1	0	41	53	17	4.4	<0.5	54	221	5.2	11	158	19
08-704	18	1	0.15	13.4	31849	4.6	5	58	4	33	0.26	0.51	151	546	5.2	13	69	56
08-670	12	2	0.06	53.1	205	3.3	2	43	51	46	4.34	<0.5	85	307	9.9	6	32	46
08-705	18	0	0.14	14.5	22280	5	2	75	8	36	1.35	<0.5	75	780	10.2	27	128	56
08-706	12	0	0.15	33.2	37735	5.1	5	77	24	23	0.79	0.75	111	855	12.7	41	173	71
08-671	14	2	0.13	8.7	350	3.5	2	62	25	51	1.79	<0.5	71	412	9.8	6	62	50
08-707	11	1	0.13	73.8	77315	5	2	101	20	24	0.34	<0.5	186	1225	3.7	65	153	67
08-672	19	0	0.21	14.6	13913	4.9	1	124	79	43	0.56	0.7	66	656	5.7	16	203	86
08-708	3	2	<0.05	30.6	46650	5.6	0	313	0	6	0.27	<0.5	114	639	3.1	52	216	8
08-673	10	0	0.14	32.8	25356	5.1	4	92	17	28	0.37	<0.5	87	498	4.2	33	169	46
08-709	22	0	0.15	14.3	8417	4.5	8	85	1	7	0.99	0.71	36	726	6.4	38	120	76
08-674	30	1	0.18	14.2	15412	4.6	4	66	7	52	0.35	0.76	70	662	7.8	14	74	108
08-675	20	0	0.16	20.9	22075	4.5	7	80	34	32	0.46	0.8	71	546	6.1	29	123	116
08-741	6	3	0.23	14.9	568	2.6	3	30	20	13	5.04	2.69	20	67	2.3	12	8	57
08-742	10	4	0.28	11.8	1520	3	1	50	11	24	6.06	2.31	21	119	6.2	8	15	52
08-676	8	3	0.11	43.9	62521	6.2	1	115	42	23	0.7	<0.5	137	503	3.3	58	267	49
08-743	17	2	0.2	20.1	6606	4.6	2	100	54	76	3.12	1.22	29	504	7.3	25	93	84
08-677	28	0	0.19	9.1	22895	4.7	5	66	23	57	0.65	0.86	46	708	8.1	22	140	92
08-744	24	1	0.08	28.1	2358	6.4	5	68	52	33	1.89	1.11	21	346	7.3	19	59	134
08-678	24	2	0.18	13.6	52725	5.7	5	73	24	64	1.11	0.94	106	900	22.4	33	220	97
08-745	30	1	0.15	32.4	38884	5.8	4	162	11	66	0.45	1.1	183	817	24.4	38	149	90
08-679	13	2	0.13	41.4	67801	5.7	1	91	42	27	1.05	<0.5	135	1688	13.6	59	319	42
08-746	25	1	0.15	50.1	35169	6.1	5	190	11	37	2.07	1.31	193	682	3.9	52	118	120
08-680	7	3	0.12	41.7	81479	6	0	356	122	18	9.12	<0.5	161	1076	10.4	53	284	31
08-681	23	1	0.17	6	4314	3.6	7	49	0	42	0.16	0.57	21	445	2.5	18	89	107
08-747	20	0	0.16	36.7	23965	5.4	10	140	22	26	0.53	0.94	147	572	4.6	49	114	86
08-682	18	2	0.12	28.3	40635	4.7	2	185	54	20	0.37	<0.5	103	793	8.3	38	177	60
08-748	14	0	0.16	55.6	43158	7	2	246	8	33	0.46	0.96	227	586	6.1	78	138	63
08-749	10	1	0.2	51.8	75752	16.9	0	310	12	45	0.78	0.57	305	597	6.1	91	174	53
08-636	10	8	0.6	14.5	1020	3.5	3	25	21	24	1.99	2.84	12	169	2.4	11	22	62
08-637	16	5	0.62	28.2	2439	4.6	4	53	30	28	2.61	3.56	18	216	10.7	21	55	96
08-750	14	0	0.14	41.1	52127	7	2	263	14	39	1	0.73	194	601	2.8	87	171	54
08-638	9	3	0.1	28.6	1067	4.1	1	59	22	16	1.45	1.71	13	145	8.5	21	73	45
08-751	11	0	0.16	48.2	57483	5.4	1	206	20	32	0.88	0.77	224	652	6	90	170	54
08-639	15	1	0.16	54.8	540	4.8	3	105	42	20	1.96	0.64	15	240	18	34	87	91
08-752	9	1	0.15	62.6	91981	6.4	2	279	18	20	0.7	<0.5	304	856	3.3	112	257	36
08-640	15	1-	0.14	46.4	5505	5.9	1	141	24	29	1.95	<0.5	29	369	18.3	53	185	64
08-753	4	0	0.07	30.8	45935	4.2	1	157	10	12	0.38	<0.5	148	371	2.1	41	121	21
08-641	22	2	0.15	21.4	4955	5.8	1	114	14	39	0.68	0.69	22	471	6.9	43	151	70
08-754	2	0	<0.05	23.3	35196	3.7	0	217	4	6	0.3	<0.5	98	229	3.2	29	107	13
08-755	0	1	<0.05	18.6	25836	4.4	0	151	5	5	0.51	<0.5	93	164	1.5	36	90	11
08-642	18	0	0.16	25.1	12502	6.6	2	188	18	31	1.15	<0.5	57	431	10.6	36	286	60
08-756	0	1	<0.05	13.2	18283	4.6	0	143	5	4	0.32	<0.5	52	170	2	38	112	5
08-643	20	2	0.16	24.7	7587	5.9	2	165	13	16	0.76	<0.5	34	467	8.1	39	271	65
08-757	1	0	0.08	13.6	12653	5	0	91	0	4	0.4	<0.5	46	197	3.1	48	123	7
08-644	9	0	0.08	26.9	14935	7	0	147	4	9	0.34	<0.5	51	379	3.6	63	354	19
08-645	0	1	<0.05	22.3	12843	5.8	2	114	10	9	0.39	<0.5	53	316	3.3	58	270	17
08-646	3	2	0.14	25.3	9899	6	2	116	7	15	0.52	<0.5	40	390	3.1	65	257	24
08-647	5	0	0.05	18.6	13774	6	0	124	34	28	1.31	<0.5	53	248	3	60	411	24
08-648	14	3	0.11	9.7	11105	5.6	0	65	10	77	0.69	<0.5	106	352	9.2	32	156	47
08-649	13	4	0.13	9.9	8441	4.3	0	78	10	29	0.31	<0.5	85	369	2.9	34	193	52

Metamorphic Grade	:	Amphibolite Facies
Structural Attributes	:	Relatively Undeformed
Gross Features	:	Veins of grey quartz and felsic dykes
Profile Truncation	:	Within saprolite
Depth to Fresh Rock	:	15 m
Location	:	Trial Hill Tin Mine, Central Queensland
Reference	:	Robertson (1990); Robertson and Eggleton (1991)

Geomorphology and regolith

Weathering has taken place beneath a pre-Pliocene lateritic surface; the whole has been eroded by a river channel, which was subsequently filled with debris-flow sediments, and capped by the Pliocene-Pleistocene Nulla olivine basalt (Figure G1-1). Thus the profile has been truncated within the saprolite.

Fresh rock

The fresh biotite granite is pink, (Figure G1-2C) and medium-grained and consists of pink perthitic (vein and patch) K-feldspar ($Ab_{4.3}An_{0.0}Or_{95.8}$; Figure G1-2E), clusters of creamy, rather sausseritized, stumpy, subhedral laths of plagioclase ($Ab_{97.5}An_{1.8}Or_{0.7}$; Figure G1-2D), glassy, grey quartz, partly chloritized biotite and minor muscovite. There is a trace of apatite, epidote and muscovite, some radiation damage in the micas and XRD analysis indicates minor illite. Plagioclase appears to have crystallized first, followed by K-feldspar and then quartz. The quartz shows strain lamellae normal to the c axis. Where the granite has been cut by quartz veins, there has been local kaolinization of the granite, due to penetration of water along vein margins.

Saprock

The contact between fresh granite and its saprock was obscured but small corestones of saprock occur in granite saprolite (Figure G1-2B). The colour and fabric of the granite are perfectly preserved but the saprock is friable, due to weathering along grain margins, and individual minerals may be broken free easily (Figure G1-2A).

In places, the plagioclase has been partly altered to a mass of very low birefringent kaolinite. SEM examination shows that the plagioclase surfaces are covered by round, cellular encrustations of smectite, with a cornflake-like fabric (Figure 8B), set with a few rods of halloysite. Similar smectite cornflake-like fabrics were found on etched microcline. SEM examination of the chlorite showed small pockets of smectite and halloysite. This illustrates that an intermediate smectite phase is produced during weathering of feldspar and chlorite.

Small dots of Mn oxides occur on crystal faces of feldspar and quartz and a black manganiferous material penetrates small cracks. XRD and SEM examination (Robertson, 1990) indicates that it is an indeterminate Mn wad which coats pre-existing clays (kaolinite, smectite and halloysite).

Saprolite

The granitic grain-size and fabric are perfectly preserved in the saprolite (Figure G1-2C) but the feldspars are extensively kaolinized and the rock is white. The contact with the saprock is sharp (Figure G1-2B). Quartz, which occurs as anhedral, strained grains (0.5-2.0 mm) is the only completely unaltered mineral. Anhedral K-feldspar, showing twin structures and a slightly undulose extinction, is all that remains of the perthite; it is partly clouded by ultra-fine kaolinite. The plagioclase component of the perthite has been converted entirely to extremely fine-grained clay (Figure G1-2F).

SEM examination shows that the K-feldspar is deeply etched along its cleavages to give a delicate lace-like structure (Figure 8A). A vermiform mesh of randomly oriented halloysite rods, 3 μm in length, meander in the etched feldspar and pseudomorphs the plagioclase of the perthite. Where weathering is more advanced, the K-feldspar is broken into domains, separated by zones of intense kaolinization, which consists of an open mesh of kaolinite crystals (2-3 μm) and randomly oriented halloysite rods. The halloysite cross sections are not round but have planar faces parallel to their long axes. In many instances the halloysite rods lie upon the kaolinite plates and appear to be partly fused with them.

A dominant clay phase, pseudomorphing the separate plagioclase, consists of a mat of fine-grained (0.005 mm), low birefringent kaolinite, set with clusters, larger flakes, books and distorted stacks of a more birefringent (white to yellow) kaolinite-muscovite mixture, containing Fe and K. These are weathered sericite flakes (Figure G1-2F). Clay and muscovite are intimately interlaminated on a <0.1 μm scale (Figure 8C), resulting in an apparently optically homogeneous material (Figure G1-2G) of moderate birefringence (yellow). Apart from muscovite, there are no preserved mafic minerals (biotite or chlorite).

Arenose zone

Not present, as the profile has been truncated within the saprolite

Mineral stability

Quartz survives throughout the profile. Plagioclase feldspar, both as a component of the perthite and as a discrete phase, survives only partly in the saprock. Initial plagioclase breaks down to smectite but this transitory phase occurs only on the surfaces of feldspar crystals; it continues its alteration to kaolinite and/or halloysite over a very short distance. Potassium-feldspar begins to break down within the lower saprolite. Biotite and chlorite break down to smectites and clay within the saprock and do not occur in the saprolite.

Muscovite and sericite survive only in part in the saprolite, where progressive alteration of muscovite is shown as wedges and lenses of clay within discrete muscovite. Alteration of sericite produces an intimate interlamination of mica and clay, to give an apparently optically homogeneous material, which is only seen to be inhomogeneous at very high (sub-micron) resolution.

References

Robertson, I.D.M. 1990. Weathering at the Trial Hill Tin Mine - Queensland. Occasional Publication No 1. Centre for Australian Regolith Studies, Australian National University, ACT. 48 pp.

Robertson, I.D.M. and Eggleton, R.A. 1991. Weathering of granitic muscovite to kaolinite and halloysite and plagioclase-derived kaolinite to halloysite. Clays and Clay Minerals 39. 113-126.

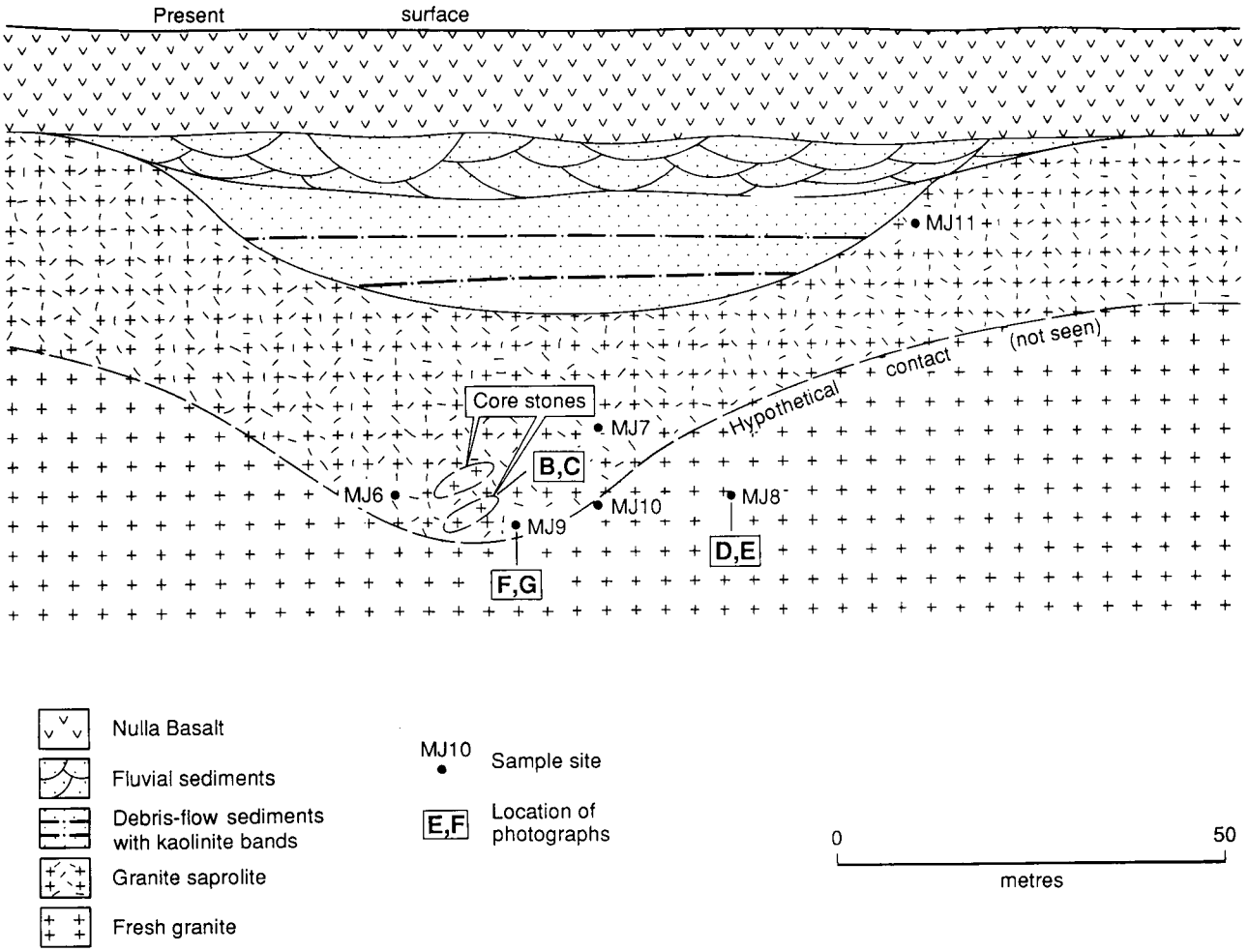

Figure G1-1. Profile at Trial Hill Tin Mine showing locations of samples and photographs.

FIGURE G1-2

Saprock

A. Partly weathered granite saprock. Weathering has penetrated grain boundaries and loosened the component mineral grains which readily crumble to a grus. Road cutting, Trial Hill, Queensland.

Fresh granite, saprock corestones and saprolite

B. Corestones of pink, crumbly, slightly weathered granite saprock (CS) set in white granite saprolite (SA). Central open cut, Trial Hill Tin Mine, Queensland.

C. The identical fabrics of fresh, pink granite (left) and the white saprolite (right) formed from it. Central open cut, Trial Hill Tin Mine, Queensland.

Feldspars of fresh granite

D. Slightly sericitized plagioclase (PL), showing mica inclusions (MC), with quartz (QZ) in fresh granite. Specimen MJ8. Trial Hill Tin Mine, Queensland. Photomicrograph with crossed polarizers.

E. Slightly turbid but otherwise fresh microcline crystal (MC) containing clear, fresh vein perthitic plagioclase (PL). Specimen MJ8. Trial Hill Tin Mine, Queensland. Photomicrograph with crossed polarizers.

Kaolinized plagioclase and sericite of saprolite

F. Very fine-grained low-birefringent kaolinite (KA), flecked with patches of mixed kaolinite and mica (MK); the whole forms a pseudomorph after sericitized plagioclase with included sericite. Granite saprolite. Specimen MJ9. Trial Hill Tin Mine, Queensland. Photomicrograph with crossed polarizers.

G. Accordion structure of mixed kaolinite and mica (MK). The birefringence varies from first order yellow to grey. Granite saprolite. Specimen MJ9. Trial Hill Tin Mine, Queensland. Photomicrograph with crossed polarizers.

FIGURE G1-2


A

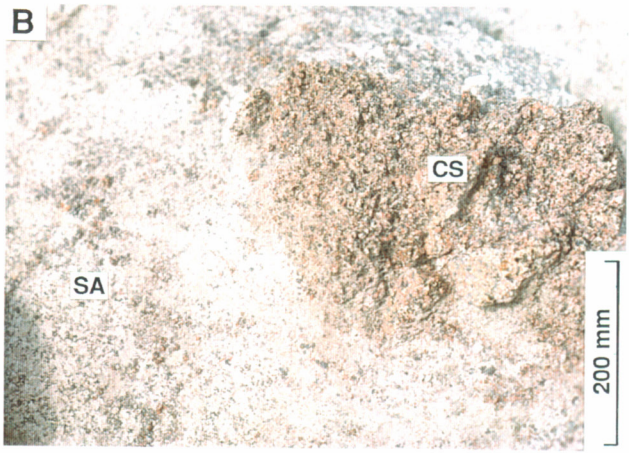
B
CS
SA
200 mm


C
200 mm

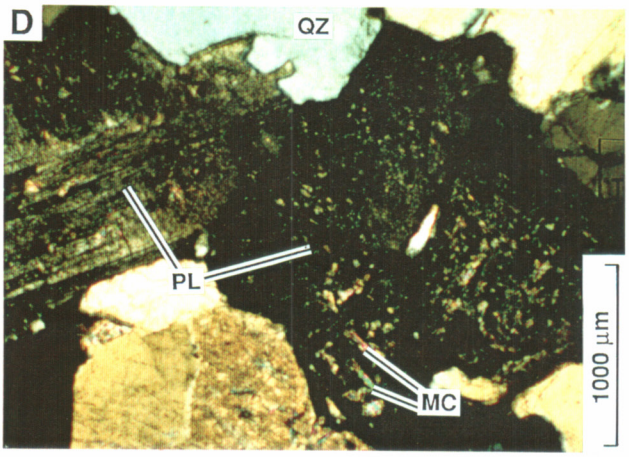
D
QZ
PL
MC
1000 µm

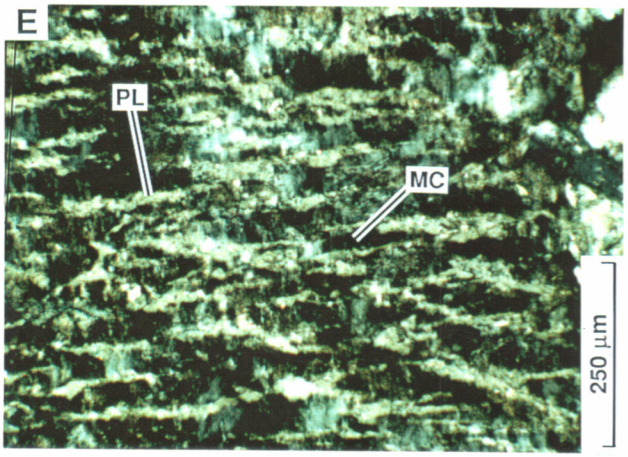
E
PL
MC
250 µm

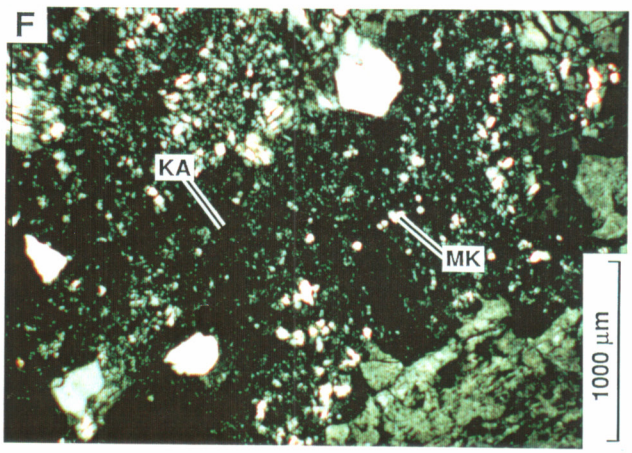
F
KA
MK
1000 µm

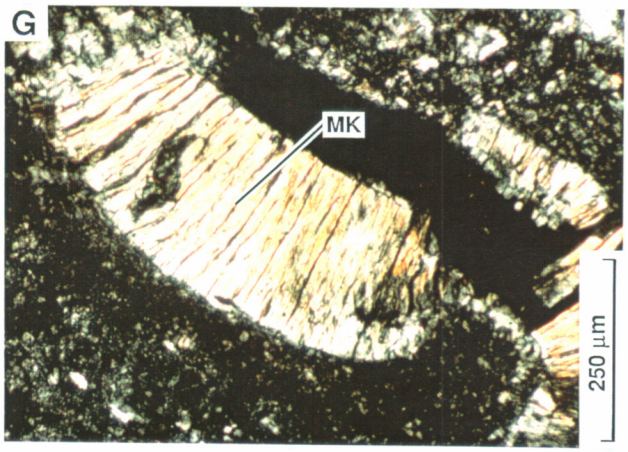
G
MK
250 µm

GRANITE G1
GEOCHEMISTRY

Sample	Type	XRF SiO2 %	XRF TiO2 %	XRF Al2O3 %	XRF Fe2O3 %	XRF MgO %	XRF CaO %	XRF Na2O %	XRF K2O %	XRF P2O5 %	XRF MnO %	XRF S %	GRV H2O+ %	GRV H2O- %	GRV CO2 %	- Total %	GRV S.G. %
MJ8	Fresh	76.94	0.06	12.35	1.14	0.14	0.18	3.22	4.91	0.03	0.04	0.00	0.57	0.25	0.02	99.81	2.49
MJ10	Fresh	77.11	0.06	12.76	0.65	0.17	0.19	2.73	5.05	0.01	0.01	0.00	0.94	0.42	0.02	100.10	2.41
MJ6	Sap	70.06	0.07	17.81	0.63	0.24	0.11	0.36	4.43	0.02	0.01	0.00	4.79	1.11	0.06	99.69	1.98
MJ7	Sap	72.80	0.08	16.86	0.47	0.23	0.11	0.29	2.58	0.01	0.01	0.00	5.01	1.40	0.03	99.87	1.83
MJ9	Sap	73.63	0.08	16.71	0.48	0.24	0.12	0.30	2.30	0.01	0.01	0.00	4.67	1.25	0.03	99.83	1.86
MJ11	Sap	73.30	0.07	15.47	0.75	0.17	0.10	0.35	5.18	0.01	0.01	0.00	3.53	0.83	0.15	99.91	1.90

Fresh = Fresh Granite; Sap = Saprolite

Sample	Type	XRF Ba ppm	XRF C e ppm	XRF Cr ppm	XRF Cu ppm	XRF Nb ppm	XRF Nl ppm	XRF P b ppm	XRF Rb ppm	XRF S n ppm	XRF Sc ppm	XRF Sr ppm	XRF V ppm	XRF Y ppm	XRF Zn ppm	XRF Zr ppm
MJ8	Fresh	52	61	0.50	0.50	12	0.50	25	414	15	0.50	23	1	68	28	90
MJ10	Fresh	52	57	0.50	5	13	2	27	424	15	0.50	23	1	69	33	93
MJ6	Sap	66	75	2	5	12	0.50	48	364	20	0.50	17	4	66	26	104
MJ7	Sap	70	26	1	8	13	0.50	36	217	20	0.50	14	3	71	37	125
MJ9	Sap	66	15	2	8	15	0.50	34	200	25	0.50	14	3	77	36	128
MJ11	Sap	64	46	0.50	9	14	0.50	28	461	45	0.50	17	4	43	35	96

Metamorphic Grade	:	Amphibolite Facies
Structural Attributes	:	Relatively Undeformed
Gross Features	:	Veins of quartz and 'sandstone' dykes
Profile Truncation	:	No truncation
Depth to Fresh Rock	:	>30 m
Location	:	Barr-Smith Range, Western Australia
Reference	:	Butt, 1985

Geomorphology and regolith

The Barr-Smith Range is a south-east trending line of breakaways that extend in an arc for over 100 km, terminating 93 km, south south-east of Wiluna. The range is underlain by granitic bedrock, weathered to a depth of 30 m or more. There are a few fresh or near fresh outcrops on the pediments (granite, granodiorite and tonalite) but these may not necessarily represent the parent material for the weathered rocks.

The weathered profile consists of kaolinized saprolites with upper horizons of silcrete, sandstone and grit. Ferruginous materials are generally absent. Saprolites and sandstones are surface hardened by exposure and, near the tops of breakaways, show some ferruginization, generally only as a thin surface Fe-oxide coating. There are no massive or pisolitic ferruginous horizons. Ferruginous pisolites have formed in the sand plains and unconsolidated sediments back from the breakaways and are rarely seen on the escarpment. The pisolites (0.1-15 mm) are dominantly argillaceous, with those greater than 4 mm being more ferruginous.

The upper surface of the Range, mantled by sand plains with aeolian characteristics, is being eroded by pedimentation under the present semi-arid climate. The sand plains are separated from the breakaways by up to 500 m of partly stripped pavements of silcrete, silcrete rubble, cemented sandstone and hardened granitic saprolite. The breakaways have near-vertical falls (3-18 m) and are generally slightly undercut, with a lower debris slope which merges into an upper pediment, crossed by numerous drainage channels. The Waterfall Profile has exposed a saprolite to colluvial sandstone section, complete with quartz vein and stone line, in a small gorge and there is a vertical face of about 7 m. At Dam Bore, silcrete columns are exposed, penetrating saprolite.

Waterfall profile

Kaolinitic granitic saprolite is exposed at the base which passes gradationally into sandstone at the top. A quartz vein may be traced upwards, where it becomes disorganized (Figure G2-1A) and terminates in a stone line. The fabric of the weathered granite is perfectly preserved at the base but, further up, where the quartz vein becomes disorganized, quartz grains of the saprolite become closely packed. About 800 mm below the stone line, all granitic fabric has been destroyed and the rock has the fabric of a sandstone with identical characteristics above and below the stone line. Silcrete occurs as a discontinuous horizon 100-300 mm thick about 500-800 mm below the stone line and is associated with pebbles and cobbles in the overlying sandstones. Above the stone line, the sandstone is transported; the stone line formed beneath a creeping mass of soil or colluvium. The quartz vein and its derived stone line are evidence of a complete residual profile, and the profile shows a gradational, *in situ* change from granitic saprolite to silcrete and sandstone. The changes from granitic to sandstone fabric are illustrated in Figure G2-2

Saprolite: The kaolinitic granitic saprolite shows relict fabrics after original feldspar (specimen 01-4989). There are two varieties of clay: a grey, streaky kaolinite, probably after microcline

perthite, and a finer grained kaolinite, very rich in included sericite, probably after plagioclase (Figures G2-2A, B, C). Numerous compound crystals of granitic quartz are set in the clay mass.

Higher in the profile (01-4991), the plagioclase-related kaolinite is still very fine-grained but is poorer in sericite and forms equant patches. The streaky fabric of the K-feldspar-related kaolinite hints at its perthitic origin and it is interstitial to the fine-grained kaolinite. Compound patches of unaltered granitic quartz are set in this inhomogeneous mass of clays. There does not appear to have been any significant decrease in the clay content, although the fabric has been weakly impregnated with aluminosilicate cement which, being isotropic, partly obscures the domain fabrics and 'books' of the kaolinite matrix (Figures G2-2D, E, F). This aluminosilicate cement may have originally been amorphous allophane but high-resolution electron microscopy shows that it is now recrystallized, on a sub-micron scale, to a mixture of kaolinite, opaline silica and anatase (Butt, 1983; Singh, Gilkes and Butt, 1992). The profile shows a progressive upward *in situ* change from kaolinitic saprolite with a granite fabric to a variably cemented quartz sand below the stone line.

Pedolith - silcrete: Higher still, but below the stone line (Figure G2-1A), there has been considerable collapse of the quartz fabric, due to removal of some kaolinite by dissolution and the granite fabric is lost, leaving, in part, a clast-supported quartz breccia (01-4992). The quartz grains are disrupted, corroded and more closely spaced. In places, the matrix to the quartz is fine-grained kaolinite, in others aluminosilicate cement has replaced the kaolinite. After a clast-supported material was achieved, further removal of kaolinite left voids, which were subsequently filled with aluminosilicate cement.

From 800 mm below the stone-line, the near-vertical quartz vein has partly collapsed and appears folded and 'crumpled'. Just below where the quartz vein becomes partly disaggregated, silcrete is partly developed. Intergranular voids are filled by both QAZ-cement[1] and strongly banded aluminosilicate (Figure G2-2G, H, I). Anatase is in part intergrown with quartz and concentrated around voids. The abundance of aluminosilicate cement increases upwards (specimen 01-4993). The QAZ-cemented silcretes have an unsupported or floating fabric (Figure G2-2H) but, as the proportion of brown aluminosilicate rises, the framework becomes grain-supported and more densely packed (specimen 01-4995; Figures G2-2J, K, L).

The medium-grained sandstones above the silcrete layer consist of poorly-sorted angular to sub-rounded quartz grains, mostly as single crystals. There are a few discrete masses of yellowish anatase, after ilmenite, throughout. The cement is predominantly colloform aluminosilicate, consisting of siliceous allophane, and/or kaolinite with opaline silica. There is some minor QAZ-cement, mainly associated with the larger quartz clasts, incorporating very fine, angular quartz, adhering to upper surfaces and penetrating fine cracks (specimen 01-4997). Some coarse grains with this QAZ-cement define weak, sub-horizontal layers.

Colluvial Material. There is no distinct change in the sandstone fabric above the stone-line, even though it is the contact between residual and transported material. The quartz grains become smaller, more closely packed and more rounded from about 1 m above the stone-line. The amount of QAZ-cement decreases but a few pebbles of QAZ-cemented silcrete (<30 mm) are present. Although apparently rounded, the pebble boundaries are irregular in detail, with sub-angular quartz grains protruding into the enclosing aluminosilicate cement. The sandstone is stained brown by goethite (specimen 01-4999) near the surface.

---

[1]The porous QAZ cement consists of zircons (1->20 μm), in a groundmass of quartz and anatase (Butt, 1983; Butt, 1985). QAZ-cements appear to have formed by physical illuviation, concentrating zircon, although there also appears to have been some chemical activity (etching of quartz and zircons, precipitation of cryptocrystalline quartz and intergrowth of anatase) under continued acid conditions but a more arid climate with impeded drainage. QAZ-silcretes are less common south of 30°S on the Yilgarn Block.

Cements. The QAZ-cemented silcretes and the aluminosilicate-cemented sandstones are layered at three scales. The QAZ-cement is abundant in a horizon 500-800 mm below the stone-line (Figure G2-1A), but it becomes less abundant above, where aluminosilicate cements predominate. The QAZ-cement forms sub-horizontal layers in the silcrete horizon (Figure G2-1A) that cement very poorly sorted quartz grains, the smaller grains being very angular. Each QAZ layer is overlain by an aluminosilicate-cemented layer (Figure G2-1C) enclosing poorly-sorted quartz, but generally without very fine, angular grains. The aluminosilicate cement is colloform and appears to be a late void infilling above earlier QAZ-cementation. The QAZ-matrix is segregated into portions complementarily richer and poorer in anatase and quartz.

Dam Bore profile

Thick silcretes and sandstone-silcrete columns penetrate the saprolite at Dam Bore. These columns reach 3 m depth, are 1-1.5 m in diameter and 1-4 m apart. At the top, the columns merge laterally into a continuous silcrete-sandstone sheet (Figure G2-1B). Some columns show a horizontal lamination towards the base as thin mm scale layers and segregations of QAZ-cement; the skeletal quartz grains show no other lamination. The boundaries of the columns appear to be sharp but, generally, the adjacent saprolite has been partly eroded and the contacts themselves are not preserved. The erosion generally results in marked undercutting with caves and natural bridges supported by silcrete columns. The sandstone columns were formed by solution of kaolinite along preferred zones in the saprolite and this was followed by settling of resistant quartz grains, supplemented by quartz sand from above.

The rough pavement above the breakaways exposes sandstone, silcrete and hardened saprolite and is strewn with quartz and silcrete pebbles and boulders. The tops of some sandstone columns are exposed close to the edge of the scarp. Quartz veins preserve their attitude in the sandstone and silcretes as in the underlying saprolite which indicates the sandstones and silcretes formed *in situ* and the profiles are essentially residual. Some veins are partly disrupted at the surface, with a scatter of quartz fragments derived from them cemented into the adjacent sandstone. By analogy with the Waterfall profile, the disruption of the veins is considered to be at the stone-line and hence the Dam Bore profiles are somewhat truncated.

Fresh rock: In the fresh granitoid (specimen 01-4979), subhedral crystals of zoned plagioclase are set in interstitial quartz and microcline. Accessory minerals are biotite and apatite. The microcline is slightly perthitic and the margins of some plagioclase grains show myrmekitic overgrowths. Microcline is poikiloblastic in specimen 01-4952.

Saprolite: The saprolites retain their granitic fabric and consist of kaolinite set with quartz grains, some of which are compound grains, the boundaries of which have become progressively separated by kaolinite. Kaolinite pseudomorphs after two feldspars are indicated by different sericite contents and by differing kaolinite granularity. In some, the kaolinite has a turbid, smoky appearance, due to permeation by aluminosilicate cement, which also fills cracks (specimen 01-4968).

Upwards, the quartz grains become increasingly disrupted, angular, ragged and corroded but also increase in overall concentration. As at the Waterfall profile, the saprolite merges to sandstone by loss of kaolinite, settling of quartz and introduction of cementing aluminosilicate. In the transition, saprolite occurs as remnants surrounded by generally quartz-rich material, showing streaking and banding resembling flow structures. Introduced aluminosilicate is patchily distributed throughout the saprolite, where it permeates and obscures the kaolinitic matrix and forms colloform void infillings. It becomes increasingly abundant upwards and is dominant in the quartz-rich bands, where marked optical orientation indicates recrystallization to kaolinite with opaline silica.

Pedolith - silcrete: In many places, the transition from saprolite to silcrete is sharp. Although this contact may appear unconformable, quartz veins continue through it, so the sandstone and silcrete must be residual. The silcretes, both in the horizontal sheets and in the vertical columns, consist of highly angular, very poorly-sorted quartz grains 'floating' in a very fine grained, cream-coloured QAZ cement. Although some large grains are rounded, the shard-like smaller quartz grains tend to have re-entrant, ragged surfaces, suggesting corrosion. In some Ti-rich silcretes, the cement forms rounded blebs, <1 mm diameter, rich in anatase and zircon, surrounded by slightly more quartzose material. Large zircons show preferential solution of some zones. The cement separates individual quartz crystals and penetrates fine cracks in optically continuous crystals, separating them into highly angular fragments.

The silcrete layers are up to 1.0 m thick and are transitional upwards to medium- or coarse-grained sandstone and grit, cemented by aluminosilicate. In the transitional zone, which is also present within the columns, there are ill-defined bands of QAZ-cemented silcrete and aluminosilicate-cemented sandstone; on the margins of such bands, intergranular voids are filled by both cements, generally aluminosilicate overlying QAZ. The amount of QAZ cementation declines upwards, with very minor quantities throughout the sandstone, adhering to the upper surfaces of larger grains and penetrating along cracks.

The sandstone and grit are generally less well cemented and less massive than the silcretes, with an irregular fracture. Their quartz grains are sub-angular to sub-rounded, are individual crystals with a closely packed, framework supported fabric. Intact quartz veins indicate these materials are essentially *in situ*. The cement is predominantly colloform aluminosilicate, partly crystallized to kaolinite and opaline silica; some narrow cracks are infilled by opaline silica alone. Ilmenite relics, now anatase, are common.

Mineral stability

As the fresh rock and saprock are not exposed, the feldspars and minor mafic minerals are all completely weathered to kaolinite at the exposed base of the profile. Quartz is the only mineral to survive and even it is split into shards and corroded by the QAZ cement. This cement is later dissolved and is, in part, replaced by aluminosilicate (allophane) cement, which subsequently recrystallizes to opaline silica, kaolinite and anatase on a sub-micron scale.

There appear to have been at least four phases in the development of the profile:- (i) formation of a kaolinitic saprolite - quartz sand profile under acid, humid conditions; (ii) Cementation by QAZ cement, under continued acid conditions but a more arid climate with impeded drainage, and its later partial dissolution; (iii) cementation by an aluminosilicate (first precipitated as a gel) and its subsequent recrystallization, and (iv) erosion and exposure. Kaolinization of the bedrock probably continued throughout, but may have been most active during the first phase.

QAZ-silcretes are widely distributed over granitic rocks in the north-eastern Yilgarn Block but they are of restricted geomorphic occurrence. They form duricrust protected cuesta-like landforms. Their prominence in outcrop tends to belie their true abundance as their extent back from these scarps may not be great (100-200 m). Sandstones and saprolites with aluminosilicate cements have been found in outcrop and drill core over a wide area of the Yilgarn Block and elsewhere; these materials tend to disaggregate near the surface so their abundance is easily underestimated.

Geochemistry

In comparing local outcropping 'fresh' granitoids (Roddick *et al*, 1976) and from elsewhere in the north east Yilgarn Block (Davy, 1976), all samples show the expected depletion in K, Ca, Mg, Na, Mn Fe, Rb and Sr on weathering. Aluminium and Ga are relatively enriched in the saprolite,

due to Si loss during kaolinization, but they decline upward as kaolinite is destroyed. Aluminium is virtually absent in silcretes, but the sandstones contain 5-11% Al_2O_3. Although total Si contents are lower in the saprolite than in unweathered rock, silica-as-quartz , increases steadily up the profile, a largely relative enrichment due to the loss of other components, with maxima exceeding 90% in some QAZ-silcretes. Iron contents are very low in the weathered rocks, Fe having been leached from primary biotite, ilmenite and pyrite. Where Fe staining is visible, there is generally only a minor increase in total Fe as the staining is due to only a small amount of Fe oxide in the cement. The brown colour-zonation of some aluminosilicates from the Barr-Smith Range profiles, as seen in transmitted light, appears due to variations in Ti.

Concentration of Ti and Zr, with Nb, Pb, Th, U, V and Y, occurs particularly in the silcretes with maxima >5% TiO_2 and >5000 ppm Zr. This is due to relative enrichment during weathering with some absolute enrichment Accurate mass balance calculations are difficult to make as silicon (as quartz), Ti and Zr have been physically and chemically mobile.

References

Butt, C.R.M. 1985. Granite weathering and silcrete formation on the Yilgarn Block, Western Australia. Australian Journal of Earth Sciences, 32: 415-432.

Davy, R. 1976. Geochemical variations in Archaean granitoids in part of the northeast Yilgarn Block. West Australian Geological Survey Annual Report for 1975. 137-142

Butt, C.R.M. 1983. Aluminosilicate cementation of saprolites, grits and silcretes in Western Australia. Journal of the Geological Society of Australia. 30: 179-186.

Roddick, J.C., Compston, W., and Durney, D.W. 1976. The radiometric age of the Mt. Keith granodiorite, a maximum age estimate for an Archaean greenstone sequence in the Yilgarn Block, Western Australia. Precambrian Research. 3: 55-78.

Singh, B., Gilkes, R.J. and Butt, C.R.M. 1992. Micromorphology and composition of an aluminosilicate cement in silcrete. 9th International working meeting on soil micromorphology, Townsville, Australia.

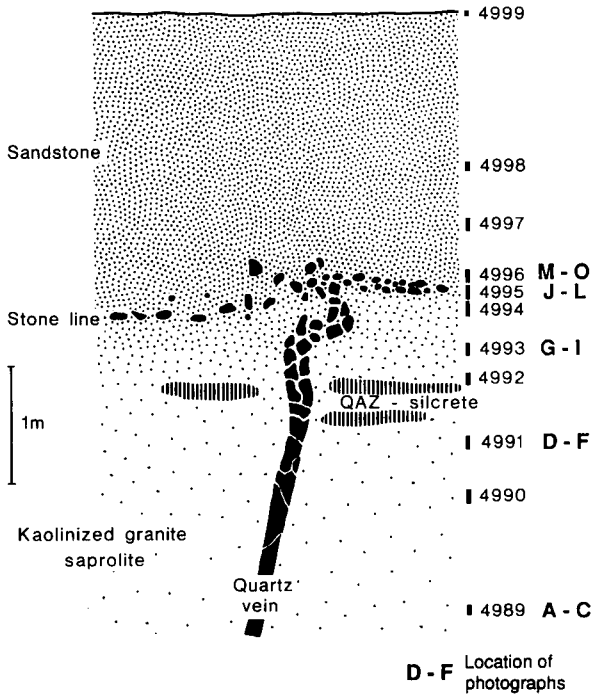

Figure G2-1A. Quartz vein in granite saprolite and arenose materials - Waterfall profile.

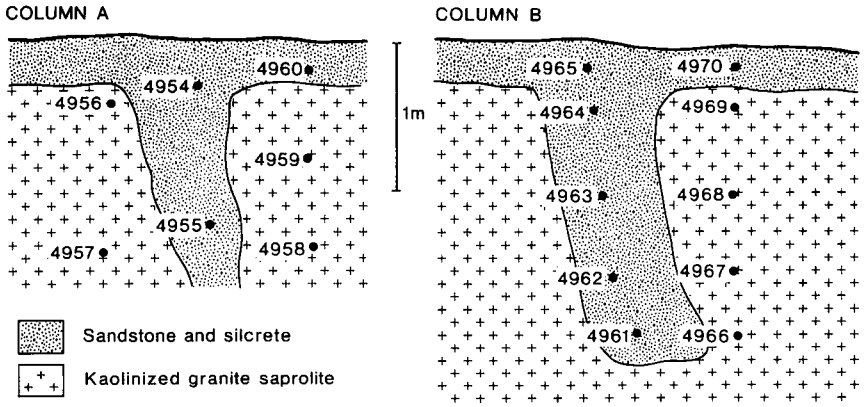

Figure G2-1B. Silcrete and sandstone columns penetrating granitic saprolite - Dam Bore profile.

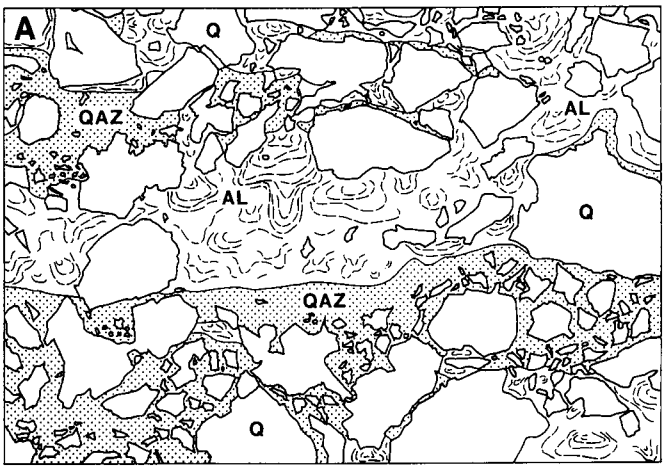

Figure G2-1C. Colloform aluminosilicate cement overlying QAZ cement; field width 750 µm.

FIGURE G2-2

Pedolith - Silcrete

M Large and small shard-like to subangular quartz grains (QZ) are closely packed in a slightly porous aluminosilicate cement (AC). Close-up photograph of 'dry' surface.

N The quartz grains (QZ) are clast-supported, are more closely packed than K and are set in an aluminosilicate cement (AC). Specimen 01-4996. Polished section in oblique reflected light.

O Closely packed, shard-like to subangular quartz grains (QZ) are cemented by pale brown aluminosilicate (AC). Specimen 01-4996. Photomicrograph in plane polarized light.

J Large and small angular quartz grains (QZ) are closely packed in a slightly porous aluminosilicate cement (AC). Specimen 01-4995. Close-up photograph of 'dry' surface.

K The quartz (QZ) grains are more closely packed (compare to H) and are set in an aluminosilicate cement (AC). Specimen 01-4995. Polished section in oblique reflected light.

L Angular to shard-like quartz grains (QZ) are set in brown aluminosilicate cement (AC). Specimen 01-4995. Photomicrograph in plane polarized light.

G The angular quartz fragments (QZ) are more closely packed than in the saprolite (D) and are set in creamy QAZ cement (ZQ) and in white aluminosilicate cement (AC). Specimen 01-4993. Close-up photograph of 'dry' surface.

H Matrix-supported angular quartz fragments (QZ) are set in alternating lenses and layers of QAZ cement (ZQ) and banded aluminosilicate cement (AC). Specimen 01-4993. Polished section in oblique reflected light.

I Angular quartz grains (QZ) are set in an early, black, QAZ (ZQ) cement and a later, banded aluminosilicate cement (AC). Specimen 01-4993. Photomicrograph in plane polarized light.

Saprolite

D Quartz crystals (QZ) of compound quartz clusters show early separation by thin layers of kaolinite (KS). The spaces between kaolinite pseudomorphs (KA) after plagioclase are filled with an aluminosilicate cement (AC). Specimen 01-4991. Close-up photograph of 'dry' surface.

E Quartz crystals (QZ) of compound quartz clusters show early separation by thin layers of kaolinite (KS). The spaces between kaolinite pseudomorphs after plagioclase (KA) are filled with an aluminosilicate cement (AC). Specimen 01-4991. Photomicrograph with crossed polarizers.

F Flaky kaolinite with included muscovite (KA) after plagioclase and interstitial low birefringent kaolinite (KB) after K-feldspar and quartz grains (QZ). The compound quartz grains are separated by kaolinite (KS) and aluminosilicate cement (AC). Specimen 01-4991. Photomicrograph with crossed polarizers.

A Grey and brown granitic quartz (QZ) and two types of kaolinite, a white, massive type after plagioclase (KA) and a pale grey interstitial type after K-feldspar (KB). Specimen 01-4989. Close-up photograph of 'dry' surface.

B Flaky kaolinite, after plagioclase (KA) is set with complex quartz grains (QZ) which have sutured margins. The margins of one grain shows the first signs of separation (QS). A few low-birefringent patches of kaolinite (KB) are after K-feldspar. Specimen 01-4989. Photomicrograph with crossed polarizers.

C Kaolinite after two types of feldspar, (i) streaky, low birefringent kaolinite (KB) from microcline microperthite probably contains some K-feldspar remnants and (ii) coarser-grained, more birefringent kaolinite (KA) from plagioclase, containing remnant sericite. Specimen 01-4989. Photomicrograph with crossed polarizers.

FIGURE G2-2

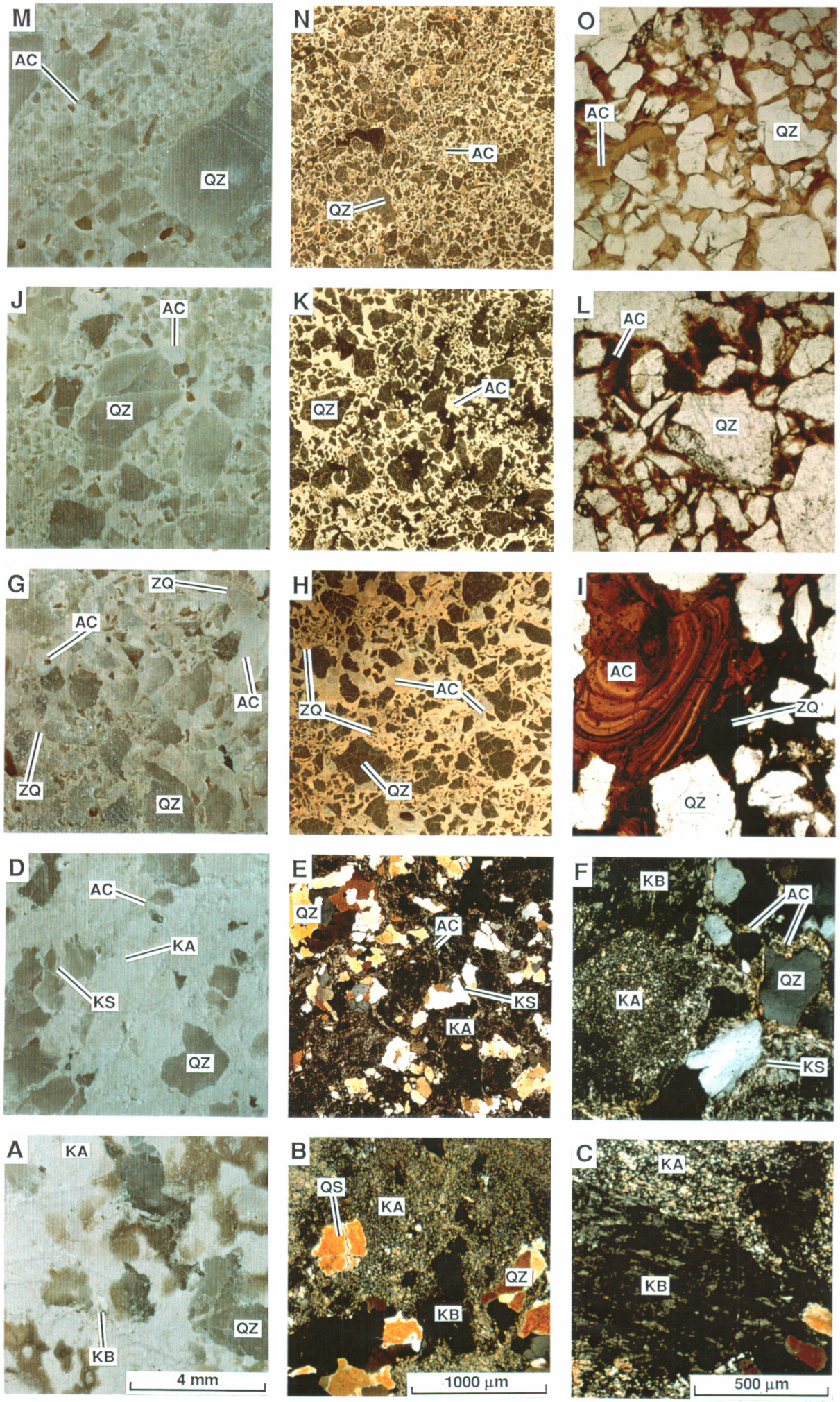
M
AC
QZ
N
AC
QZ
O
AC
QZ
J
AC
QZ
K
AC
QZ
L
AC
QZ
G
ZQ
AC
AC
ZQ
QZ
H
AC
ZQ
QZ
I
AC
ZQ
QZ
D
AC
KA
KS
QZ
E
QZ
AC
KS
KA
F
KB
AC
QZ
KA
KS
A
KA
QZ
KB
4 mm
B
QS
KA
QZ
KB
1000 µm
C
KA
KB
500 µm

GRANITE G2
GEOCHEMISTRY

Sample	Depth cm	Type	XRF SiO2 %	XRF Al2O3 %	XRF Fe2O3 %	XRF MgO %	XRF CaO %	XRF Na2O %	XRF K2O %	XRF TiO2 %	XRF LOI %	INAA Ag ppm	INAA As ppm	INAA Au ppb	XRF Ba ppm	INAA Br ppm	INAA Ce ppm	XRF Co ppm	XRF Cr ppm	INAA Cs ppm	XRF Cu ppm	INAA Eu ppm	XRF Ga ppm
01-4960	25	Ssil-A	87.67	2.99	0.23	0.07	0.05	<.01	0.02	6.13	1.87	4	226	4	163	1.6	21.1	89	24	1.0	0	0.7	16
01-4954	40	Ssil-A	89.87	2.90	0.09	0.02	0.05	<.01	0.02	2.55	2.00	3	143	3	266	1.2	5.2	108	11	0.6	0	0.1	11
01-4955	140	Ssil-A	85.42	4.22	0.14	0.12	0.03	0.28	0.05	4.81	3.43	3	370	6	96	1.4	7.1	137	19	0.6	3	0.2	24
01-4956	40	Sap-A	71.60	16.81	0.23	0.05	0.05	<.01	0.02	1.12	7.96	4	866	5	72	2.5	3.9	71	15	0.6	1	0.1	53
01-4959	90	Sap-A	62.01	23.75	0.15	0.05	0.05	0.02	0.03	1.26	10.59	3	102	3	233	0.5	5.1	31	14	0.5	1	0.4	110
01-4957	140	Sap-A	60.71	25.00	0.22	0.05	0.04	0.02	0.01	1.30	11.04	3	425	5	42	1.3	3.0	36	11	0.6	2	0.2	93
01-4958	150	Sap-A	56.71	28.50	0.36	0.09	0.05	<.01	0.03	0.35	12.11	4	241	4	10	0.7	5.2	29	10	0.8	6	0.1	119
01-4970	25	Ssil-B	87.70	6.17	0.39	0.04	0.05	0.01	0.02	1.62	3.06	2	1	4	56	0.8	6.2	86	5	0.4	5	0.2	24
01-4965	30	Ssil-B	93.54	0.34	0.10	0.07	0.03	<.01	0.01	3.74	0.43	3	1	6	97	1.0	13.0	146	10	0.6	0	0.4	4
01-4964	60	Ssil-B	88.85	5.68	0.30	0.05	0.04	<.01	0.02	1.16	2.88	5	14	6	103	1.0	23.1	118	9	5.2	0	0.5	17
01-4963	110	Ssil-B	89.67	5.30	0.26		0.04	0.01	0.02	1.15	2.74	5	17	6	48	1.0	19.1	119	6	1.1	11	0.5	19
01-4962	160	Ssil-B	91.51	0.32	0.15	0.06	0.04	<.01	0.03	5.61	0.89	5	79	13	241	2.0	13.6	164	16	0.8	0	0.1	2
01-4961	210	Ssil-B	88.47	0.95	0.22	0.12	0.03	<.01	0.17	8.31	1.01	5	298	49	186	0.9	15.9	136	25	0.9	0	0.2	8
01-4969	60	Sap-B	65.77	22.23	0.55	0.06	0.04	0.01	0.02	1.70	9.78	2	1	3	76	0.8	6.0	34	12	0.3	2	0.2	102
01-4968	110	Sap-B	59.93	26.28	0.52	0.12	0.04	<.01	0.03	2.15	11.05	2	1	3	49	0.6	5.6	30	14	0.3	0	0.2	105
01-4967	160	Sap-B	61.17	26.00	0.39	0.04	0.04	<.01	0.04	0.94	11.36	2	0	2	388	0.5	4.5	17	7	0.3	4	0.1	114
01-4966	210	Sap-B	60.71	26.08	0.51		0.04	<.01	0.08	1.14	11.57	2	1	3	120	1.4	5.2	20	11	0.4	4	0.1	101
01-4952	-	FGran	68.47	14.88	2.09	0.71	2.29	0.17	2.26	0.36	0.79	3	104	3	982	0.6	3.9	87	0	0.6	1	0.1	22
01-4979	-	FGran	68.78	14.97	2.78	0.88	2.14	4.97	2.98	0.41	0.93	5	1	8	970	1.3	191.9	100	0	3.9	71	2.0	22
01-4999	250	Ssil	88.10	6.38	0.37	0.24	0.06	0.01	0.08	0.61	3.19	2	1	4	252	1.8	3.1	7	17	0.4	16	0.1	15
01-4998	80	Ssil	89.22	5.51	0.23	0.03	0.09	<.01	0.03	0.22	3.18	3	1	4	613	0.9	2.5	25	6	0.4	4	0.1	11
01-4997	50	Ssil	89.08	6.35	0.21	0.09	0.14	<.01	0.04	0.29	3.55	2	1	5	242	1.2	8.2	13	5	0.8	0	0.3	13
01-4995	5	Ssil	89.62	5.21	0.22	0.12	0.08	<.01	0.03	0.70	3.24	2	1	5	127	0.8	3.0	21	6	0.4	0	0.2	14
01-4996	5	Ssil	90.33	4.97	0.18	0.08	0.10	<.01	0.04	0.28	3.02	2	1	5	142	1.9	3.0	11	3	0.9	3	0.1	12
01-4994	-15	Ssil	89.42	5.10	0.21	0.09	0.09	<.01	0.03	1.00	3.27	3	1	5	149	2.0	7.0	17	6	0.5	4	0.2	15
01-4993	-50	Ssil	87.75	5.43	0.25	0.10	0.06	<.01	0.04	2.77	3.24	3	1	5	333	0.8	11.6	22	18	0.6	0	0.3	16
01-4992	-80	Ssil	88.26	3.19	0.20	0.06	0.12	0.01	0.06	4.26	2.50	3	1	5	175	0.9	19.1	16	17	0.6	1	0.4	12
01-4991	-140	Sap	72.47	17.89	0.54	0.01	0.10	0.01	0.73	0.40	7.19	2	1	4	126	0.8	4.7	5	12	1.7	1	0.2	51
01-4990	-190	Sap	68.41	18.86	1.34	0.51	0.05	0.07	2.51	0.34	6.15	3	1	4	707	1.5	0.7	7	11	4.8	1	0.1	77
01-4989	-290	Sap	67.13	21.29	0.81	0.17	0.06	0.03	0.88	0.38	8.38	2	1	4	173	0.7	4.3	2	11	0.9	8	0.2	29

FGran = Fresh Granitoid; Sap = saprolite; Ssil = sandstone or silcrete

GRANITE G2
GEOCHEMISTRY

Sample	XRF Ge ppm	INAA Hf ppm	INAA Ir ppb	INAA La ppm	INAA Lu ppm	XRF Mn ppm	INAA Mo ppm	XRF Nb ppm	XRF Ni ppm	XRF Pb ppm	XRF Rb ppm	INAA Sb ppm	INAA Sc ppm	XRF Se ppm	INAA Sm ppm	XRF Sn ppm	XRF Sr ppm	INAA Ta ppm	XRF Th ppm	INAA U ppm	XRF V ppm	XRF Y ppm	INAA Yb ppm	XRF Zn ppm	XRF Zr ppm
01-4960	0	1.2	10.70	9.0	0.2	14	4	147	0	16	0	1.4	17.2	2	2.4	13	3	0.6	39	1.5	116	18	1.5	6	1319
01-4954	0	0.2	8.40	2.2	0.1	0	3	60	0	17	0	0.7	7.0	1	0.5	3	2	0.3	25	1.1	42	12	0.3	4	1308
01-4955	0	0.4	8.60	2.9	0.1	13	4	105	0	10	0	1.4	7.3	0	0.6	19	2	0.4	25	1.3	80	11	0.4	2	752
01-4956	1	0.4	10.20	2.1	0.0	0	4	24	0	3	0	3.0	7.5	0	0.5	5	0	0.4	10	1.6	24	5	0.3	1	226
01-4959	2	0.2	6.40	2.4	0.0	7	3	29	0	6	2	2.3	5.1	0	0.6	5	4	0.3	8	0.9	32	2	0.4	5	227
01-4957	1	0.3	13.90	1.8	0.0	5	3	29	0	4	0	1.5	6.5	0	0.4	2	1	0.4	9	1.3	22	4	0.3	2	232
01-4958	1	0.4	8.80	2.1	0.0	10	3	9	2	5	1	1.0	9.8	0	0.5	4	0	0.4	5	1.2	15	0	0.5	4	147
01-4970	0	13.3	10.80	3.8	0.3	2	8	39	0	5	0	0.5	3.7	0	0.9	6	3	4.8	13	4.9	16	7	1.2	1	609
01-4965	0	49.0	14.10	3.5	0.7	8	20	91	0	12	0	1.1	9.1	4	1.3	4	3	11.0	32	11.7	55	18	3.7	3	2225
01-4964	0	1.8	11.50	11.0	0.2	0	4	26	0	3	0	0.2	27.2	1	2.4	1	1	0.9	9	1.5	20	4	1.5	0	485
01-4963	0	1.6	11.50	9.5	0.2	7	4	25	0	3	0	0.6	22.5	1	2.0	3	2	0.6	8	1.5	16	4	1.4	0	328
01-4962	0	1.4	10.60	6.5	0.2	2	4	172	0	25	0	0.4	19.4	6	1.4	9	4	0.5	36	1.4	78	43	1.1	4	5417
01-4961	0	1.3	10.70	7.0	0.1	18	4	236	0	39	7	3.3	20.9	2	1.7	18	13	0.5	39	1.5	136	22	0.8	7	2232
01-4969	1	6.3	7.20	3.7	0.2	8	7	36	0	5	1	0.4	2.9	0	0.8	8	3	4.0	13	4.3	28	5	1.1	1	307
01-4968	2	8.2	7.50	4.1	0.2	2	9	50	0	5	0	0.6	3.5	0	0.8	15	0	5.1	12	4.9	43	7	1.5	5	388
01-4967	1	4.8	6.10	3.1	0.1	1	7	24	0	5	2	0.2	2.0	0	0.6	16	2	2.8	6	3.7	18	3	0.8	4	225
01-4966	2	5.5	6.30	2.7	0.1	7	8	26	0	3	2	0.3	2.3	0	0.6	5	7	2.7	9	4.8	29	3	1.0	5	257
01-4952	0	0.4	7.70	2.3	0.0	391	3	5	0	24	101	0.7	7.6	0	0.5	0	400	0.3	17	1.1	21	19	0.3	57	185
01-4979	0	4.6	16.00	122.4	0.4	374	6	16	14	27	162	0.2	3.9	0	14.4	0	473	1.4	32	3.2	28	43	2.6	83	224
01-4999	0	4.5	11.20	1.6	0.2	11	5	10	0	5	1	0.4	3.5	0	0.4	6	4	1.7	11	1.5	17	2	0.6	1	246
01-4998	0	2.7	11.80	1.5	0.1	38	5	3	0	9	2	0.1	2.0	0	0.4	0	15	1.9	5	1.5	3	1	0.5	4	143
01-4997	0	2.4	12.40	5.6	0.2	27	7	5	0	11	2	0.2	2.3	1	1.2	1	11	2.1	4	1.6	6	6	0.7	4	138
01-4995	0	3.8	12.50	2.8	0.2	45	4	12	0	9	2	0.3	2.7	2	0.7	1	9	3.1	8	1.9	8	5	0.8	5	209
01-4996	0	2.2	12.70	2.7	0.2	28	7	7	0	5	2	0.3	2.0	1	0.8	1	5	2.5	6	1.7	1	2	0.5	3	136
01-4994	0	6.7	13.40	4.0	0.3	71	4	21	0	8	2	0.4	4.0	2	1.0	2	11	3.9	15	3.0	14	8	1.0	6	352
01-4993	0	19.0	13.50	3.1	0.4	15	12	55	5	10	0	0.8	9.3	1	1.3	4	10	6.4	31	6.8	41	14	2.1	3	868
01-4992	0	20.2	13.80	6.5	0.5	86	18	88	3	15	1	1.0	11.4	2	1.6	5	13	9.0	27	10.3	71	15	2.8	6	894
01-4991	0	3.3	10.70	5.4	0.1	180	4	7	0	8	53	0.1	2.4	0	0.8	0	11	1.6	3	1.5	17	5	0.5	9	170
01-4990	0	3.3	11.10	0.4	0.1	50	5	8	0	1	200	0.1	2.7	0	0.2	0	6	0.4	2	2.9	33	1	0.4	18	169
01-4989	1	4.0	10.60	1.5	0.1	32	7	5	0	3	71	0.2	2.8	0	0.4	1	4	1.1	4	1.7	23	3	0.4	8	193

Metamorphic Grade	:	-
Structural Attributes	:	-
Gross Features	:	Gravel layers near base
Profile Truncation	:	Colluvial top part of profile only
Depth to Fresh Rock	:	Unknown
Location	:	Tammin, Western Australia
Reference	:	Stace *et al.*, (1968).

Geomorphology and regolith

Plains of yellow-brown clay sand (Figure G3-1A) mantle a large part of the granitic terrain of the Yilgarn Block of SW Australia. This sandy material, which is the product of colluviation of a granite arenose zone, dominates the upper regolith of many of the drainage divides and is particularly extensive on the watershed between the Avon, draining to the west, and the eastward trending drainages of the Goldfields. The plains form broadly undulating tracts with lateritic duricrust and ferruginous gravels on the crests and thick sand sheets that extend to the adjacent valley floor. Away from the major divides, the sandplains become increasingly fragmented and here are, in part, flanked by breakaways and associated erosional terrain.

The colluvial sands, which tend to thicken down slope from the laterite outcrops, were formed from detritus from the slight truncation of the deep weathered profiles upslope. At depth (1-2 m), bands and lenses of clearly-defined ferruginous gravels occur (Figure G3-1C, D), which support their transported origin. Although colluvial action is their most likely origin, reworking by aeolian action is suggested by rare, linear dunes. Their origin as a transported mantle contrasts with earlier suggestions that they are the upper parts of an ancient soil profile. They generally show minimal pedogenic differentiation so it would seem they are relatively young soils developed on highly weathered granitic parent material (sandy colluvium). In places their colluvial nature is clear, where they rest directly on a truncated saprolite profile (Figure G3-1B) but, in most locations, the underlying rocks are not exposed.

Some mottling occurs in the subsoil of these profiles and some of this has hardened into nodules. These nodules are generally not as hard as the colluvial gravels, nor are they clearly differentiated from the sandy matrix; they seem to have been developed *in situ,* subsequent to the deposition of the sand. The soils on this colluvium are relatively porous and friable and some show slight increases with clay at depth but very little colour change. Their pH ranges from 5.0-6.5. The sand is largely quartz but there may be an appreciable component of kaolinite-rich spherules. Kaolinite dominates the clay fraction (5-15%) and goethite and aluminosilicate are the cementing agents.

Tammin profile

This colluvial profile is exposed in a road material quarry adjacent to the Tammin Cemetery, immediately west of Tammin and north of the Great Eastern Highway. Here, about 1.5 m of light yellow, structureless sand overlies a lower layer containing strata rich in slightly ferruginous nodules (Figure G3-1D). The upper layer of sandy colluvium consists of a loosely-cemented, framework-supported mass of angular quartz, set in partly opaque, smoky-brown aluminosilicate cement. This has been lightly stained by goethite. Much of the aluminosilicate cement has recrystallized to ultra-fine kaolinite. The cement is incomplete and there are numerous irregular voids. Where disaggregated, it has the appearance of a slightly clay-bearing sand. A few well-defined, small (8 mm) nodules are set in the sandy material (Figure G3-1E). These consist of a similar mass of closely-packed quartz fragments, set in a slightly less opaque, hematite-stained aluminosilicate matrix (Figure G3-1F).

The ferruginous nodules of the lower, stratified layers consist of largely framework-supported, angular and, in places, shard-like quartz grains, set in flaky kaolinite, cemented by aluminosilicate. Some quartz grains show re-entrant angles and appear to have been corroded by the matrix. Whether or not this corrosion is real is difficult to determine, because much of the quartz was probably derived by disaggregation of interlocking, sutured, compound grains of granitic quartz. The matrix of the inside of the nodules is largely stained yellow with goethite but the rim is stained red-brown with a mixture of goethite and hematite. The inner and outer boundaries of the hematitic rim are gradational (Figure G3-1G, H). There are numerous, small, irregular voids throughout the matrix.

Mineral stability.

It seems that the aluminosilicate cement is metastable; it quickly reverts to an ultra-fine mixture of quartz and kaolinite, giving this material a variable opacity, although its banded structure remains.

Reference

Stace, H.C.T., Hubble, G.D., Brewer, R., Northcote, K.H., Sleeman, J.R., Mulcahy, M.J. and Hallsworth, E.G. 1968. Handbook of Australian soils. Rellim Technical Publications, S. Australia. p48.

FIGURE G3-1

Field appearance of sandplains over granitoids

A. A gently undulating sandplain of the wheat belt of WA. The original scrub and heath communities have been cleared for farming. Some of the swales are occupied by shallow, ephemeral lakes. Ten km north of Meckering. Photo HMC.

B. A truncated, white, kaolinized, granite saprolite (GS) overlain by yellow, colluvial granitic sands and nodular material (SS). Rail cutting, 13 km north-east of Merredin. Photo HMC.

C. A particularly dense concentration of Fe-cemented nodules (FN) at the base of a sandy soil of a sandplain (SS). This material is probably colluvial. Gravel pit, 30 km south-east of Corrigin. Photo HMC.

D. A largely structureless colluvial sand (SS), with a few, small, Fe-oxide-cemented nodules, overlying bands of layered nodules (FN). Small road-material pit, adjoining the cemetery, west of Tammin.

Detail of materials from Tammin road material quarry

E. Structureless yellow sand (SS) containing a small Fe-cemented nodule (FN) from the upper part of the profile (see SS in Figure G3-1D). The angular sand grains are cemented with goethite-stained aluminosilicate. The nodule has been more effectively cemented with hematite. Specimen Tammin 2. Close-up photograph of "wet" surface. The sand sample has been resin impregnated prior to cutting.

F. Petrographic detail of E. Angular to shard-like quartz grains (QS) are cemented by the hematite (HM) of the nodule. Outside the nodule, the sand grains are angular but less shard-like and are cemented by brown, Fe-stained aluminosilicate (AL), largely recrystallized to kaolinite. Specimen Tammin 2. Photomicrograph in plane polarized light.

G. A slightly porous, large, Fe-cemented nodule from the lower part of the profile (see FN of G3-1D). Its outer part (OP) is stained red by hematite and its inner part (IP) is yellow, due to goethite. Specimen Tammin 1. Close-up photograph of "wet" surface.

H. Petrographic detail of G. Framework-supported, angular to subrounded quartz grains (QZ), cemented by Fe-oxide-stained aluminosilicate cement (AL). The cement of the outer part is stained with hematite and that of the inner part with goethite. Specimen Tammin 1. Photomicrograph in plane polarized light.

FIGURE G3-1

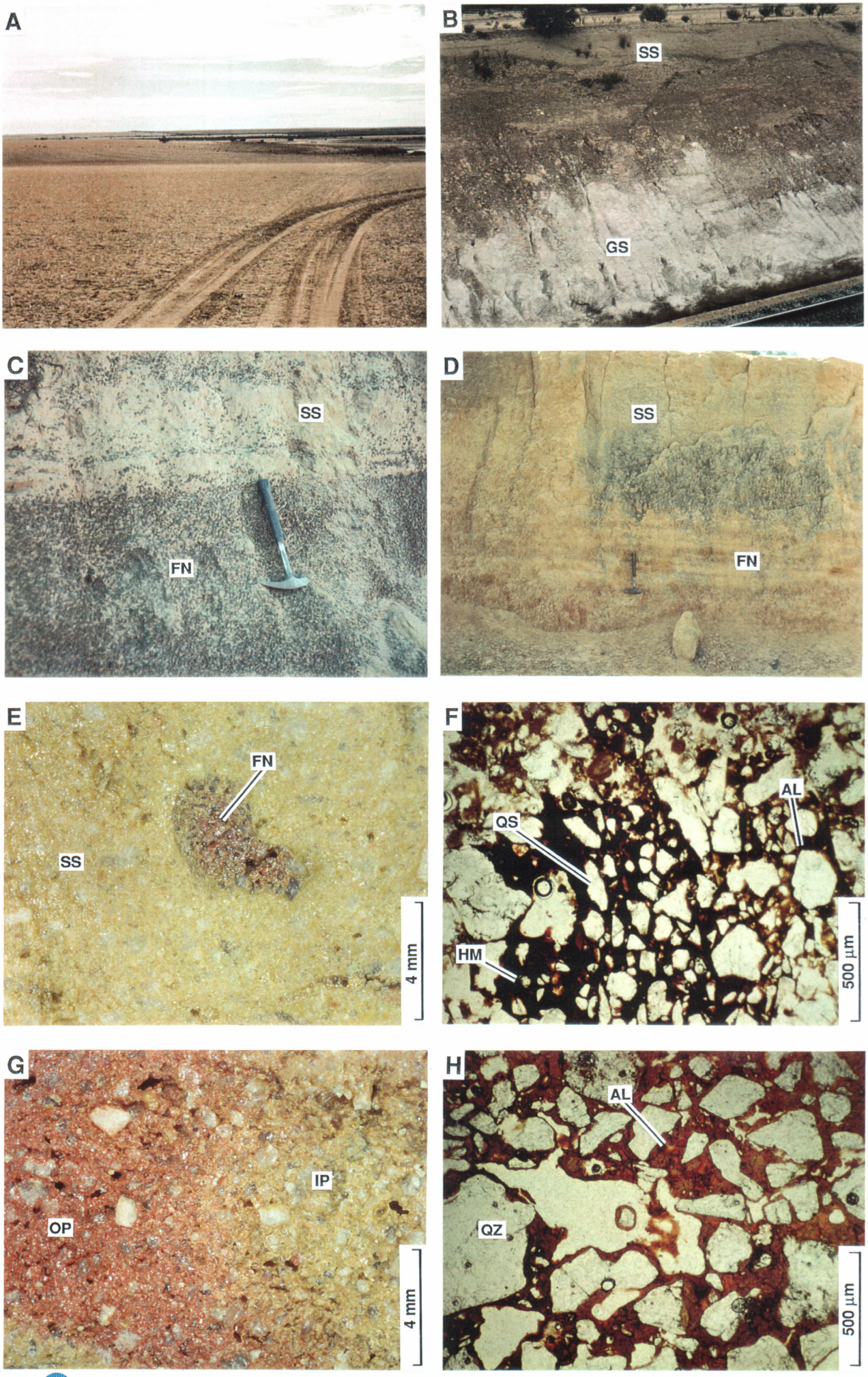

Metamorphic Grade	:	-
Structural Attributes	:	-
Gross Features	:	Stony pavement on a variety of rocks
Profile Truncation	:	Variable
Depth to Fresh Rock	:	-
Locations	:	Beasley Ck, Laverton, Western Australia, Bottle Creek, Western Australia, Lights of Israel, Davyhurst, Western Australia, Ora Banda Sill, Ora Banda, Western Australia.
References	:	Robertson, 1989; Robertson, 1990; Butt *et al.*, 1992; Robertson and Wills, 1993; Robertson, 1996a.

Definition, origin and distribution

Lag is a veneer or thin pavement of fragments of diverse origin and/or composition on the land surface; fragments may be faceted, rounded or varnished. In highly weathered terrain, the term is commonly applied to highly ferruginous concretions (Butt and Zeegers, 1992). This material also has been referred to as 'desert armour', 'surface laterite fragments', 'surface pea gravels', 'lateritic pisolites', 'ferricrete fragments' and 'loam concentrates'. Lag or lag gravel are probably the best terms.

Lag is common on the Yilgarn Craton and ferruginous lag is particularly abundant over mafic and ultramafic lithologies where it helps to protect the soil from wind erosion. It can develop by a combination of processes that concentrate stony fragments at the surface through:-

1) Residual accumulation, following preferential erosion by wind (deflation) or water (e.g., sheetwash). Such fragments were derived from above the present surface, from previously overlying laterite or soil layers.

2) Upward displacement by:-
   i) Churning related to wetting and drying of swelling clays (smectites) (see Butt, 1992; p 101-2; Figure I.6-2).
   ii) Bioturbation: by burrowing insects and animals; by root plucking.

A veneer of lag may develop over a stone-free soil and lag fragments can be transported upward through fine-grained, allochthonous (e.g., aeolian) overburden. It concentrates readily on flat areas where it is dispersed largely by sheet wash. Thus, lag may represent either the underlying material or a largely-removed, pre-existing lateritic or other cover. It has considerable geochemical potential and has been used extensively in the search for Au and base metals (Carver *et al.*, 1987, Robertson, 1996b) in relict and erosional areas, having complete and partly truncated lateritic regoliths. Its ability to retain pathfinder elements, because of its high goethite content, and its generally limited dispersion leads to strong anomalies of slightly greater area than those of corresponding soils; however, the petrographic potential of lag for identification of underlying rocks has neither been fully recognised nor exploited.

Geomorphology and regolith

The combined effects of deep, lateritic weathering and differential erosion have led to a variety of lag gravels. Their distribution and characteristics are generally related to the regolith substrate and to processes of erosion and deposition. For example, (i) lag of cellular gossan may be dispersed around gossan outcrop and subcrop (Figure Lg1-1A), (ii) a lag of pisoliths and nodules may occur on relict landform regimes (Figure Lg1-1B), overlying a complete or nearly

complete laterite profile or (iii) a lag of saprolite and ferruginous saprolite (Figure Lg1-1D) may occur largely on erosional areas, overlying partially truncated profiles. In places, these may be highly ferruginous and form a very dark, shiny gravel (Figure Lg1-1C). Lastly, (iv) allochthonous lag of mixed origins, comprising lithic fragments, quartz and lateritic pisoliths, is generally abundant on colluvial-alluvial outwash plains. The outward appearance of the lag gives clues as to the nature of the underlying regolith (Anand *et al.*, 1993). However it is the interior fabrics of the lag that can contain evidence of the parent rocks and their weathering history.

Remnants and pseudomorphs

Many lag fragments are lithorelics. Iron oxides, principally goethite and hematite, largely pseudomorph the original minerals. Identification of original minerals from the pseudomorphs can be difficult, particularly since there may have been intermediate stages such as kaolinite, kaolinite interlaminated with illite and even smectite derived from the primary minerals. The presence of minor amounts of Si and Al in some goethite pseudomorphs suggests that some of these intermediate silicates are preserved on a sub-micron scale or that the goethite has incorporated some of the Si and Al into its lattice. However, if recognisable elements of the original fabric remain intact (pseudomorphed) despite these mineralogical changes, vital information will survive.

Where ferruginisation takes place deep in the profile (during the early stages of weathering), a wide variety of primary rock fabrics may be well preserved. If ferruginisation takes place higher in the saprolite (late stage of weathering), secondary fabrics may also be preserved. If ferruginisation has occurred after pedoplasmation, most primary fabric elements are lost. However, an important feature of the weathering process is that it tends to be incomplete. Thus, pockets of earlier fabrics may be preserved among newer ones; these remnants can be found by careful search.

Collection of lag for petrographic examination

It is generally necessary to examine several specimens of coarse lag (>10 mm) to find easily recognisable remnants of primary lithic fabrics. Petrographic investigation of fine lag (<10 mm) is generally less effective, as the fabrics are fragmented and the proportion of secondary structures is generally greater. Several (>3) polished blocks of the lag should be made from each locality, and examined in oblique and normally reflected light.

Primary and secondary fabrics

Primary phyllitic fabrics (Beasley Creek)

Lag formed from phyllitic schist, from the ore host, clearly preserves its schistose fabric. Islands of preserved, original and secondary fabrics, now largely replaced by goethite, are set in bright, massive, to spongy goethite (Figure Lg1-1V) with open vesicles. The original fabric contains mica remnants (10-100 μm), some of which have been split along their cleavages by the enclosing goethite (Figure Lg1-1F). The mica of these remnants still contains some potassium. There are also some fine-textured pseudomorphs of layer silicates, probably after kaolinite and interstratified kaolinite and mica. The mica remnants and kaolinite pseudomorphic fabrics are identical to those of unferruginised, phyllitic mica and kaolinite, seen in saprolite in diamond drill core (Robertson and Gall, 1988). See also Section Ar1-2 (this Atlas).

Primary and secondary fabrics of mafic schist (Beasley Creek)

Preserved schistose fabrics in lag fragments, overlying mafic schists, consist of numerous, very fine-grained, matted, layer silicate pseudomorphs that form a confused fingerprint fabric (Figure Lg1-1J). These fabrics are secondary, formed in the saprolite by kaolinite and smectite replacing primary feldspar and amphibole, themselves now replaced and pseudomorphed by goethite. This fabric is similar to those of less ferruginised saprolite of the footwall amphibolite seen in diamond drill core (Robertson and Gall, 1988). Although the primary fabric of the amphibolite

appears to have been lost, clustering of the layer silicate minerals into equant groups could reflect a granoblastic or decussate primary fabric.

Primary and secondary fabrics in ultramafic schist (Beasley Creek)
Lag overlying ultramafic schists is yellowish brown or red-brown, mottled blue-black (Figure Lg1-1I). The fabric consists of a matted, pseudomorphed layer-silicate fabric, probably after smectites, in a few places showing a confused fingerprint structure, similar to that of the mafic rocks, but at a very fine scale.

Primary tillite fabrics (Beasley Creek)
The lag, overlying Permian glacial sediments, consists of diverse, polymictic fragments (Figure Lg1-1G), several mm in size, with faint secondary fabrics and a breccia-like structure, set in an apparently relatively fine grained, matrix-supported, arenaceous matrix (Figure Lg1-1H). The parent rocks appear to be sedimentary breccias; the fabric of the lag thus accurately reflects the underlying tillites and arenites that have been weathered to clay-rich saprolites and mottled materials that have all the characteristics of lateritic weathering.

Primary cumulate fabrics (Ora Banda Sill)
Primary igneous fabrics are preserved in lag overlying the peridotite and pyroxenite of the Ora Banda Sill (Butt *et al.*, 1992). Many subangular fragments consist of hematite or hematitic goethite, in which hematitic pseudomorphs after olivine abound, and a few goethitic pseudomorphs after talc-altered pyroxene (Figures Lg1-1K, L). These olivine and pyroxene fabrics occur in various stages of preservation. Serpentine-filled cracks in the olivine have been faithfully pseudomorphed by hematite, but the olivines are now voids, leaving only the outline of the olivine (Figure Lg1-1L). The preservation of the complete primary fabric of pyroxene and olivine depends on ferruginisation having occurred prior to partial destruction of the fabric. If this does not occur, the most that may be found are disaggregated olivine pseudomorphs or only very indistinct pseudomorphs after smectitic clays.

Abundant, drop-like crystals of weathered, pinkish grey chromite are also characteristic of this lag. The polished surfaces of some chromite crystals are extensively pitted, others have a reticulate pattern of goethite-filled cracks that penetrate the crystal from its margin. These cracks appear to reflect weathering of the chromite and become progressively narrower towards the centres of the grains. The crack pattern has almost destroyed the outline of some small chromite crystals.

The primary fabrics of the pyroxenites are not nearly as well preserved as those of the peridotites. In general, all that can be discerned is a fine-scale, parallel, goethitic structure that appears to indicate amphibole, talc or, rarely, pyroxene. There are a few indistinct pseudomorphs after sheet silicates, probably smectites and vermiculites, set in dark, spongy goethite. The lag is significantly poorer in hematite and richer in goethite than that overlying the peridotite; it is also poorer in chromite. The chromite grains are smaller and poorly formed.

Phyllic and oxide-sulphide primary alteration fabrics (Bottle Creek)
Lag overlying the phyllic alteration halo at Emu, Bottle Creek (Robertson and Wills, 1993) contains significant quantities of granular quartz, euhedral K-mica (Figures Lg1-1O, P) and preserved quartz 'eyes'. Mica is visible by hand lens examination of the cut surface of lag fragments. In others, alternating layers of quartzose and ferruginised, argillaceous material suggests either a graded argillaceous metasediment or the 'zebra rock' typical of the ore environs. Linear mica flakes and equant, subhedral hematite pseudomorphs after magnetite and/or sulphide (Figures Lg1-1M, N) are set in massive to spongy goethite. Although some of the hematite pseudomorphs are martite, which still preserves the internal trellis structure of pre-existing magnetite, others are internally massive or show internal brush structures more typical of

sulphide pseudomorphs. There are traces of As in the hematite pseudomorphs and in the surrounding goethite.

Secondary fabrics in goethite and hematite

Pseudomorphed mineral fabrics may be destroyed by secondary iron oxides (Figures Lg1-1S, T, U, V). In places, there is evidence for multiple cycles of iron dissolution and precipitation. After dissolution of parts of the fabric, to form voids, goethite has precipitated as colloform, delicately banded structures (Figure Lg1-1T) as linings on the walls of open spaces. In places, these open spaces have been completely or almost completely filled. In others, the fabric has been replaced progressively by spongy to massive goethite. In many cases, fabric destruction is incomplete, leading to partly erased (palimpsest) fabrics (Figures Lg1-1U, V).

Hematite fabrics

Hematite occurs overtly, as small lozenge-shaped crystals (Figures Lg1-1P, V) and as poikiloblasts, but it also occurs covertly, with goethite, as an ultra fine-grained mixture, a product of goethite dehydration. It leads to a wide variety of goethite colours and reflectances, from dull brownish-grey, through lead-grey to goethite of increasing brightness as dehydration progresses. Thus, the hematite content is generally greater than is apparent from a cursory study of polished sections. Dehydration is accompanied by a reduction in volume, resulting in desiccation cracking or a spongy appearance. Morris (1985) suggested this process is selective in the iron ores of the Hamersley Province, with goethite pseudomorphs after quartz being the most easily transformed, followed by silicate and finally carbonate pseudomorphs. Such dehydration appears to be related to long exposure of the goethite above the water-table and is most prevalent near the surface; a similar process may be equally applicable to an accumulation of lag.

Accordion fabrics

Accordion-like layer silicate pseudomorphs are common. These form vermicular structures and are generally mixed with, or occur on the periphery of, preserved silicate remnants, close to, and intimately associated with, secondary goethite structures (Figures Lg1-1W, X). Very similar accordion-like structures have been described in authigenic kaolinite of argillaceous rocks (Williams *et al.*, 1955) and in kaolinites derived from granite weathering (Robertson and Eggleton, 1991; also in this Atlas). It is suggested that these pseudomorphs represent authigenic recrystallisation of kaolinite in the saprolite (see Figures G1-2G; Um1-2K, L), that have since suffered iron replacement, preserving these accordion fabrics from saprolite re-texturing and collapse. In some places, widespread development of accordion structures form fabric-destroying blasts in the upper saprolite.

Duricrust-related lag

Lag developed from lateritic granules and duricrust has had a particularly complex history and incorporates numerous types of fragments which may be either lateritic or lithic in origin. Some are clay-rich and ferruginous, nodular and pisolitic, and include angular quartz, set in one or more generations of red-brown to yellow-brown clay (Figure Lg1-1Q, R). These fragments may be gibbsitic in part (Robertson and Wills, 1993). The ferruginous nodules are dominated by pseudomorphs of secondary fabrics formed in the saprolite. Incomplete goethite cutans on the ferruginous nodules suggest precipitation and re-solution of goethite prior to clay deposition.

The interiors of lag fragments overlying lateritic duricrust vary widely in colour (blue-grey, dark red-brown, mottled yellow and honey-brown) and fabric (a very few retain patches of primary fabrics). These remnants are set in secondary goethite (some fibrous), bright, polygonal grains of hematite and, in turn, in various goethite- and hematite-stained clays. The latter also have a wide variety in colour, indicating a range in hematite content (Figure Lg1-1Q). The outer parts generally tend to be yellow or goethitic, whereas the interiors are red or hematitic. This could be related to water access, which may either influence the equilibrium between goethite and hematite,

during Fe-oxide precipitation, or the solid state hydration of hematite to goethite. In some duricrust-related lag fragments, a history of at least two clay phases is shown by the presence of fragmentary or complete clay pisoliths, some with yellow clay cutans (argillan), now set in a second generation clay matrix (Figures Lg1-1Q). Some pisoliths contain dark goethite granules Small crystals of hematite occur scattered in the clay (Figure Lg1-1R). Solution cavities are filled with ooliths of flocculated yellow clay (Figures LG1-1Q, R). In places, goethite fills the channelways that link vesicles in the clay, and the goethite has permeated outwards from the channel into the clay for a short distance.

Voids

Vesicles in lag fragments vary from round and cavernous to vermiform and some are strung together to form channelways, linked by hairline fractures. Some fractures are open, others are filled with clay or goethite. Some vesicles are lined with a thin layer of goethite, which is, in places, colloform, fibrous or both; other voids are lined with or filled by white, banded, opaline silica. Some solution cavities are filled with brown, siliceous, ferruginous clay. Alternatively, numerous, small, angular fragments of goethitic, nodular material and angular quartz are set in a brown, void filling of hardpanised clay soil.

References

Anand, R.R., Churchward, H.M., Smith, R.E., Gozzard, J.R., Craig, M.A., and Munday, T.J. 1993. Classification and atlas of regolith-landform mapping units. CSIRO Division of Exploration and Mining Restricted Report 440R.

Butt, C.R.M. 1992. Physical weathering and dispersion. In C.R.M. Butt and H. Zeegers (Editors). Regolith exploration geochemistry in tropical and subtropical terrains. Handbook of Exploration Geochemistry, Vol 4. Elsevier, Amsterdam, 97-113.

Butt, C.R.M., Williams, P.A., Gray, D.J., Robertson, I.D.M., Schorin, K.H., Churchward, H.M., McAndrew, J., Barnes, S.J. and Tenhaeff, M.F.J. 1992. Geochemical exploration for platinum group elements in weathered terrain. CSIRO Division of Exploration Geoscience Restricted Report 332R.

Butt, C.R.M. and Zeegers, H. (Editors) 1992. Regolith exploration geochemistry in tropical and subtropical terrains. Handbook of Exploration Geochemistry, Vol 4. Elsevier, Amsterdam, 607 pp.

Carver, R.N., Chenoweth, L.M., Mazzucchelli, R.H., Oates, C.J. and Robins, T.W. 1987. "Lag" - A geochemical sampling medium for arid regions. Journal of Geochemical Exploration. 28, 183-199.

Morris, R.C. 1985. Genesis of iron ore in banded iron-formation by supergene and supergene-metamorphic processes - a conceptual model. In K.H. Wolf (Ed). Handbook of strata-bound and stratiform ore deposits. Regional studies and specific deposits. Vol 13. Elsevier. 73-235.

Robertson, I.D.M. 1989. Geochemistry, petrography and mineralogy of ferruginous lag overlying the Beasley Creek Gold Mine - Laverton, WA. CSIRO Division of Exploration Geoscience Restricted Report 27R.

Robertson, I.D.M. 1990. Mineralogy and geochemistry of soils overlying the Beasley Creek Gold Mine - Laverton, WA. CSIRO Division of Exploration Geoscience Restricted Report 105R.

Robertson, I.D.M. 1996a. Interpretation of fabrics in ferruginous lag. AGSO Journal of Australian Geology & Geophysics, 16 (3), 263-270.

Robertson, I.D.M. 1996b. Ferruginous lag geochemistry on the Yilgarn Craton of Western Australia; practical aspects and limitations. Journal of Geochemical Exploration, 57 139-151

Robertson, I.D.M. and Eggleton, R.A. 1991. Weathering of granitic muscovite to kaolinite and halloysite and of plagioclase-derived kaolinite to halloysite. Clays and Clay Minerals, 39. 113-126.

Robertson, I.D.M. and Gall, S.F. 1988. A mineralogical, geochemical and petrographic study of rocks of drillhole BCD1 from the Beasley Creek Gold Mine - Laverton, WA. CSIRO Division of Exploration Geoscience Restricted Report MG 67R, 44 pp.

Robertson, I.D.M. and Wills, R. 1993. Petrology and geochemistry of surface materials overlying the Bottle Creek Gold Mine, WA. CSIRO Division of Exploration and Mining Restricted Report 394R.

Williams, H., Turner, F.J. and Gilbert, C.M. 1955. Petrography - an introduction to the study of rocks in thin section. W.H. Freeman and Co, San Fransisco. 406 pp.

FIGURE Lg1-1

LAG TYPES AND PRIMARY FABRICS

Lag-strewn surfaces

A. An abundant, coarse, black lag of highly ferruginous, cellular gossan (GN) overlying the central part of the orebody subcrop at Beasley Creek; Robertson (1989). Scattered among it is a subordinate lag of white vein quartz (QZ). This is typical of an erosional regime.

B. A very coarse, relatively pale, yellow-brown, nodular lag, derived from the duricrust overlying a pyroxenite of the Ora Banda Sill; Butt *et al.*, (1992). It consists largely of goethite and abundant ferruginous clays and is typical of a slightly stripped 'relict regime'.

C. A thin soil masked by a shiny, blue-black 'buckshot' lag, overlying peridotitic rocks of the Ora Banda Sill; Butt *et al.* (1992). This is typical of lag overlying saprolite in an erosional regime.

D. A lag of lithic fragments of ferruginous saprolite (FS) and minor, white, vein quartz (QZ) overlying mafic-ultramafic schists at Beasley Creek; Robertson (1989). This is typical of a lag overlying an erosional regime.

Metasediments and sediments

E. A deep red-brown, ferruginised lithorelic of ore host phyllite, showing a preserved and folded schistosity (SC) with a high proportion of fine-grained, glistening mica relics (MU). Compare Figure Lg1-1F. Beasley Creek; Robertson (1989). Specimen 08-108D. Close up photograph of polished block in oblique reflected light.

F. Mica relics (MU) set in porous goethite (GO) with small vesicles (VS). Goethite has, in part, wedged the mica apart along cleavages. From a coarse, black lag fragment overlying the ore host phyllite at Beasley Creek, Robertson (1989). Compare Figure Lg1-1E. Specimen 08-108B. Photomicrograph in normally reflected light.

G. A ferruginised lithorelic of polymictic fragments set in a ferruginised, arenaceous matrix, derived from Permian glacial sediments at Beasley Creek; Robertson (1989). Compare Figure Lg1-1H. Specimen 08-120B. Close up photograph of polished block in oblique reflected light.

H. A lithorelic of matrix-supported, polymictic sediment, including fragments of sub-angular, bright goethite (GO), a few ferruginised saprolite fragments (SP), after mafic-ultramafic schists, quartz fragments (QZ) and shadowy lithorelics (HS), all comprising a ferruginised Permian glacial sediment from Beasley Creek; Robertson (1989). Compare Figure Lg1-1G. Specimen 08-120B. Photomicrograph in normally reflected light.

FIGURE Lg1-1

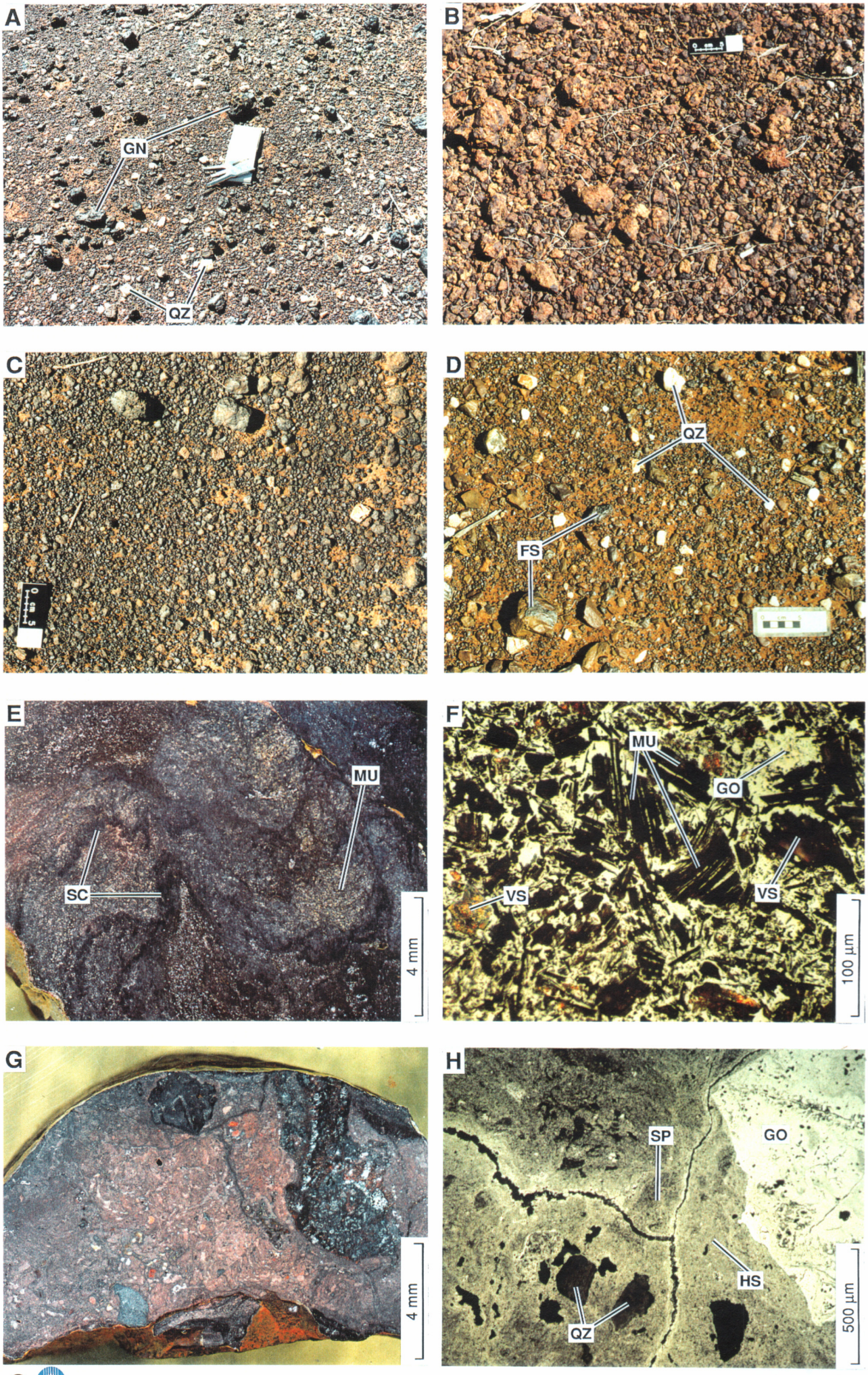

FIGURE Lg1-1 (Contd)

PRIMARY FABRICS

Secondary fabrics developed in saprolite

I. Islands of yellow-brown goethite (YG), with a very fine-scale, preserved schistosity, containing very fine-grained, layer-silicate pseudomorphs after a saprolite of an ultramafic rock. This is veined by dark brown goethite (DG). Specimen 08-117B from Beasley Creek; Robertson (1989). Close up photograph of polished block in oblique reflected light.

J. A coarse, black, ferruginous lag fragment over mafic footwall rocks, showing a matted layer silicate pseudomorph (LS), with a fingerprint fabric, probably after secondary kaolinite or smectite of the saprolite. Specimen 08-113C. Beasley Creek; Robertson (1989). Photomicrograph in normally reflected light.

Peridotite Fabric

K. Pseudomorphs of serpentinised olivine (OL) and talc-altered pyroxene (PX) perfectly replaced by goethite and hematite. Peridotite of Ora Banda Sill; Butt *et al.*, (1992). Compare Figure Lg1-1L. Specimen 08-1498. Close up photograph of polished block in oblique reflected light.

L. Olivine (OL) and pyroxene (PX) pseudomorphed in a lag overlying a peridotite of the Ora Banda Sill. The serpentinised cracks in the olivine are preserved by hematite (HE) but the olivine has been dissolved and is now a void (VO). The outline and cleavage of the pyroxene are preserved in goethite (GO). Compare Figure Lg1-1K. Specimen 08-1498; Butt *et al.* (1992). Photomicrograph in normally reflected light.

Ore-related Fabrics

M. Lithorelic lag from the eastern edge of the Emu Pit. Goethite pseudomorphs after magnetite (MT) are set in a red-brown goethite (GO). Ferruginised saprolite. Bottle Creek; Robertson and Wills (1993). Specimen 06-0190. Compare Figure Lg1-1N. Close up photograph of polished surface in oblique reflected light.

N. Euhedral to subhedral goethite pseudomorphs after magnetite (GM) and possibly some pyrite (GP), surrounded by finer-grained, similar pseudomorphs and remnants of sericite (MU). Compare Figure Lg1-1M. Specimen 06-0190. Bottle Creek; Robertson and Wills (1993). Photomicrograph in normally reflected light.

O. Lithorelic lag from the eastern edge of the Emu Pit. Patches of glistening sericite (MU) are set in red-brown goethite (GO). The original banded rock fabric remains. Ferruginised saprolite. Compare Figure Lg1-1P. Specimen 06-0190. Bottle Creek; Robertson and Wills (1993). Close-up photograph of polished block in obliquely reflected light.

P. Well-defined, euhedral flakes of sericite (MU) are set in grey goethite (GO) with equant grains of hematite (HM). Compare Figure Lg1-1O. Specimen 06-0190. Bottle Creek; Robertson and Wills (1993). Photomicrograph in normally reflected light.

FIGURE Lg1-1 (Contd)

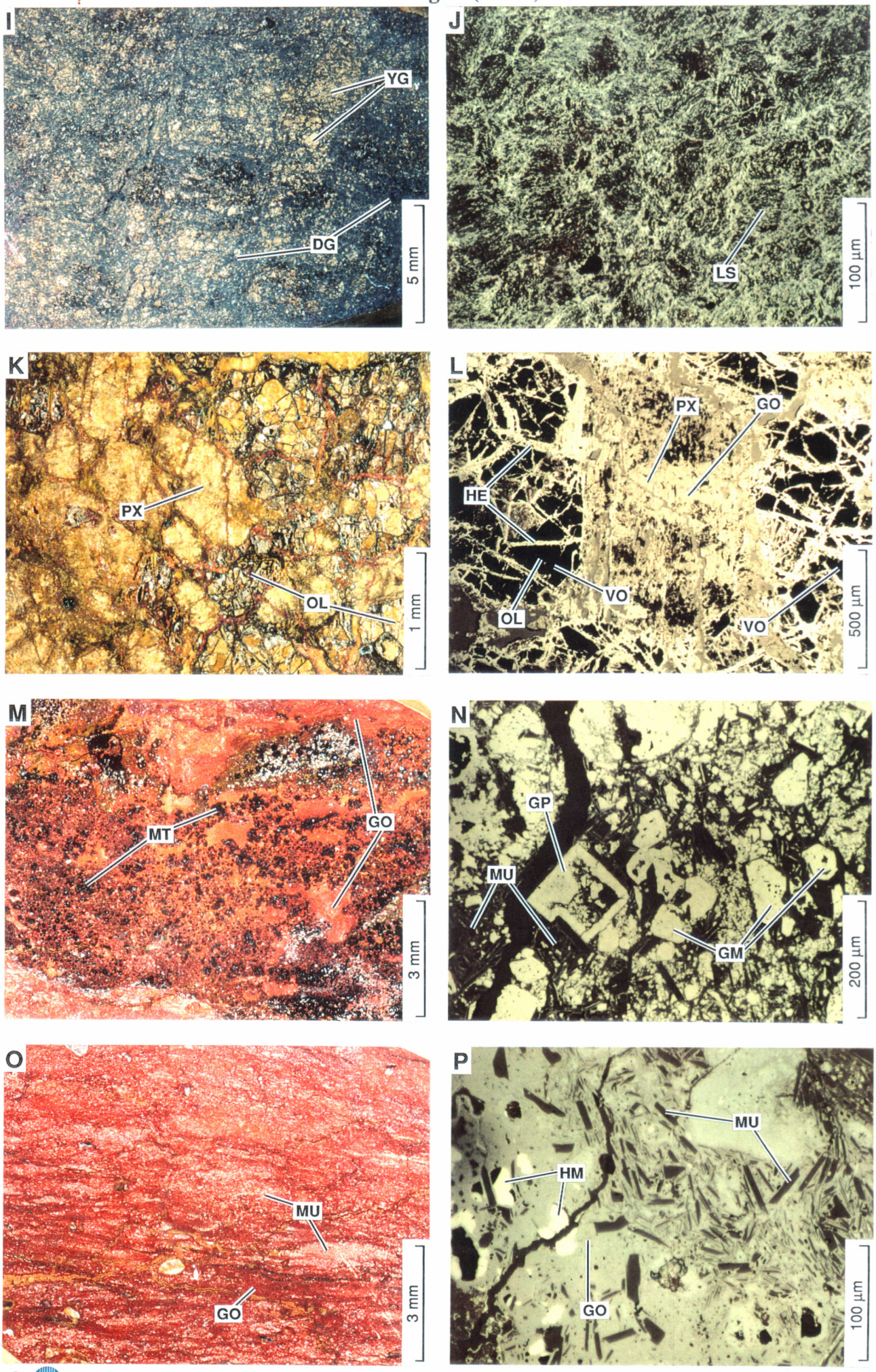

FIGURE Lg1-1 (Contd)

SECONDARY FABRICS

Duricrust fabrics

Q. Duricrust-related lag showing a red, hematitic clay fragment (HC), containing ferruginous clay pisoliths (CP) and pisolith fragments set in a mass of oolitic, yellow, clay spherules (CS) which may have been precipitated chemically in a solution cavity. Duricrust covering hangingwall of Beasley Creek orebody. Compare Figure Lg1-1R. Specimen 08-130D; Robertson (1989). Close up photograph of polished block in oblique reflected light.

R. Dark, concentrically zoned, red clay pisoliths (PC), set in a nodule of red clay (RC). The zonation is due to variations in the concentration of goethite which stains the clay. Small crystals of hematite (HM) are scattered in the clay matrix. Duricrust overlying the hangingwall of the Beasley Creek orebody. Compare Figure Lg1-1Q. Specimen 08-130D; Robertson (1989). Photomicrograph in normally reflected light.

Void fill fabrics

S. A fine-grained, flinty lithorelic, largely replaced by cauliflower-like secondary goethite (SG). This is cut by later stylolitic veins (SV) of black goethite. Beasley Creek. Specimen 08-104B; Robertson (1989). Close up photograph of polished block in oblique reflected light.

T. Delicately banded botryoidal structures in alternating layers of goethite (GO) and hematite (HM) on the edge of a lag granule from above the orebody at Beasley Creek. Specimen 08-216; Robertson (1989). Photomicrograph in normally reflected light.

Palimpsest fabrics

U. A very fine-grained, ferruginised lithorelic. Though some schistosity is preserved, much of the original fabric has been replaced by dark brown, secondary goethite. Ore host phyllite at Beasley Creek. Specimen 08-108C; Robertson (1989). Close up photograph of polished block in oblique reflected light.

V. Islands of layer-silicate pseudomorphs (LS) and a few mica remnants (MC), set in dull goethite (G1), invaded by, and now set in, bright goethite (G2). A few lozenge-shaped hematite crystals (HM) are scattered in the fabric. A coarse black, ferruginous lag from Beasley Creek. Specimen 08-104A; Robertson (1989). Photomicrograph in normally reflected light.

Accordion fabrics

W. A pedogenically recrystallised fabric of yellowish-brown goethite from Bottle Creek. Compare Figure Lg1-1X. Specimen 06-1624; Robertson and Wills (1993). Close up photograph of polished block in oblique reflected light.

X. Relicts of well-developed accordion fabrics (AC) of pedogenically recrystallised kaolinite, set in grey goethite (GO) from Bottle Creek; Robertson and Wills (1993). Compare Figure Lg1-1W. Specimen 06-1624. Photomicrograph in normally reflected light.

FIGURE Lg1-1 (Contd)

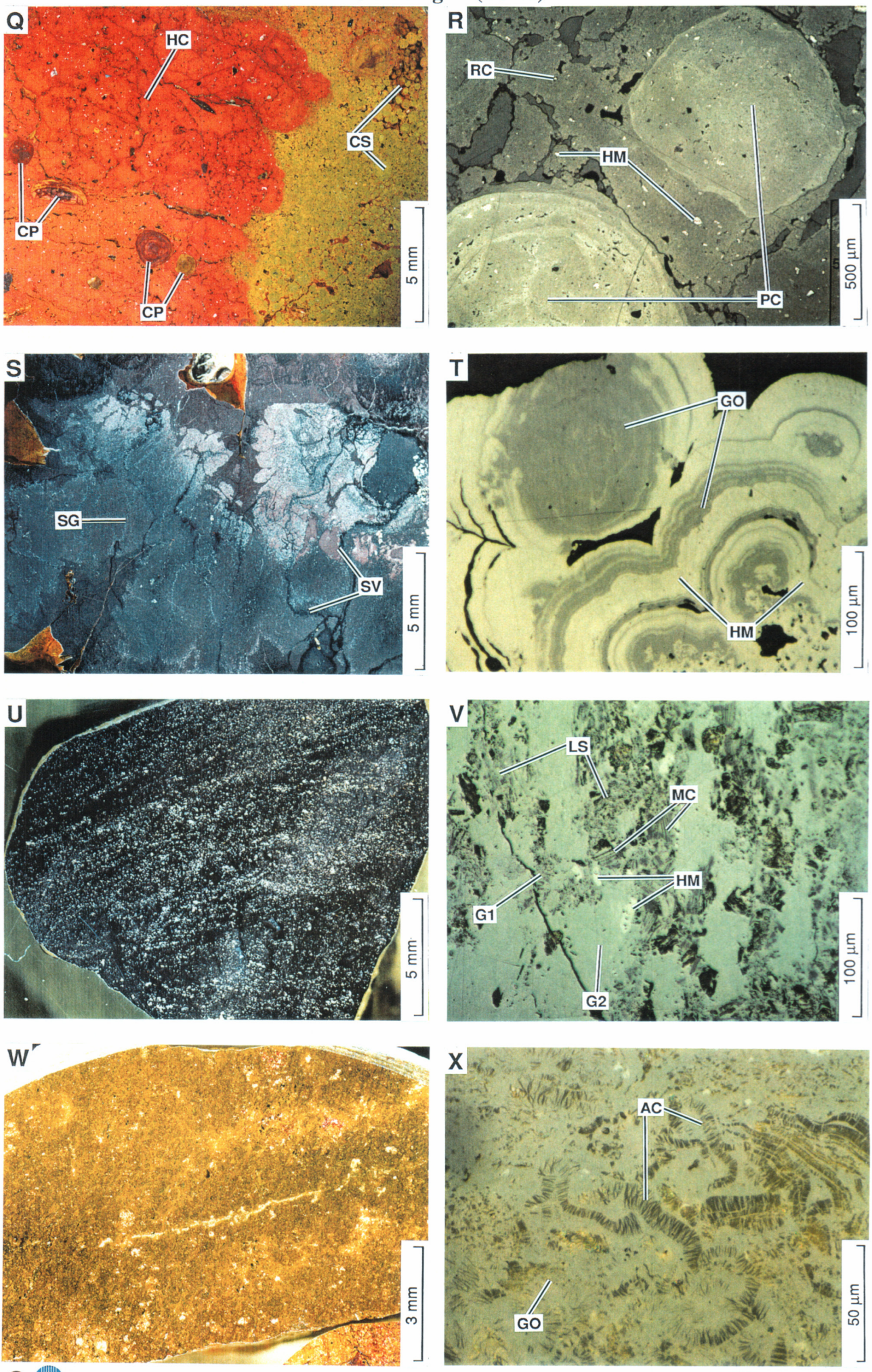

Metamorphic Grade	:	Amphibolite Facies
Structural Attributes	:	Strongly sheared
Gross Features	:	Possible deformed pillows
Profile Truncation	:	Near base of Mottled Zone
Depth to Fresh Rock	:	70 m
Location	:	Reedy, near Cue: North of Menzies Line
Reference	:	Robertson, Chaffee and Taylor, 1990

Geomorphology and profile

The Reedy Mine is situated on a gently sloping, stony, erosional plain, which forms a portion of the low divide between minor elements of the drainage systems into the playa lakes Austin and Annean. There are a few stony rises and low hills which expose weathered, generally ferruginized, Archaean greenstones and a few patches of lateritic duricrust. Deeply weathered country rocks are overlain by a dominantly fine, gravelly, ferruginous alluvium, up to 2 m thick, much of which has been hardpanized. A shallow (<0.5 m), acidic, stony, friable, fine, sandy, red to brown, clay loam overlies the hardpan. This contains lateritic and ferruginized lithorelic gravels which form a surface lag.

At the Rand Pit, where the profile was studied, the regolith has been stripped to the base of the mottled zone. The depth of weathering varies between rock types, but generally has penetrated to 70-80 m. The south face of the Rand Pit has exposed granitoid porphyry pods set in interstratified mafic, ultramafic and mica schists (Figure M1-1). The mafic schists are described here.

Fresh rock

Where comparatively fresh, these rocks consist of granular quartz, untwinned albite and lenticular patches of chlorite, cut by a strong foliation marked by muscovite and talc (Figures M1-2A and B). In turn, this is cut by a later, open-spaced cleavage, filled with schistose chlorite. Sinuous quartz veins follow the cleavage. Magnetite and ilmenite show very slight weathering with release of a trace of goethite, which locally stains grain boundaries and penetrates the cleavage (Figure M1-2A). In places, these rocks are unusually coarse-grained and probably are intrusives or thick flows.

Saprock

The onset of weathering occurs at about 70 m and is indicated by white or cream turbidity in the albite that has been partly altered to very fine-grained kaolinite (Figure M1-2C). Only slightly higher, the albite is almost completely kaolinized (Figure M1-2D). A few cubic goethite structures pseudomorph pyrite and goethite has stained the rock more extensively (Figure M1-2C). The cleavage is followed by sinuous quartz lenses.

Saprolite

Complete kaolinization of plagioclase and oxidation of sulphides marks the base of the saprolite and this is accompanied by widespread to patchy goethite staining along quartz veins. Chlorite has altered to smectite and this, in part, has altered to kaolinite, but the schistose fabric remains. Near the top of the saprolite, the primary fabric is partly obliterated, quartz grains in vein quartz become separated, solution cavities and channelways occur and the saprolite grades into the pedolith above.

Chlorite is partly altered to smectite (Figure M1-2D) at 50 m depth; alteration is complete at 30 m depth. Sulphides, lying both within the rock and along the margins of small quartz veins, have

oxidized completely to goethite and hematite and ferruginous staining has spread along the vein margins and along the cleavage of the partly altered chlorite (Figure M1-2E, F). Some saprolites have a well-preserved schistose fabric (Figure M1-2G, H), whereas others, which contain sinuous quartz patches, now consist of very fine-grained, low birefringent kaolinite, some talc and a kaolinite-smectite mixture that has a slightly higher birefringence than kaolinite alone. This mixed phase occurs as patches with a sworled fabric. The rock is cut by vermiform fractures and solution channels. Most of these rocks are saprolitic, though some pedolithic fabrics occur on a small scale (Figure M1-2G).

The saprolite at 10 m depth generally consists of a very fine- to relatively coarse-grained, schistose mat of kaolinite and talc, with some muscovite and smectite after a chloritic cleavage, and fine-grained granular quartz. This is cut by cleavage-associated quartz, in which the individual quartz grains are separated by a clay matrix. There are also numerous solution channels and vesicles, some of which are infilled with fragments of saprolite, set in a matrix of clay. Saprolitic fabrics are preserved in these rocks as palimpsest schistosities, now consisting of clays and quartz, but pedolithic fabrics (matted clay fabrics and vesicles) become increasingly important.

Plasmic zone
At 30 m depth, the mafic rocks consist of a schistose fabric of talc, chlorite and quartz, which has become reorganized progressively by recrystallization of kaolinite. The fabric reorganization has taken several forms:-

a) Initially, small, globular blasts of very fine-grained, secondary, pedogenic kaolinite (Figures M1-2K and L) occur in the original, schistose, saprolitic fabric. This progressively becomes more marked, with considerable reorganization of the primary fabric. Blasts of very fine-grained kaolinite have developed and these have swept remnant quartz grains into clusters (Figures M1-2M and N).

b). Some saprolite has formed a breccia, which consists of fragments of round to subangular kaolinitic saprolite and vein quartz, set in a variably goethite-stained, coarser-grained matrix of flaky kaolinite and smectite.

c). Some of the reorganized saprolite variety contains two distinct clay phases: (i) an older, low birefringent kaolinite, set with quartz grains (their wide size range and strained nature suggests they are fragmented vein quartz) and vermiform books, stacks and accordion structures of recrystallized kaolinite; (ii) a later, very fine-grained, pinkish yellow, very low birefringent kaolinite, containing minor smectite, which contains fragments of all the earlier components and cuts the previous clay phase.

This reorganization causes loss of the original rock fabric and marks the transition from saprolith to pedolith. The restructured plasmic materials close to the surface (2-10 m) become increasingly more closely cut by small channelways and voids, many of which are lined with kaolinite and completely or partly infilled with mixed kaolinite and smectite. Some of the open channelways are occupied by roots.

Mottled zone
Not sampled.

Mineral stability.
Quartz is stable throughout the exposed profile but it appears to decrease slightly in abundance although this may reflect crystallinity (poorly crystalline quartz giving a lesser XRD peak). Feldspar (albite) is completely kaolinized at the base of the saprolite, although some chlorite

survives about half way through the saprolite zone. Talc survives throughout the saprolith but is partly altered in the plasmic zone, whereas muscovite survives to the present surface, presumed to be at the base of the original mottled zone. Smectite is present throughout both the saprolith and the pedolith.

Reference

Robertson, I.D.M., Chaffee, M.A., and Taylor, G.F. 1990. The petrography, mineralogy and geochemistry of weathering profiles developed on felsic, mafic, ultramafic and sedimentary rocks, Rand Pit, Reedy Mine, Western Australia. CSIRO Division of Exploration Geoscience Restricted Report 102R. 205 pp.

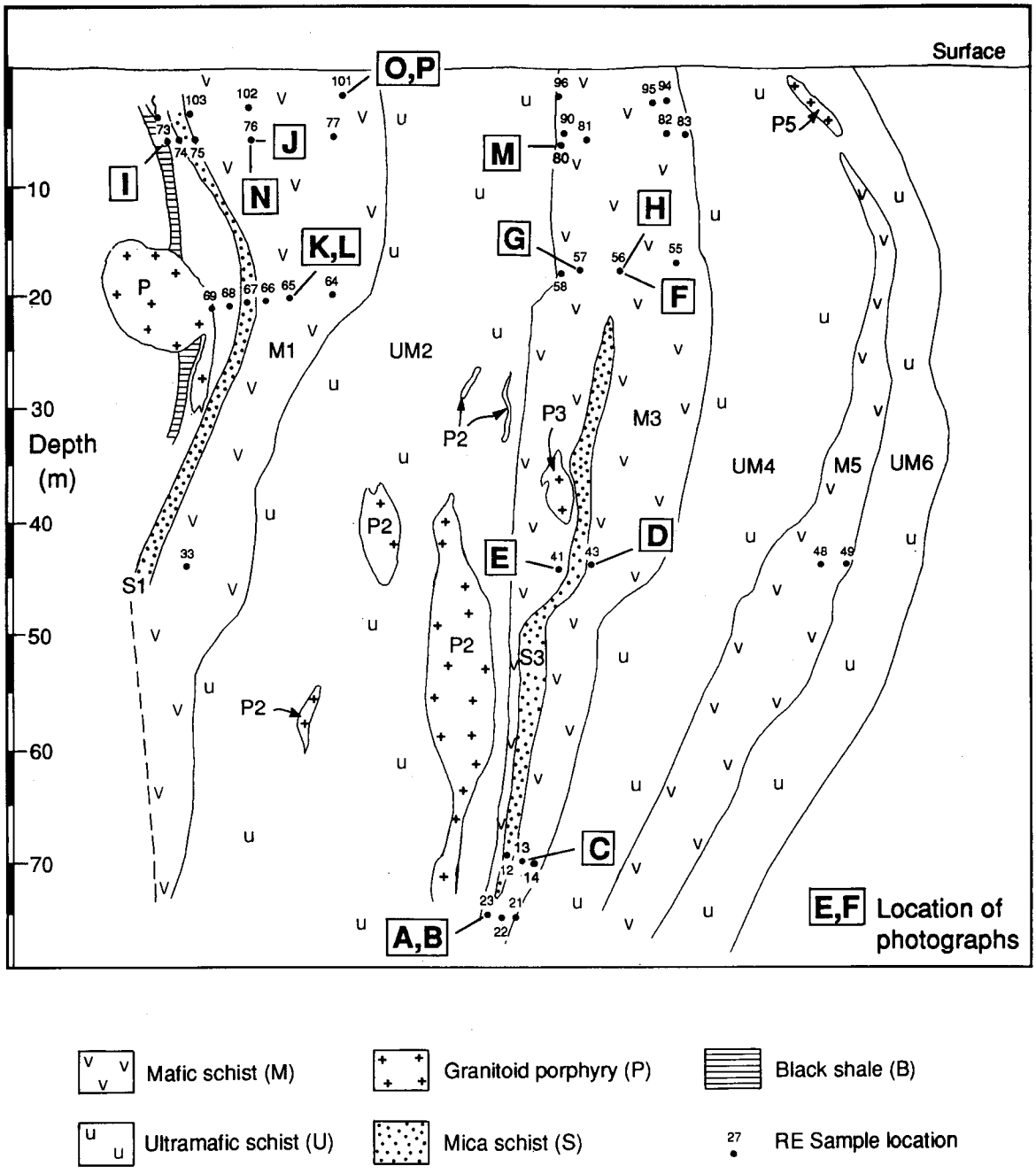

Figure M1-1. Profile at Rand Pit showing locations of samples and photographs.

FIGURE M1-2

Foliation preserved in clays - Saprolite

G. Kaolinite-smectite-quartz schist. A strong foliation is preserved in wavy bands of green smectite (SM) and white, secondary kaolinite (KA) with quartz. Creamy, feathery patches are anatase (AN), after ilmenite and/or sphene. Red-brown powdery goethite patches (GO) stain the fabric. There are also a few small voids and channelways (VO). Compare with Figure M1-2H. Specimen RE 57. Depth 21 m. Mafic band M3. Close-up photograph of "wet" surface.

H. Quartz-kaolinite schist. A groundmass of granular quartz and kaolinite, after plagioclase (KQ), is cut by lenses of kaolinite which accurately pseudomorph two acutely intersecting, previously chloritic, cleavages (KL). Compare with Figure M1-2G. Specimen RE 56: Depth 21 m. Mafic band M3. Photomicrograph with crossed polarizers.

Iron oxide staining following a quartz vein - Saprolite

E. A quartz vein (QV) intersects a dark green chloritic schist (CL). Sulphides within the schist and along the margins of the quartz vein have altered to deep red-brown hematite (HE) and have stained the chlorite intensively along its cleavage. Feathery, cream-coloured patches are anatase (AN) after ilmenite. Compare with Figure M1-2F. Specimen RE 41: Depth 47 m. Mafic band M3. Close-up photograph of "wet" surface.

F. A quartz vein (QV) intersects a quartz-kaolinite schist. Goethite staining (GO) is limited to the margins of the quartz vein and has spread from weathered magnetite (MT). Compare with Figure M1-2E. Specimen RE 56. Depth 21 m. Mafic band M3. Photomicrograph in plain polarized light.

Saprock

C. Quartz-chlorite schist. Bands rich in chlorite (CL) alternate with bands of quartz and opaque, completely kaolinized feldspar (QF). The kaolinite has been pervasively stained yellow with goethite but a more intense brown stain (BS) has spread outward from granules of goethite replacing pre-existing magnetite or pyrite. Compare with Figure M1-2D. Specimen RE13: Depth 69 m. Mafic band M3. Close-up photograph of "wet" surface.

D. Quartz-chlorite-kaolinite-muscovite schist. The albite has been completely altered to very fine-grained kaolinite (KA), leaving the quartz (QZ) and muscovite (MU) unaltered. The chlorite (CH) is turbid and has begun to alter to smectite. Lenses of goethite (GO) lie in the cleavage. Compare with a similar fabric in Figure M1-2C. Specimen RE 43: Depth 47 m. Mafic band M3. Photomicrograph with crossed polarizers.

Relatively fresh rock

A. A nearly fresh, quartz-feldspar-chlorite schist. It consists of fresh, glassy vein quartz (QZ) and lightly stained albite (AB), set with flakes of chlorite (CH). The strong, chloritic cleavage is parallel to x-y. Red-brown goethite stains (GO) have spread from small, partly weathered magnetite grains. Compare with Figure M1-2B. Specimen RE 23: Depth 73 m. Mafic band M3. Close-up photograph of "wet" surface.

B. Quartz-feldspar-chlorite schist. An unweathered schistose fabric of granular quartz (QZ), untwinned albite (AB), muscovite (MU) and chlorite is cut by an open-spaced fracture cleavage marked by chlorite (CH). Compare with Figure M1-2A. Specimen RE 23: Depth 73 m. Mafic band M3. Photomicrograph with crossed polarizers.

FIGURE M1-2

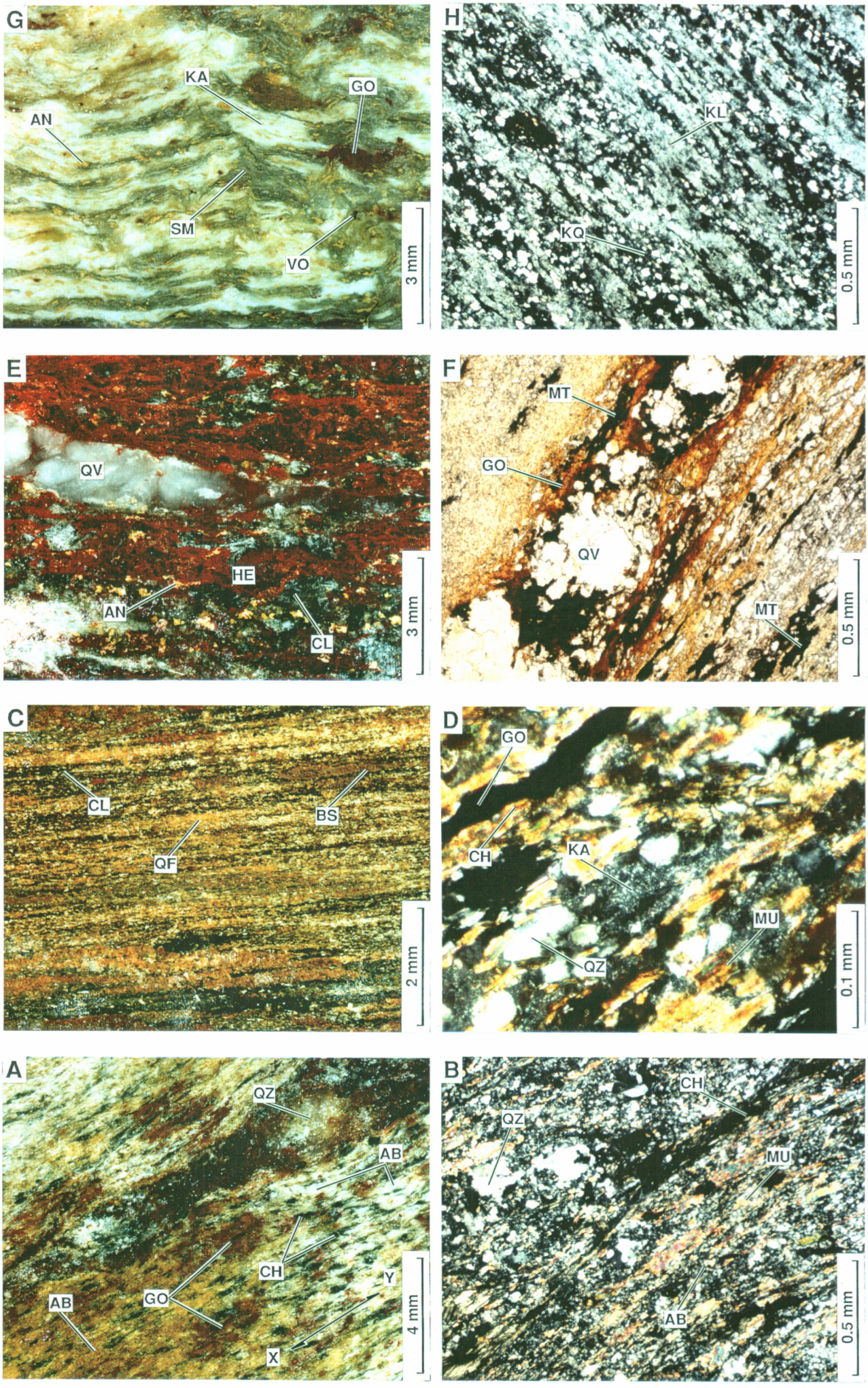
G
KA
GO
AN
SM
VO
3 mm
H
KL
KQ
0.5 mm
E
QV
HE
AN
CL
3 mm
F
MT
GO
QV
MT
0.5 mm
C
CL
BS
QF
2 mm
D
GO
CH
KA
MU
QZ
0.1 mm
A
QZ
AB
CH
Y
AB
GO
X
4 mm
B
CH
QZ
MU
AB
0.5 mm

FIGURE M1-2 (contd)

Voids and Solution Channels - Plasmic Zone

O. A quartz-kaolinite rock. Light brown patches of early kaolinite and quartz (KQ) are separated by several generations of arcuate channels, now largely filled with a lining of white kaolinite (KA) and a discontinuous grey core of mixed kaolinite and smectite (KS). These link small clay-lined vesicles (VO). Compare with Figure M1-2P. Specimen RE 101: Depth 2 m. Mafic band M1. Close-up photograph of "wet" surface.

P. A quartz-kaolinite rock. A mat of fine-grained kaolinite (KA) and granular quartz is cut by an arcuate solution channel (CH) which is lined with low birefringent clay (LC) and partly filled with a core of kaolinite and smectite (KS). Compare with Figure M1-2O. Specimen RE 101: Depth 11 m. Mafic band M1. Photomicrograph with crossed polarizers.

Kaolinite blasts and quartz segregations - Plasmic Zone

M. A quartz-kaolinite rock. White patches of secondary kaolinite (KA) and segregations of quartz grains (QZ) show considerable reorganization of the rock fabric. Small cracks, vermiform vesicles (V) and irregular cavities, some partly lined with Mn minerals (MN) are now filled with impregnating resin. Compare with Figure M1-2N and with similar, but less well-developed, fabrics in Figures M1-2K, L. Specimen RE 80: Depth 8 m. Mafic band M3. close-up photograph of "wet" surface.

N. Kaolinite-quartz schist. The fabric has, in places, been completely replaced by secondary, fine-grained kaolinite structures (KA) which form globular segregations around which the quartz (QZ) has been concentrated. Compare with similar fabrics in Figures M1-2M. Specimen RE 76: Depth 8 m. Mafic band M1. Photomicrograph with crossed polarizers.

Early kaolinite blasts and quartz segregations - Plasmic Zone

K. A quartz-chlorite-talc-smectite schist. Granular quartz and the overall schistose fabric are all that remain of the original rock. The schistose fabric (SH) is being progressively destroyed by expanding patches of very fine-grained, white secondary kaolinite (KA). Compare with Figure M1-2L and with similar, but better developed, fabrics in Figures M1-2M, N. Specimen RE 65: Depth 24 m. Mafic band M1. Close-up photograph of "dry" surface.

L. Quartz-chlorite-talc-smectite schist. Globular patches of recrystallized, very fine-grained kaolinite (KA) lie in a slightly schistose mass of granular quartz and flaky chlorite, smectite and kaolinite (QC). Compare with Figure M1-2K. Specimen RE 65: Depth 24 m. Mafic band M1. Photomicrograph with crossed polarizers.

Palimpsest cleavage - transition from Saprolite to Plasmic Zone

I. Quartz-kaolinite-smectite rock. A mat of white to creamy, slightly stained kaolinite (KA) is cut by a very weakly-developed and largely palimpsest smectite-kaolinite cleavage (CL). Numerous cracks, voids and channelways (CH) intersect the fabric and serve to camouflage the relict cleavage. Compare with Figure M1-2J. Specimen RE 73: Depth 8 m. Mafic band M1. Close-up photograph of "wet" surface.

J. Kaolinite-quartz schist. A mat of slightly shard-like quartz granules (QZ) and flaky kaolinite (KA) is cut by a palimpsest and kaolinized remnant of a phyllosilicate cleavage (KC). Compare with Figure M1-2H, where this fabric is more clearly developed and with Figure M1-2N where the fabric has been completely overprinted by secondary kaolinite structures in the same slide. Compare with Figure M1-2I. Specimen RE 76: Depth 8 m. Mafic band M1. Photomicrograph with crossed polarizers.

FIGURE M1-2 (Contd)

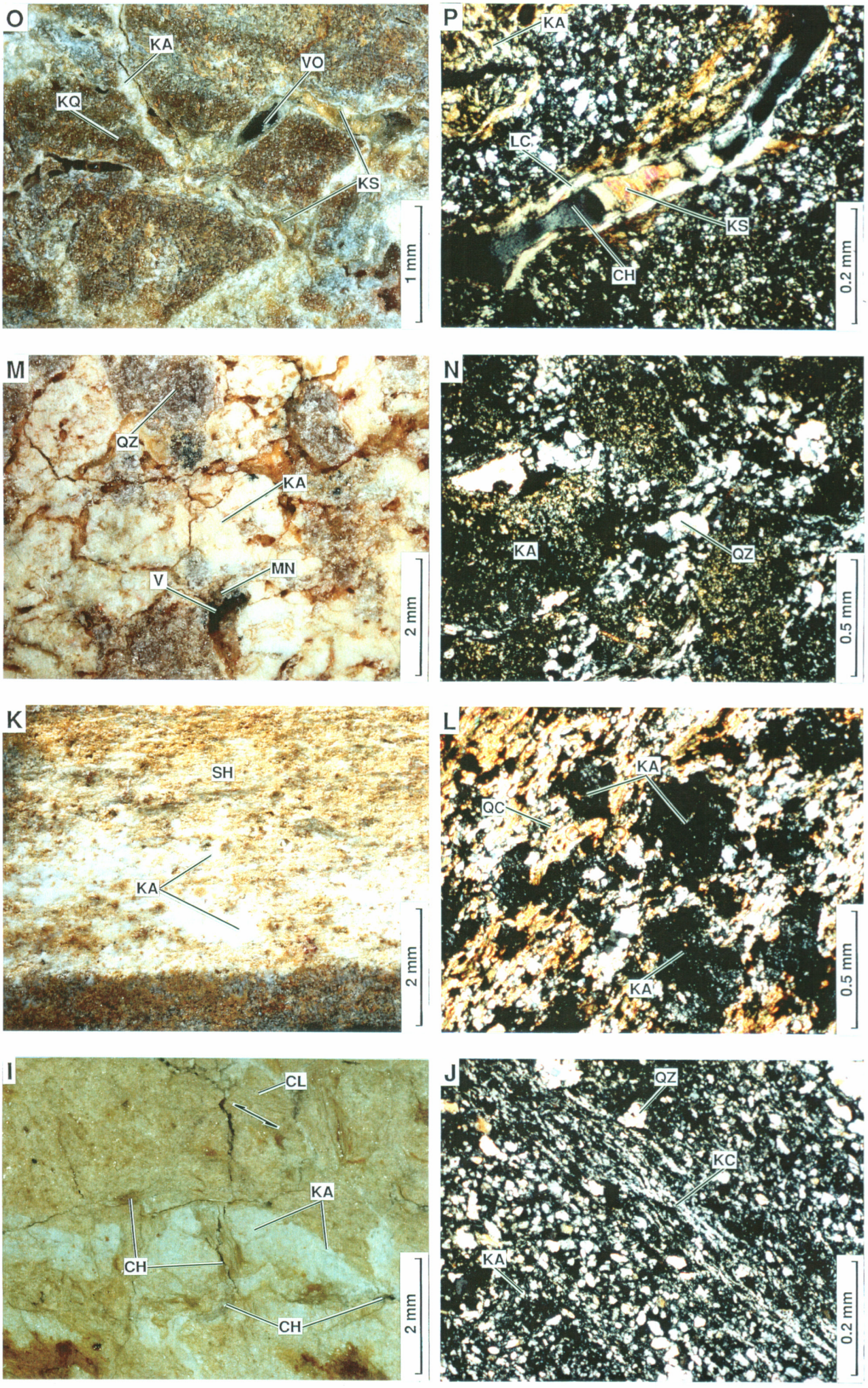

MAFIC VOLCANIC M1
MINERALOGY

Lib No	Depth	Class	Quartz	Fspar	Musc	Talc	Trem	Kaolin	Chlor	Smect	Hemat	Goeth	Halite
08-488	2	Plasmic Z	58	0	0	0	0	46	0	167	0	43	0
08-493	2	Plasmic Z	54	0	0	0	0	47	4	0	0	0	0
08-486	3	Saprolite*	9	0	0	0	0	29	0	23	0	106	0
08-495	4	Plasmic Z	67	0	5	0	0	48	0	128	0	5	0
08-494	4	Plasmic Z	75	0	5	0	0	119	0	71	0	0	0
08-499	4	Plasmic Z	78	0	0	0	0	85	0	11	0	0	0
08-498	4	Plasmic Z	139	0	13	0	0	37	0	149	0	5	0
08-497	4	Plasmic Z	151	0	0	0	4	60	0	28	0	5	0
08-496	4	Plasmic Z	8	0	5	2	0	42	0	117	0	5	0
08-071	7	Plasmic Z	128	0	6	47	0	99	0	70	0	6	0
08-073	8	Saprolite	137	0	5	33	0	110	5	0	0	5	0
08-077	8	S/Plasmic Z	28	0	0	30	4	86	4	0	0	0	0
08-070	8	Saprolite	217	0	6	31	0	74	0	180	0	6	0
08-069	8	Plasmic Z	171	0	5	36	0	88	0	124	0	0	0
08-067	8	Plasmic Z	160	0	5	52	0	140	0	36	0	0	0
08-052	21	Saprolite	260	0	4	52	0	43	3	0	0	0	0
08-053	21	Saprolite	66	0	6	165	0	88	0	88	0	88	0
08-054	21	Plasmic Z	10	0	0	20	0	91	0	131	0	5	0
08-060	24	Saprolite	207	0	0	269	0	63	457	88	0	0	0
08-065	24	Saprolite	211	0	6	64	0	102	0	110	0	70	0
08-066	25	Saprolite	133	0	6	67	0	155	27	6	0	0	0
08-044	46	Saprock	216	25	6	6	0	0	662	229	0	0	0
08-043	47	Rock	151	58	50	50	0	0	576	324	0	0	0
08-037	47	Saprock	114	0	7	64	0	0	268	54	7	0	0
08-011	69	Saprock	141	0	7	48	0	40	315	67	0	0	7
08-020	73	Rock	152	76	69	7	0	7	193	55	0	7	0
08-021	73	Rock	210	81	68	7	0	0	231	7	0	0	0

* Mottled

MAFIC VOLCANIC M1
GEOCHEMISTRY

Lib No	Depth	Class	SiO2	Al2O3	Fe2O3	MgO	CaO	Na2O	K2O	TiO2	LOD	LOI	S.G.	Ag	As	Au	Ba	Be	Bi	Br
-	m	-	%	%	%	%	%	%	%	%	%	%	-	ppm	ppm	ppb	ppm	ppm	ppm	ppm
08-488	2	Plasmic Z	68.10	14.10	2.86	0.85	0.25	0.06	0.08	0.79	2.36	9.90	2.25	-	3	121	56	0	0	3
08-493	2	Plasmic Z	64.30	21.60	0.86	0.32	0.12	0.03	0.04	0.94	1.42	10.60	2.04	-	1	58	156	1	0	1
08-486	3	Saprolite*	47.30	23.70	15.87	0.45	0.18	0.05	0.09	1.00	1.89	12.80	1.92	-	1	8	79	0	0	1
08-495	4	Plasmic Z	60.00	17.80	6.43	0.78	0.30	0.05	0.14	0.93	4.34	13.40	1.72	-	1	39	203	0	0	1
08-494	4	Plasmic Z	57.40	25.00	4.15	0.54	0.17	0.02	0.02	1.06	2.12	12.50	1.97	-	2	6	190	0	0	1
08-499	4	Plasmic Z	55.60	25.40	3.43	0.34	0.11	0.02	0.02	1.54	1.37	11.80	2.04	-	5	5	26	0	1	1
08-498	4	Plasmic Z	60.90	19.40	3.00	1.05	0.26	0.03	0.41	0.93	3.08	11.70	2.08	-	3	16	241	0	2	1
08-497	4	Plasmic Z	58.80	22.00	4.72	0.49	0.13	0.02	0.03	1.07	1.64	11.40	2.20	-	8	15	36	0	0	1
08-496	4	Plasmic Z	60.50	17.10	6.00	0.78	0.25	0.04	0.26	0.88	2.87	11.80	2.00	-	4	19	96	0	0	1
08-071	7	Plasmic Z	63.40	17.22	7.58	0.78	0.29	0.04	0.10	0.84	4.40	12.70	1.87	0	5	16	61	0	1	2
08-073	8	Saprolite	62.56	21.20	5.86	0.00	0.09	0.06	0.12	1.12	1.03	10.10	1.59	0	5	929	58	0	2	2
08-077	8	Plasmic Z	56.27	26.87	1.57	0.00	0.19	0.11	0.14	1.17	1.41	12.80	1.74	0	4	229	186	0	0	1
08-070	8	Saprolite	68.28	11.61	8.86	0.80	0.26	0.05	0.49	0.63	4.02	9.80	1.94	2	18	19	185	0	0	1
08-069	8	Plasmic Z	60.70	18.76	5.43	0.67	0.21	0.04	0.04	0.86	3.73	12.00	1.98	0	6	12	29	0	0	1
08-067	8	Plasmic Z	61.72	24.24	3.86	0.63	0.21	0.02	0.03	0.73	2.93	12.40	1.88	2	3	3	59	0	1	1
08-052	21	Saprolite	66.78	21.62	1.00	0.00	0.04	0.04	0.01	0.97	0.37	8.40	1.63	1	28	17	9	0	0	1
08-053	21	Saprolite	50.95	29.83	6.00	1.35	0.17	0.03	0.02	1.94	2.05	13.50	1.78	1	23	2060	26	0	5	1
08-054	21	Plasmic Z	46.31	29.71	5.00	1.63	0.20	0.04	0.02	2.03	2.91	14.80	1.80	2	20	689	25	0	8	2
08-060	24	Saprolite	56.36	18.08	9.72	4.10	0.23	0.04	0.22	0.89	2.49	10.60	1.81	0	10	4	36	0	0	1
08-065	24	Saprolite	57.85	19.63	10.29	0.58	0.16	0.03	0.05	1.02	1.97	11.00	1.73	1	22	16	67	0	0	1
08-066	25	Saprolite	57.54	27.54	5.72	0.00	0.11	0.03	0.10	1.66	1.86	12.00	1.47	2	6	5	26	0	1	1
08-044	46	Saprock	51.75	12.75	10.72	11.10	0.52	0.81	0.06	0.59	4.05	11.00	2.22	0	1	10	23	0	2	1
08-043	47	Rock	56.27	14.18	12.58	8.92	0.52	1.35	0.80	0.67	3.63	10.00	2.42	0	2	7	199	0	1	1
08-037	47	Saprock	56.23	14.36	10.87	11.70	0.13	0.04	0.01	1.17	1.58	8.70	1.78	0	16	89	17	0	1	1
08-011	69	Saprock	53.81	16.81	10.29	8.98	0.22	0.55	1.92	0.85	2.32	9.10	2.07	1	3	43	192	0	0	1
08-020	73	Rock	64.18	14.31	10.15	2.23	0.26	4.30	1.94	0.72	2.03	5.40	2.26	1	12	6420	145	0	1	1
08-021	73	Rock	55.60	14.89	9.86	7.35	0.40	2.31	2.97	0.85	1.11	5.30	2.34	4	6	918	493	0	0	1

* Mottled

MAFIC VOLCANIC M1
GEOCHEMISTRY

Lib No -	Cd ppm	Ce ppm	Co ppm	Cr ppm	Cs ppm	Cu ppm	Eu ppm	Ga ppm	Ge ppm	Hf ppm	In ppm	Ir ppb	La ppm	Li ppm	Lu ppm	Mn ppm	Mo ppm	Nb ppm	Ni ppm	Pb ppm	Rb ppm
08-488	1	8	24	852	1	38	0	17	1	2	0	9	2.4	32	0.2	119	3	5	173	0	3
08-493	0	5	8	964	1	39	0	23	1	5	1	10	3.2	23	0.3	17	3	9	107	4	2
08-486	0	5	23	987	2	123	1	22	0	4	0	12	5.9	32	0.3	60	3	6	206	4	6
08-495	0	6	32	543	2	62	0	20	1	4	0	9	6.8	41	0.2	47	3	8	130	5	11
08-494	0	118	28	518	1	78	1	29	1	4	0	11	4.2	21	0.5	646	3	6	99	18	2
08-499	0	7	11	457	1	62	0	29	2	3	0	12	3.0	34	0.2	53	3	4	110	7	0
08-498	1	46	28	554	7	83	0	25	1	4	0	10	6.8	19	0.3	607	3	5	76	5	29
08-497	0	6	13	1189	1	82	0	23	2	4	0	12	2.7	30	0.2	28	3	6	122	6	2
08-496	2	4	17	561	4	72	0	21	2	3	0	9	5.1	20	0.2	35	3	5	108	3	16
08-071	1	5	43	420	1	95	0	19	0	3	3	8	5.3	18	0.2	31	4	4	116	5	6
08-073	2	9	9	382	1	351	1	25	1	4	0	12	4.4	30	0.4	32	5	5	89	29	8
08-077	0	6	10	1360	1	91	0	29	2	5	0	11	2.0	52	0.4	14	5	7	228	3	9
08-070	0	5	22	351	7	89	0	15	1	3	3	8	5.2	15	0.2	41	5	5	105	6	25
08-069	0	2	34	901	1	203	0	20	0	3	1	10	3.7	18	0.2	38	3	6	139	5	2
08-067	0	21	28	325	1	109	0	25	2	5	0	8	4.4	32	0.3	192	2	6	134	11	2
08-052	2	4	9	1110	1	35	0	23	1	3	0	17	1.4	52	0.3	36	3	6	104	2	0
08-053	0	6	9	1340	1	43	1	39	2	6	0	11	6.0	25	0.5	28	5	12	121	23	1
08-054	0	6	9	1760	1	46	0	40	3	7	0	13	6.1	28	0.5	27	5	13	136	22	1
08-060	0	68	71	170	2	120	2	21	2	4	0	10	39.0	36	0.6	671	5	5	339	7	18
08-065	3	54	27	1060	1	196	1	21	1	4	0	11	14.6	27	0.5	289	4	7	179	18	5
08-066	0	5	14	108	1	91	0	30	3	2	2	14	5.9	49	0.2	86	5	1	164	4	9
08-044	0	8	58	861	1	30	0	16	2	2	1	10	4.7	51	0.2	633	3	3	377	3	4
08-043	0	25	88	415	1	54	1	16	0	3	0	10	17.7	40	0.3	858	5	3	289	7	23
08-037	0	19	55	957	1	23	1	28	2	4	4	10	12.1	68	0.5	1205	3	4	219	13	1
08-011	1	56	87	346	2	209	2	21	1	3	1	12	35.9	72	0.8	554	3	2	531	6	49
08-020	2	21	68	117	1	19	1	15	1	2	0	12	14.6	13	0.4	718	5	4	228	12	48
08-021	2	33	91	299	1	67	1	18	1	3	0	14	25.0	69	0.3	884	4	3	448	6	72

MAFIC VOLCANIC M1
GEOCHEMISTRY

Lib No -	Sb ppm	Sc ppm	Se ppm	Sm ppm	Sn ppm	Sr ppm	Ta ppm	Te ppm	Th ppm	U ppm	V ppm	W ppm	Y ppm	Yb ppm	Zn ppm	Zr ppm
08-488	0.2	39.5	0	0.7	2	30	1	0.13	3.4	1	285	15	7	1.1	6	106
08-493	0.1	55.5	0	1.1	2	16	1	0.02	7.6	1	282	5	12	1.7	3	223
08-486	0.1	50.1	1	2.0	0	20	1	0.06	9.3	1	418	1	12	2.1	36	154
08-495	0.1	40.7	0	1.1	0	40	0	0.06	5.0	1	128	5	8	1.2	25	162
08-494	0.3	57.5	0	2.8	0	13	1	0.09	11.0	1	204	9	17	2.7	10	199
08-499	0.6	71.0	1	0.8	3	10	0	0.11	2.7	1	373	2	5	1.1	19	123
08-498	0.3	43.3	0	1.6	2	25	0	0.15	3.1	1	148	7	11	1.7	14	159
08-497	0.7	62.8	2	0.7	2	11	0	0.09	6.5	1	305	5	6	1.1	13	155
08-496	0.1	37.9	0	1.0	0	22	1	0.14	4.6	1	241	10	7	1.1	20	154
08-071	0.3	35.9	0	1.0	0	25	1	0.03	3.7	1	261	11	7	0.9	24	146
08-073	0.1	57.5	2	2.0	0	9	1	0.18	8.4	1	375	8	12	2.3	13	178
08-077	0.2	66.8	1	1.0	0	35	1	0.05	9.6	1	368	4	15	2.2	7	206
08-070	0.1	24.2	0	1.0	2	23	1	0.20	4.6	1	219	14	9	1.1	23	112
08-069	0.7	43.1	0	0.7	1	20	1	0.04	4.1	1	248	20	7	1.0	61	132
08-067	0.1	30.4	0	1.3	2	16	1	0.00	5.9	1	138	1	11	2.0	15	207
08-052	0.2	61.4	0	0.8	1	3	1	0.03	5.3	1	386	14	14	1.7	10	144
08-053	0.2	68.0	0	1.5	6	15	1	21.00	7.2	1	465	13	23	2.8	23	290
08-054	0.2	85.8	0	1.5	3	17	2	8.00	8.7	2	391	12	26	2.9	20	283
08-060	0.1	41.2	0	7.8	0	20	1	0.06	5.8	1	240	23	34	3.4	218	133
08-065	0.6	49.2	0	4.6	0	13	1	0.10	6.2	2	430	2	16	3.0	95	145
08-066	0.9	82.9	0	2.0	0	8	0	0.10	0.8	1	509	2	8	1.3	29	95
08-044	0.1	32.4	1	1.6	1	46	1	0.04	3.8	2	231	4	12	1.3	58	96
08-043	0.1	32.8	0	3.3	3	48	1	0.02	4.5	1	256	2	19	2.0	81	107
08-037	0.1	53.1	2	3.4	0	10	1	0.25	5.7	1	741	14	20	3.1	176	145
08-011	0.1	38.4	2	7.7	1	41	1	0.08	5.8	1	308	16	48	4.5	444	129
08-020	0.2	28.6	0	2.9	0	66	1	0.26	4.2	2	280	12	21	1.9	172	105
08-021	0.2	34.2	0	3.2	0	207	2	0.05	4.4	2	308	7	18	1.8	304	122

Metamorphic Grade	:	Greenschist Facies
Structural Attributes	:	Partly sheared and mineralized
Gross Features	:	Xenoliths of fuchsitic material and carbonate alteration
Profile Truncation	:	Complete profile
Depth to Fresh Rock	:	50-70 m
Location	:	Mt. Percy Mine, Kalgoorlie
Reference	:	Butt, 1991.

Geomorphology and regolith
Mt. Percy is relatively high in the landscape (total relief only a few tens of metres) and its upper parts are armoured with a lateritic duricrust or cuirasse. This is developed particularly strongly over the associated mafic and ultramafic rocks. Samples were collected during mining along two sections, of which one (15850N) has been studied petrographically (Figure P1-1)

Fresh porphyry
There are minor variants of these feldspar-phyric rocks, some containing additional quartz and others altered mafic phenocrysts; the groundmass consists of albite, quartz and carbonate ± K-feldspar. Where fresh (specimen MW-1809) the porphyry is fine-grained and light grey, flecked with greenish and khaki patches of chlorite and carbonate, and dotted with small, equant grains of magnetite (Figure P1-2A). The groundmass consists of semi-aligned laths of K-feldspar and albite, with some interstitial, fine-grained quartz granules and muscovite flakes. Patches of carbonate, quartz and chlorite, scattered throughout, represent pseudomorphed mafic phenocrysts or micro-xenoliths (Figure P1-2B).

Saprock
Above the weathering front (55 m depth), the porphyry (MW-1937) is stained a pale brown by goethite. It consists of white plagioclase and grey quartz with pale green micaceous patches (Figure P1-2C). It is relatively fresh but all contained pyrite and magnetite have been altered to goethite. The porphyry consists of a groundmass of laths of plagioclase and interstitial quartz in which are set microcline phenocrysts. The feldspars show some sericitization and kaolinization (Figure P1-2D). Clots of matted sericite and irregular patches of muscovite, stained with goethite, appear to represent either severely altered micro-xenoliths or altered mafic phenocrysts.

Saprolite
The porphyry saprolite at 47.5 m (MW-1723) is particularly rich in small (2-10 mm) polymictic xenoliths, which make up almost half the rock (Figure P1-2E). The fine-grained groundmass is medium brown; although some of the groundmass feldspar has been kaolinized, the porphyritic fabric remains. Laths of plagioclase have been completely kaolinized in patches, leaving the interstitial quartz unaffected (Figure P1-2F). Some of the quartz phenocrysts are corroded glomerocrysts.

Higher in the saprolite (40 m depth), the almost completely kaolinized and brown-stained groundmass is set with numerous polymictic xenoliths and grains or quartz (Figure P1-2G). Alteration of the felsic component of the groundmass, which is a very pale brown, is essentially complete, though XRD analysis indicates a trace of remnant feldspar (MW-1697), however, the kaolinized feldspars of the groundmass maintain their lath-like shapes where protected by quartz (Figure P1-2H).

Near the top of the saprolite (MW-1625; depth 25 m), where feldspar has been completely consumed, the kaolinized groundmass is patchily stained brown and is set with small, greenish

and brown xenoliths (Figure P1-2I). The groundmass consists of a mass of patchy, matted kaolinite and sericite, set with quartz grains and compound grains of quartz. The fabric of the kaolinite which, lower down, had preserved the feldspar fabric, has been reorganized and the detailed lath-like feldspar pseudomorphic fabric is largely lost (Figure P1-2J). A few white, vein-like patches and rounded blasts of secondary kaolinite, with a slightly high birefringence, meander in the fabric. The loss of primary fabric and the appearance of secondary kaolinite indicate early pedogenesis and transition to the plasmic zone.

Clay saprolite, plasmic and mottled clay zone

Globular blasts of white, pedogenic kaolinite (MW-1530) mark the complete destruction of the igneous fabric at 25 m depth (Figure P1-2K, L). The yellow-brown, flaky kaolinitic and sericitic groundmass has been patchily stained pink by traces of hematite. The re-texturing is very incomplete, its extent variable and the kaolinite blasts are, in places, less distinct (MW-1457). A few vermiform patches and knots of highly goethite-stained material probably represent channelways and root passages.

Pedogenic and saprolitic fabrics co-exist on the cm scale illustrating the incompleteness of the pedogenesis. A 17.5 m depth (MW-1292) the porphyry has a light-brown, highly kaolinized groundmass (Figure P1-2M), set with a few very small patches of blastic kaolinite. Highly ferruginized knots and tubes mark root passages. It is particularly quartz rich and is intensely stained with goethite, however, although the original felsic groundmass is no longer recognizable in the main, a few completely kaolinized feldspar laths (Figure P1-2N) remain unstained by goethite and locally preserve the igneous micro-fabric.

Much higher in the profile (8 m depth), the original fabric has been completely destroyed. Here, a creamy-coloured mass of very fine-grained, pedogenic kaolinite, with no pseudomorphed igneous fabric, is set with remnant quartz grains and ferruginized tubules and channelways (Figure P1-2O). Other parts of the kaolinized mass are intensely stained with hematite. Globular to subangular fragments of quartz glomerocrysts are set in a groundmass of goethite-stained, flaky kaolinite (MW-0741; Figure P1-2P). There is comparatively little muscovite. Even where the goethite staining is less intense, no saprolitic groundmass fabric is recognizable.

Higher still (5 m depth), approaching the cementation front, granules of goethite become important. Creamy-brown, goethite-stained, very fine-grained pedogenic kaolinite, with no recognizable primary fabric (MW-0570), is set with remnant quartz grains and nodules of goethitic material. There are two types of kaolinite, an older goethite-kaolinite fabric is cut by a younger fabric of fine-grained but stained kaolinite, set with chips of quartz and a few ferruginous granules.

Duricrust

The porphyries yield a pisolitic to fragmental duricrust (LT202, LT205; Anand *et al*, 1989); the pisolitic type is the most common. The pisolites are, in part, cored by black, subrounded to subangular fragments rich in goethite and hematite. Others consist of goethite- and hematite-stained clays. Some are coated with honey-brown goethite, others with yellow clays.

Near the base of the duricrust (MW-0399; depth 2.5 m), large (10-15 mm) clay-rich, brown to yellow-brown pisolites lie in, and are supported by, a matrix of similar finer-grained material and all are set in a dark brown clay-rich cement. Many of the larger pisoliths have multi-layered cutans. A low proportion (10%) are cored with angular hematitic goethite fragments set in porous goethite. Most of these angular fragments only show dehydration structures, and seem to have replaced quartz phenocrysts; a very few outwardly round fragments contain relics of very fine-grained layer-silicates, apparently after saprolitic kaolinite. The larger pisoliths have thin

ocherous coatings of yellow-brown clay. The small pisoliths have cores of ferruginous clay, with a few patches and fragments of hematitic goethite, and very thick cutans (over 50% by volume).

Higher in the profile (specimen MW-0181A; 0.4 m depth), black, subrounded to subangular hematitic goethite fragments, only containing secondary structures, are cemented by dark brown goethite. Parts of this goethite cement have been dissolved, leaving irregular, branching cavities which have, in part, been infilled with clays and clay micropisoliths. In a very few places in the cores, fine-grained layer silicate pseudomorphs are preserved in large patches, some showing accordion structures, after pedogenic kaolinite and a few angular goethite fragments with no internal structure, possibly after disaggregated primary quartz glomerocrysts. There are also a very few mica remnants.

Specimen MW-0182 (0.3 m depth) is part of a complex nodule of black, hematitic goethite fragments, set in a yellow-brown ferruginous clay, containing pisoliths. Only secondary structures are apparent in the hematitic goethite fragments, many of which have attached pisolitic material. The matrix is spongy, lead-grey goethite, with a few incipient pisolitic structures. Specimen MW-0183 (0.1 m depth) consists of black subangular to subrounded hematitic goethite fragments, set in a red-brown goethitic matrix which shows evidence of at least three phases of matrix dissolution, re-cementing and infilling. Secondary dehydration fabrics dominate the early fragments, although some structureless fragments within them could be after angular quartz. The lead-grey goethite matrix is very porous and contains numerous incipient pisoliths.

In the duricrust formed from porphyry, the only preserved fabrics are those after saprolitic and pedogenic kaolinite, and some rare primary muscovite remnants; none of these are diagnostic of the underlying bedrock. The only primary porphyry fabric preserved in the duricrust are the relatively featureless, but typically angular, hematitic goethite fragments which may have replaced disaggregated quartz glomerocrysts but these are unlikely to be diagnostic.

Mineral stability.

Most of the mineralogy of the porphyries survive in the saprock, only pyrite oxidizing to goethite and extensively staining the rock. Part of this reaction would be expected to be buffered by the extensive carbonate alteration. Feldspars, particularly K-feldspar, survive into the saprolite zone but they are absent at the top of the saprolite. Muscovite begins to weather in the plasmic zone but some survives into the duricrust; muscovite is a comparatively minor component of the fresh rock. Quartz survives throughout the saprolith and lower pedolith but appears to be replaced by Fe oxides in the duricrust.

Reference

Butt, C.R.M. 1991. Dispersion of gold and associated elements in the lateritic regolith, Mystery Zone, Mt Percy, Kalgoorlie, Western Australia. CSIRO Division of Exploration Geoscience Restricted Report 156R.

Anand, R.R., Smith, R.E., Innes, J., Churchward, H.M., Perdrix, J.L. and Grunsky, E.C. 1989. Laterite types and associated ferruginous materials, Yilgarn Block. CSIRO Division of Exploration Geoscience Restricted Report 60R.

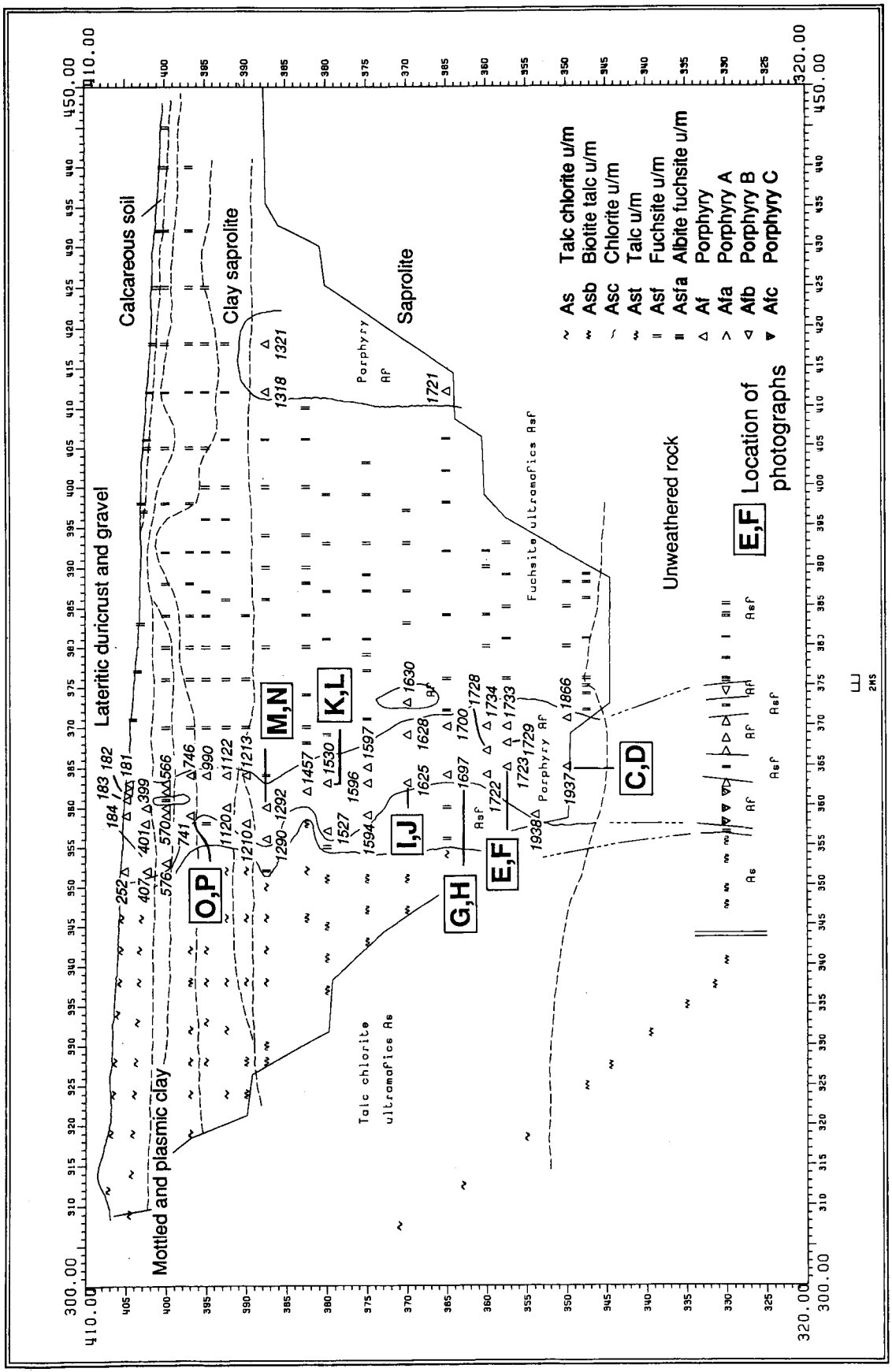

Figure P1-1. Section 15850N showing a steep-dipping porphyry, enclosed in various talcose, chloritic and fuchsitic ultramafics, passing from duricrust to fresh rock.

FIGURE P1-2

Saprolite

G. Polymictic micro-xenoliths (XN) dominate the matrix, which is set with small quartz phenocrysts (QZ). Specimen MW-1697. Depth 40 m. Close-up photograph of 'dry' surface.

H. Kaolinization of the feldspars (KA) is complete (virtually no birefringence), but the fabric of the feldspars is preserved by surrounding quartz (QZ). Specimen MW-1697. Depth 40 m. Photomicrograph with crossed polarizers.

E. The porphyry is particularly rich in polymictic micro-xenoliths (XN), set in a partly kaolinized feldspathic groundmass (GM). Specimen MW-1723. Depth 47.5 m Close-up photograph of 'wet' surface.

F. Petrographic detail of P1-2E. Although kaolinization of the feldspar (KA) is almost complete, shown by its very low birefringence, the surrounding quartz (QZ) has preserved the feldspar fabric. The feldspathic fabric is surrounded by matted muscovite (MU). Specimen MW-1723. Depth 47.5 m. Photomicrograph with crossed polarizers.

Saprock

C. The saprock is stained a pale brown. Small voids (VS) are left by dissolution of carbonates from among the micaceous patches. The feldspars (FS) are still relatively fresh. Specimen MW-1937. Depth 55 m. Close-up photograph of "wet" surface.

D. Petrographic detail of P1-2C. Relatively fresh feldspar (FS) remains, although some is partly kaolinized (KA). Cubic goethite pseudomorphs (GO) after magnetite and pyrite dot the fabric and are largely associated with micaceous patches (MP). A small, corroded quartz phenocryst (QZ) occurs in the centre of the section. Specimen MW-1937. Depth 55 m. Photomicrograph with crossed polarizers.

Fresh Rock

A. A fabric of grey quartz (QZ) and white feldspar (FS) is dotted with minor magnetite (MT) and a trace of pyrite. Muscovite, chlorite and carbonate form yellowish green irregular patches (MF) and some lath-like shapes, suggest altered and pseudomorphed mafic phenocrysts. Specimen MW-1808. Depth 121 m. Close-up photograph of "wet" surface.

B. Petrographic detail of P1-2A. Semi-aligned laths of K-feldspar and albite (FS) with scattered magnetite (MT) surround irregular patches of very fine-grained mica, chlorite and carbonate (MC) after micro-xenoliths. Specimen MW-1808. Depth 121 m. Photomicrograph with crossed polarizers.

FIGURE P1-2

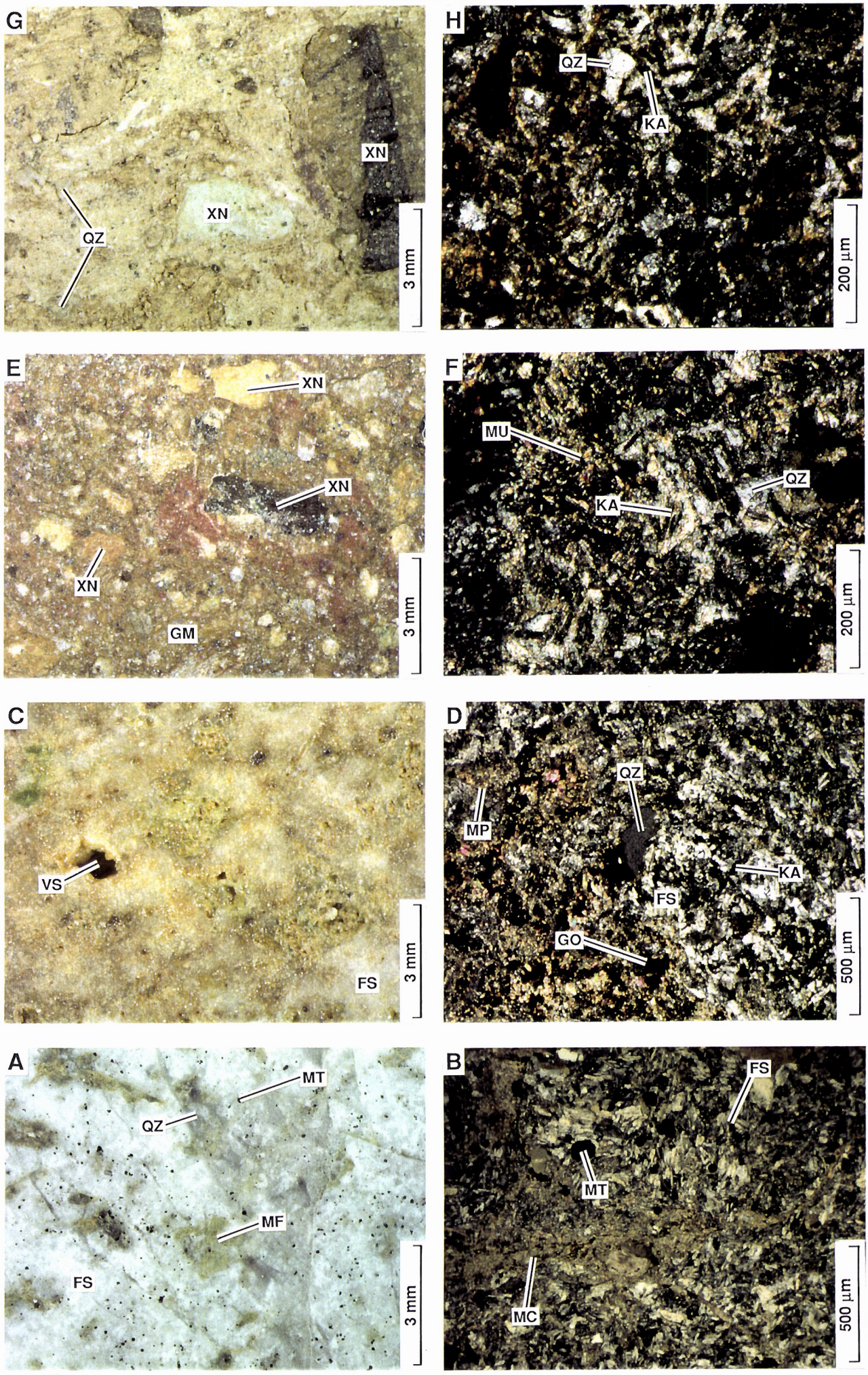

FIGURE P1-2 (Contd)

Clay saprolite, plasmic and mottled clay zone

O. The original fabric has been destroyed and is replaced with cream-coloured pedogenic kaolinite. Only quartz phenocrysts (QZ) remain. Numerous voids (VO) mark root passages. Specimen MW-741. Depth 8.0 m. Close-up photograph of 'dry' surface.

P. Petrographic detail of P1-2I. A fine grained mat of pedogenically restructured, Fe-stained kaolinite and sericite (KM) is set with relics of compound quartz phenocrysts (QZ), which are the only part of the original fabric to survive. Specimen MW-741. Depth 8.0 m. Photomicrograph with crossed polarizers.

M. The incompleteness of pedogenic processes is illustrated by a preserved saprolitic fabric of yellow clay and quartz (KQ), set with quartz phenocrysts (QZ) and goethite-rich patches (GO). Specimen MW-1292. Depth 17.5 m. Close-up photograph of 'dry' surface.

N. Petrographic detail of P1-2M. Although completely altered to kaolinite, the feldspar lath fabric (LF) is preserved in quartz (QZ) despite restructuring of clays by pedogenesis below (see P1-2K and L). Specimen MW-1292. Depth 17.5 m. Photomicrograph with crossed polarizers.

K. Globular blasts of white pedogenic kaolinite (KA) dominate a groundmass of kaolinite and sericite, variously stained yellow by goethite (GO) and pink by hematite (HM). Specimen MW-1530. Depth 25.0 m. Close-up photograph of "dry" surface.

L. Petrographic detail of P1-2K. Blasts of very fine-grained, matted kaolinite (KA) are set in matted sericite, kaolinite and quartz (MQ). Specimen MW-1530. Depth 25.0 m. Photomicrograph with crossed polarizers.

Saprolite

I. A pale-yellow, clay- and quartz-rich, fine-grained groundmass (KQ) is set with quartz phenocrysts, lath-like patches of goethite-stained, fine-grained mica (GM), probably after mafic phenocrysts, and minor, small goethite cubes (GO) after pyrite and/or magnetite. A few diffuse patches of white kaolinite (KA) indicate early stages of saprolite restructuring. Specimen MW-1625. Depth 25.0 m. Close-up photograph of "dry" surface.

J. Petrographic detail of P1-2I. The feldspar has been completely consumed and restructuring of the groundmass has led to the loss of much of the lath-like feldspar microfabric (compare with P1-2H and F). The saprolite consists of a fine-grained mat of quartz, kaolinite and mica (MA), with a few relics of feldspar structures (RF), set with goethite cubes (GO) after pyrite and magnetite. Specimen MW-1625. Depth 25.0 m. Photomicrograph with crossed polarizers.

FIGURE P1-2 (Contd)

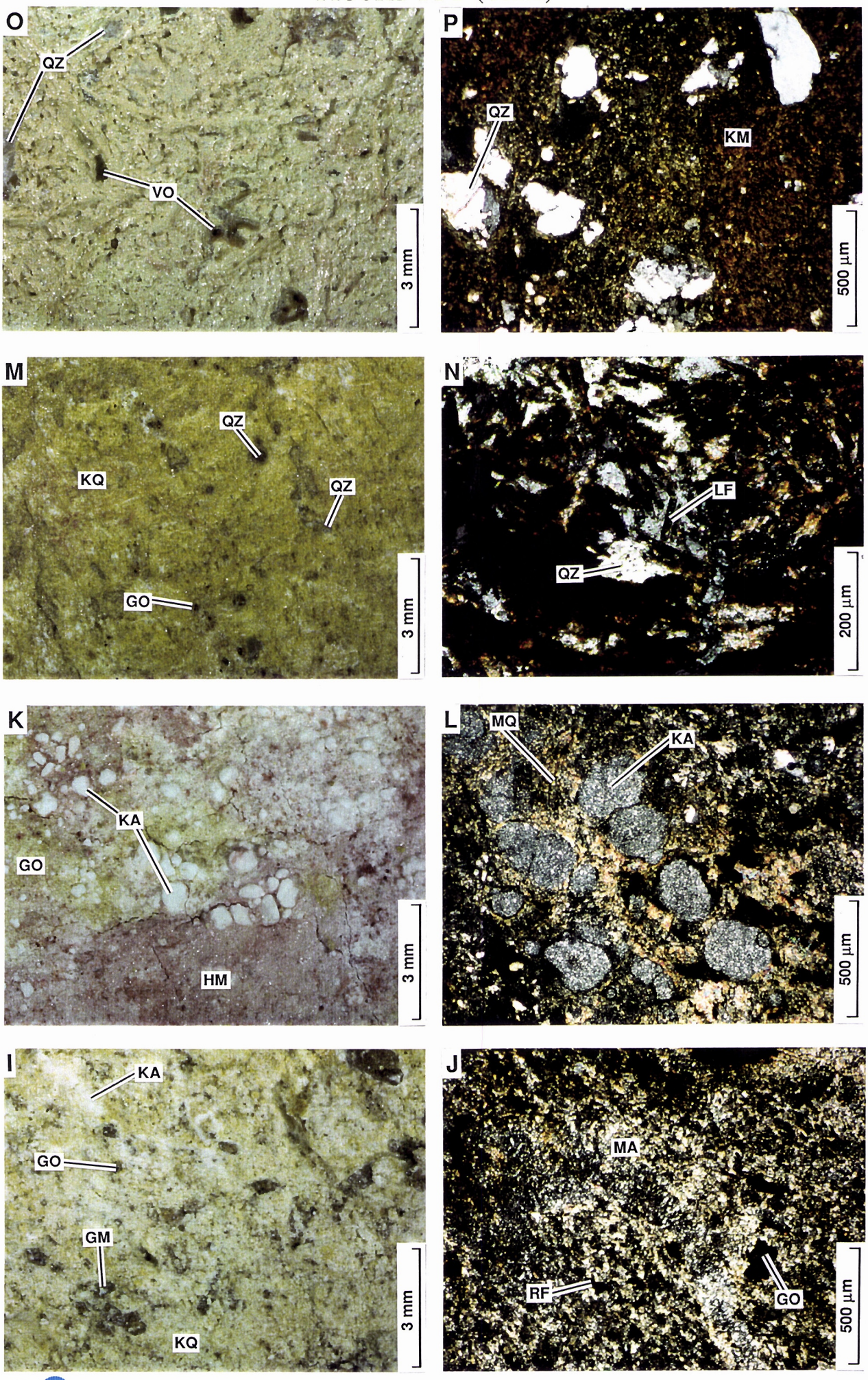

-	-	-	ICP	ICP	INAA	XRF	ICP	ICP	AAS	AAS	INAA	INAA	XRF
-	-	-	%	%	%	%	%	%	ppm	ppm	ppm	ppb	ppm
Sample	Depth	Regolith Unit	SiO2	Al2O3	Fe2O3	TiO2	CaO	MgO	Na2O	K2O	As	Au	Ba
MW-184	0.0	Duricrust	19.80	8.50	62.33	8.61	0.32	0.17	-	-	44	450	289
MW-252	0.0	Duricrust + carbonate	13.30	9.70	47.61	4.94	9.95	0.78	-	-	29	554	162
MW-183	0.1	Duricrust	7.16	5.70	72.20	11.87	0.01	0.10	-	-	78	350	298
MW-182	0.3	Duricrust + carbonate	19.29	8.80	61.19	8.21	0.68	0.15	-	-	65	723	308
MW-181	0.4	Duricrust + carbonate	21.67	8.90	57.62	8.12	0.38	0.16	-	-	57	698	269
MW-222	0.5	Duricrust + carbonate	9.23	21.00	45.18	7.43	1.17	0.32	705	348	70	943	145
MW-100	0.5	Duricrust + carbonate	24.60	15.00	38.60	3.76	2.91	0.65	1420	2340	110	3590	644
MW-244	0.7	Duricrust + carbonate	15.30	17.00	33.45	4.94	9.48	0.81	1590	925	56	1090	455
MW-401	2.4	Duricrust + carbonate	15.60	16.00	47.04	6.21	0.56	0.31	-	-	160	260	168
MW-399	2.5	Duricrust	21.92	20.50	42.03	2.61	0.01	0.24	-	-	394	380	120
MW-407	2.6	Duricrust + carbonate	10.90	18.00	47.04	7.04	0.18	0.36	-	-	71	380	88
MW-451	4.0	Mottled clay	27.90	22.00	33.17	1.61	0.15	0.35	2420	5290	140	150	110
MW-566	5.0	Plasmic clay	52.56	14.90	23.73	0.66	0.01	0.31	-	-	150	26	589
MW-567	5.0	Plasmic clay	59.61	18.00	9.39	1.13	0.01	0.48	-	-	35	54	689
MW-569	5.0	Plasmic clay	53.37	21.20	13.64	1.17	0.01	0.24	-	-	246	35	353
MW-570	5.0	Plasmic clay	30.40	19.00	33.60	1.61	0.03	0.24	-	-	600	76	185
MW-576	5.0	Plasmic clay	22.80	23.00	29.31	3.89	0.02	0.11	-	-	77	16	137
MW-660	7.0	Plasmic clay	38.30	26.00	19.73	1.32	0.03	0.38	3820	8440	120	110	191
MW-671	7.0	Plasmic clay	39.90	27.00	18.73	1.45	0.03	0.51	2630	14600	200	49	784
MW-501	8.0	Mottled clay	27.60	27.00	32.17	1.07	0.05	0.25	2940	3370	87	77	120
MW-491	8.0	Mottled clay	38.30	20.00	31.88	0.66	0.06	0.35	1720	13500	170	18	776
MW-741	8.0	Mottled clay	42.80	22.00	19.87	0.94	0.09	0.25	-	-	305	38	344
MW-746	8.0	Plasmic clay	56.70	16.00	14.44	0.69	0.04	0.48	-	-	170	39	1003
MW-920	9.0	Clay saprolite	40.40	20.00	28.17	1.10	0.04	0.46	1850	15400	318	30	690
MW-925	9.0	Clay saprolite	47.30	20.00	16.87	1.05	0.01	0.53	2160	25700	74	22	235
MW-990	10.0	Clay saprolite	69.40	16.00	5.00	0.68	0.04	0.72	-	-	33	69	1716
MW-620	11.0	Mottled clay	27.30	19.00	38.17	0.85	0.05	0.87	1470	31200	283	22	758
MW-1098	11.5	Mottled clay	45.00	15.00	27.74	0.73	0.06	1.12	3740	12100	240	44	363
MW-1101	11.5	Mottled clay	58.30	19.00	11.44	1.06	0.03	0.73	2470	23800	34	18	371
MW-1120	12.5	Clay saprolite	71.21	14.10	5.72	0.61	0.01	0.47	-	-	20	420	780
MW-1122	12.5	Clay saprolite	68.00	17.00	3.57	0.69	0.02	0.65	-	-	15	86	1326
MW-860	13.0	Mottled clay	33.40	19.00	31.88	0.83	0.04	0.81	1570	36800	331	12	539
MW-865	13.0	Mottled clay	37.20	22.00	24.45	0.74	0.01	0.77	1920	25000	180	10	1422
MW-870	13.0	Mottled clay	49.00	29.00	5.29	0.92	0.01	0.55	2130	25800	24	3	1140
MW-1210	15.0	Mottled clay	71.60	9.70	10.18	0.42	0.02	0.31	-	-	140	44200	494
MW-1213	15.0	Saprolite	85.50	1.40	10.88	0.05	0.02	0.05	-	-	150	682	70
MW-1073	15.5	Saprolite	62.10	29.00	3.43	0.91	0.01	0.68	1820	29000	33	75	714
MW-1268	16.5	Saprolite	51.70	17.00	15.44	1.09	0.01	0.69	2420	29000	62	200	1074
MW-1271	16.5	Saprolite	53.70	17.00	10.98	1.20	0.03	0.97	2540	39300	17	210	915
MW-1290	17.5	Saprolite	61.50	17.00	5.58	0.62	0.03	0.65	-	-	80	43	1420
MW-1292	17.5	Saprolite	67.30	20.00	4.29	0.67	0.02	0.75	-	-	60	410	1547
MW-1367	19.0	Saprolite	46.80	14.00	17.16	0.93	0.05	1.46	8690	20900	190	744	860
MW-1234	20.5	Clay saprolite	59.90	18.00	6.72	0.76	0.01	0.18	1650	8220	13	8	263
MW-1236	20.5	Clay saprolite	48.70	22.00	2.14	0.53	0.01	0.48	4070	46200	48	551	928
MW-1239	20.5	Clay saprolite	60.90	18.00	7.81	0.68	0.01	0.62	1660	21900	59	3750	1060
MW-1241	20.5	Clay saprolite	65.40	16.00	5.00	0.79	0.02	0.69	2350	28500	74	200	946
MW-1440	21.5	Saprolite	48.70	17.00	20.16	0.98	0.01	0.68	1830	31700	180	100	286
MW-1443	21.5	Saprolite	51.90	16.00	18.30	1.00	0.03	0.57	2710	22500	208	791	1185
MW-1445	21.5	Saprolite	23.20	8.00	51.33	0.47	0.02	0.46	1160	21000	472	512	960
MW-1448	21.5	Saprolite	53.20	12.00	23.73	0.71	0.05	0.31	1690	9940	180	79	419
MW-1457	22.5	Saprolite	54.60	17.00	9.41	0.58	0.03	0.57	-	-	76	3180	1026
MW-1337	23.0	Saprolite	75.90	13.00	2.72	0.57	0.03	0.75	1500	35800	120	140	1005
MW-1342	23.0	Saprolite	60.30	19.00	2.29	0.65	0.02	0.46	3440	29300	37	430	1045
MW-1527	25.0	Saprolite	45.60	13.00	28.31	0.50	0.03	0.36	-	-	555	795	606
MW-1530	25.0	Saprolite	59.10	19.00	8.39	0.61	0.01	0.56	-	-	82	2270	1182
MW-1411	25.5	Saprolite	63.40	19.00	3.86	0.61	0.01	0.38	1470	16600	43	23	481

-	-	INAA	INAA	INAA	INAA	INAA	XRF	INAA	XRF	XRF	INAA	INAA	INAA	XRF	XRF	XRF	XRF
-	-	ppm	ppm	ppm	ppm	ppm	ppm	ppm	ppm	ppm	ppm	ppm	ppm	ppm	ppm	ppm	ppm
Sample	Depth	Br	Ce	Co	Cr	Cs	Cu	Eu	Ga	Ge	Hf	La	Lu	Mn	Nb	Ni	Pb
01-184	0.0	5.8	11.0	48	812	2.6	26	0.94	75	1	7.7	10	0.64	430	9	84	20
01-252	0.0	8.4	34.0	42	500	0.5	26	0.85	81	1	5.3	10	0.47	123	10	102	16
01-183	0.1	4	10.0	70	636	0.5	28	0.79	98	1	9.1	5	0.83	168	15	71	13
01-182	0.3	6.3	20.0	39	1020	2.6	41	0.91	86	4	8.2	10	0.71	244	14	92	19
01-181	0.4	9.3	20.0	51	923	3.2	43	0.86	71	4	8.0	10	0.67	437	10	101	17
01-222	0.5	4.1	10.0	54	1050	1.1	29	1.00	75	1	8.7	10	0.61	321	13	150	16
01-100	0.5	9.1	16.0	61	1810	1.3	49	0.80	47	1	5.6	7	0.37	211	8	236	15
01-244	0.7	11	16.0	40	820	1.6	43	0.91	53	1	6.6	10	0.53	447	8	138	13
01-401	2.4	25	7.2	39	1320	0.5	50	0.69	77	2	6.1	5	0.43	123	8	165	19
01-399	2.5	24	7.5	30	1960	1.4	72	0.25	45	4	4.8	3	0.26	123	6	242	15
01-407	2.6	10	11.0	75	589	1.7	72	0.25	58	1	7.3	4	0.41	1052	10	154	12
01-451	4.0	24	8.3	34	2530	4.3	63	0.25	34	2	3.5	2	0.20	49	5	342	19
01-566	5.0	17	3.7	5	1380	4.7	51	0.25	27	2	4.0	3	0.10	13	3	89	10
01-567	5.0	28	5.5	6	1860	8.7	33	0.25	30	3	3.8	3	0.10	50	4	112	6
01-569	5.0	30	3.8	10	2150	8.4	36	0.25	28	5	3.5	2	0.10	34	4	136	4
01-570	5.0	41	2.4	14	3590	5.4	56	0.25	38	3	3.2	2	0.10	29	6	145	7
01-576	5.0	40	2.8	21	2510	0.5	52	0.25	55	2	5.5	2	0.24	130	8	253	19
01-660	7.0	32	1.0	18	2690	9.4	48	0.25	30	2	3.1	2	0.10	19	3	335	9
01-671	7.0	21	5.6	18	2040	14.0	92	0.25	35	4	6.7	2	0.10	7	4	463	10
01-501	8.0	17	70.0	46	2400	3.8	47	0.25	28	3	4.2	5	0.10	37	4	355	25
01-491	8.0	22	1.0	10	704	8.0	46	0.25	25	3	4.2	1	0.10	3	2	90	20
01-741	8.0	21	3.6	12	2330	6.2	55	0.25	29	5	3.6	2	0.10	26	5	171	7
01-746	8.0	20	5.8	5	1100	5.0	48	0.25	29	4	3.9	4	0.10	8	3	80	6
01-920	9.0	33	5.4	14	1050	8.8	178	0.53	27	3	4.4	2	0.10	11	3	277	12
01-925	9.0	24	5.5	9	539	18.0	57	0.25	25	2	4.2	2	0.20	4	7	139	1
01-990	10.0	10	9.5	2	460	4.9	17	0.25	28	2	4.7	6	0.10	2	5	57	2
01-620	11.0	14	2.7	39	3470	11.0	173	0.25	23	3	1.8	2	0.10	184	1	444	26
01-1098	11.5	22	6.6	40	2070	7.3	134	0.57	20	3	2.0	4	0.10	119	1	524	7
01-1101	11.5	20	5.8	17	1010	14.0	44	0.25	24	3	3.6	3	0.10	35	4	187	2
01-1120	12.5	8.1	4.4	2	1680	4.1	24	0.25	22	3	3.9	2	0.10	12	4	64	5
01-1122	12.5	13	4.5	2	420	5.4	13	0.25	29	3	4.7	2	0.10	3	3	59	1
01-860	13.0	12	3.8	34	3830	14.0	99	0.25	21	2	2.3	2	0.10	40	2	258	19
01-865	13.0	12	5.1	47	1560	8.7	94	0.25	31	1	3.7	2	0.10	52	3	257	7
01-870	13.0	9.4	4.1	4	871	8.5	23	0.25	39	2	6.2	1	0.10	5	4	89	4
01-1210	15.0	12	3.7	30	822	3.3	59	0.25	15	1	2.5	3	0.10	27	3	145	18
01-1213	15.0	3.9	1.0	2	200	0.5	21	0.25	2	1	0.5	1	0.10	27	1	18	5
01-1073	15.5	7.1	4.1	3	390	7.2	33	0.25	37	2	5.8	1	0.10	6	4	89	5
01-1268	16.5	16	22.0	20	350	11.0	103	0.67	27	1	4.9	14	0.10	88	6	323	2
01-1271	16.5	15	23.0	25	140	10.0	53	0.81	30	2	5.2	16	0.25	200	5	342	7
01-1290	17.5	7.4	3.5	13	400	6.0	35	0.25	27	1	4.0	2	0.10	12	4	108	6
01-1292	17.5	6.2	5.6	8	330	5.4	40	0.25	29	3	4.1	2	0.10	12	4	120	2
01-1367	19.0	21	11.0	30	1080	7.1	139	0.63	22	3	3.7	7	0.10	107	4	518	8
01-1234	20.5	20	4.6	14	1850	3.8	69	0.25	21	3	3.0	2	0.10	36	1	213	4
01-1236	20.5	34	7.3	8	260	4.3	90	0.25	24	4	4.0	4	0.10	5	3	55	12
01-1239	20.5	8.8	5.7	16	773	5.1	41	0.25	29	2	4.3	4	0.10	54	2	197	3
01-1241	20.5	10	2.7	10	1390	5.8	64	0.25	23	3	3.4	2	0.10	36	2	142	5
01-1440	21.5	8.7	19.0	26	250	8.2	107	0.73	22	1	3.9	6	0.25	24	7	555	8
01-1443	21.5	10	14.0	13	280	5.8	206	1.00	24	1	4.4	9	0.21	24	3	441	12
01-1445	21.5	6.5	22.0	42	450	6.2	326	1.30	8	3	2.3	13	0.10	70	1	1419	12
01-1448	21.5	10	7.9	22	2300	2.1	185	1.20	16	1	2.0	6	0.29	33	2	715	7
01-1457	22.5	14	9.2	3	290	4.1	55	0.25	26	1	3.7	7	0.10	1	4	83	14
01-1337	23.0	7.3	4.0	6	2310	5.4	69	0.25	17	3	2.2	3	0.10	20	1	124	4
01-1342	23.0	16	6.0	6	310	4.9	52	0.25	27	2	4.1	3	0.10	16	1	78	8
01-1527	25.0	13	19.0	51	1530	4.6	278	1.30	16	2	2.4	8	0.10	205	2	682	23
01-1530	25.0	14	12.0	5	370	5.2	63	0.25	26	2	3.7	11	0.10	9	2	140	21
01-1411	25.5	7.4	10.0	5	230	4.8	38	0.25	26	2	4.6	3	0.10	20	6	95	3

-	-	XRF	XRF	INAA	INAA	INAA	XRF	INAA	INAA	XRF	INAA	XRF	INAA	XRF	XRF
-	-	ppm	ppm	ppm	ppm	ppm	ppm	ppm	ppm	ppm	ppm	ppm	ppm	ppm	ppm
Sample	Depth	Rb	S	Sb	Sc	Sm	Sr	Ta	Th	V	W	Y	Yb	Zn	Zr
01-184	0.0	10	0.000	8.9	25.2	2.4	19	1.30	6.6	2857	31	29	3.50	18	238
01-252	0.0	3	0.000	5.9	26.0	2.4	212	1.20	3.0	2361	22	24	2.70	7	166
01-183	0.1	3	0.000	13.0	17.6	1.9	9	2.00	3.0	4426	54	32	4.30	19	225
01-182	0.3	10	0.000	10.0	27.1	2.8	24	0.50	8.1	2705	35	31	3.70	39	227
01-181	0.4	12	0.000	9.2	24.7	2.7	28	1.70	6.1	2443	34	26	3.40	38	215
01-222	0.5	3	0.000	8.0	25.0	2.7	37	1.40	5.7	1327	32	28	3.20	15	291
01-100	0.5	12	0.000	8.1	30.3	2.0	94	0.25	5.1	790	28	19	2.10	24	199
01-244	0.7	4	0.000	5.6	22.2	2.8	143	0.67	5.1	872	20	22	2.70	15	220
01-401	2.4	5	2.000	8.8	31.0	1.6	54	0.71	3.6	2076	33	19	2.50	19	198
01-399	2.5	6	1.000	5.2	35.3	1.3	33	0.50	5.2	1309	13	11	1.40	54	143
01-407	2.6	1	0.000	5.8	30.6	1.4	22	1.90	4.2	1786	22	19	2.40	26	223
01-451	4.0	21	0.000	10.0	34.7	0.8	19	0.25	4.4	631	27	7	1.00	29	145
01-566	5.0	45	0.000	10.0	16.7	0.8	25	0.50	6.2	476	25	5	0.75	13	125
01-567	5.0	65	0.000	8.1	21.3	0.8	32	0.50	5.0	397	21	8	1.00	14	134
01-569	5.0	34	0.000	5.6	20.7	0.7	20	0.50	3.9	555	23	6	0.74	10	129
01-570	5.0	25	0.000	8.3	35.7	0.7	13	0.58	4.4	1384	19	1	0.84	6	117
01-576	5.0	3	1.000	6.1	42.9	0.6	34	1.40	4.8	1613	12	11	1.40	13	213
01-660	7.0	38	0.000	12.0	36.8	0.7	7	0.25	3.3	403	31	7	0.83	16	133
01-671	7.0	59	0.000	14.0	41.4	1.3	19	0.66	8.2	656	83	9	1.00	15	273
01-501	8.0	11	0.000	10.0	49.4	1.2	15	0.25	10.0	573	20	7	0.84	7	169
01-491	8.0	41	0.000	8.2	24.4	0.5	9	0.25	8.6	207	21	1	0.25	8	164
01-741	8.0	31	0.000	8.6	31.7	0.8	13	0.25	4.3	370	27	7	0.85	37	145
01-746	8.0	66	0.000	27.1	28.6	1.2	33	0.25	7.5	262	28	7	0.67	13	172
01-920	9.0	54	0.000	11.0	56.1	1.2	9	0.25	6.1	331	40	7	0.79	24	183
01-925	9.0	89	0.000	5.7	28.3	0.9	9	0.25	4.8	181	13	7	1.00	22	181
01-990	10.0	86	0.000	9.4	22.3	1.3	42	0.65	7.5	131	23	7	0.73	12	202
01-620	11.0	106	0.000	15.0	38.1	1.1	15	0.25	2.3	469	25	6	0.82	67	77
01-1098	11.5	42	0.000	11.0	41.1	1.4	9	0.25	2.7	289	27	9	0.87	41	83
01-1101	11.5	78	0.000	7.4	24.9	1.0	13	0.25	4.2	210	13	10	0.92	31	168
01-1120	12.5	58	0.000	8.5	23.3	0.9	20	0.50	5.1	175	40	8	0.89	16	146
01-1122	12.5	76	0.000	7.0	19.8	1.0	34	0.25	7.7	138	18	7	0.72	13	218
01-860	13.0	104	0.000	17.0	53.6	0.9	18	0.25	2.2	635	20	9	0.87	41	82
01-865	13.0	96	0.000	10.0	28.9	1.1	25	0.77	7.0	399	28	7	0.70	43	174
01-870	13.0	67	0.000	5.7	25.3	0.9	28	0.25	10.0	212	29	9	0.78	14	278
01-1210	15.0	31	0.000	11.0	26.5	0.9	13	0.25	3.4	169	18	6	0.76	57	109
01-1213	15.0	6	0.000	2.2	14.3	0.3	2	0.25	1.4	49	13	1	0.25	1	16
01-1073	15.5	73	0.000	7.2	19.8	1.0	27	0.25	9.0	177	27	9	1.00	17	260
01-1268	16.5	79	0.000	10.0	27.4	2.0	24	0.25	6.3	219	36	10	1.30	60	214
01-1271	16.5	112	0.000	7.8	20.7	2.8	26	0.25	6.6	229	18	14	1.50	80	240
01-1290	17.5	80	0.000	6.6	16.8	1.0	25	0.25	7.8	133	25	8	0.77	42	186
01-1292	17.5	77	0.000	7.0	16.7	0.9	28	0.25	7.0	155	31	7	0.73	41	203
01-1367	19.0	64	0.000	11.0	44.4	2.2	14	0.25	5.0	250	44	10	1.30	59	165
01-1234	20.5	17	1.000	5.0	45.3	0.9	15	0.25	3.2	208	17	12	1.20	17	133
01-1236	20.5	62	4.000	5.4	34.0	1.0	60	0.68	5.6	143	20	6	0.71	28	183
01-1239	20.5	60	0.000	7.8	20.6	1.4	26	0.25	7.2	174	29	9	0.84	46	182
01-1241	20.5	72	0.000	10.0	24.8	0.8	21	0.25	5.0	282	19	8	0.79	29	147
01-1440	21.5	92	0.000	9.3	26.0	3.0	14	0.78	6.1	173	16	14	1.40	62	192
01-1443	21.5	62	0.000	14.0	36.1	3.0	17	0.25	6.1	244	60	11	1.10	42	187
01-1445	21.5	58	0.000	9.4	45.7	4.3	7	0.25	4.5	156	21	11	0.74	82	80
01-1448	21.5	29	0.000	8.5	32.8	3.1	5	0.61	2.8	209	14	11	1.40	79	84
01-1457	22.5	62	2.000	7.7	22.8	1.1	33	0.25	6.9	193	27	6	0.59	15	175
01-1337	23.0	94	0.000	6.9	22.7	1.0	24	0.25	2.8	228	16	8	0.90	33	94
01-1342	23.0	59	2.000	5.9	18.7	1.0	37	0.84	7.4	150	25	7	0.66	35	196
01-1527	25.0	40	0.000	24.7	67.3	4.2	10	0.25	3.8	455	20	10	1.00	100	105
01-1530	25.0	59	1.000	7.0	23.7	1.3	33	0.66	5.9	146	31	5	0.69	24	168
01-1411	25.5	48	0.000	7.9	13.9	1.3	9	0.75	7.0	151	37	9	1.00	54	222

-	-	-	ICP	ICP	INAA	XRF	ICP	ICP	AAS	AAS	INAA	INAA	XRF
-	-	-	%	%	%	%	%	%	ppm	ppm	ppm	ppb	ppm
Sample	Depth	Regolith Unit	SiO2	Al2O3	Fe2O3	TiO2	CaO	MgO	Na2O	K2O	As	Au	Ba
MW-1415	25.5	Saprolite	63.80	19.00	2.14	0.64	0.01	0.56	2120	31900	26	110	1135
MW-1418	25.5	Saprolite	63.40	19.00	2.43	0.70	0.02	0.56	2390	26700	33	31	1216
MW-1497	28.0	Saprolite	65.00	20.00	5.00	0.60	0.01	0.54	2310	26700	23	64	936
MW-1581	29.0	Saprolite	36.40	12.00	36.60	0.72	0.03	0.33	1290	14500	451	4040	656
MW-1583	29.0	Saprolite	54.40	23.00	8.72	1.29	0.01	0.65	2450	27800	50	49	1363
MW-1585	29.0	Saprolite	58.00	21.00	7.53	1.20	0.01	1.15	2470	47100	49	1250	1688
MW-1594	30.0	Saprolite	58.60	17.00	15.58	0.59	0.02	0.41	-	-	180	260	358
MW-1596	30.0	Saprolite	60.90	15.00	9.14	0.53	0.02	0.71	-	-	242	644	1097
MW-1597	30.0	Saprolite	58.60	17.00	4.00	0.55	0.03	0.52	-	-	62	3	1061
MW-1553	33.0	Saprolite	59.90	22.00	5.43	0.61	0.01	0.31	2060	8080	28	3490	287
MW-1561	33.0	Saprolite	65.10	21.00	2.57	0.65	0.01	0.56	1990	23700	26	350	847
MW-1625	35.0	Saprolite	58.90	17.00	6.72	0.62	0.00	0.67	-	-	71	79	1029
MW-1628	35.0	Saprolite	57.40	18.00	4.43	0.68	0.02	0.57	-	-	16	23	1315
MW-1630	35.0	Saprolite	44.10	27.00	13.17	1.60	0.03	0.50	-	-	66	6480	730
MW-1645	38.0	Saprolite	66.90	21.00	4.86	0.56	0.01	0.88	4520	30000	31	240	1148
MW-1646	38.0	Saprolite	63.60	19.00	6.86	0.68	0.07	2.20	13200	24100	43	190	963
MW-1697	40.0	Saprolite	56.10	13.00	7.95	0.20	0.04	2.17	-	-	61	632	393
MW-1700	40.0	Saprolite	83.70	6.60	2.14	0.24	0.01	0.23	-	-	18	821	514
MW-1722	45.0	Saprolite	71.60	16.00	3.86	0.54	0.03	0.68	-	-	28	913	1136
MW-1728	45.0	Saprolite	79.80	17.00	3.72	0.48	0.03	0.73	-	-	25	1080	1074
MW-1734	45.0	Saprolite	65.50	16.00	7.49	0.76	0.02	0.82	-	-	100	2090	1227
MW-1723	47.5	Saprolite	71.40	16.00	4.00	0.52	0.03	0.68	-	-	31	1250	1175
MW-1729	47.5	Saprolite	80.00	17.00	3.72	0.49	0.03	0.73	-	-	26	1120	1082
MW-1733	47.5	Saprolite	70.90	15.00	2.50	0.73	0.01	0.57	-	-	30	300	1345
MW-1846	48.0	Saprolite	71.80	15.00	7.42	0.43	0.05	0.69	44900	15900	37	754	443
MW-1848	48.0	Saprolite	73.00	17.00	4.15	0.55	0.05	0.74	40400	27400	18	516	1134
MW-1850	48.0	Saprolite	71.30	16.00	4.43	0.57	0.06	0.67	47900	25200	13	51	961
MW-1852	48.0	Saprolite	69.50	16.00	4.43	0.56	0.05	0.53	48200	21700	17	190	1056
MW-1847	50.5	Saprolite	69.10	14.00	9.31	0.50	0.05	0.73	35900	19900	37	542	730
MW-1849	50.5	Saprolite	74.20	15.00	3.86	0.49	0.05	0.57	49100	21000	18	410	1015
MW-1851	50.5	Saprolite	66.70	15.00	4.15	0.53	0.05	0.58	41500	24100	31	170	1231
MW-1853	50.5	Saprolite	63.90	18.00	6.72	0.82	0.05	0.74	38700	28500	26	84	1269
MW-1938	51.0	Saprolite	70.25	15.90	3.72	0.47	0.02	0.42	-	-	6	700	1368
MW-1904	53.0	Saprolite	66.03	14.30	4.29	0.48	0.02	0.54	42500	22700	23	320	849
MW-1907	53.0	Saprolite	68.68	13.60	4.29	0.46	0.03	0.49	42400	20600	28	330	955
MW-1908	53.0	Saprolite	66.51	14.90	6.29	0.51	0.02	0.87	32400	25500	26	94	1009
MW-1866	55.0	Saprolite	59.43	13.90	10.35	0.77	0.25	1.18	-	-	225	602	604
MW-1937	55.0	Saprolite	69.83	15.90	3.29	0.50	0.23	0.52	-	-	26	517	722
MW-1905	55.5	Saprolite	65.49	14.10	4.29	0.48	0.03	0.59	43900	25600	29	290	1068
MW-1906	55.5	Saprolite	66.75	14.70	3.86	0.48	0.03	0.47	58200	19300	23	968	841
MW-1827	56.0	Fresh	68.43	15.70	3.29	0.52	0.05	0.59	53800	19700	13	17	812
MW-1828	61.0	Fresh	68.87	16.70	3.86	0.54	0.05	0.76	57300	23200	26	140	858
MW-1829	65.0	Fresh	63.28	13.90	3.15	0.45	4.01	3.94	48600	465	10	140	804
MW-1815	119.0	Fresh	48.49	13.50	6.15	0.81	5.85	6.63	30500	33000	1	150	1154
MW-1816	119.5	Fresh	49.23	14.20	6.58	0.85	4.25	6.07	35000	32600	1	33	1797
MW-1802	121.0	Fresh	61.26	12.50	3.43	0.43	3.84	4.47	52200	10900	56	828	482
MW-1803	121.5	Fresh	61.50	13.70	3.43	0.46	3.47	4.12	52700	14600	55	470	533
MW-1804	122.0	Fresh	59.98	13.40	3.29	0.46	4.33	3.96	53300	13200	28	4990	566
MW-1805	122.5	Fresh	64.75	12.20	3.15	0.40	3.61	3.66	44500	15300	21	1580	669
MW-1806	123.0	Fresh	61.10	14.00	3.29	0.46	3.06	4.00	45100	21700	19	290	793
MW-1807	123.5	Fresh	60.17	13.40	3.43	0.43	3.62	3.90	48700	16900	22	460	622
MW-1808	124.0	Fresh	60.58	13.40	3.43	0.45	3.84	3.80	42200	21200	69	2220	756
MW-1809	126.0	Fresh	66.80	11.30	3.43	0.41	2.91	3.26	15500	29700	59	5450	1202
MW-1810	127.0	Fresh	63.58	13.40	3.29	0.45	3.21	3.64	46200	17800	34	1070	770
MW-1811	127.5	Fresh	62.58	12.80	3.43	0.42	3.21	4.02	54000	12600	6	310	634

-	-	INAA	INAA	INAA	INAA	INAA	XRF	INAA	XRF	XRF	INAA	INAA	INAA	XRF	XRF	XRF	XRF
-	-	ppm	ppm	ppm	ppm	ppm	ppm	ppm	ppm	ppm	ppm	ppm	ppm	ppm	ppm	ppm	ppm
Sample	Depth	Br	Ce	Co	Cr	Cs	Cu	Eu	Ga	Ge	Hf	La	Lu	Mn	Nb	Nl	Pb
01-1415	25.5	7.7	7.8	3	310	5.7	23	0.25	28	3	4.2	2	0.10	9	3	65	6
01-1418	25.5	8.3	4.1	2	300	4.9	30	0.25	29	2	4.2	3	0.10	10	1	51	5
01-1497	28.0	12	18.0	5	260	4.2	45	0.25	27	2	4.0	3	0.10	86	2	125	9
01-1581	29.0	7.9	23.0	67	604	4.7	260	1.10	14	1	2.5	9	0.25	100	4	906	5
01-1583	29.0	7.1	49.0	10	320	4.9	104	1.30	31	2	5.3	18	0.32	8	7	450	5
01-1585	29.0	6.6	63.0	7	310	9.0	79	1.50	31	2	5.5	35	0.32	10	5	255	4
01-1594	30.0	5.3	31.0	131	1690	2.9	150	0.87	24	3	3.3	5	0.10	883	2	923	15
01-1596	30.0	6.9	89.0	62	1020	3.8	233	0.25	23	1	3.3	49	0.10	189	2	736	45
01-1597	30.0	12	218.0	7	450	2.7	98	1.40	24	2	5.4	202	0.10	26	1	190	109
01-1553	33.0	8.5	8.6	12	566	4.4	67	0.55	25	2	4.1	2	0.25	27	4	353	2
01-1561	33.0	6.4	21.0	6	320	3.4	27	0.61	29	2	4.2	7	0.10	14	2	121	13
01-1625	35.0	5.1	52.0	38	597	5.0	36	0.92	26	2	3.8	23	0.10	115	4	395	13
01-1628	35.0	6	67.0	17	250	4.8	12	1.20	31	2	4.5	40	0.10	42	3	141	17
01-1630	35.0	11	190.0	48	79	3.9	139	2.00	37	2	7.5	76	0.50	282	10	436	19
01-1645	38.0	8.6	51.0	13	280	5.2	26	0.72	26	3	3.8	25	0.10	83	4	130	14
01-1646	38.0	15	27.0	45	805	4.5	57	0.53	25	3	3.3	12	0.10	367	3	462	9
01-1697	40.0	9.4	56.0	52	1170	4.2	29	1.60	17	2	3.1	33	0.20	220	1	342	34
01-1700	40.0	3.3	15.0	10	160	1.2	49	0.25	9	1	1.6	8	0.10	76	1	76	11
01-1722	45.0	2.2	61.0	37	240	2.9	14	2.30	23	2	3.3	61	0.10	333	2	212	14
01-1728	45.0	3.3	63.0	31	200	3.2	28	2.80	22	2	2.8	61	0.10	474	2	161	22
01-1734	45.0	4.8	88.0	73	555	4.9	68	3.40	23	1	4.0	82	0.37	856	4	365	21
01-1723	47.5	3.7	61.0	35	250	4.2	21	3.40	23	1	3.5	79	0.24	339	1	218	13
01-1729	47.5	2.5	62.0	32	210	3.0	25	2.90	21	1	3.0	61	0.24	442	2	166	23
01-1733	47.5	1	61.0	58	190	2.5	26	3.10	22	2	3.2	69	0.26	865	2	153	20
01-1846	48.0	4	63.0	88	790	2.5	33	1.70	19	2	2.7	40	0.27	433	3	589	18
01-1848	48.0	2.2	62.0	43	300	4.1	26	2.60	23	1	3.1	54	0.29	527	4	216	13
01-1850	48.0	1	63.0	50	310	3.5	16	3.40	23	1	2.6	78	0.29	765	2	188	14
01-1852	48.0	2.6	130.0	42	250	3.8	23	3.70	24	2	3.3	82	0.35	742	1	171	33
01-1847	50.5	5.3	62.0	89	1430	4.3	50	1.40	20	3	1.9	30	0.28	462	1	667	9
01-1849	50.5	2.3	58.0	36	220	3.4	21	1.50	21	1	2.9	42	0.10	486	2	177	13
01-1851	50.5	1	60.0	57	240	4.1	17	2.90	22	1	3.1	66	0.25	663	4	182	15
01-1853	50.5	3.1	120.0	78	180	5.2	50	5.70	26	2	4.5	112	0.52	949	4	326	18
01-1938	51.0	3.2	62.0	21	140	4.2	14	1.60	20	1	3.7	35	0.10	373	2	305	3
01-1904	53.0	1	55.0	54	330	3.2	32	0.85	21	2	3.0	37	0.10	852	2	226	14
01-1907	53.0	3.2	55.0	63	220	3.8	20	1.30	20	2	3.0	38	0.10	1297	3	198	14
01-1908	53.0	4.1	53.0	77	644	4.8	28	1.70	20	2	3.0	41	0.10	809	1	374	9
01-1866	55.0	11.4	78.0	50	1110	4.2	87	2.07	20	1	4.6	52	0.20	318	2	571	10
01-1937	55.0	2.9	60.0	13	220	3.0	12	1.20	22	1	3.5	36	0.10	230	4	85	9
01-1905	55.5	1	59.0	29	260	4.1	20	1.20	21	1	3.2	35	0.10	489	1	173	18
01-1906	55.5	3.3	60.0	30	210	2.9	27	1.10	20	1	3.4	37	0.10	456	4	183	16
MW-1827	56.0	-	49.0	34	200	3.4	18	1.20	23	1	3.6	39	-	469	3	156	13
MW-1828	61.0	-	50.0	10	210	2.7	13	0.94	23	1	3.8	38	-	82	5	132	11
MW-1829	65.0	-	43.0	11	170	3.4	33	1.00	19	1	2.9	30	-	407	2	67	8
MW-1815	119.0	-	110.0	24	23	5.2	53	2.40	17	3	3.7	61	-	713	6	68	6
MW-1816	119.5	-	110.0	28	15	4.8	80	2.70	18	3	3.9	66	-	735	5	51	3
MW-1802	121.0	-	45.0	14	190	1.6	14	1.00	15	1	2.6	27	-	415	2	69	6
MW-1803	121.5	-	49.0	16	170	2.4	10	0.89	19	1	2.9	29	-	439	3	66	7
MW-1804	122.0	-	46.0	15	170	1.4	38	0.71	17	2	2.7	28	-	448	3	59	11
MW-1805	122.5	-	42.0	16	160	1.9	18	0.66	16	2	2.5	26	-	365	2	59	6
MW-1806	123.0	-	48.0	15	180	2.4	5	1.20	20	3	2.8	31	-	401	1	69	4
MW-1807	123.5	-	48.0	14	170	2.4	10	1.10	18	2	2.6	30	-	456	2	64	6
MW-1808	124.0	-	49.0	16	180	2.0	19	0.94	18	1	3.1	30	-	402	3	63	9
MW-1809	126.0	-	42.0	15	160	3.0	147	0.85	19	2	2.7	26	-	282	3	63	109
MW-1810	127.0	-	51.0	15	170	1.6	24	1.20	19	2	3.2	30	-	395	2	54	11
MW-1811	127.5	-	46.0	17	190	1.1	27	0.72	19	1	2.7	29	-	424	3	67	9

-	-	XRF	XRF	INAA	INAA	INAA	XRF	INAA	INAA	XRF	INAA	XRF	INAA	XRF	XRF
-	-	ppm	ppm	ppm	ppm	ppm	ppm	ppm	ppm	ppm	ppm	ppm	ppm	ppm	ppm
Sample	Depth	Rb	S	Sb	Sc	Sm	Sr	Ta	Th	V	W	Y	Yb	Zn	Zr
01-1415	25.5	75	1.000	4.6	16.5	0.9	36	0.25	7.3	105	21	7	0.66	32	196
01-1418	25.5	67	0.000	6.5	14.8	1.0	27	0.25	7.6	128	30	7	0.75	16	212
01-1497	28.0	62	1.000	5.0	16.0	1.1	27	0.86	6.8	127	24	7	0.56	51	189
01-1581	29.0	36	0.000	10.0	37.3	4.0	14	0.25	3.7	219	14	13	1.40	174	104
01-1583	29.0	72	0.000	10.0	21.2	4.4	28	0.25	7.6	247	36	17	2.00	51	262
01-1585	29.0	129	0.000	8.3	20.2	6.3	32	0.62	7.9	242	31	16	1.70	59	240
01-1594	30.0	47	0.000	8.5	38.2	2.0	11	0.62	3.7	236	27	10	1.10	197	132
01-1596	30.0	80	0.000	11.0	38.2	3.6	59	0.25	5.2	201	23	8	1.00	198	128
01-1597	30.0	61	2.000	6.8	50.6	8.3	164	1.80	7.2	132	29	6	0.85	23	169
01-1553	33.0	23	0.000	6.6	22.4	1.2	4	0.25	6.5	159	27	10	1.00	24	209
01-1561	33.0	60	0.000	6.0	13.3	1.5	22	0.25	8.0	133	23	10	0.86	41	205
01-1625	35.0	77	0.000	7.3	18.5	3.2	25	0.25	6.4	187	31	8	0.89	57	177
01-1628	35.0	68	0.000	7.2	16.5	4.8	24	0.25	7.3	134	33	8	0.95	70	202
01-1630	35.0	50	0.000	21.8	40.5	12.0	16	0.25	15.0	317	48	21	2.10	128	309
01-1645	38.0	75	0.000	6.1	12.6	3.1	27	0.25	7.1	101	18	7	0.89	56	182
01-1646	38.0	65	0.000	7.5	18.2	2.2	24	0.72	6.4	163	18	10	0.87	68	161
01-1697	40.0	56	0.000	6.3	19.9	5.7	76	0.25	4.5	69	23	11	1.20	57	130
01-1700	40.0	25	0.000	4.8	5.4	1.2	9	0.25	2.2	64	13	2	0.25	19	67
01-1722	45.0	60	0.000	5.9	10.0	8.8	243	0.25	5.9	132	22	16	0.85	59	156
01-1728	45.0	52	0.000	6.0	8.9	11.0	211	3.10	5.2	133	21	16	1.00	62	150
01-1734	45.0	76	0.000	10.0	17.6	14.0	120	0.25	6.7	192	30	30	1.80	93	171
01-1723	47.5	60	0.000	5.7	10.3	12.0	255	0.25	6.2	128	22	18	1.00	60	157
01-1729	47.5	52	0.000	6.1	8.9	11.0	215	2.10	5.5	136	22	15	1.10	62	150
01-1733	47.5	53	0.000	5.9	9.3	12.0	198	0.25	5.9	135	23	15	1.30	63	153
01-1846	48.0	45	0.000	7.4	15.8	7.5	119	3.50	4.2	120	35	18	1.20	118	119
01-1848	48.0	73	0.000	6.5	10.9	9.5	204	1.70	6.3	109	20	16	1.20	60	152
01-1850	48.0	68	0.000	4.9	11.0	14.0	290	0.25	5.5	106	18	16	1.40	63	151
01-1852	48.0	56	0.000	5.7	10.8	16.0	227	0.25	6.3	108	24	18	1.70	56	161
01-1847	50.5	57	0.000	8.8	21.7	6.3	129	1.60	3.1	167	28	15	1.40	123	112
01-1849	50.5	57	0.000	7.4	9.4	6.3	233	2.10	5.6	98	18	14	0.78	54	152
01-1851	50.5	65	0.000	4.8	10.0	11.0	248	2.70	5.8	108	19	16	1.20	56	155
01-1853	50.5	75	0.000	8.5	15.3	22.4	159	2.00	8.0	170	20	32	2.50	80	195
01-1938	51.0	62	0.000	8.4	8.3	6.0	180	0.25	5.6	72	40	17	0.63	75	164
01-1904	53.0	57	0.000	6.8	10.5	4.7	186	0.25	5.8	115	20	9	0.62	57	145
01-1907	53.0	52	0.000	4.5	9.2	4.9	219	1.60	5.4	92	20	11	0.61	59	140
01-1908	53.0	66	0.000	4.9	14.3	6.2	155	0.25	5.5	118	14	16	0.66	59	135
01-1866	55.0	57	0.000	13.4	22.2	9.1	121	0.50	4.8	191	17	16	1.11	98	142
01-1937	55.0	57	0.000	5.0	10.0	5.0	350	0.25	5.9	92	22	7	0.25	41	149
01-1905	55.5	65	0.000	4.8	10.0	4.7	202	1.10	5.9	98	17	7	0.58	60	150
01-1906	55.5	48	0.000	4.4	9.2	5.0	265	1.50	6.2	107	23	9	0.57	51	151
MW-1827	56.0	52	0.013	4.4	9.0	5.0	292	3.10	5.0	97	21	9	0.25	56	157
MW-1828	61.0	63	0.011	4.2	10.0	5.4	232	3.40	5.0	101	26	9	0.25	45	164
MW-1829	65.0	48	0.494	3.6	7.9	4.2	473	4.00	4.7	84	15	7	0.25	51	136
MW-1815	119.0	99	0.284	8.0	14.1	10.0	310	0.25	7.4	156	17	17	1.30	75	166
MW-1816	119.5	100	0.125	6.7	14.7	11.0	289	0.25	8.0	156	13	19	1.30	76	179
MW-1802	121.0	29	0.931	3.1	8.3	3.9	402	0.25	4.4	104	24	6	0.25	58	125
MW-1803	121.5	37	0.766	4.2	7.8	4.1	356	0.25	5.2	104	29	6	0.25	52	132
MW-1804	122.0	35	1.068	6.8	7.7	3.9	448	0.25	4.8	122	27	6	0.25	40	129
MW-1805	122.5	40	0.728	5.0	7.1	3.7	374	0.25	4.4	85	20	5	0.25	41	117
MW-1806	123.0	58	0.495	4.5	8.4	4.2	346	0.25	4.8	103	23	6	0.60	60	135
MW-1807	123.5	46	0.568	5.5	8.1	4.2	439	0.25	5.1	97	17	6	0.25	51	132
MW-1808	124.0	58	0.933	5.9	8.1	4.2	396	1.30	5.2	191	19	5	0.25	43	132
MW-1809	126.0	78	1.016	34.2	7.4	3.6	277	0.25	4.7	640	23	5	0.25	38	114
MW-1810	127.0	46	0.942	4.2	8.3	4.2	345	0.25	5.2	157	27	7	0.52	37	129
MW-1811	127.5	34	0.642	6.9	7.9	4.0	392	0.25	4.6	98	22	6	0.25	53	125

Metamorphic Grade	:	Amphibolite Facies
Structural Attributes	:	Strongly sheared
Gross Features	:	Schistose, banded
Profile Truncation	:	Near base of Mottled Zone
Depth to Fresh Rock	:	70 m
Location	:	Reedy, near Cue: North of Menzies Line
Reference	:	Robertson, Chaffee and Taylor, 1990

Geomorphology and profile

The Reedy Mine is situated on a gently sloping, stony, erosional plain, which forms a portion of the low divide between minor elements of the drainage systems into the playa lakes Austin and Annean. There are a few stony rises and low hills which expose weathered, generally ferruginized, Archaean greenstones and a few patches of lateritic duricrust. Deeply weathered country rocks are overlain by a dominantly fine, gravelly, ferruginous alluvium, up to 2 m thick, much of which has been hardpanized. A shallow (<0.5 m), acidic, stony, friable, fine, sandy, red to brown, clay loam overlies the hardpan. This contains lateritic and ferruginized lithorelic gravels which form a surface lag.

At the Rand Pit, where the profile was studied, the regolith has been stripped to the base of the mottled zone. The depth of weathering varies between rock types, but generally has penetrated to 70-80 m. The south face of the Rand Pit has exposed granitoid porphyry pods set in interstratified mafic, ultramafic and mica schists (Figure Um1-1). The ultramafic schists are described here.

Fresh rock

These rocks are almost fresh at 70 m depth. They are greenish-grey, in part tremolitic talc schists and are cut by an open-spaced chloritic cleavage. The talc forms slightly schistose mats and islands (Figure Um1-2D), in places set with decussate tremolite (Figure Um1-2A, B). Small amounts of graphite are found in a pre-chlorite, talcose schistosity. In parts, the cleavage is intense, the tremolite is needle-like and aligned to the cleavage and the rock is closely banded (Figure Um1-2C). Where the cleavage crosses tremolite crystals, these crystals are broken. Although most of these rocks are relatively quartz-poor, introduced quartz is locally important and occurs as chains of grains, closely associated with the cleavage, or as clusters in pressure shadows, where it occurs with coarse talc. Accessory minerals are chromite, magnetite and ilmenite, as well as hypidiomorphic sphene (Figure Um1-2A).

Saprock

In places, groundwater has penetrated the cleavage, etching it, and has deposited small amounts of goethite. Iron staining first occurs along the cleavage and in small fractures around 50 m depth. Goethite, from the weathering of granules of magnetite and ilmenite, stains the talc (Figure Um1-2F) and spreads along the cleavage or follows stylolitic fractures and the margins of quartz veins. In places, goethite pseudomorphs pyrite cubes. Small amounts of cryptomelane follow fractures. Ilmenite, which is generally found aligned to the cleavage, has a feathery appearance and shows early alteration to anatase and goethite. Sphene is opaque to semi-opaque and has been altered to creamy-coloured anatase lenses in the cleavage. The cleavage-related chlorite is yellow brown, slightly opaque and dusted with yellowish smectite. Tremolite needles have been dissolved and replaced in part by goethite (Figures Um1-2G, H).

Saprolite
Around 30 m depth, the talc of the saprolites has remained unaltered, though weathering of chlorite to smectite is advanced. Tremolite is represented only by goethite-lined or infilled cavities, sphene and ilmenite are altered entirely to anatase, all traces of Ca have been leached from the sphene but the characteristic feathery structures of ilmenite remain. Goethite occurs both in the talcose schistosity, where it has intensely stained the rock (Figures Um1-2I, J) and in the later chloritic cleavage, where it has been exsolved during the alteration of chlorite to smectite, and it also penetrates quartz vein margins. Some fractures are filled with asbolane ($Mn[O,OH]_2.[Co,Ni,Ca]_x.OH_{2x}.nH_2O$) and an indeterminate secondary V mineral. Some of these saprolites show lensoid cavities.

Plasmic zone
Kaolinite is an important component of these ultramafics at and above 10 m depth. In places kaolinite occurs as an alteration product of smectite, which was produced from largely cleavage-associated chlorite; here it contains relict "islands" of talc. In other places it is more pervasive. Fragments of the talc mat are surrounded with fine-grained kaolinite, suggesting alteration of talc to kaolinite (Figures Um1-2M, N). Some of the kaolinite has recrystallized to stumpy stacks (Figures Um1-2K, L) and books of coarser-grained kaolinite. Kaolinite, and mixtures of smectite and kaolinite, make up most of the rock and some of this is pervasively Fe-stained. Some of the talc relicts contain voids after tremolite which have been partly filled with goethite. The rock is pockmarked with vesicles which form chains, linked by solution channels.

Goethite staining is quite pervasive in some parts and is restricted to specific parts of others. Unaltered chromite still survives. Some fractures are lined with pyrolusite and barian cryptomelane. Cryptomelane is, in places, found developed in the clay fabric. Although some saprolitic fabrics remain, pedogenic fabrics are common.

Very close to the surface, some of these rocks are polymictic breccias, containing a variety of angular, partly Fe-stained saprolite fragments (Figures Um1-2O, P) consisting of matted kaolinite and kaolinite mixtures. One such specimen contained palygorskite, set in a matrix of smaller, angular aggregates of kaolinite.

Mottled zone
Not sampled.

Duricrust
None.

Lag and soil
Not sampled.

Reference
Robertson, I.D.M., Taylor, G.F, and Chaffee, M.A. 1990. The petrography, mineralogy and geochemistry of weathered profiles developed on felsic, mafic, ultramafic and sedimentary rocks, Rand Pit, Reedy Mine, Western Australia. CSIRO Division of Exploration Geoscience Restricted Report 102R. 205 pp.

FIGURE P1-2 (Contd)

Clay saprolite, plasmic and mottled clay zone

O. The original fabric has been destroyed and is replaced with cream-coloured pedogenic kaolinite. Only quartz phenocrysts (QZ) remain. Numerous voids (VO) mark root passages. Specimen MW-741. Depth 8.0 m. Close-up photograph of 'dry' surface.

P. Petrographic detail of P1-2I. A fine grained mat of pedogenically restructured, Fe-stained kaolinite and sericite (KM) is set with relics of compound quartz phenocrysts (QZ), which are the only part of the original fabric to survive. Specimen MW-741. Depth 8.0 m. Photomicrograph with crossed polarizers.

M. The incompleteness of pedogenic processes is illustrated by a preserved saprolitic fabric of yellow clay and quartz (KQ), set with quartz phenocrysts (QZ) and goethite-rich patches (GO). Specimen MW-1292. Depth 17.5 m. Close-up photograph of 'dry' surface.

N. Petrographic detail of P1-2M. Although completely altered to kaolinite, the feldspar lath fabric (LF) is preserved in quartz (QZ) despite restructuring of clays by pedogenesis below (see P1-2K and L). Specimen MW-1292. Depth 17.5 m. Photomicrograph with crossed polarizers.

K. Globular blasts of white pedogenic kaolinite (KA) dominate a groundmass of kaolinite and sericite, variously stained yellow by goethite (GO) and pink by hematite (HM). Specimen MW-1530. Depth 25.0 m. Close-up photograph of "dry" surface.

L. Petrographic detail of P1-2K. Blasts of very fine-grained, matted kaolinite (KA) are set in matted sericite, kaolinite and quartz (MQ). Specimen MW-1530. Depth 25.0 m. Photomicrograph with crossed polarizers.

Saprolite

I. A pale-yellow, clay- and quartz-rich, fine-grained groundmass (KQ) is set with quartz phenocrysts, lath-like patches of goethite-stained, fine-grained mica (GM), probably after mafic phenocrysts, and minor, small goethite cubes (GO) after pyrite and/or magnetite. A few diffuse patches of white kaolinite (KA) indicate early stages of saprolite restructuring. Specimen MW-1625. Depth 25.0 m. Close-up photograph of "dry" surface.

J. Petrographic detail of P1-2I. The feldspar has been completely consumed and restructuring of the groundmass has led to the loss of much of the lath-like feldspar microfabric (compare with P1-2H and F). The saprolite consists of a fine-grained mat of quartz, kaolinite and mica (MA), with a few relics of feldspar structures (RF), set with goethite cubes (GO) after pyrite and magnetite. Specimen MW-1625. Depth 25.0 m. Photomicrograph with crossed polarizers.

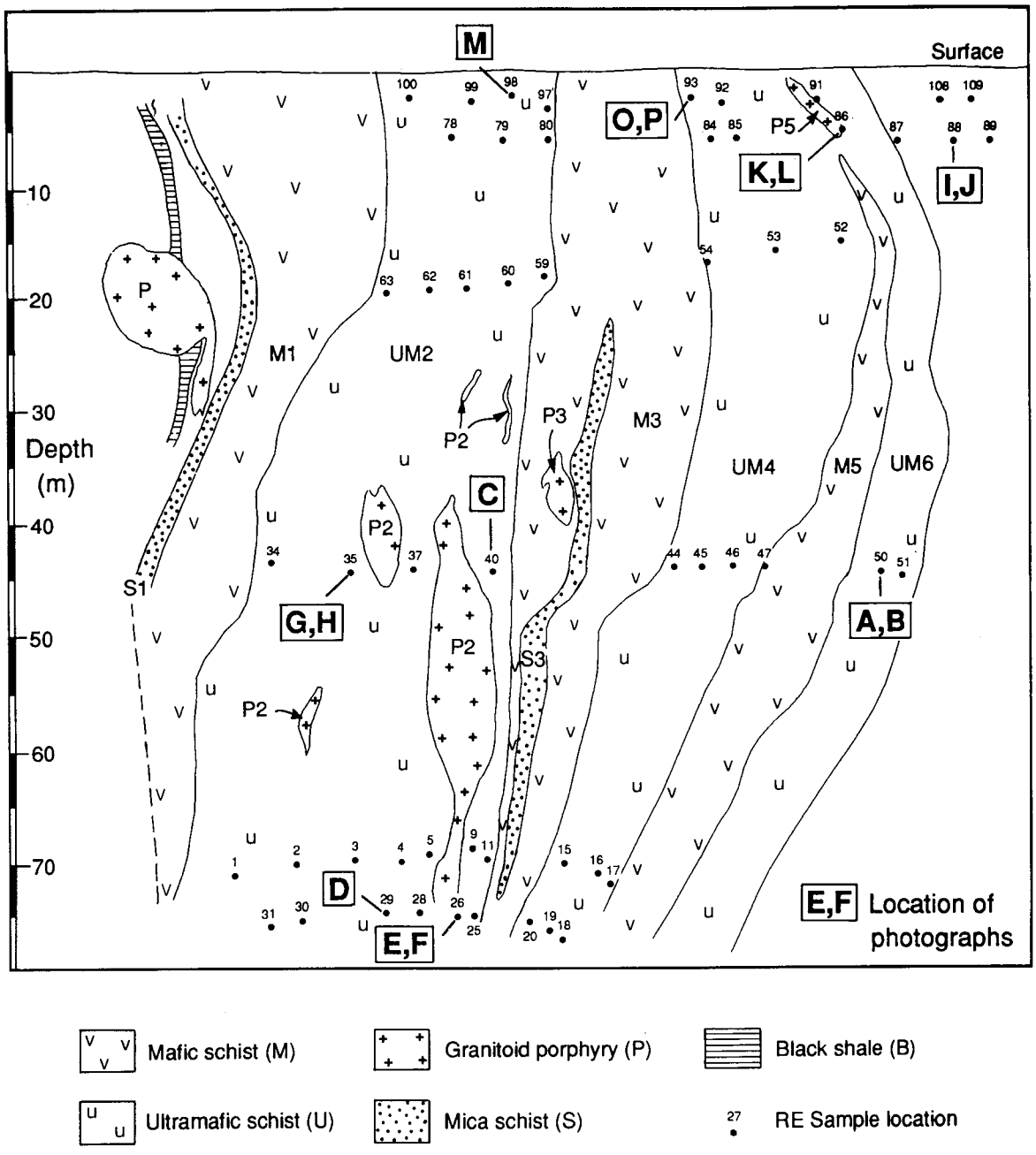

Figure Um1-1. Profile at Rand Pit showing locations of samples and photographs.

FIGURE Um1-2

Saprock

G. A weathered talc-chlorite schist. A schistose groundmass of white talc (TC) and grey chlorite (CH) rich layers, are lightly but variably stained with goethite (GO). This is set with needles of tremolite which have been largely dissolved and replaced by goethite (GT). Specimen RE 35: Depth 49 m. Ultramafic band UM2. Compare with Figure Um1-2H. Close-up photograph of "dry" surface.

H. Partly weathered talc-chlorite schist. A brown, goethite-stained mat of talc and chlorite (TL), set with patches and granules of quartz (QZ). Pre-existing tremolite (TM) has been dissolved, leaving needle-like voids, some of which have been filled or partly filled with goethite (GO). Specimen RE 35: Depth 49 m. Ultramafic band UM2. Compare with Figure Um1-2G. Photomicrograph in plain polarized light.

E. Largely fresh talc-chlorite schist. White talc (TC) and green chlorite (CL) show a schistose fabric. This is set with dark brown granules of goethite pseudomorphs (GT) after magnetite or pyrite, surrounded by a pale-brown goethite stain (GS). Compare to Figure Um1-2F. Specimen RE 26: Depth 73 m. Ultramafic band UM2. Close-up photograph of "wet" surface.

F. Largely fresh talc-chlorite schist. Goethite pseudomorphs (GO) after pyrite and/or magnetite are surrounded by a goethite stain (GS) in the talc mat (TC). Ilmenite grains (IL) are unaltered. Compare to Figure Um1-2E. Specimen RE 26: Depth 73 m. Ultramafic band UM2. Photomicrograph with crossed polarizers.

Relatively fresh rock

C. A fresh talc-chlorite schist showing a very strong foliation of alternating bands of white talc (TC) and green chlorite (CL). Weathering has started by altering sphene to pale flecks of anatase (AN). Specimen RE 40: Depth 48 m. Ultramafic band UM2. Close-up photograph of "wet" surface.

D. Talc-chlorite schist. Islands of fresh matted talc (TC), with some quartz, cut by a chlorite-filled cleavage (CH). Specimen RE 29: Depth 73 m. Ultramafic band UM2. Photomicrograph with crossed polarizers.

A. Needles and blades of fresh, pale green tremolite (TR) in dark green chlorite (CH). Small flecks of sphene (SP) are also completely unaltered. Tremolite has survived higher in the regolith than in Ultramafic band UM 2, apparently due to being remote from oxidizing sulphides around the ore shoots. Compare to Figure Um1-2B. Specimen RE 50: Depth 46 m. Ultramafic band 6. Close-up photograph of "wet" surface.

B. A fresh tremolite-chlorite schist consisting of poorly-defined lens-like islands of bladed tremolite (TM) with quartz and feldspar, set in highly schistose, flaky chlorite (CL) and needle-like tremolite (TN). Compare to Figure Um1-2A. Specimen RE 50: Depth 46 m. Ultramafic band 6. Photomicrograph with crossed polarizers.

FIGURE Um1-2

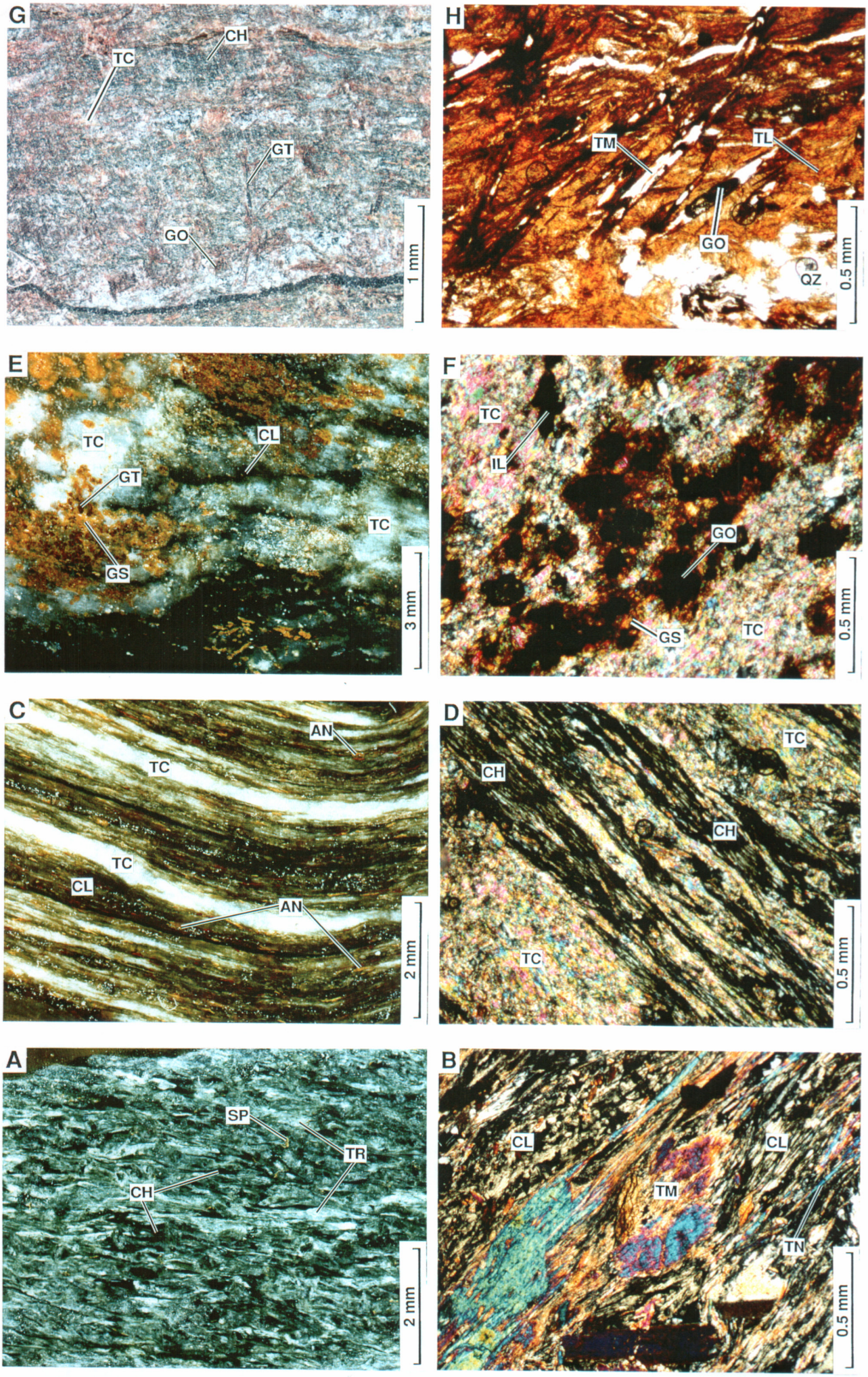
G
TC
CH
GT
GO
1 mm
H
TM
TL
GO
QZ
0.5 mm
E
TC
CL
GT
TC
GS
3 mm
F
TC
IL
GO
GS
TC
0.5 mm
C
AN
TC
TC
CL
AN
2 mm
D
TC
CH
CH
TC
0.5 mm
A
SP
TR
CH
2 mm
B
CL
CL
TM
TN
0.5 mm

FIGURE Um1-2 (Contd)

Filled voids and root channels - Plasmic Zone

O. A saprolite-fragment breccia. This consists of a loosely-cemented, clast-supported polymictic breccia of saprolite fragments. Most fragments consist of matted kaolinite, some containing smectite and palygorskite. Some still retain a schistose fabric (SH), others are matted (MT). They show varying stages of goethite staining from intense and largely replaced (GO) through lightly stained (LS) to unstained kaolinite (KA). Specimen RE 93: Depth 2 m. Ultramafic band UM4. Compare with Figure Um1-2P. Close-up photograph of "wet" surface.

P. Saprolite-fragment breccia. A wide variety of texturally different, polymictic, round to sub-angular saprolite fragments which form a loosely clay-cemented breccia. The saprolite fragments are of matted kaolinite and some are mixed with smectite and palygorskite. Some show clay-rich skins and there are also a few goethitic granules. Specimen RE 93: Depth 2 m. Ultramafic band UM4. Compare with Figure Um1-2O. Photomicrograph in plain polarized light.

Development of structureless kaolinite mat and breakdown of talc - Plasmic Zone

M. Segregations of quartz (QZ) in a mat of secondary kaolinite and smectite (KS). The quartz has been swept aside into patches and any pre-existing schistose fabric has been destroyed Specimen RE 98: Depth 2 m. Ultramafic band UM2. Compare with Figure Um1-2N. Close-up photograph of "wet" surface.

N. Relict primary talc (TC) surrounded by and apparently altering to secondary kaolinite (KA). Photomicrograph with crossed polarizers.

Kaolinite accordion structure - Plasmic Zone

K. A strongly weathered ultramafic - now a kaolinite-quartz rock. It consists of patches of white, coarse-grained recrystallized kaolinite (KS), with a stumpy stack micro-fabric, set in yellowish fine-grained kaolinite (KY). The whole contains small vesicles (V) and has been variably stained pink with Fe oxides. The blue patch is quartz (QZ). Specimen RE 86: Depth 6 m. Ultramafic band UM4. Compare with Figure Um1-2L. Close-up photograph of "wet" surface.

L. Kaolin-quartz rock. A mass of stumpy books of secondary kaolinite (KB), set in flakes of fine-grained kaolinite (KA). These are the precursors to accordion structures. Specimen RE 86: Depth 6 m. Ultramafic band UM4. Compare with Figure Um1-2K. Photomicrograph with crossed polarizers.

Saprolite - intense Fe staining

I. Intensely Fe-stained talc-kaolinite-smectite schist. The schistosity has been preserved, by the resistance of talc to weathering, to a point very close to the surface. Compare with Figure Um1-2P. Specimen RE 88: Depth 6 m. Ultramafic band UM6. Close-up photograph of "wet" surface.

J. Intensely goethite-stained talc-kaolinite-smectite schist. Despite the weathering of some of the major minerals and their intense staining so as to be petrographically unrecognizable, they are set with lath-like crystals of unaltered ilmenite (IL), parallel to the cleavage. Compare with Figure Um1-2I. Specimen RE 88: Depth 6 m. Ultramafic band UM6. Photomicrograph in plane polarized light.

FIGURE Um1-2 (Contd)

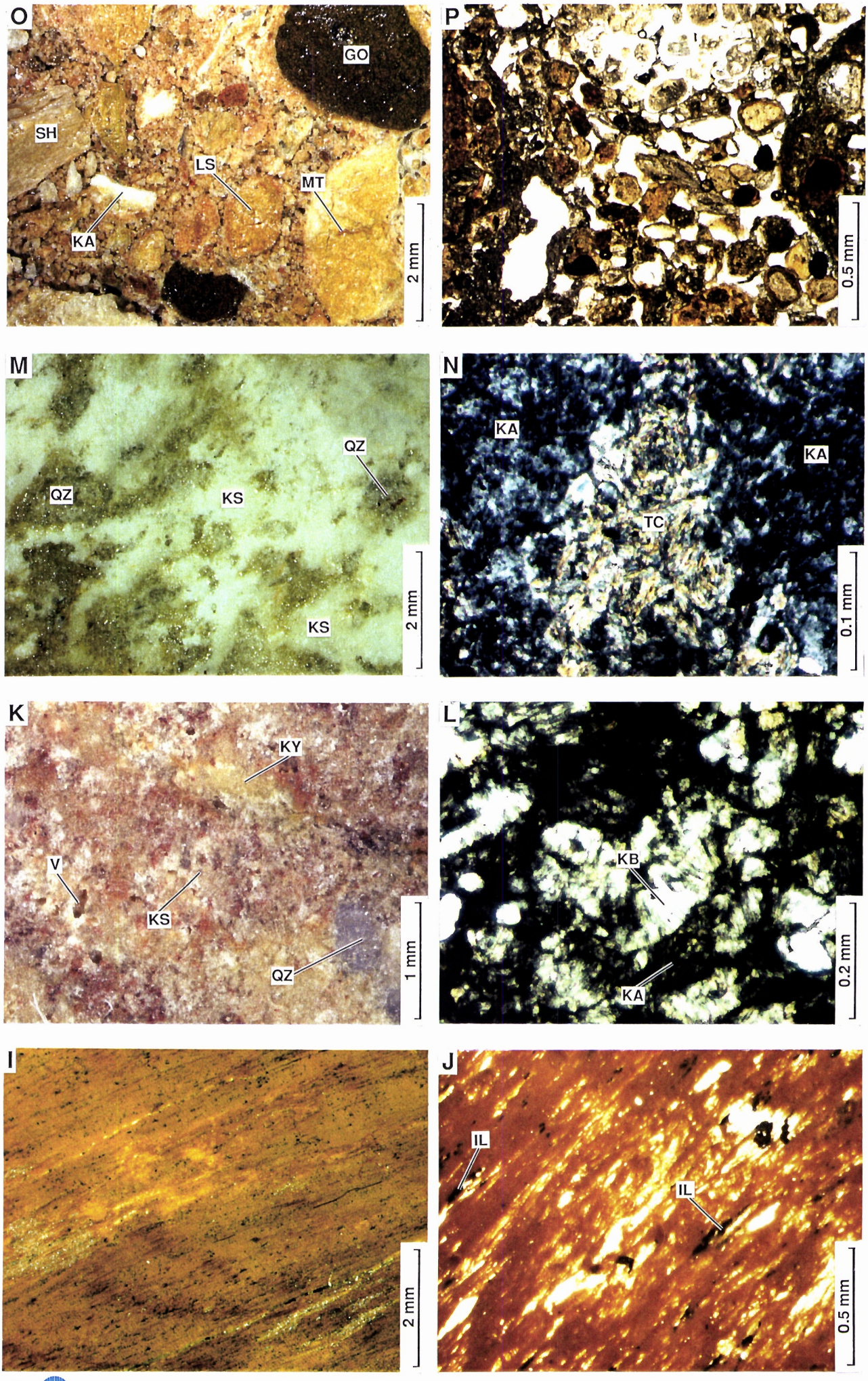

ULTRAMAFIC VOLCANIC UM1
MINERALOGY

Lib No	Depth	Class	Quartz	Fspar	Musc	Talc	Trem	Kaolin	Chlor	Smect	Hemat	Goeth	Halite
08-492	2	Saprolite	36	0	0	1757	5	28	0	0	0	0	0
08-490	2	Plasmic Z	62	0	0	9	0	60	0	60	0	52	0
08- 484	3	Plasmic Z	5	0	0	0	0	43	0	154	0	108	0
08-500	3	Saprolite	1	0	0	1656	0	7	0	1159	0	0	0
08-501	3	Plasmic Z*	0	0	0	579	0	18	0	502	0	112	0
08-480	6	Saprolite	0	0	0	1060	10	208	0	165	0	0	0
08-481	7	Saprolite	0	0	0	100	0	399	0	0	0	377	0
08-479	7	Saprock	0	0	6	74	0	5	0	1472	0	0	0
08-080	8	Saprolite	39	0	6	22	0	83	0	232	0	0	0
08-081	8	Saprolite	129	0	6	6	0	259	0	141	0	6	0
08-049	19	Saprolite	142	0	6	62	0	62	371	297	0	0	0
08-050	20	Saprock	138	0	6	1268	0	0	646	231	0	0	0
08-058	23	Saprock	6	0	0	2731	0	0	801	340	0	0	0
08-059	24	Saprock	268	0	0	2096	0	0	675	116	0	0	0
08-046	46	Rock	120	7	7	42	396	0	410	0	0	0	0
08-047	46	Rock	122	50	0	43	690	0	475	7	0	0	0
08-042	47	Saprock	162	7	54	27	257	0	542	135	0	0	7
08-041	47	Saprock	0	0	0	2156	0	0	439	146	0	0	0
08-033	48	Rock	146	0	0	2225	0	0	759	187	0	0	0
08-036	48	Saprock	12	0	0	4963	0	0	886	414	0	0	0
08-013	69	Rock	105	0	62	1997	0	0	567	0	0	0	6
08-003	69	Rock	60	0	0	2090	28	0	438	0	0	0	6
08-004	69	Rock	66	0	0	2319	0	0	676	0	0	0	0
08-015	69	Rock	149	7	7	7	607	0	694	0	0	0	0
08-001	69	Rock	94	0	7	1193	603	0	362	7	0	0	7
08-027	73	Saprock	82	0	7	2552	393	0	628	0	0	0	7
08-026	73	Saprock	143	0	1	1409	65	0	349	50	0	0	0
08-023	73	Rock	12	0	0	3521	0	0	763	0	0	0	6
08-024	73	Rock	20	0	0	3102	0	0	453	0	0	0	6
08-016	74	Rock	219	0	0	480	439	0	411	0	0	0	0
08-017	74	Saprock	47	0	6	1998	0	0	343	6	0	0	6

ULTRAMAFIC VOLCANIC UM1
GEOCHEMISTRY

Lib No	Depth	Class	SiO2	Al2O3	Fe2O3	MgO	CaO	Na2O	K2O	TiO2	LOD	LOI	S.G.	Ag	As	Au	Ba	Be	Bi
-	m	-	%	%	%	%	%	%	%	%	%	%	-	ppm	ppm	ppb	ppm	ppm	ppm
08-492	2	Saprolite	60.70	15.20	4.43	9.27	0.12	0.05	0.07	0.57	0.78	8.90	1.77	-	5	34	120	0	0
08-490	2	Plasmic Z	66.00	16.40	3.15	1.25	0.27	0.05	0.14	0.41	2.80	11.50	1.94	-	2	21	556	0	0
08- 484	3	Plasmic Z	46.00	18.60	17.16	0.88	0.27	0.06	0.11	1.05	3.25	14.30	1.95	-	3	22	164	0	5
08-500	3	Saprolite	47.40	12.20	13.58	10.50	0.44	0.09	0.07	0.82	5.10	14.20	1.75	-	1	11	13	0	0
08-501	3	Plasmic Z	44.50	16.00	15.87	3.63	0.31	0.06	0.05	1.61	4.65	14.70	2.03	-	1	16	42	0	0
08-480	6	Saprolite	38.60	14.20	25.73	6.73	0.24	0.07	0.06	1.64	3.12	13.30	1.59	-	1	4	96	0	1
08-481	7	Saprolite	32.30	18.00	31.74	0.99	0.11	0.06	0.04	1.67	1.32	12.90	1.48	-	2	5	35	0	2
08-479	7	Saprock	46.50	15.40	10.44	11.30	0.61	0.04	0.02	0.48	5.80	15.50	1.96	-	1	4	14	0	0
08-080	8	Saprolite	46.62	27.50	7.43	1.21	0.28	0.03	0.03	1.33	4.69	16.30	1.82	2	1	9	134	0	0
08-081	8	Saprolite	51.04	25.66	8.44	0.74	0.20	0.03	0.04	1.25	3.52	14.60	1.92	0	1	16	52	0	0
08-049	19	Saprolite	54.02	18.28	9.29	6.62	0.39	0.03	0.27	0.93	4.06	13.20	1.73	0	1	4	52	0	0
08-050	20	Saprock	59.29	8.06	7.29	18.60	0.26	0.03	0.01	0.38	2.42	9.10	2.26	1	1	6	31	0	0
08-058	23	Saprock	53.83	9.23	8.86	20.60	0.31	0.04	0.02	0.38	3.22	10.30	2.20	0	5	4	6	0	0
08-059	24	Saprock	54.71	7.43	7.86	22.60	0.24	0.03	0.01	0.34	1.70	8.80	2.14	0	15	4	19	0	0
08-046	46	Rock	50.47	8.85	10.01	18.90	6.24	0.31	0.02	0.29	0.23	5.50	2.76	0	1	3	3	0	0
08-047	46	Rock	51.99	9.14	10.44	17.70	5.85	0.98	0.03	0.32	0.64	5.10	2.78	0	1	3	6	0	0
08-042	47	Saprock	52.36	9.68	10.15	16.80	3.51	0.25	0.20	0.41	1.27	7.60	2.65	0	1	3	62	0	0
08-041	47	Saprock	52.85	5.72	9.29	24.70	0.11	0.03	0.01	0.21	1.16	7.40	2.63	0	0	2	2	0	1
08-033	48	Rock	57.00	6.43	8.01	20.60	0.24	0.06	0.07	0.28	2.52	8.70	2.54	0	4	13	6	0	0
08-036	48	Saprock	52.12	7.03	8.72	23.00	0.18	0.05	0.01	0.23	2.27	9.10	2.49	1	3	57	1	0	0
08-013	69	Rock	56.80	7.66	8.86	21.70	0.31	0.03	0.01	0.27	0.53	6.70	2.70	2	1	4	3	0	2
08-003	69	Rock	55.79	6.34	9.01	23.40	0.90	0.03	0.01	0.26	0.58	6.70	2.52	0	0	32	6	0	0
08-004	69	Rock	55.65	6.53	8.44	22.90	0.22	0.08	0.36	0.28	1.87	8.10	2.60	2	0	2	30	0	2
08-015	69	Rock	54.88	9.49	10.01	17.60	5.88	0.85	0.09	0.30	0.28	4.78	2.74	0	1	15	11	0	0
08-001	69	Rock	51.15	6.50	8.86	22.20	5.59	0.13	0.02	0.22	0.38	5.60	2.72	1	0	2	0	0	0
08-027	73	Saprock	56.15	6.86	8.44	21.50	3.67	0.11	0.16	0.33	0.77	6.20	2.68	2	0	3	21	0	0
08-026	73	Saprock	55.65	6.01	9.01	20.70	1.55	0.05	0.03	0.20	0.79	6.80	2.55	1	2	19	0	0	0
08-023	73	Rock	47.87	8.23	8.86	24.50	0.14	0.03	0.00	0.37	0.15	7.70	2.43	0	2	19	0	0	1
08-024	73	Rock	50.42	6.44	9.01	24.30	0.23	0.03	0.08	0.32	0.49	7.20	2.68	1	1	3	15	0	2
08-016	74	Rock	54.23	7.61	9.44	20.70	4.74	0.07	0.01	0.23	0.17	5.20	2.68	1	1	3	1	0	0
08-017	74	Saprock	57.74	15.44	8.86	11.00	0.40	0.03	0.00	0.21	0.53	6.50	2.61	1	1	9	0	0	0

ULTRAMAFIC VOLCANIC UM1
GEOCHEMISTRY

Lib No -	Br ppm	Cd ppm	Ce ppm	Co ppm	Cr ppm	Cs ppm	Cu ppm	Eu ppm	Ga ppm	Ge ppm	Hf ppm	In ppm	Ir ppb	La ppm	Li ppm	Lu ppm	Mn ppm	Mo ppm	Nb ppm	Ni ppm
08-492	1	1	9	29	3019	1	136	0	19	1	2	0	13	4.7	12	0.2	122	4	2	338
08-490	2	1	23	24	621	1	48	0	19	1	2	0	8	5.2	18	0.1	88	2	4	98
08- 484	1	0	2	40	1266	1	154	0	26	1	5	0	12	4.1	33	0.2	65	3	5	341
08-500	4	0	7	117	4140	1	144	1	18	0	1	1	11	8.0	15	0.3	275	4	0	1618
08-501	3	0	3	54	3611	1	130	0	30	2	4	3	12	3.1	10	0.1	251	4	4	614
08-480	2	0	8	112	4403	3	345	2	27	0	3	0	14	6.3	15	0.3	747	4	2	1626
08-481	2	0	5	52	4409	1	475	1	36	2	4	2	16	2.8	10	0.3	419	5	6	1168
08-479	1	0	40	97	3946	1	51	2	18	2	2	2	13	30.4	37	0.3	430	4	4	774
08-080	1	2	9	50	744	1	82	0	29	2	5	2	11	4.1	51	0.2	478	3	10	369
08-081	1	1	4	26	1140	1	129	0	31	1	4	5	18	3.3	51	0.2	91	3	6	398
08-049	1	0	71	62	489	1	78	2	21	3	4	0	10	45.8	41	0.6	723	3	5	273
08-050	1	0	27	122	2930	1	88	1	9	1	1	0	9	16.0	35	0.3	819	3	2	881
08-058	1	0	14	107	3330	1	15	1	12	2	2	5	9	10.2	40	0.3	580	3	1	919
08-059	1	0	15	143	3580	1	5	0	9	1	2	1	7	6.0	47	0.2	844	4	5	942
08-046	1	0	14	71	2360	1	0	1	9	1	2	4	8	8.2	45	0.2	1278	3	3	552
08-047	1	1	9	69	2170	1	3	1	12	2	1	1	10	4.5	40	0.2	1273	3	3	533
08-042	1	1	15	73	1690	1	31	1	11	1	2	0	8	9.7	49	0.2	1024	3	3	436
08-041	0	0	5	89	2570	1	16	0	6	1	1	0	10	3.1	23	0.1	633	3	0	1236
08-033	0	1	5	74	2490	1	22	0	9	1	1	0	7	2.7	49	0.2	673	3	5	614
08-036	0	3	17	79	2860	1	322	1	13	1	1	0	8	12.0	38	0.2	826	3	1	600
08-013	0	0	10	80	2270	1	0	0	8	0	1	1	8	6.5	44	0.2	819	3	3	624
08-003	0	0	7	90	2650	1	8	0	8	1	1	0	8	5.3	52	0.2	1113	3	2	666
08-004	1	0	10	80	2700	5	13	0	11	0	1	0	8	6.4	80	0.2	739	3	3	673
08-015	1	0	13	67	1740	1	23	1	11	1	2	0	9	7.6	36	0.2	1294	3	3	452
08-001	1	0	6	74	2790	1	0	1	9	0	1	0	7	3.5	52	0.2	1396	3	0	599
08-027	1	0	10	73	2400	2	3	0	7	0	1	0	8	5.9	64	0.2	1077	3	0	616
08-026	1	0	9	124	2670	1	0	0	7	1	1	0	8	6.1	63	0.1	1007	3	4	984
08-023	1	0	13	61	3070	1	204	1	18	1	1	0	8	7.7	53	0.2	1240	3	4	371
08-024	0	0	8	70	3330	1	35	0	13	1	1	2	9	4.8	53	0.2	958	3	2	536
08-016	1	0	13	77	2650	1	0	1	7	1	1	2	8	8.1	32	0.2	1309	3	3	510
08-017	1	0	7	84	2720	1	4	0	7	1	1	0	7	5.3	35	0.1	748	3	1	695

ULTRAMAFIC VOLCANIC UM1
GEOCHEMISTRY

Lib No -	Pb ppm	Rb ppm	Sb ppm	Sc ppm	Se ppm	Sm ppm	Sn ppm	Sr ppm	Ta ppm	Te ppm	Th ppm	U ppm	V ppm	W ppm	Y ppm	Yb ppm	Zn ppm	Zr ppm
08-492	8	4	0.1	65.7	0	1.4	1	19	0	0.09	6.1	2	304	3	10	1.6	29	128
08-490	1	8	0.2	26.0	0	0.9	0	42	1	0.14	4.1	1	154	11	7	0.8	9	107
08- 484	6	8	0.2	52.9	1	1.1	0	30	1	0.17	15.5	1	644	5	8	1.2	10	199
08-500	0	23	0.1	35.4	2	3.6	4	35	1	0.05	0.3	1	315	1	13	1.4	133	65
08-501	4	3	0.3	59.9	1	1.3	0	24	1	0.06	0.9	2	494	1	7	1.0	60	142
08-480	4	26	0.2	59.9	1	4.7	0	21	1	0.06	0.6	2	593	1	20	2.2	165	116
08-481	7	2	0.3	80.9	2	3.3	0	10	1	0.06	0.6	2	797	2	15	2.0	99	155
08-479	0	1	0.1	49.1	0	7.6	0	38	1	0.02	4.0	1	191	1	16	1.7	89	105
08-080	5	3	0.1	51.7	0	1.2	0	25	1	0.15	4.9	1	312	1	12	1.4	31	196
08-081	6	2	0.1	74.3	0	1.2	0	17	1	0.05	6.2	1	435	1	10	1.5	7	193
08-049	9	35	0.2	42.3	0	8.3	0	26	1	0.03	5.6	1	257	2	52	3.8	104	142
08-050	3	1	0.5	32.3	0	3.0	1	18	1	0.02	2.2	1	150	1	13	1.5	198	55
08-058	0	2	0.1	38.3	0	2.4	2	24	0	0.24	2.4	1	188	1	9	1.5	161	63
08-059	2	0	0.1	16.6	0	1.6	0	16	0	0.02	1.9	1	128	2	8	1.0	160	52
08-046	0	1	0.1	30.1	0	1.9	3	11	0	0.01	2.3	1	160	1	12	1.4	65	57
08-047	3	1	0.2	29.3	0	2.0	1	32	1	0.01	2.5	1	166	1	14	1.2	65	55
08-042	4	5	0.1	31.9	1	2.3	0	13	1	0.02	2.9	1	159	2	17	1.5	74	71
08-041	3	1	0.1	17.4	1	0.8	0	6	0	0.00	1.6	1	92	1	5	0.6	80	41
08-033	2	2	0.1	21.0	0	0.8	0	16	0	0.07	2.2	1	107	3	6	0.7	88	57
08-036	2	1	0.2	20.2	0	2.2	0	12	0	0.09	1.5	1	141	1	8	0.9	219	36
08-013	0	0	0.2	25.9	0	1.5	0	3	0	0.02	2.7	1	147	2	11	1.0	64	51
08-003	2	1	0.1	22.9	1	1.1	0	6	0	0.01	1.9	1	122	1	9	1.0	78	46
08-004	3	15	0.1	22.2	0	1.3	0	14	0	0.03	1.8	1	161	1	8	0.8	111	44
08-015	1	2	0.1	30.3	0	2.1	0	19	1	0.02	2.8	1	177	1	14	1.5	51	66
08-001	3	0	0.1	25.0	0	1.4	1	11	0	0.01	1.9	1	117	1	11	1.1	62	44
08-027	0	6	0.1	23.9	0	1.4	0	15	0	0.01	2.0	1	118	1	9	0.9	59	47
08-026	4	2	0.1	29.2	0	1.3	1	7	0	0.00	1.9	1	150	1	11	0.9	118	40
08-023	7	1	0.5	27.3	13	1.6	0	3	1	0.13	2.7	1	377	1	12	1.2	233	62
08-024	3	3	0.1	26.1	0	1.3	0	3	0	0.03	2.0	1	312	1	12	1.0	129	48
08-016	2	0	0.1	27.4	0	1.7	0	4	1	0.24	2.3	1	156	1	11	1.0	73	50
08-017	3	1	0.1	23.6	0	1.2	0	1	1	0.00	1.7	1	128	1	8	0.8	68	40

6 ACKNOWLEDGEMENTS

Thin and polished sections were prepared by R.J. Bilz, A.G. Bowyer and I. Pontifex. Geochemical analyses were by M.K.W. Hart (XRF), J.E. Wildman (ICP) at CSIRO and by Becquerel Laboratories (INAA) at Lucas Heights. H.M. Churchward provided geomorphological input. X-ray diffraction analysis was by M.K.W. Hart and A. Horne. Debye-Scherer XRD was by E. Nickel. Artwork was prepared by A.D. Vartesi and C. R. Steel. Permission to publish electron photomicrographs was granted by the Centre for Australian Regolith Studies. R.R. Anand commented on the manuscript. N.A. Campbell assisted with multivariate statistics. D.J.Gray and W. Jones helped with with colour graphics. Technical assistance was by E.G. Barbour and V.M. Baker assisted with document formatting. All this is acknowledged with appreciation.

7 REFERENCES

Anand, R.R., Gilkes, R.J., Armitage, T.M. and Hillyer, J.W. 1985. Feldspar weathering in lateritic saprolite. Clays and Clay Minerals, 33: 31-43.

Anand, R.R. and Gilkes, R.J. 1987. Muscovite in Darling Range bauxitic laterite. Australian Journal of Soil Research. 25: 445-450.

Anand, R.R. and Butt, C.R.M., 1988. The terminology and classification of the deeply weathered regolith. Discussion paper, CSIRO Australia, Division of Exploration Geoscience, Perth. (Unpublished), 29p.

Anand, R.R., Smith, R.E., Innes, J., Churchward, H.M., Perdrix, J.L. and Grunsky, E.C., 1989. Laterite types and associated ferruginous materials, Yilgarn Block, WA. Terminology, classification and atlas. CSIRO Division of Exploration Geoscience Restricted Report 60R.

Box, G.E.P. and Cox, D.R., 1964. An analysis of transformations. Journal of the Royal Satistical Society, Series B. 26. 211-252.

Butt, C.R.M., 1991. Geochemical dispersion in the regolith, Mystery Zone, Mt. Percy, Kalgoorlie, Western Australia. CSIRO Division of Exploration Geoscience Restricted Report 156R. 226 pp.

Campbell, N.A., 1980. Robust procedures in multivariate analysis. I. Robust covariance estimation. Applied Statistics. 29: 231-237.

Campbell, N.A., 1982. Robust procedures in multivariate analysis. II. Robust canonical variate analysis. Applied Statistics. 31: 1-8.

Campbell, N.A., 1986. Censored, grouped and truncated geochemical data.. CSIRO Division of Mathematics and Statistics Technical Files.

Eggleton, R.A. and Buseck, P.R., 1980. High resolution electron microscopy of feldspar weathering. Clays and Clay Minerals, 88: 173-178.

Grunsky, E., 1991. Strategies and methods for the interpretation of geochemical data. Discussion paper applied to laterite geochemistry. CSIRO Division of Exploration Geoscience. 77p.

Hallberg, J.A., 1984. A geochemical aid to igneous rock identification in deeply weathered terrain. Journal of Geochemical Exploration, 20: 1-8.

Hart, M.KW., 1989. Analysis for total iron, chromium, vanadium and titanium in varying matrix geological samples by XRF, using pressed powder samples. Standards in X-ray analysis. Australian X-ray Analytical Association (WA Branch) Fifth State Conference. 117-129.

Jensen, L.S. 1976. A new cation plot for classifying subalkalic volcanic rocks. Ontario Division of Mines. Misc. Paper 66. 22 pp.

Llorca, S.M., 1989. Mineralogy and geochemistry of the Glasson gold deposit, Callion, Yilgarn Block, WA. CSIRO Division of Exploration Geoscience Restricted Report 58R. 33 pp.

Norrish, K and Hutton, T.J., 1969. An accurate X-ray spectrographic method for the analysis of a wide range of geological samples. Geochimica et Cosmochimica Acta. 33: p 431.

Norrish, K and Chappell, B.W., 1977. X-ray fluorescence spectrometry. In J. Zussman (ed). Physical methods in determinative mineralogy. Academic Press, London 201-272.

Robertson, I.D.M., 1989. Geochemistry, petrography and mineralogy of ferruginous lag overlying the Beasley Creek Gold Mine - Laverton, WA. CSIRO Division of Exploration Geoscience Restricted Report 27R. 181 pp.

Robertson, I.D.M., 1990. Mineralogy and geochemistry of soils overlying the Beasley Creek Gold Mine - Laverton, WA. CSIRIO Division of Exploration Geoscience Restricted Report 105R. 158 pp.

Robertson, I.D.M., 1990. Weathering at the Trial Hill tin mine - Queensland. Occasional Paper, 1. Centre for Australian Regolith Studies, Canberra, 48 pp.

Robertson, I.D.M., Chaffee, M.A., and Taylor, G.F. 1990. The petrography, mineralogy and geochemistry of weathering profiles developed on felsic, mafic, ultramafic and sedimentary rocks, Rand Pit, Reedy Mine, Western Australia. CSIRO Division of Exploration Geoscience Restricted Report 102R. 205 pp.

Robertson, I.D.M. and Eggleton, R.A., 1991. Weathering of granitic muscovite to kaolinite and halloysite and of plagioclase-derived kaolinite to halloysite. Clays and Clay Minerals, 39. 113-126.

Robertson, I.D.M., and Tenhaeff, M.F.J., 1992. Petrography, mineralogy and geochemistry of soil and lag overlying the Lights of Israel Gold Mine, Davyhurst, Western Australia.. CSIRO Division of Exploration Geoscience Restricted Report 232R.

Savarajasingham, S, Alexander, L.T., Cady, J.G., and Cline, M.G., 1962. Laterite. Advances in Agronomy, 14: 1-60.

8 APPENDIX 1

Data Disc.

Type README.DOC for contents and formats